

Cartographic modelling for automated map generation

Citation for published version (APA):

Reimer, A. (2015). *Cartographic modelling for automated map generation*. [Phd Thesis 2 (Research NOT TU/e / Graduation TU/e), Mathematics and Computer Science]. Technische Universiteit Eindhoven.

Document status and date:

Published: 01/01/2015

Document Version:

Publisher's PDF, also known as Version of Record (includes final page, issue and volume numbers)

Please check the document version of this publication:

- A submitted manuscript is the version of the article upon submission and before peer-review. There can be important differences between the submitted version and the official published version of record. People interested in the research are advised to contact the author for the final version of the publication, or visit the DOI to the publisher's website.
- The final author version and the galley proof are versions of the publication after peer review.
- The final published version features the final layout of the paper including the volume, issue and page numbers.

[Link to publication](#)

General rights

Copyright and moral rights for the publications made accessible in the public portal are retained by the authors and/or other copyright owners and it is a condition of accessing publications that users recognise and abide by the legal requirements associated with these rights.

- Users may download and print one copy of any publication from the public portal for the purpose of private study or research.
- You may not further distribute the material or use it for any profit-making activity or commercial gain
- You may freely distribute the URL identifying the publication in the public portal.

If the publication is distributed under the terms of Article 25fa of the Dutch Copyright Act, indicated by the "Taverne" license above, please follow below link for the End User Agreement:

www.tue.nl/taverne

Take down policy

If you believe that this document breaches copyright please contact us at:

openaccess@tue.nl

providing details and we will investigate your claim.

Cartographic Modelling for Automated Map Generation

Andreas Reimer

Cartographic Modelling for Automated Map Generation

PROEFSCHRIFT

ter verkrijging van de graad van doctor aan de Technische Universiteit
Eindhoven, op gezag van de rector magnificus prof.dr.ir. F.P.T. Baaijens,
voor een commissie aangewezen door het College voor Promoties, in het
openbaar te verdedigen op maandag 1 juni 2015 om 16:00 uur

door

Andreas Wolfgang Reimer

geboren te Berlijn, Duitsland

Dit proefschrift is goedgekeurd door de promotoren en de samenstelling van de promotiecommissie is als volgt:

| | |
|--------------|--|
| voorzitter: | prof.dr. E.H.L. Aarts |
| promotor: | prof.dr. B. Speckmann |
| co-promotor: | dr. W.A. Mackaness (University of Edinburgh) |
| leden: | prof.dr. M.T. de Berg |
| | prof.dr. J. Dykes (City University London) |
| | prof.dr. M.J. Kraak (Universiteit Twente) |
| | prof.dr. J.J. van Wijk |
| | prof.dr. A. Zipf (Heidelberg University) |



UNIVERSITÄT
HEIDELBERG
ZUKUNFT
SEIT 1386



Part of the work in this thesis was funded by the German Research Foundation (DFG) in the GRK 1324.

Part of the work in this thesis was funded by Ordnance Survey Great Britain and remains crown copyright as indicated.

Part of the work in this thesis was funded by Heidelberg University.

Part of the work in this thesis was funded by the Federal Highway Research Institute bast.

Implementations used for experimental results made in Python using the Eclipse IDE. OpenMapSurfer TMS tiles generated with MapSurfer.NET. Geodata was handled and stored with PostGIS/PostgreSQL and QGIS. Figures were created in the Inkscape and IPE vector graphics editors. Typed on a Unicomp Model M.

© Andreas Reimer. All rights are reserved. Reproduction in whole or in part is prohibited without the written consent of the copyright owner.

Cover Design: Andreas Reimer
Printing: Eindhoven University Press

A catalogue record is available from the
Eindhoven University of Technology Library
ISBN: 978-90-386-3856-0

Dedicated to the memory of Marija Reimer, née Žunac.
Born: February 5, 1951, in Zrenjanin, Yugoslavia
Died: January 7, 1990, in West-Berlin

Contents

| | |
|---|------------|
| Acknowledgments | vii |
| 1 Introduction | 1 |
| 1.1 Automated map generation | 4 |
| 1.1.1 Generalisation as linchpin of automation | 5 |
| 1.1.2 Knowledge acquisition in generalisation research | 6 |
| 1.2 Contributions | 7 |
| 1.3 Definitions | 10 |
| 2 Labelling | 15 |
| 2.1 Introduction | 16 |
| 2.2 Multi-criteria model for point feature labelling | 18 |
| 2.2.1 Quality evaluation function | 19 |
| 2.2.2 Experimental results | 23 |
| 2.2.3 Conclusion | 26 |
| 2.3 Considering base map details | 26 |
| 2.3.1 Cartographic principles | 26 |
| 2.3.2 Measures of feature overprinting and type legibility | 27 |
| 2.3.3 Aggregated measure | 31 |
| 2.3.4 Computational complexity | 32 |
| 2.4 Labelling islands | 32 |
| 2.4.1 Cartographic guidelines | 34 |
| 2.4.2 Candidate position generation | 34 |
| 2.4.3 Position quality evaluation | 35 |
| 2.4.4 Modelling the labelling of groups of islands | 36 |
| 3 Schematisation in the Context of Cartographic Generalisation | 47 |
| 3.1 Generalisation research and schematisation | 47 |
| 3.1.1 A classification of schematised maps | 47 |
| 3.2 Defining schematisation | 50 |
| 3.2.1 What is cartographic schematisation? | 50 |
| 3.3 Governing the generalisation process in schematisation | 53 |

| | | |
|----------|---|------------|
| 3.4 | Schematisation operators | 57 |
| 3.4.1 | Forms of schematisation | 57 |
| 3.5 | Efficient derivation and caricature of urban settlement boundaries for 1:250k | 60 |
| 3.5.1 | Introduction and related work | 61 |
| 3.5.2 | Approach | 61 |
| 3.5.3 | Results | 67 |
| 3.5.4 | Summary and outlook | 70 |
| 4 | Chorematic Diagrams | 71 |
| 4.1 | Chorematic diagrams defined | 72 |
| 4.2 | Chorematic diagrams explained | 73 |
| 4.3 | Taxonomy | 79 |
| 4.3.1 | Descriptive analysis | 80 |
| 4.3.2 | Taxonomy | 83 |
| 4.4 | Graphical and geometric analysis | 86 |
| 4.4.1 | Across classes | 87 |
| 4.4.2 | Symmetric chorematic models | 97 |
| 4.4.3 | Asymmetric chorematic models | 99 |
| 4.4.4 | Synthetic chorematic models | 99 |
| 4.4.5 | Chorematic maps | 102 |
| 4.4.6 | Synthetic chorematic maps | 102 |
| 4.4.7 | Chorematic overlays | 103 |
| 4.5 | Validation of the taxonomy | 104 |
| 4.5.1 | Non-parametric tests | 108 |
| 4.6 | Methodology | 110 |
| 4.6.1 | Collection of base data | 111 |
| 4.6.2 | Analysis methods | 112 |
| 4.6.3 | Taxonomy validation methods | 117 |
| 5 | Modelling Chorematic Diagrams | 121 |
| 5.1 | Design principles | 121 |
| 5.1.1 | Overarching design goals | 122 |
| 5.1.2 | Composition | 129 |
| 5.1.3 | Thematic encoding | 132 |
| 5.1.4 | Shape | 136 |
| 5.1.5 | Chorematic design principles and cartographic merit | 138 |
| 5.2 | Modelling for automation | 142 |
| 5.2.1 | Necessary input | 142 |
| 5.2.2 | Task definition | 142 |
| 5.3 | Chorematic constraint modelling | 145 |
| 5.3.1 | General guidelines | 146 |
| 5.3.2 | Composition constraints | 148 |
| 5.3.3 | Encoding constraints | 149 |
| 5.3.4 | Shape constraints | 153 |

| | | |
|----------|--|------------|
| 5.4 | Procedural model | 157 |
| 5.5 | Exemplary validation | 158 |
| 5.5.1 | Parallelism in chorematic diagrams | 159 |
| 5.5.2 | Curved subdivisions for chorematic diagrams | 174 |
| 6 | Stenomaps | 183 |
| 6.1 | Design choices | 186 |
| 6.2 | Technical preliminaries | 187 |
| 6.3 | Algorithm | 188 |
| 6.3.1 | Feature points | 189 |
| 6.3.2 | Regions | 190 |
| 6.3.3 | Backbone | 192 |
| 6.3.4 | Glyphs | 193 |
| 6.4 | Glyph types | 193 |
| 6.4.1 | Simple | 193 |
| 6.4.2 | Locally intersecting | 194 |
| 6.4.3 | Tree-based | 195 |
| 6.5 | Cartographic applications | 195 |
| 6.5.1 | Stenomaps as thematic maps | 196 |
| 6.5.2 | Use case: variations on glyphs as cartographic lines | 198 |
| 6.5.3 | Use case: spatial uncertainty | 200 |
| 6.5.4 | Use case: cross-boundary phenomena | 202 |
| 6.6 | Discussion and future work | 203 |
| 7 | Conclusion | 207 |
| 7.1 | Main findings | 207 |
| 7.2 | Looking forward | 208 |
| | Bibliography | 211 |
| | Summary | 233 |
| | Curriculum Vitae | 235 |

Acknowledgments

If one pictures research results as a rough, unhewn stone, then a thesis is the result of careful smoothing of said stone to make it fit into the ever-growing building of science. It is only logical, that there is generally no great interest in the person who wielded the hammer and even less interest in the parts that had to be removed. But some people did care and were interested, and thus deserve my sincerest thanks. Without false modesty, I think I have earned the right to claim my research as well as my life have encountered above-average external adversity. It directly follows that the support, inspiration and help I did receive, are all the more precious to me.

First of all, I would like to thank my supervisor Bettina Speckmann and my co-supervisor William Mackaness for their encouragement, feedback and passion for maps. I met Bettina at the GIScience conference in 2010 during the workshop "Geometric Algorithms and Efficiency for GIScience". It wasn't long after that, that I could visit Eindhoven (not for the last time, thankfully) and learn so much about research and scientific writing during our early collaborations. During all the time we worked together, she has been a model of an advisor: fiercely loyal, receptive to ideas and a savant in scientific questions both big and small. I am very thankful, that, when things got rough academically, she was there and showing a way out. I met William at a Dagstuhl seminar, and I was quite surprised to see him walking towards me with one of my early papers in his hands. His passion for my research topic has inspired me greatly. I am especially thankful for educating me on how critical thinking and a quick-wit can talk sense to the stuffy old lady that cartography research sometimes is. During my visit to Edinburgh, he spent much time in order to educate me on how to structure a scientific narrative for the first version of my thesis. I hope William and I will continue to collaborate and keep rattling the cage of topographic map generation for some time to come.

The GIScience group at the University of Heidelberg has been a great working environment. My first thanks here go to Alexander Zipf, who provided me with the chance to become part of this highly dynamic group. I was not only readily accepted in the group, but my skills and contributions were valued and put to use immediately. I further want to thank Oliver Roick, Michael Auer, Jo Lauer, Christopher Barron, Pascal Neis, Lukas Loos, Enrico Steiger and Timothy Ellersiek for bringing me up to speed with OpenStreetMap and for generally providing a helpful office atmosphere. Special thanks go to René Westerholt for many research discussions and much appreciated grading help. My admir-

ation and sincere thanks go to Maxim Rylov, it is always a pleasure to work with him. His open ear, dedication to high quality mapping and interest in *doing it properly* along with his skills make him stand out as a researcher. Thanks also go to the student assistants Christian Kempf, Sarah Lohr and Susanne Heuser.

Many thanks also go to Herman Haverkort, Anne Driemel, Kevin Verbeek, Dirk Gerits, Chris Volk and Quirijn Bouts as members of the Algorithms Group in Eindhoven. I always felt sincerely welcome and we had a lot of fun discussions that often unexpectedly detoured into philosophy or research results. Special thanks go to Arthur van Goethem and Wouter Meulemans, both impressively skilled researchers that taught me so much computational geometry. I am honoured to call them co-authors as well as friends.

A knowing nod goes to my former colleagues Sören Haubrock, Falko Theisselmann, Joachim Fohringer, Anastasia Galkin, Mathias Schroeder and Kathrin Poser. Without them, it would have been much worse.

Next I would like to thank my collaborators from other institutes, namely Jo Wood, Guillaume Touya, Maxwell Roberts and Marc van Kreveld.

Thanks go, of course, also to the members of my graduation committee, Mark de Berg, Jason Dykes, Menno-Jan Kraak, Jack van Wijk and Alexander Zipf, for perusing my thesis and providing valuable feedback and suggestions. Special thanks go to Jason Dykes for being supportive of my work at an early stage, helping me go to my first Dagstuhl Seminar.

I am also indebted to Peter Tainz and Wolfram Pobanz from the FU Berlin. It was P. Tainz who introduced me to chorematic diagrams. Wolfram Pobanz handed me down many maps and Atlases that are regularly being used for my research and teaching. Wolf-Dieter Rase deserves thanks for pointing me towards Bunge and sending me a parcel with hard-to-get literature.

On a more personal note, I wish to thank the librarians of the Stadtteilbibliothek Heerstraße for guarding a spot for curious children.¹ I was one of them. Special thanks also to Hans-Jürgen Schroeder-Fürst and his brothers for guarding a spot equally important. Personal thanks also go to my aunts Annemarie and Uschi as well as my uncle Bob for help across the Atlantic. I also wish to express my gratefulness to my aunt Katica, who found me via the Red Cross. Further thanks go to Ulrike Gruhl and Yvonne Landes for helping with the kids while I was away on conferences.

My undying love and gratefulness are reserved for my wife Ulrike. Any hardship, any task that is thrown our way is answered by her pragmatically, smartly and, above all, with humour and grace. Our children, Paul, Johannes, Annemarie and Viktoria, are to be thanked for generally being awesome. Experience has shown, that being a father and at the same time pursuing scientific research is a bit like having a secret identity at night. Neither realm takes the demands of the other serious. Ulrike bridged that gap the last years with an amount of tenacity, wisdom and faith that humbles me deeply. She is the best companion any aspiring Doctor could hope for.

¹http://commons.wikimedia.org/wiki/File:Stadtteilbibliothek_Heerstra%C3%9Fe.JPG

Chapter 1

Introduction

Somewhen in the second century A.D. the Greek polymath Claudius Ptolemy sat down at the Library of Alexandria to write the *Geographia*. In addition to being an ordered set of instructions describing the known ancient world in lists of coordinates it was accompanied by copious amounts of maps. For those maps he could draw upon the long line of tradition of spatial charting that started in the deep well of history with its murky beginnings in the Upper Palaeolithic. Perpetuated by the scribes of Byzantium, Ptolemy's work remained unsurpassed for 1,400 years. Upon its rediscovery by the Latin world, the *Geographia* helped to usher in the Renaissance of scientific cartography after its long dark slumber through the middle ages. The Dark Ages had brought the downfall of the monetary system and with it a wide-ranging destruction of urban culture and division of labour. Until the Age of Discovery, the peculiar skill-sets of geometers, surveyors and cartographers did not provide anyone with a living any more, consequently they were forgotten and medieval maps show that.¹

It would be comforting to mentally confine such forced forgetfulness to history, but the story of map production of the last decades is paradoxical: The means of production are becoming ever cheaper, the data much more encompassing and easier to collect. New data-handling techniques and algorithms now allow one person to do in weeks what took the cartographers of yore their lifetimes. The demand for maps is increasing at a greater rate than the means of accessing them. The maps produced, though, have been of lower quality than what was deemed to be acceptable forty years ago. Whereas the currently produced maps arguably serve the purposes of the large majority of use-cases, the great technical advances have narrowed the uses-cases for which it is economically feasible to produce maps for. The demand for timely communication of spatial phenomena of all kinds is increasing as society becomes ever more complex and refined. This effect is multiplied by a growing population, so that there is increased demand for making the production of specialised maps economically more feasible. In this day and age, only automatically produced maps can be thought of as worth their cost. In order to automate

¹cf. Harley and Woodward 1987 [130]

map generation, a sound body of formalised design principles is needed for each type of map. Showing ways to derive and model such design principles is the subject of this thesis.

Let us illustrate some of the statements above. We start with an example of why we need automated thematic mapping at all. Among the many endeavours where maps play a functional role are time-critical activities such as disaster response. A study conducted at the German Research Centre for Geosciences (GFZ) leading up to a comprehensive workflow adaptation model [101] revealed that in order to make a decision on whether a team of seismologists should quickly travel to the site of a given earthquake, many different maps are used. The internal documentation of that study ² include the following geographical information being used in the form of (or transformed into) maps:

- **epicentre**
- **aftershock**
- historical earthquakes
- earthquake zones
- **tactical pilot charts**
- GPS stations
- **topographic maps (roads, hydrology, orography)**
- tectonics
- great fault lines, recent and historic
- volcanoes, recent and historic
- thermal springs
- potable water
- groundwater level
- soils
- land use/land cover
- land development
- climate and weather
- population
- other statistical data on the population
- bridges (load class and make)
- gas and energy networks

The bold entries are those that can be thought of as currently being generated automatically. In other words, even this very specific example would benefit greatly from having many more thematic map types available faster and, if automatically generated, on-demand for arbitrary regions.

To provide some exemplary corroboration to the claim that many specialised (thematic) maps are currently of a lower quality and thus of lower usefulness compared to 40 years ago, we invite the reader to inspect Fig. 1.1. We chose examples aiming for a fair

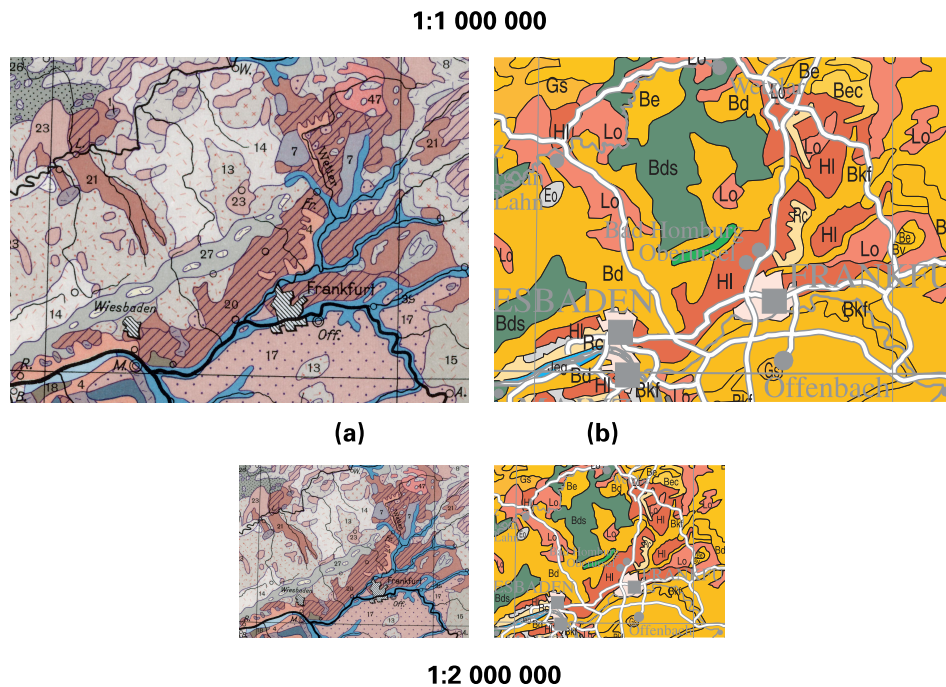


Figure 1.1 Comparison of soil maps, cut outs are from the same area around Frankfurt am Main. (a) Soil map for the Federal Republic of Germany, 1:1000000, 1963 [57] (b) Soil map for Germany and Switzerland, 1:2000000, 2005 [100, Plate 7].

comparison: both are prepared by official government agencies for basically the same purpose and on the very same subject.

Fig. 1.1a was manually generalised and drafted from larger scale soil maps. As can be seen, the subdivision is drawn with gentle curves. An elaborate colour and hachure regime is effectively applied to provide detailed and shape-preserving soil information. The topographical situation is depicted by a black-ink, generalised hydrographic network and large urban areas are elevated by a drop-shadowed black-white hachure. The 2005 map (Fig. 1.1b) is automatically generated from the EUROSTAT GISCO database. The subdivision uses polylines and is decidedly not gently flowing, adding micro-vibrations that are uneasy on the eye. The colours are much brighter and not well-coordinated, not following any harmony, and no hachures or textures are employed. The labelling is both more invasive (abbreviations) and harder to read (grey sans-serifs font for populated places). Additional visual complexity is added by a badly generalised road network drawn with a bordered line. Built up areas and soil polygons are visually not well separated. The river

²courtesy of Dirk Fahland, Timo Glässer, Falko Theisselmann and Heiko Woith.

network is also less generalised and, against extant cartographic convention, drawn with a rasterised grey instead of a fully saturated hue. Note that a similar Atlas was published in 2014 for Latin America with the very same techniques. Nine years have brought no improvement whatsoever, save for the addition of white halos around placenames as brute force *Schriftfreistellung*. We can see that the 1963 cartographer applied many techniques that are not currently employed by the automatically generated sample. We think it is safe to say that the usefulness of the 1963 map is all around higher even when photographically reduced to 1:2000000, that being the alleged optimal viewing scale for the 2005 map.

1.1 Automated map generation

Generating readily usable maps automatically with a minimum of human intervention has been a goal in several areas, driven by distinct groups of people. Two of the most prominent of these areas and groups are (1) large-scale topographic map generalisation driven by cartographic engineers in the interest of National Mapping Agencies (NMAs) and (2) tile-based web-maps mainly for land navigation purposes mirroring pre-digital road maps created by software engineers (for example, Google maps or OpenStreetMap). In addition, computer scientists, most notably from the area of computational geometry, have studied and solved a diverse collection of specific algorithmic problems from the area of automated cartography.

The problems considered so far centred on the areas of metro-map schematisation, automated label placement and some isolated thematic mapping techniques [299]. We argue that in all cases, the usefulness of the output for actual map generation is not only a function of the technical or algorithmic sophistication of the solution, but also critically depends on the degree of insight into the governing cartographic design principles. Viewed as such, proper cartographic modelling is a necessary albeit not sufficient prerequisite for meaningful and high-quality automated map generation. In the case of the popular algorithmic problem of label-placement, for example, many design rules are known in principle, but they are not formalized to a sufficient degree to find their way into the algorithmic design process. Furthermore, the cartographic knowledge concerning the great variety of specialized (thematic) maps has, for the most part, not been formalized at all, beyond textual descriptions and examples.

Consequently, the gap between technical and algorithmic sophistication on the one hand and insight into design specifications on the other hand has widened. This is particularly true for the area of non-topographic and non-navigational maps, that is, thematic maps. Thematic maps are currently created in the graphical no-man's-land of desktop GIS, which occupy the area between proper industry-scale automation and sophisticated manual authoring support. One result is the unrepentant proliferation of semi-automated choropleth and pie chart maps and in turn the neglect of the great expanse of thematic mapping techniques common till the early '80s.

1.1.1 Generalisation as linchpin of automation

Essentially, a map can be thought of as a graphical model³ of the surface of the earth and selected phenomena. With this interpretation, automated map generation is essentially a model transformation: from a geometric model of the earth's surface to a graphical model. The field that has the most experience with such geographic model transformations is called cartographic generalisation. As we will discuss in broader detail later (Chapter 3), every map has some purpose or intent. For topographical maps, the scale of the map equals its intent. And it is exactly here, in the model transformation from one scale into another scale, where cartographic generalisation approaches are most effective.

The excluded middle. With all the advances of the last decades, it is surprising that even for topographic mapping only a rather narrow band of scales has been fully understood. In automated generalisation, large-scale maps in the $50 - 100k$ range have been the focus of attention and can be produced fully automatically. On the other end of the extreme, mainly advanced by computational geometers, C-restricted schematic maps inspired by the London tube map saw the greatest attention. This leaves a rather large excluded middle, displayed in grey in Fig. 1.2a (also cf. Fig. 3.3). Our depiction characterises the missing knowledge as being much too expansive as to be surmounted in a single dissertation project. This motivates our strategy of investigating maps and schematisations at the edges of what is known, so as to move slowly inward by investigating chorematic diagrams and medium-scale maps (Fig. 1.2b). Note that our work on labelling (Chapter 2) is concerned with deficiencies in extant automated labelling that appear specifically in medium and small scale mapping. It is also clear that our approach presupposes that generalisation and schematisation are intimately linked, although they have been pursued in some isolation until recently (cf. Chapter 3).

³For this thesis, we stay confined to the Bertinian preliminaries of graphics in the sense of his semiology; that is barring 3D representations, interactivity, change of lighting and viewing distance and so forth.

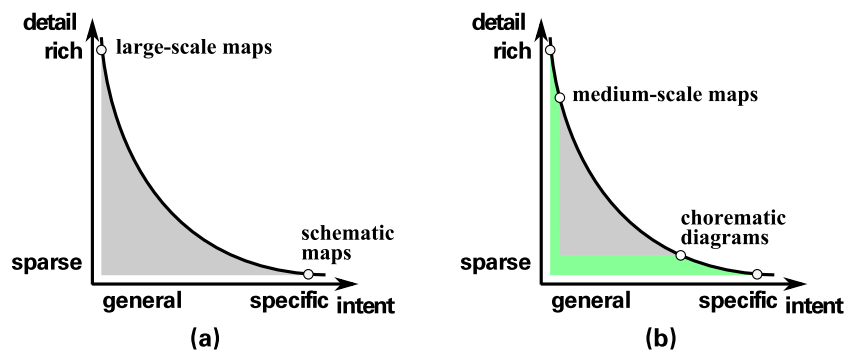


Figure 1.2 (a) The excluded middle of operationalised map knowledge in grey.
(b) Scope of this thesis in green.

1.1.2 Knowledge acquisition in generalisation research

This section provides a brief overview of the current state of knowledge acquisition in generalisation research. The aim is not for a complete reproduction of historical developments but rather to later motivate and contextualise the methodological choices. Various overview articles (most notably [60, 176, 244, 305]) have been written concerning generalisation research to which we direct the reader if more detail is needed.

While formalisation of tacit and practical knowledge is a core activity of many academic endeavours, the term of knowledge acquisition in the narrow sense is closely linked to the rise of digital data manipulation in several fields. This holds for academic cartography too: even without access to (then) state of the art computing machinery, the subtexts of Töpfer's and Pillewizer's seminal works [281, 282, 283] are about mathematical formalisation for reproducibility using machines. Automated map production was the obvious goal for generalisation research, but automation ideas were present in nearly all subfields of academic cartography by the '60s the latest [209].

Generalisation research. The problem of collecting and formalising extant knowledge about map generalisation was identified as the major task for academic generalisation research in the late '80s, resulting in the publication of the book 'Map generalization: Making rules for knowledge representation' [62, preface]. It included both the thinking of its time in the form of a predisposition upon expert-systems, as well as the seed from which full automation would blossom: constraint-based knowledge representation [23]. The predominance of rule based approaches was a technological hindrance and the successes of expert systems in non-spatial fields like business process planning could not be repeated. But the rule based approaches made it abundantly clear that any system will only be as effective as the knowledge that informs it. For cartography and other fields, it was recognised that the necessary theoretical and procedural knowledge was not acquired fast and reliably enough, no matter which technological frameworks was to later use it. This became known as the Knowledge Acquisition Bottleneck in Map Generalization [305, 306].

Four basic strategies for knowledge acquisition were identified and grouped by the sources they use, namely Human Experts, Text Documents, Maps or Traced Processes [306]. A slightly different and expanded version was presented in [305], that added machine-learning and neural networks as potential additional methods and re-framed the Human Experts strategy by calling its corresponding strategy 'conventional knowledge engineering'. All these acquisition techniques had a noticeable topographic mapping subtext, both in their description as well as their implementation. The most detailed investigation into modelled cartographic knowledge naturally had national mapping agencies (NMAs) and their products and processes as subject: the EuroSDR 'generalisation project' [268].

Recent developments. The strong emphasis on the needs of topographic maps continues today [182]. Recently, two NMAs successfully amalgamated research technological developments and the acquired knowledge in order to fully automatise production of large-scale topographic maps [234, 269]. With these successes in sight or partially achieved,

NMAs and researchers have begun to shift attention towards modelling user requirements and matching ontologies for on-demand maps [15, 106, 122]. These efforts only implicitly address issues of thematic generalisation. As such, they do not broaden the base of knowledge on *existing* thematic or schematised maps. Rather, assuming user requests can be mapped to certain information needs, on-demand mapping as an idea presupposes that appropriate (thematic) mapping techniques are available.

1.2 Contributions

In this thesis we present our efforts to further automated map generation by analysing and modelling design principles from automated label placement, schematisation (with a special focus on chorematic diagrams), and small-scale map generalisation. One of the approaches this work pursues to structure the diversity within schematisations is dissection & classification. Naturally, differentiations can only be as clear as the underlying definitions. These are presented in Section 1.3.

Beyond the contributions included in this thesis, I (co)-authored articles on bivariate colour maps [224], 4D-cartography [233], scale in volunteered geographic information datasets [229, 285], curved schematisation [232, 292], pairwise Line Labelling [241] and on disaster mapping [228].

Automated map labelling. In the second chapter of the thesis, we investigate the state of automated map labelling. We show that automated label placement algorithms can, if informed by a soundly designed model, be used to solve placement problems automatically to a degree that was formerly only attainable by human cartographers. Our approach

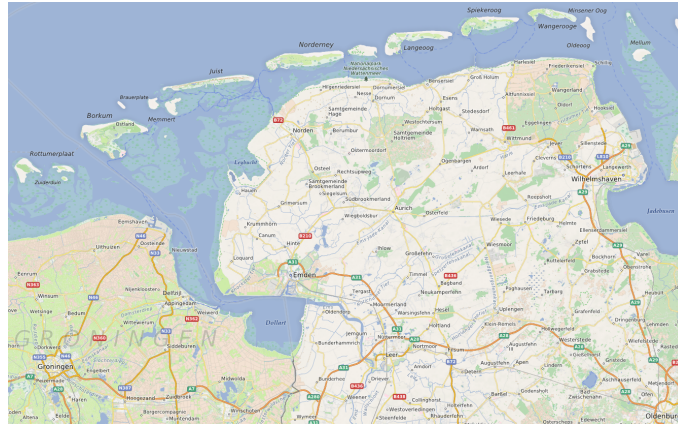


Figure 1.3 OSM Roads layer in OpenMapSurfer of the Frisian Islands (zoom level 10, depicted at $\approx 1 : 750000$) and environs labelled fully automatically by our algorithm. Map data: ©OpenStreetMap contributors.

for the first time considers disambiguation between labels and base map detail alongside some more specialized techniques, such as island labelling (Fig. 1.3). The results compare favourably to commercial solutions even for industrial scale data sets generated from OpenStreetMap data.⁴

This chapter is based on joint work with Maxim Rylov. This work is composed from journal articles published in *Geoinformatica* [239], *Cartographica* [238], and the *Cartographic Journal* [240]. Section 2.4 includes joint work with Arthur van Goethem, Maxim Rylov, Marc van Kreveld and Bettina Speckmann and has been accepted for publication in *CaGIS* [230].

Schematisation and generalisation. Chapter 3 provides a contextualizing overview of schematisation interpreted as a subfield of map generalisation. We argue that the governing metric for schematisation must be map complexity instead of target map scale. We introduce *cartographic line frequency* as a robust measure for said complexity. Furthermore, we give a comprehensive taxonomy of schematisation operators and contrast it with the well-known generalisation operators. Using this taxonomy, we show that especially polygonal caricature and curved stylisation have seen little algorithmic developments so

⁴For an interactive side-by-side comparison, please peruse <http://mc.bbbike.org/mc/?lon=6.982443&lat=53.487614&zoom=9&num=4&mt0=mapnik&mt1=google-map&mt2=bing-map&mt3=osm-roads>

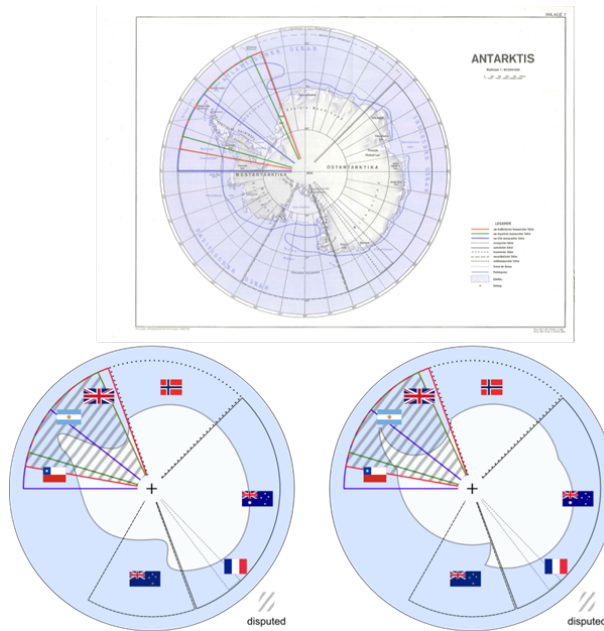


Figure 1.4 Curved schematisations using Bézier curves and circular arcs [292].

far (see Fig. 1.4 for one of the few exceptions). We then describe how schematisation and generalisation combine to generate caricatured angle-restricted polygons for real-world medium-scale maps.

This chapter is partially based on joint work with William Mackaness. Parts of this work have been published in a chapter for the 2014 book of the ICA Commission on Generalisation & Multiple Representation [182], Section 3.5 was published in the proceedings of the 17th Workshop of the same commission and is joint work with Christian Kempf [225].

Modelling chorematic diagrams. Chapters 4 and 5 represent a comprehensive investigation of chorematic diagrams (examples are Fig. 1.5 and Fig. 1.7). Chorematic diagrams are a fascinating type of thematic maps that represent the largest corpus of schematisations produced under a single unifying graphical idea. They are intriguing both because of their known effectiveness as well as the supposed impossibility of modelling their design rules in a formal way. We describe the first comprehensive cartographic model for chorematic diagrams using qualitative as well as quantitative and empirical methods.

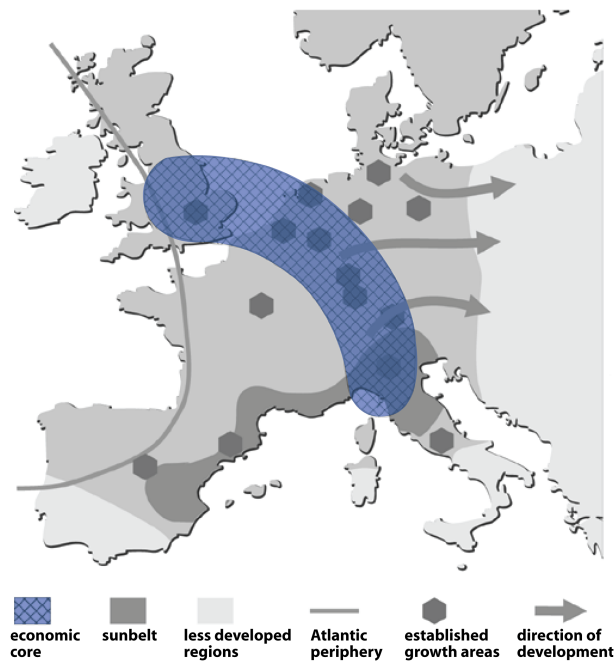


Figure 1.5 *Rahmenkarte*: The Blue Banana, highlighting the main axis of economic and societal development in the EU, and the fact that Paris is in danger of being excluded. This rendition is translated and coloured from: [31].

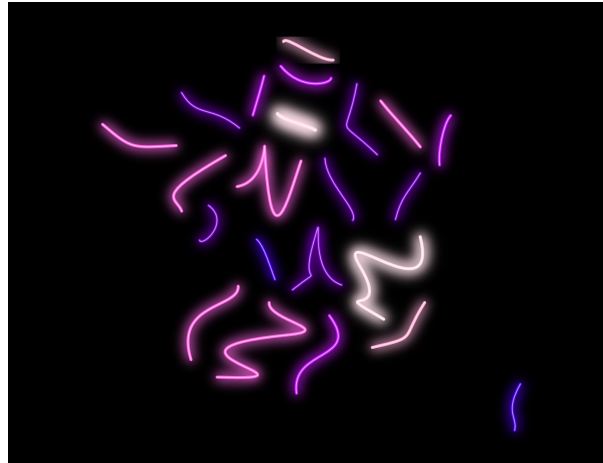


Figure 1.6 Stenomaps depicting the energy consumption in France in 2010.

Chapter 4 is an expansion of the journal Article [223]. Parts of that chapter were submitted as joint work with William Mackaness [226]. Section 5.5.1 is based on joint work with Wouter Meulemans and was published in the Proceedings of the 14th Workshop of the ICA Commission on Generalisation & Multiple Representation [227]. Section 5.5.2 is based on joint work with Chris Volk and was published in the Proceedings of the 15th Workshop of the ICA Commission on Generalisation & Multiple Representation [231].

Stenomaps. Chapter 6 presents Stenomaps: the first area-to-curve collapse technique (Fig. 1.6). Stenomaps fill a gap in the schematisation taxonomy. The Chapter also shows exemplary how cartographic modelling is not bound to emulate existing techniques but can be applied to planfully widen the cartographic design space. This chapter is based on joint work with Arthur van Goethem, Wouter Meulemans and Bettina Speckmann. This work was published in the IEEE Transactions on Visualisation and Computer Graphics [294].

1.3 Definitions

For historical, cultural and linguistic reasons, German academic cartography has produced elaborate collections of definitions of cartographic terms. Examples are three cartographic dictionaries [32, 208, 310] and the two Multilingual dictionaries of technical terms in Cartography that use German terms as baseline [195, 203]. We provide the most essential translations as definitions. Also provided are definitions created or selected among others for convenience by the author. When no English shorthand is available, we will use the German word as terminus technicus in *italicised* form.

Map. A *map* is the ground plot of a planet or its parts including the concrete and abstract phenomena within the depicted space; it further is:

- scale reduced
- generalised
- symbol-encoded
- textually annotated
- horizontally projected

This definition is an elaboration of IMHOF's definition as developed by Wolfgang Scharfe in 1995 at the Free University Berlin.

Map-like Diagram. A map-like diagram is a diagram that conforms to most, but not all, of the characteristics that define a map following Scharfe 1995. They include side views, panoramas or *stumme Karten* (see below). In the following text, we will often omit *map-like* when it is clear from the context that *diagram* refers to map-like diagrams.

Regular Map. A regular or conventional map (from ger. *Karte im engeren Sinne*; lit. 'map in the strict sense') is:

A map constructed from precise measurements, in which the outlines of features are shown as accurately as possible within the limitations of scale [195, §811.1] .

Thematic Map. A thematic map is

A map designed to demonstrate particular [geographic] features or concepts.
In conventional use this term excludes Topographic Maps.

modified from [195, §811.7], parenthesised term added by author.

Topographic Map. A topographic map is:

A map whose principal purpose is to portray and identify the features of the Earth's surface as faithfully as possible within the limitations imposed by scale.

Schematised Map. A schematised map is:

A map representing features in a much simplified or diagrammatic form.

adapted from [195, §811.4], the entry there is for schematic maps. In the last decade, 'schematic map' has come to be used for a much narrower subset, i. e. metro maps. A more thorough discussion of schematised maps, schematic maps and their definition, as well as the relation between generalisation and schematisation, will be presented in Chapter 3.

Chorematic Diagram.

All those maps and map-like diagrams, which have explicitly been created according to the chorematic principles laid down by French geographer Roger Brunet, especially those created by members and associates of the GIP-RECLUS institution (changed from [223]).

Naturally, a detailed discussion, definition and characterisation of chorematic diagrams will run through Chapters 4 and 5.

Generalisation. Generalisation is the:

Selection and simplified representation of detail appropriate to the scale and/or the purpose of a map.

[195, §51.8]. As lemma concerning the underlying goal of generalisation in the wider context of all geosciences we present:

Generalization should be seen as a process allowing [...] to perform a change in the perception level of geographic data. Precision and geometry changes are no more than consequences of this process [237, p. 74].

Stumme Karte. A *Stumme Karte* (literally: silent map) is (Fig. 1.5):

A map without names or descriptive lettering on its face [195, §811.7].

Inselkarte. An *Inselkarte* (lit. "island map") is (Fig. 1.7)

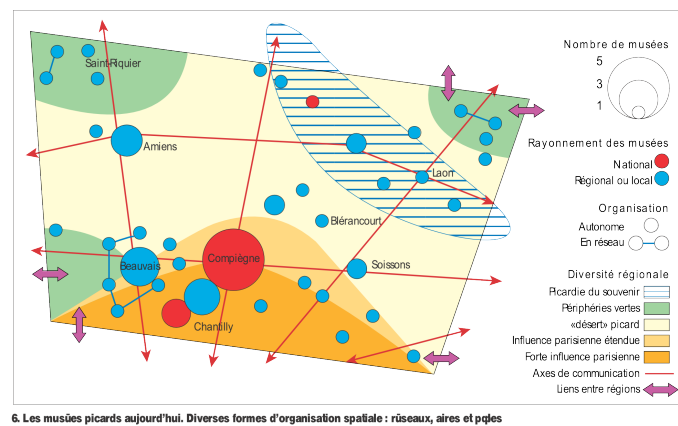


Figure 1.7 *Inselkarte*: Museums in Picardie. This is one of only two examples of chorematic diagrams that show quantitative information [139].

A map on which only a selected area is mapped in full; or a map on which detail does not extend over the whole of the Map Face [195, §818.1].

Rahmenkarte. A *Rahmenkarte* (lit. "frame map") is (Fig. 1.5):

A map on which the detail extends over the whole area enclosed by the Neat Line or to a Bleeding Edge [195, §818.2].

Schriftfreistellung. *Schriftfreistellung* is defined as:

The clearing of detail relevant to the positioning of Lettering [195, §652.9].

This process of clearing detail for crossing/intersecting elements of the same colour by partial omissions and interruptions can also be applied to line symbols instead of lettering. One can then generally talk about *Freistellung*. Halos around type and edge casing are the most simple techniques of clearing detail when more advanced methods are not available.

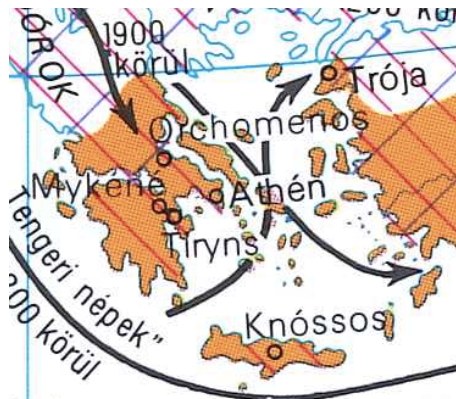


Figure 1.8 *Schriftfreistellung*: Clearing of detail to enhance visibility of crossing arrows, and labels in a map on ancient Greece. Note how simplistic halos and line casings would be unable to replicate the effect: [1].

Chapter 2

Labelling

Textual annotation is one of the defining features of maps (see Section 1.3). The whole process and especially the placement of labels is very laborious if conducted manually. Therefore, automated map labelling is one of the major components of automated map generation. Scientifically, automated label placement problems play an important and critical role in several disciplines such as cartography [200, 320], geographic information systems [109], and graph drawing [22, 159]. While industrial-scale solutions for automated map labelling exist, they produce rather crude results that work mostly for large scale road annotation and sparse point feature labelling. Industrial solutions use the degrees of freedom gained by only allowing low toponym densities. Many known guidelines used in manual placement that enhance the functionality of a map and allow high toponym densities remained desiderata (exemplified in Fig. 2.1). In this chapter we provide an overview of our recent advances in modelling and implementing many of the missing rules. In Section 2.2 we introduce a comprehensive multi criteria model that covers more cartographic placement rules than other existing solutions. We show the practical applicability by implementation and experiment. The following Section 2.3 introduces a more powerful modelling of the consideration of basemap detail using a raster approach. In Section 2.4 we address the problem of automated labelling of area features such as islands on small and medium scales. We prepared and published a web map that is based on the global dataset provided by the OpenStreetMap project. It is available online on the OpenMapSurfer web page (OSM Roads layer).¹ The name placement on small scales (zoom levels 2 – 12) is done using the multi-criteria model presented here. In lieu of the detailed comparisons with existing labelling engines which are available in the original papers [238, 239, 240], we point the readers to the OpenMapSurfer webpage to investigate how the solutions work in practice.

While the extant written guidelines on label placement were sufficient to inform the above problems, for *groups* of islands nearly everything remained tacit knowledge until now. Subsection 2.4.4 details our approach for modelling the placement guidelines

¹openmapsurfer.uni-hd.de

themselves from existing maps. The main idea here is to compare the results of manual labelling from atlases with placements that analytically optimise certain distance measures.



Figure 2.1 (a) Map of Sicily with automated label placement from GoogleMaps. ©2013 Google. (b) Map of Sicily with manual labelling. Source: Encyclopaedia Britannica World Atlas ©RM Acquisition, LLC d/b/a Rand McNally. Reproduced with permission, License No. R.L. 14-S-002.

2.1 Introduction

Over the last four decades many attempts have been made to automate the process of map labelling; see the bibliography of papers on this topic maintained by [314]. The main reason is to reduce the cost of manual label placement. The cartographic lettering problem comprises [149]:

- (1) toponym considerations (for example exonyms vs. endonyms, multilingual labelling and gazetteers)
- (2) toponym selection in respect to task
- (3) typeface (e.g. font choice, font form (spacing, colouring, italics etc.), font size, font color)
- (4) geometric placement of labels.

Automated label placement research has concentrated on the geometric placement and assumes the preceding problems have been solved, becoming input parameters. A general function to measure the geometric quality of label placement was proposed by [288], but neither implemented nor experimentally evaluated.

Geometric label placement. Being one of the more difficult and complex problems of the disciplines mentioned at the start of the chapter, the label placement problem is generally split up into smaller and simpler independent sub-problems (or subtasks). These subtasks are (see Fig. 2.2):

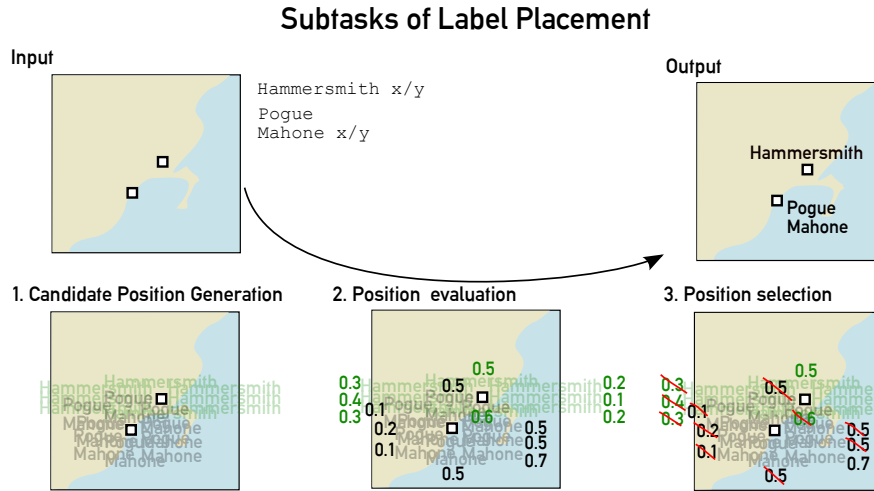


Figure 2.2 Subtasks of Label Placement.

- (1) Candidate position generation
- (2) Position evaluation
- (3) Position selection

The first subtask (Candidate position generation) consists of generating a set of label candidates for each map feature by taking into account its type (point, line and polygon), shape, as well as well-defined cartographic principles [149, 316]. There are various research works which devised different solutions to tackle this subtask. Point-feature label placement (PFLP) is the problem of assigning text to point features objects (settlements, mountain peaks, points of interest, etc.). The PFLP is known to be an NP-hard problem [108, 160, 188]. For point-like objects two different labelling models are differentiated, namely, fixed position [140, 320] and sliding label models [164, 270, 295]. The task of tagging linear features (for example roads, rivers or boundaries) requires special and more sophisticated methods of generating potential positions. The research for labelling these feature types was conducted by Barrault and Lecordix [18], Edmondson et al. [97], Chirié [68] and Wolff et al. [313]. Areal features are usually labelled first due to lesser placement flexibility. This issue is the most challenging due to the possible complexity of shapes. Nevertheless, some practical solutions for placing names inside polygons were suggested by Carstensen [64], van Roessel [296], Pinto and Freeman [215], Barrault [17] and Dörschlag et al. [86].

The second subtask (Position evaluation) is the process of evaluating the quality of possible positions by measuring how well a label is positioned with respect to the feature it tags and to the rest of the map content [141, 288]. Manifold metrics of evaluating quality of candidate positions for different feature types can be found in the works of

Barrault and Lecordix [18], Edmondson [97], Chirié [68], Barrault [17] and Rylov and Reimer [238, 239, 240, 241].

The third subtask (Position selection) lies in addressing the primary goal of label placement which is to preserve clarity and legibility of names. The positions must be selected as to balance the well-known cartographic precepts of good lettering on the one hand and on the other hand to maximise the number of labels. This subtask is considered as an optimisation problem. Therefore, several compelling strategies to find a feasible near-optimal labelling were proposed in previous research. In particular, these strategies and techniques are: the greedy best-first search algorithm [320], a discrete gradient-descent method [140], exhaustive search algorithms [5, 72, 84, 110, 157], 0-1 integer programming [323], simulated annealing [69, 324], a depth-first search [69], a genetic algorithm [300], an ant colony system [249], tabu search algorithm [319], and POPMUSIC partial optimisation meta-heuristic [6, 273].

2.2 Multi-criteria model for point feature labelling

The currently implemented, fully automated solutions are limiting computer generated maps in their expressive power. In this section, we present a comprehensive multi-criteria model that complies with almost all well defined cartographic placement principles and requirements for Point Feature Label Placement (PFLP). This allows for a significant increase in toponym density without effecting legibility. The proposed model expressed as a quality evaluation function can be employed by any mathematical optimisation algorithm for solving the automated label placement problem. An application of the proposed model was tested on volunteered geographic information data and sample parameter settings were devised. The results illustrate that a high level of cartographic quality for PFLP can be achieved through the integrated approach. The resulting quality is comparable to the lettering produced by an expert cartographer.

The extant guidelines [36, 149, 316] that refer to labelling of point features can be divided into two categories: rules and constraints.² The list of rules adapted to the requirements of our purposes is as follows:

- R1 Type arrangement should reflect the classification, importance and hierarchy of objects.
- R2 Labels should be placed horizontally.
- R3 The lettering to the right and slightly above the symbol is prioritized.
- R4 Names of coastal settlements should be written in water.
- R5 Labels should be placed completely on the land or completely on the water surface.
- R6 Names should not be too close to each other.
- R7 Labels should not be excessively clustered nor evenly spread out.
- R8 Each label should be easily identified with its point feature. Ambiguous relationships between symbols and their names must be avoided.

²Note that the usage of the terms *rule* and *constraint* is slightly different in label placement compared to cartographic generalisation.

R9 Labels should not overlap other significant features of the cartographic background or do this as little as possible.

The constraints are:

C1 Names must not overlap point feature symbols.

C2 Two names must not overlap each other.

C3 Two point feature symbols must not have any overlap.

| Research Article | PFLP Requirements and Constraints Applied in Research Article | | | | | | | | | | | |
|--|---|----|----|----|----|----|----|----|----|----|----|----|
| | R1 | R2 | R3 | R4 | R5 | R6 | R7 | R8 | R9 | C1 | C2 | C3 |
| Yoeli (1972) | X | X | X | | | | | | | X | X | X |
| Hirsch (1982) | X | X | X | | | | | | X | X | X | X |
| Zoraster (1986) | | X | X | | | | | | | X | X | X |
| Doerschler and Freeman (1992) | X | X | X | | | | | | X | X | X | X |
| Edmondson and others (1997) | X | X | X | | | | | | X | X | X | X |
| Strijk and van Kreveland (1999) | X | X | | | | | | | X | X | X | X |
| Huffman and Cromley (2002) | X | X | X | | | | | | | X | X | X |
| Ebner, Klau, and Weiskircher (2003) | | X | X | | | X | X | | | | | |
| van Dijk, Thierens, and de Berg (2004) | | X | | | | | | | | X | X | X |
| Stadler, Steiner, and Beiglbock (2006) | X | X | | | | X | | | X | X | X | X |
| Mote (2007) | X | X | X | | | | | | | X | X | X |
| Luboschik, Schumann, and Cords (2008) | X | X | X | | | | | | X | X | X | X |
| Bae and others (2011) | | X | X | | | | | | | | | |
| Gomes, Ribeiro, and Lorena (2013) | | X | X | | | X | X | | | | | |

Figure 2.3 The PFLP requirements and constraints in previous research works.

| | R1 | R2 | R3 | R4 | R5 | R6 | R7 | R8 | R9 | C1 | C2 | C3 |
|--|----|----|----|----|----|----|----|----|----|----|----|----|
| | X | X | X | X | X | X | X | X | X | X | X | X |

Figure 2.4 The PFLP requirements and constraints in the presented model.

It is important to note, that R6 and especially R8 are in fact the most important of all rules according to the literature, as the whole usability of the map hinges upon them. Previous work often concentrates on avoiding overlapping (C1-C3) labels with few regards to disambiguation (Fig. 2.1 and 2.5).

2.2.1 Quality evaluation function

We have written out the requirements for good label placement. These requirements are also metrics for the quality evaluation function. The requirement that a point feature can be labelled only once or even can be left unlabelled can be written as:

$$\sum_{i=1}^{P_n} x_{i,j} \leq 1, \forall j = 1 \dots N \quad (2.1)$$

where $x_{i,j} \in 0, 1$ is the decision variable that defines whether the j th point feature is labelled in the i th position and N is the number of map features to be labelled and P_n is the number of possible label positions for one feature. In our implementation $P_n = 8$, being a common model in PFLP. An important constraint of map lettering is that no two labels may in any way overlap each other or point features. This is expressed with the inequality: $x_{i,j} + x_{k,m} \leq 1$, which is valid for all intersections between the i th position of the j th point feature and the k th position of the m th point feature.

The full form of the quality evaluation function of cartographic preferences is:

$$Q(x) = \left[\sum_{i=1}^{P_n} \sum_{j=1}^N (\beta_1 F_{i,j}^{prior} + \beta_2 F_{i,j}^{pos} + \beta_3 F_{i,j}^{over} + \beta_4 F_{i,j}^{disamb} + \beta_5 F_{i,j}^{clut} + \beta_6 F_{i,j}^{coast}) x_{i,j} \right] / N_v(x) \quad (2.2)$$

where $N_v(x)$ is the number of visible labels from input N , $\beta_1 \dots \beta_6$ are the weights for the corresponding measure $F_{i,j}^*$ that are explained below.

Priority of the point feature ($F_{i,j}^{prior}$). The difference in presentation of two cities helps a reader to see the difference in population, importance, or administrative status of a place [63]. Such differentiation can be done by assigning a priority to a place, often this is done by population. After normalization over the minimum and maximum of the population values at hand, the measure is in range $[0, 1]$, fulfilling requirement R1.

Positioning of the name around its point feature in terms of cartographic desirability ($F_{i,j}^{pos}$). The measure has the maximum value $[1]$ when the label position is somewhat above and to the right of its symbol, other positions are ranked lower after an ordered list such as found in [149]. In our current framework, we only generate label candidates which are horizontally aligned with the upper map edge, as it is fitting for the Mercator-like projections used in web mapping. Note that non-rectangular map projections might warrant curved labels that are axis-aligned with the curved latitude grid of such a projection. Fulfilling requirement R2 and R3.

Overlap of symbol and its label with other significant map features ($F_{i,j}^{over}$). We use a raster-based method. We prefer this method as it can be used on both small and large scales. We define a measure that can measure homogeneity of the cartographic background under a label. As an input for this measure we require a raster image I in which the non-textual objects are already rendered. Each element $p \in I$ is a pixel. Assume that we applied some image segmentation algorithm φ which transforms pixels into clusters $\varphi(I) = c^1, c^2, \dots, c^M$, where $c^m, m = 1, \dots, M$ are the clusters. This measure is designed to yield a value of 1.0 for the case when all elements within the bounding rectangle $R_{i,j}$ of a label belong to one cluster, that is, the region of the map background under a label is homogeneous. Section 2.3 explains a more powerful and detailed version of this measure. Fulfilling requirement R9.

Disambiguation ($F_{i,j}^{disamb}$). The magnitude of ambiguity between neighbouring point features and their names; measured as normalised distances between labels themselves

and between their respective centrelines. The distances are compared to certain thresholds beyond which no ambiguity can occur anymore at the given resolution. Illustrated in Fig. 2.5; Fulfilling requirements R6 and R8.

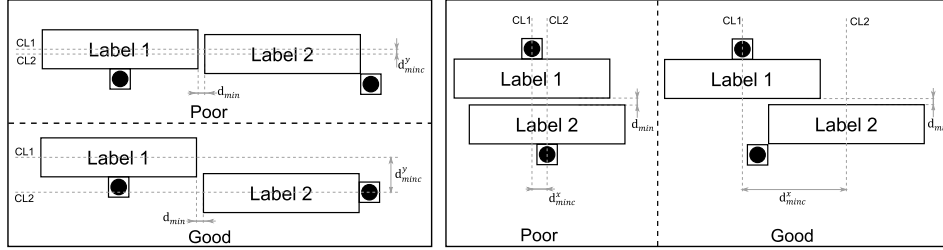


Figure 2.5 Presentation of ambiguity between two neighbouring labels.

We define the measure of disambiguation as a function that consists of two parts, each of which is representing aspects that have an influence on ambiguity:

- Two different labels should not be too close to each other
- Labels of different features that are close to each other should not be vertically or horizontally aligned.

In the following, we describe our disambiguation measure $F_{i,j}^{\text{disamb}}$ and its constituent parts in more detail. We begin by establishing some definitions. For every label $\eta \in L$, we define its bounds as $r_\eta = r_\eta^s \cup r_\eta^n$, where r_η^s and r_η^n are two rectangles on the Euclidean plane \mathbb{R}^2 , which are minimum bounding rectangles of the symbol and its toponym respectively. Further, for every two labels $\eta, \mu \in L$ we define a function that returns the Euclidean distance between them:

$$d_{\min}(\eta, \mu) = \begin{cases} 0, & \eta \text{ and } \mu \text{ overlap} \\ \min \{d_{\min r}(r_\eta^s, r_\mu^s), d_{\min r}(r_\eta^s, r_\mu^n), d_{\min r}(r_\eta^n, r_\mu^s), d_{\min r}(r_\eta^n, r_\mu^n)\} & \end{cases} \quad (2.3)$$

where $d_{\min r}(r_1, r_2) = \min\{\|p, q\| \mid p \in r_1, q \in r_2\}$ is the minimum distance between two rectangles. The norm $\|p, q\| : \mathbb{R}^2 \times \mathbb{R}^2 \rightarrow \mathbb{R}$ denotes the Euclidean distance between two points $p, q \in \mathbb{R}^2$. We also define $d_{\min}^x(r_1, r_2)$ and $d_{\min}^y(r_1, r_2)$ as functions that return the distance between x - or y -components of the centres of the two rectangles r_1 and r_2 , see Fig.2.5. We define the first as

$$d_{\min}^x(r_1, r_2) = \begin{cases} T_{dc}, & d_{\min r}(r_1, r_2) \geq T_d \\ |x_{r_1} - x_{r_2}|, & d_{\min r}(r_1, r_2) < T_d \end{cases} \quad (2.4)$$

where x_{r_1}, x_{r_2} are the x -components of the centre points of r_1 and r_2 respectively. Note that the function $d_{\min}^x(r_1, r_2)$ returns a threshold value T_{dc} in the case when two rectangles are too far apart to create any ambiguities between two labels. The parameter T_{dc}

is the threshold distance between the horizontal or vertical centrelines of the two bounding rectangles of the labels (see *CL1* and *CL2* in Fig.2.5). The function $d_{min}^y(r_1, r_2)$ is defined analogously.

We denote the function that normalises the distances and returns values in the the range $[0, 1]$ as

$$B(d, t) = \frac{d}{t} \quad (2.5)$$

where t is a threshold value that specifies the neighbourhood of a label. In our implementation, we define the neighbourhood (which is the minimum permissible distance) of a label with the parameter T_d . For each pair of labels $\eta, \mu \in L$ we define part one the proximity function as

$$A_1(\eta, \mu) = \begin{cases} B(d_{min}(\eta, \mu), T_d), & d_{min}(\eta, \mu) < T_d \\ 1, & d_{min}(\eta, \mu) \geq T_d. \end{cases} \quad (2.6)$$

The function $A_1 : L \times L \rightarrow \mathbb{R}$ was designed to yield a value of 0 for a case when the labels η, μ touch each other and 1 if they are too far apart to raise any ambiguities. Analogously we define the second function that measures the degree of alignment between two adjacent labels as

$$A_2(\eta, \mu) = \begin{cases} B(d_{minc}(\eta, \mu), T_{dc}), & d_{minc}(\eta, \mu) < T_{dc} \\ 1, & d_{minc}(\eta, \mu) \geq T_{dc} \end{cases} \quad (2.7)$$

where $d_{minc}(\eta, \mu)$ is defined as

$$d_{minc}(\eta, \mu) = \begin{cases} 0, & \text{if } \eta \text{ and } \mu \text{ overlap} \\ \min \{ d_{minc}^x(r_\eta^s, r_\mu^n), d_{minc}^x(r_\eta^n, r_\mu^s), d_{minc}^y(r_\eta^s, r_\mu^n), d_{minc}^y(r_\eta^n, r_\mu^s) \}, & \end{cases} \quad (2.8)$$

The function returns the minimum value of the set of distances between the x – or y –components of the centres of the rectangles $r_\eta^s, r_\eta^n, r_\mu^s, r_\mu^n$ which are considered for creating ambiguity between labels η and μ . Function A_2 returns 0 if the centrelines of the rectangles coincide (see *CL1* and *CL2* in Fig.2.5a). Accordingly, it returns 1, should the distance between the centrelines be greater or equal to the threshold T_{dc} . We can now combine functions A_1 and A_2 , yielding our disambiguation measure $F_{i,j}^{\text{disamb}}$ as follows:

$$F_{i,j}^{\text{disamb}} = \begin{cases} \prod_{y \in \tilde{L}(l_{i,j})} (\gamma_1 A_1(l_{i,j}, y) + \gamma_2 A_2(l_{i,j}, y)), & y \in \tilde{L}(l_{i,j}) \\ 1, & \tilde{L}(l_{i,j}) = \{\} \end{cases} \quad (2.9)$$

where A_1, A_2 are the defined distance functions; γ_1, γ_2 are weights and add up to 1, and $\tilde{L}(l_{i,j})$ is the neighbourhood of the label $l_{i,j}$ defined by T_d as the set $\tilde{L}(\eta) = \{\mu \in L \mid d_{min}(\eta, \mu) < T_d\}$. The measure is expressed as product, which means that we compute the total degree of disambiguation between label $l_{i,j}$ its neighbouring labels $\tilde{L}(l_{i,j})$.

Clutter ($F_{i,j}^{\text{clut}}$). The magnitude of ambiguity between and density of neighbouring point features and their names. Calculated with a modified version of the force-based model of [95]. Fulfilling requirements R6 and R7.

Coastal places ($F_{i,j}^{\text{coast}}$). Coastal places are measured by the percentage of water under the label for the point features that describe coastal places. The actual procedure uses an approach similar to the abovementioned raster-based technique with a separate colour mask generated from ocean polygons. Fulfilling requirements R4 and R5.



Figure 2.6 Example of the output of our approach on OpenMapSurfer at zoom level 6. Map data ©OpenStreetMap contributors.

2.2.2 Experimental results

In our implementation we used a couple of techniques that allow an increase in performance of label placement algorithms. Firstly, we made use of a quad tree data structure to store labels and examine whether any label overlaps other characters or symbols on the map. Secondly, in a pre-processing step, we construct a conflict graph, whose nodes are all labels of the map, and whose edges indicate potential overlap with other labels

(nodes). The graph-based approach is one of the most common approaches in the field of interactive and dynamic labelling [24, 201].

In order to compare effectiveness and accuracy of our model we used three well-known heuristic search algorithms for solving PFLP as a mathematical programming problem: greedy, discrete gradient descent and simulated annealing. In our experiments these algorithms are used to find a feasible solution for label placement by treating the proposed model as the objective function to be optimized. In our implementation the greedy algorithm is restricted to the selection of the first candidate position for a point feature that can be placed on a map. It follows, that the improvement of a final solution within the candidate positions of a point feature is not allowed. As an annealing schedule for the simulated annealing algorithm we chose a polynomial-time cooling schedule that was proposed by [2].

| № | N | β_1 | β_2 | β_3 | β_4 | β_5 | β_6 | Greedy | | | | Gradient Descent | | | | Simulated Annealing | | | |
|---|----|-----------|-----------|-----------|-----------|-----------|-----------|----------|-------|--------|--------------|------------------|-------|--------|--------------|---------------------|-------|--------|--------------|
| | | | | | | | | $N_v(x)$ | % | $Q(x)$ | $t_{cpu}[s]$ | $N_v(x)$ | % | $Q(x)$ | $t_{cpu}[s]$ | $N_v(x)$ | % | $Q(x)$ | $t_{cpu}[s]$ |
| 1 | 82 | 0.6 | 0.4 | 0 | 0 | 0 | 0 | 59 | 71.95 | 0.617 | 0.01908 | 66 | 80.49 | 0.657 | 0.02553 | 73 | 89.02 | 0.706 | 1.02975 |
| 2 | 82 | 0.3 | 0.2 | 0.5 | 0 | 0 | 0 | 59 | 71.95 | 0.673 | 0.08279 | 66 | 80.49 | 0.717 | 0.09524 | 73 | 89.02 | 0.784 | 1.29695 |
| 3 | 82 | 0.2 | 0.1 | 0.3 | 0 | 0 | 0.4 | 59 | 71.95 | 0.712 | 0.39249 | 66 | 80.49 | 0.761 | 0.42134 | 74 | 90.24 | 0.839 | 1.48764 |
| 4 | 82 | 0.2 | 0.1 | 0 | 0 | 0 | 0.7 | 59 | 71.95 | 0.729 | 0.34698 | 66 | 80.49 | 0.779 | 0.35373 | 74 | 90.24 | 0.858 | 1.57519 |
| 5 | 82 | 0.2 | 0.1 | 0.3 | 0.1 | 0.05 | 0.25 | 59 | 71.95 | 0.710 | 0.50949 | 66 | 80.49 | 0.760 | 0.51101 | 74 | 90.24 | 0.834 | 3.56920 |

Figure 2.7 The results of the PFLP algorithms with different parameter weights. Note that the values for Q_x can meaningfully only be compared for each parameter weight setting separately, that is within the same row.

We performed our experiments on a dataset that represents geospatial data granted by the OpenStreetMap project that is one of the most promising crowd sourced projects. The test dataset represented the northern part of Denmark. From the dataset we extracted all settlements and divided them into 4 groups. To each group we assigned a different font size and image for point features which reflect the population and administrative status of a place. The tabular data in Fig. 2.7 show the parameter weights for each of the five test runs, as well as the run-times and measured quality. In Fig. 2.8a and b we present the results of Test No 1 for the greedy and gradient descent algorithms respectively. In Test No 1 we used only two measures common in the literature such as positioning around a point-feature and feature hierarchy, as can be seen by the weights β_1, β_2 . From these figures it is clear that the resulting map is far from a high level of functionality, as the names partially hide some important and relevant geographic features such as roads (see Fig. 2.8a, ref. 2) and bays (see Fig. 2.8b, ref. 1). Moreover, we can see some distinct ambiguities between the names and the features they label (see ref. 1 in Fig. 2.8a and b).

A demonstrative example is a group of villages that consist of Møldrup, Roum, Bjerregrav, Skals. Fig. 2.8d shows the changing label configuration with simulated annealing using the weights for Test Nr. 2 [3 metrics] (i) Nr. 3 [4 metrics] (ii), Nr. 4 [3 metrics] (iii) and Nr. 5 [6 metrics] (iv). It is evident from the tabular data (see Fig. 2.7) that the

simulated annealing algorithm predominated over other algorithms in the quality of the label assignment, while the greedy heuristic is the fastest at the same time returning the worst solution. It is also clear that the computational resources required for each PFLP algorithm and parametrisation vary greatly. In order to determine how strong the impact of different metrics is upon performance, we calculated a score as the running time of Test No 5 divided by the running time of Test No 1. For the tested PFLP algorithms, this score is 26.70, 20.01 and 3.46 respectively. Comparing the scores, we can conclude that a substantial amount of computation time is spent on pre-processing for different metrics.

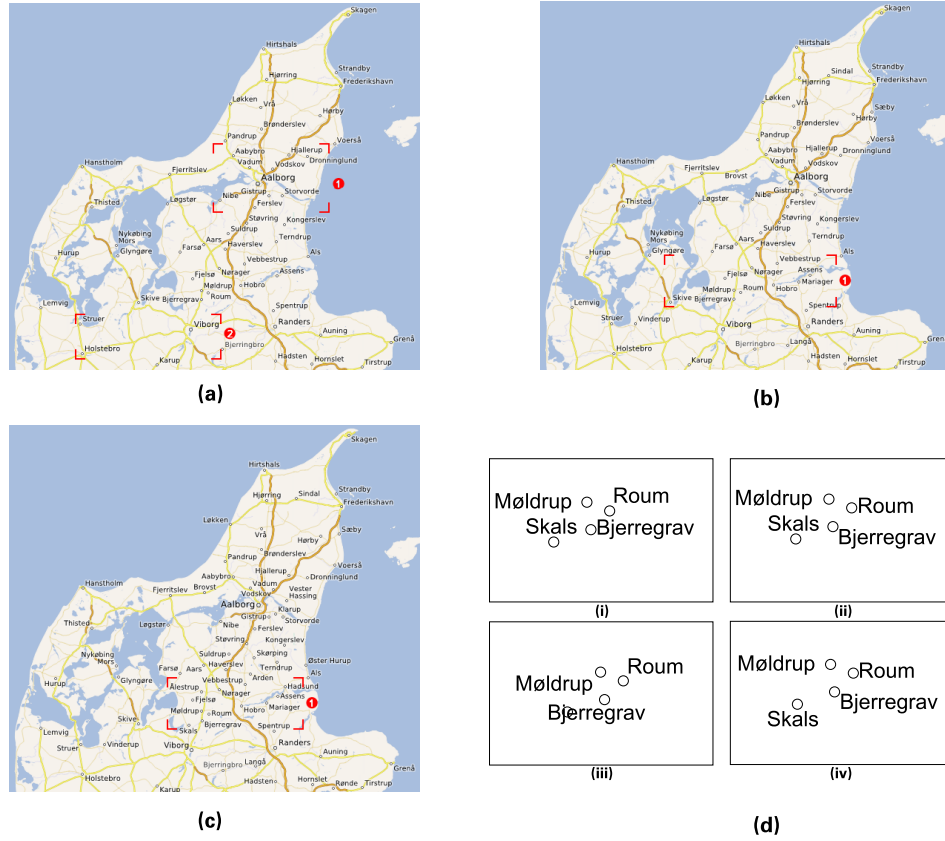


Figure 2.8 (a) The results of the greedy test run No 1. (b) The results of the gradient descent test run No 1. (c) The results of the simulated annealing test run No 5. (d) A sketch representation of ambiguity for a group of villages.

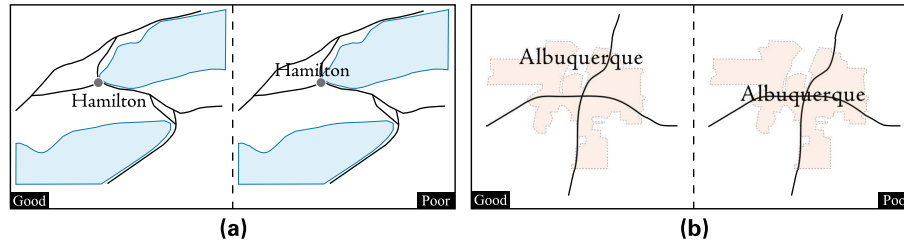


Figure 2.9 Illustrative examples of good and poor name positioning for the above-mentioned guidelines.

2.2.3 Conclusion

Our model of a quality evaluation function for the PFLP problem satisfies almost all cartographic requirements for point features. Producing unambiguously labelled maps has been traditionally recognized as being the most important aim of the whole labelling process [36, 149, 316]. To our knowledge this is the first attempt to address, among other things, the quantification of ambiguous label-feature relations. The proposed model is highly adjustable and provides a handy tool to make an appropriate label placement. It also conceptually opens the possibility to automate the preceding stages of label placement (see Introduction), which have previously been neglected in research. The experiments argue that the model together with an appropriate mathematical optimisation algorithm for PFLP, which is able to find an approximation to the global optimum, produces visually plausible lettering with high cartographic quality and is capable of considerably enhancing the functionality of the map (see Fig. 2.6). The presented model can also be used for labelling other feature types (lines, areas).

2.3 Considering base map details

In this section we introduce some further quality metrics which can measure the degree of label-feature overprinting and visual contrast between them. In other words, the metrics allow evaluating and consequently minimising distortion of map features that have been effected due to lettering. They also allow enhancing map legibility. The devised metrics are based on widely used cartographic design principles.

2.3.1 Cartographic principles

The extant cartographic guidelines referring to overlapping and text-symbol-clutter (compiled from [36, 149, 316]) are:

- G1 Move the names away from positions where they partially overlap or even totally conceal other symbols. Locating names in empty spaces is preferable (Fig. 2.9a).

- G2 Avoid interfering or overprinting a geographic feature which is running the length of the name (Fig. 2.9b).
- G3 For legibility, the name should be placed so as to minimise visual contrast of other names and space around them (Fig. 2.10).
- G4 Labels should take into account the nature and the importance of the graphical features in the layout. Overlapping or concealment of different feature classes (e.g., roads, lakes, rivers, administrative boundaries) by types should be treated differently. Positioning names on top of less important features is preferable.

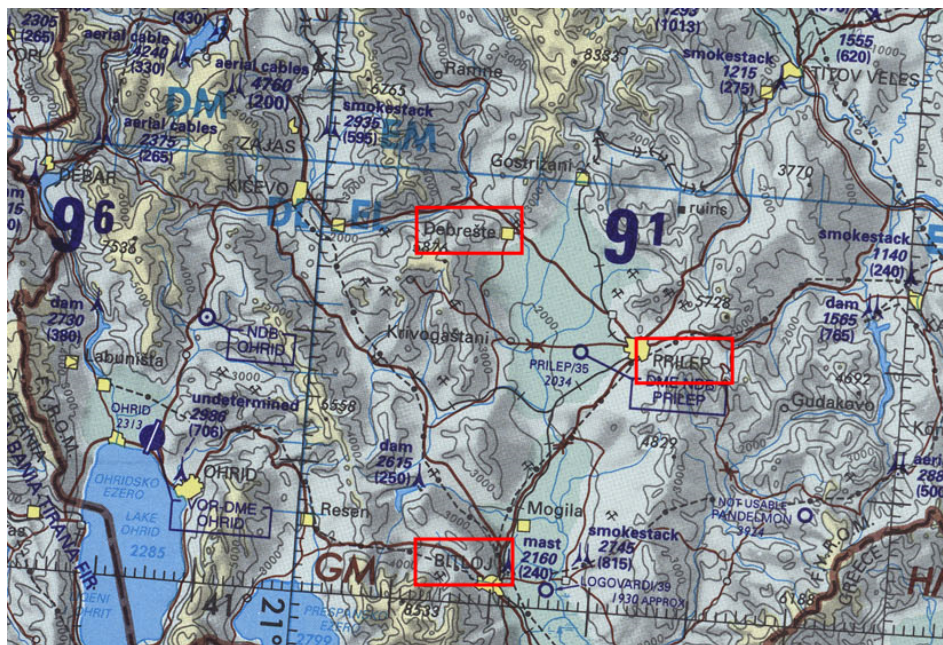


Figure 2.10 An example map lacking visual contrast between labels (examples are Prilep city, Bitola city, Debrešte village) and map background. Source: Defence Geographic and Imagery Intelligence Agency (UK) (2000), ©UK MOD Crown Copyright, 2014.

2.3.2 Measures of feature overprinting and type legibility

In the following subsection we present and describe in detail four metrics, which correspond to the cartographic guidelines given above. We conclude with a single quality evaluation function that incorporates all four metrics at once.

Preliminary definitions. Our measure depends on a raster image which represents non-textual map features. In order to make further work with raster data (pixels) easier, we

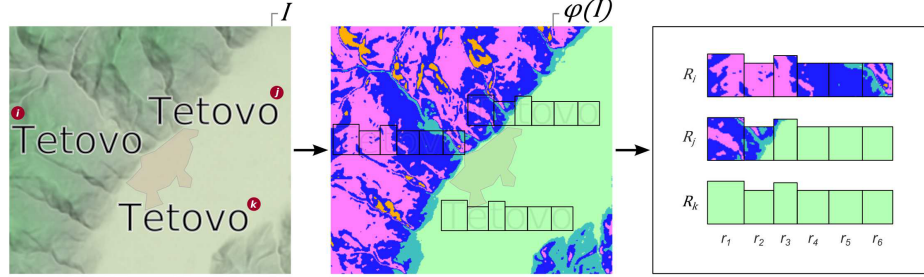


Figure 2.11 Workflow of the method. The input image I with shaded relief is transformed into a segmented image ($M=4$). Next, map background information of the segmented image is assigned to each letter of the potential labels. Note that the urban area of Tetovo is imaginary and has been provided for the sake of explanation.

chose the approach of image segmentation [128, 257]. Such representation of an image facilitates efficient and meaningful analysis of its properties. Besides, this method is extensively used for feature extraction and recognition from digital cartographic documents [175]. In our approach image segmentation helps to merge the map background regions which have similar colours. Image segmentation consists of the partitioning of an image into homogeneous regions (clusters). We note that our approach assumes clusters based on colour space only, disregarding spatial proximity. Maps in raster form can contain a large number of unique colours that can be governed by shaded relief [147, 151, 155] or bathymetry, gradient fills of polygons or colour gradations produced by the anti-aliasing technique. In this case, the clustering is crucial for further analysis as a data reduction step. Next, we omit the description of any existing image segmentation method and assume that one of them has already been chosen. The required input for our measure is a digital image, the number of clusters in the segmented image and a set of axis-aligned rectangles that represent the boundaries of the characters in a name, where each character can be a letter or other graphic symbol. In simple terms, the raster pixels are grouped and succinctly indexed by colour. We further require the boxes around the individual letters to line up with the raster grid. The following paragraph expresses this process more formally.

Let us define $I = \{1, \dots, W\} \times \{1, \dots, H\}$, where W and H are the dimensions of the input image, $I \subset \mathbb{Z}^2$. Each element $p \in I$ is a pixel that has its colour, denoted as C_p . We also denote the number of clusters in the segmented image as M . We assume that an image segmentation algorithm φ [128] has been applied to the input image I . The algorithm φ was able to assign an index of a cluster to each pixel $p \in I$. Thus, we can denote this transformation as $\varphi(I) = \{S^1, S^2, \dots, S^M\}$, where $S^m, m = 1, \dots, M$ are the clusters. Hence, each pixel $p \in I$ has the associated cluster index S_p . Further, let us assume that the name of a label $l \in L$ consists of K_l characters. Then, the set of axis-aligned rectangles that bound its characters we denote as $R_l = \{r_1, \dots, r_{K_l}\}$, where

$r_i, i = 1, \dots, K_l$ (see Fig. 2.11). In our implementation of the metrics, we demand that beforehand the coordinates and size of r_i are rounded to the pixel coordinates. In order to shorten further mathematical manipulations, we denote all pixels that lie within a certain rectangle r_i as D_{r_i} . We also define the area of an image covered by a label l as $A(R_l) = \sum_{i=1}^{K_l} a(r_i)$, where the function a returns the area of a rectangle r_i , or, in other words, the number of pixels. Note that the pixel size is only considered in the procedure of rounding the character bounds r_i . The rectangle-based representation of type letters also supports the cartographic technique known as letter-spacing which is a powerful and widely used design element. Sometimes it is called type spacing, character spacing or tracking in typography. Letter-spacing gives more freedom in making the names and the non-textual features less obscure.

Measure of background homogeneity. A good design technique is to place labels in areas where other features are less dense. The purpose of this sub-section is to define a measure that can describe background homogeneity (see $G1$). In image processing, homogeneity expresses how similar certain elements (pixels) of the image are. Homogeneity has diverse definitions and measures, which can be found in the literature [158, 211]. Pursuing our needs, we consider homogeneity only for the pixels that are covered by the characters of a label $l \in L$, namely by the set of given rectangles in R_l . Hence, we can use the concept of local homogeneity which we define as a value that represents a cluster with maximum number of elements bounded by R_l . Let us define a function that calculates the number of elements of a cluster m within R_l as follows:

$$N_{cl}(R_l, m) = \sum_{i=1}^{K_l} \sum_{q \in D_{r_i}} B(s_q, m) \quad (2.10)$$

$s_q \in 1, \dots, M$ is a cluster index of a pixel q . The function $B(d, e)$ defined as:

$$B(d, e) = \begin{cases} 1 & \text{if } d = e \\ 0 & \text{if } d \neq e \end{cases} \quad (2.11)$$

where d, e are the cluster indices.

$$Q_{BH}(R_l) = \frac{\max_{m \in M} N_{cl}(R_l, m)}{A(R_l)} \quad (2.12)$$

The function $Q_{BH}(R_l)$ can be interpreted as the percentage of the area inside R_l covered by the cluster with maximum number of elements (pixels) in R_l . Function 2.12 returns a value in the interval $[0, 1]$. This measure is designed to yield a value of 1.0 when all elements within R_l belongs to one cluster, that is the region of the map background under a label l is homogeneous.

Measure of spatial distribution. The shortcoming of the measure presented in the previous paragraph is that it does not consider the spatial distribution of the clusters over the rectangles. We use a modified measure based on the concept of entropy to remedy this

situation. We omit the details out of space considerations and point the reader to [239, p.8-10] where this measure (Q_{SD}) is discussed in full detail.

Measure of background feature priority. Toponyms may overlap non-textual background elements of different classes (land, roads, seas, woods and so forth) which of course have distinct importance (G4). Jones [157] proposed to use an overlapping priority for different feature classes, so that each colour of the background has a priority. As a label covers a set of pixels, we can conclude that the best label position is in which the sum of priorities of covered pixels is minimal. Hence, using the mentioned notations we can construct the next measure as:

$$Q_{FP}(R_l) = 1 - \frac{\sum_{i=1}^{K_l} \sum_{q \in D_{r_i}} P(s_q)}{A(R_l)} \quad (2.13)$$

where $P(s_q)$ is a function that returns the priority of a background pixel q . Function $P(s_q)$ should return normalised values, in order to take in equation 2.13 the values in the range $[0, 1]$. Measure 2.13 also helps to distinguish and refine potential label positions that are considered by the metrics Q_{BH} and Q_{SD} (=spatial distribution) as equal.

Measure of visual contrast. Here, we consider a measure that describes visual contrast (G3) between a label and the map background in terms of their colour similarity. Earlier works by Williams [308] and by Phillips and Noyes [213] showed that clutter mostly comes from symbols of similar colours. It was proven through the set of experiments that the effect of lacking visual contrast decreases the performance of map reading. Wood [315] experimentally determined that brightness difference between figure and ground is highly important for the tasks of estimation and comparison of map areas. Furthermore, Swiss cartographer Eduard Imhof asserted:

One should always combine those elements which are as different or as contrasting as possible, both in the information which they contain and in their design characteristics: in other words, those symbols which supplement each other well in what they represent and are graphically compatible. [147]
cited from the translation [151, p.334]

These facts lead us to the necessity of taking into account contrast difference in the quantification of feature overlapping, since this may positively affect the type legibility and visual search time as a whole. We base our measure on the difference between two colours. It is obvious that the difference between the colours, as they are perceived, determines the figure-ground relationship. The colour space (e.g., RGB, CMYK, HSV, etc.) plays a crucial role in measuring the colour-difference. Since we are interested in measuring visual perception of the information, the colour space should be designed in a way of good approximation of human vision. One of such colour spaces is CIE Lab (CIELAB) space (1978) which was standardized by the French Commission Internationale de l'Eclairage (International Commission on Illumination). A colour in CIELAB is expressed through three components L^* , a^* , b^* , where L^* defines lightness, a^* and b^*

denote red/green and yellow/blue values respectively. The distance between two colour values in CIELAB is defined as:

$$\Delta E(x, y) = \sqrt{(\Delta L^*)^2 + (\Delta a^*)^2 + (\Delta b^*)^2} \quad (2.14)$$

where ΔL^* , Δa^* , Δb^* are the differences between corresponding components. To compute the difference of colours between a label and the background, we need to calculate the difference between the colour of the label and colour of each pixel in R_l . Hence, we can define visual contrast measure as follows:

$$Q_{VC}(R_l) = \frac{\sum_{i=1}^{K_l} \sum_{q \in D_{r_i}} \Delta E(C_q, C_t)}{100 \cdot A(R_l)} \quad (2.15)$$

where C_q, C_t are the colours of a background pixel q and text colour respectively. The function $Q_{VC}(R_l)$ is normalised and its values fall in the range $[0, 1]$. The value 100 in the denominator represents the difference of the lightness component L^* of black and white colours. It should be noted that the problem of colour perception in cartography is much more profound than the CIELAB-space distances suggest. On a fundamental level, this is caused by the inverse optics problem [224, 311]. For our label placement problem, the CIELAB approximation works well as a proof of concept. For more sophisticated techniques trying to address simultaneous contrast and perceptual distances, we point the reader to the works like Lee et al. [173] for pixel-based techniques and Purves and Lotto [218] for more holistic approaches.

2.3.3 Aggregated measure

In the previous section, four metrics have been proposed. They quantify the cartographic guidelines given above. These metrics, which are defined in equations 2.12, 2.13 and 2.15, can be conflated into one single measure as follows:

$$Q(l) = \alpha_{BH} \cdot Q_{BH}(R_l) + \alpha_{SD} \cdot Q_{SD}(R_l) + \alpha_{FP} \cdot Q_{FP}(R_l) + \alpha_{VC} \cdot Q_{VC}(R_l) \quad (2.16)$$

where R_l is the bounds of a label $l \in L$ and $\alpha_{BH}, \alpha_{SD}, \alpha_{FP}, \alpha_{VC}$ are weighing parameters which should sum up to 1 in order to yield values of $Q(l)$ in the interval $[0, 1]$. The higher the value of the function, the more preferable a label position is. Equation 2.16 is an extension and refinement of the function $F_{i,j}^{over}$ in equation 2.2. For an exhaustive study on the issue of construction of quality functions please refer to van Dijk et al. [288]. The approach of adjustable weights allows to prefer one cartographic guideline over another. The adjustment of the weights should be undertaken to provide the most readable, legible and functional label placement. It is thus task-dependent and can currently only be determined for a specific map type as it was exemplary done for OpenMapSurfer.

2.3.4 Computational complexity

In this subsection, we discuss the factors influencing the overall computational complexity of the proposed model. It should be noted that the computation of our composite measure is performed only once, namely, after all potential label positions have been generated and before the position selection procedure (greedy, discrete gradient descent or simulated annealing algorithm, see Edmondson et al. [97]) is applied. The time complexity is determined by two main stages that constitute the two parts of our approach. They are the image segmentation algorithm and the computation of the quality score for each label using function 2.16. Let N be the number of pixels in the input image I , and let M be the number of the required clusters. Denote by V the number of pixels covered by n labels. Then, the time complexity of the model can be written in the general form as $O(F(N, M) + nM + V)$, where $F(N, M)$ is a function that defines the number of operations for the image segmentation algorithm. The second term of the total complexity $O(nM + V)$ represents the runtime which is needed to perform the labelling quality evaluation using our measure. Taking into account that M is fixed and has small values in practice, V directly depends on n and on the font size of the text, the second term can be computed in linear time $O(n)$. Note that the first term $O(F(N, M))$ depends on the type of segmentation technique and can vary greatly. For example, the seeded region growing method [3] has the time complexity of $O((M + \log N)N)$. The K-means clustering algorithm requires $O(NMr)$ execution time, where r is the number of iterations taken by the algorithm to converge [153]. Furthermore, the hierarchical agglomerative algorithm is much slower and requires $O(N^2 \log N)$ [153]. We summarize that our measure can perform its task very rapidly in comparison to the whole runtime consumed by other stages of a labelling algorithm when it deals with a moderate number of labels and a fast image segmentation algorithm.

2.4 Labelling islands

One of the subtasks of automated map labelling that has received little attention so far is the labelling of areas. Geographic areas often are represented by concave polygons which pose severe limitations on straightforward solutions due to their great variety of shape, a fact worsened by the lack of measures for quantifying feature-label relationships. We introduce a novel and efficient algorithm for labelling area features externally, in other words outside their polygonal boundary. Two main contributions are presented in the following. First, an algorithm to generate candidate placements. Second, a measure for scoring label positions. Both solutions are based on a series of well-established cartographic precepts about name positioning in the case of semantic enclaves such as islands or lakes. The results of our experiments show that our algorithm can efficiently place labels with a quality that is close to the quality of traditional cartographic products made by human cartographers.

The new algorithm presented here extends previous research by providing techniques for label position generation and evaluation for the task of external labelling of areas.

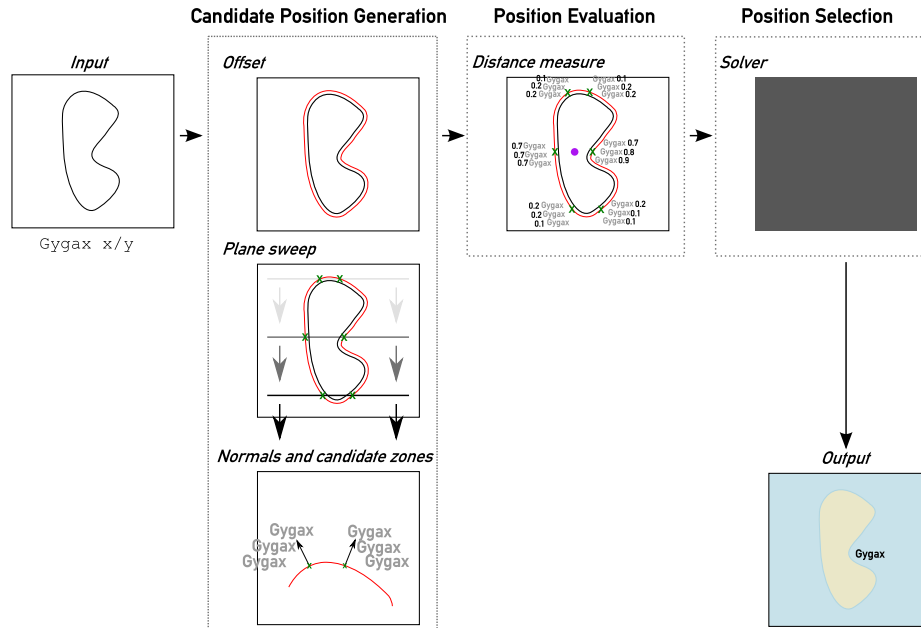


Figure 2.12 Workflow of the approach of labelling individual islands.

The output of the proposed technical approach can be further utilized as an input for the position selection subtask to find a good approximation to the global optimum of a general name placement [97]. Here we address the problem of automated labelling of area features outside their boundary on small and medium scales. Among those are natural features such as small islands, lakes, valleys, canyons or urban areas. Such a problem arises in cartography basically in two cases:

- The area is too small to place the label entirely inside.
- Any internal label overlaps other labels or completely conceals other important geographic features of the map.

On a more conceptual level, we find circumstances leading to the desire for external labelling of polygons repeat themselves. What lakes and islands have in common for the case of maps is that they are, conceptually, semantic enclaves. Such noteworthy areas within a semantic sea of the other/the rest can be encountered in other graphical domains, too. Examples where external polygon labelling might be beneficial include 2D outlier visualization and displaying classification or clustering results. Especially where the semantic enclaves are surrounded by an entity with much lower graphical density, placing text outside the area feature to be annotated is an attractive and tried technique. Positioning names in regions with lower graphic complexity is also tempting in the sense of higher

type legibility and legibility of the map as a whole. To the best of our knowledge, there are no extant automated methods for this task that can be found in the literature. Nevertheless, tools that are able to provide comparable functionality do exist. Among them are ESRI's Maplex Label Engine and MapTexts Label-EZ. However, most other popular toolkits do not have a method to place the labels outside the areal feature. Such functionality is implemented only in proprietary software packages and its description is not publicly available. Being provided in sufficient detail, the proposed algorithm can be easily reproduced. It can potentially extend capabilities of any label placement toolkit and thus, can partially fill a gap between open source and commercial packages.

2.4.1 Cartographic guidelines

The list of rules adapted to the needs of externally labelling areal features is as follows:

- R1 Labels should be placed horizontally.
- R2 Label should be placed entirely outside at some distance from the area feature.
- R3 Name should not cross the boundary of its area feature.
- R4 The name should be placed in way that takes into account the shape of the feature by achieving a balance between the feature and its name, emphasising their relationship.
- R5 The lettering to the right and slightly above the symbol is prioritized.

In the following subsections we utilize four of the five rules for two subtasks of label placement, namely, for candidate positions generation (R1, R2, and R3) and for measuring their goodness (R4). The rule R5 is applicable only in the case when the area of a polygonal feature is small and the feature can be treated and labelled as a point-feature. For a detailed study on the issue of lettering point-features for small and medium scale maps please refer to [318].

2.4.2 Candidate position generation

The candidate position generation shall be described here only in very brief form. For the full algorithm as it was implemented in our framework, we direct the reader to [240]. The basic idea is to generate an offset polygon via the Minkowski sum and generate intersection events on that offset polygon at a scale-dependent interval using a modified plane sweep algorithm (second column of Fig. 2.12). Note that the plane sweep and its associated data structure of projected edges is mostly used for implementation reasons. From these generated intersections of the sweep line with the offset polygon, we construct normals, which are used to generate candidates basically treating those points as point features to be labelled. Note that the data structure of the plane sweep is here used to again check for intersections of those candidates with the offset polygon, in order to rule out label-polygon intersections. These candidates are then evaluated using the approach described in the following subsection.

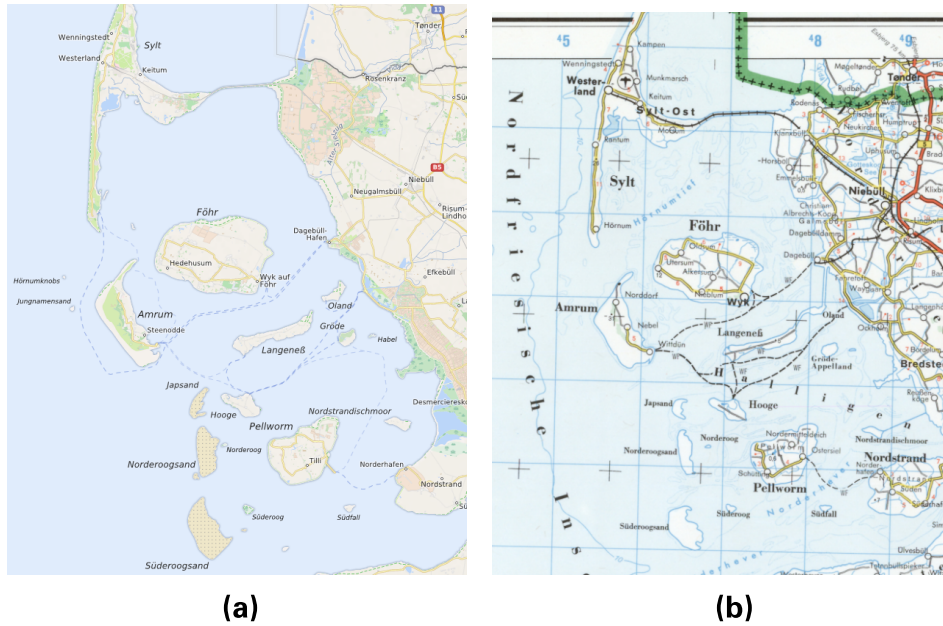


Figure 2.13 (a) A resulting map with a labelled group of the North Frisian Islands and other feature types. Projection: spherical Mercator (EPSG:3857). Data source: OpenStreetMap project (2013)
 (b) The North Frisian Islands. Projection: Equidistant conic projection (standard parallels 49° and 56°), scale 1:500,000. Source: Deutscher Militärgeographischer Dienst (1990), BGIC Licence B-14A003.

2.4.3 Position quality evaluation

The quality evaluation component of our algorithm evaluates the goodness of a label candidate position in respect to the degree of a spatial relationship between a label and the feature it tags (R4). The higher degree of their relationship the faster the information is searched and interpreted by the map reader. The distance between two spatial objects is normally measured by some proximity measure. A wide range of different proximity measures are extant in the literature (for instance, [171, 322]). Usually, proximity is expressed as a function to compute a single numeric score in the range $[0, 1]$. For our needs we use a rather simple proximity measure that is based on measuring the Euclidean distance between the centroid points of the polygon and a label. In order to convert a distance to a score value that falls into the range $[0, 1]$ we define the quality function of a label l as:

$$Q(P, l) = \frac{U_e(C(P), C(l))}{\max_{l \in L} U_e(C(P), C(l))} \quad (2.17)$$

where $C(P)$ is a function for computing the centroid point for a polygon P or bounds of a label l , L is a set of all label candidate positions of the polygon P and U_e is the Euclidean distance. It is worth noting that in our measure we choose a linear score function, however when so required, one can also use supposedly more realistic and suitable quantification functions, for example, a non-linear or a smooth Gaussian-like function. As mentioned above, our approach actually reduces the problem from the more involved and ambiguous polygon to polygon proximity measurement [171] to a point to point proximity question. This was done mostly to keep the overall complexity low. In order to accomplish this reduction, we need a point that visually best represents the whole respective polygon. While this seems easy enough for the rectangular label, for concave polygons the question is known to be strongly dependant on the use case [64]. Where centre of gravity has been shown to be a bad approximation for diagram symbol placement as it can often lie outside the polygon, for external labelling this naturally is not a problem. In fact, according to cartographic practice and literature [316], C- or U-shaped polygons can best be served by placing their label into the bay (conceptual or real). Using the distance between the centroids of both label and area feature as the proximity measure naturally guides the label into such bays with the proximity value of zero being preferred and reachable for strongly concave polygons. An example of the output of our algorithm is shown in Fig. 2.13, where it is contrasted with a similar map that was manually labelled.

2.4.4 Modelling the labelling of groups of islands

We investigate the labelling of feature groups by comparing manually generated labels to a set of formally defined, algorithmically optimal placements. By taking this systematic approach, we hope to detect if, and which, formal measures are—possibly subconsciously—used by cartographers. Furthermore, the framework allows us to define a series of precise algorithmic questions which can readily be investigated in future work.

Each cartographic design technique introduces its own requirements and challenges. The most complex and challenging task is the labelling of areal features. Areal features allow a high degree of freedom for labelling, due to the great variety of possible shapes to be labelled and the diverse set of guidelines. For example, the label can be placed inside the area, using either a horizontal, straight label or a curved label. If the feature is too small for the entire label or contains other important map elements, the label may be placed outside the area. There is one uniting aspect in all design techniques: a label should always conform to the shape and extent of the feature.

Some geographic features like archipelagos, forest patches, or sand hills can be grouped into a cluster or a chain having a common name. These feature groups should usually be labelled differently from single areal features. Surprisingly the (automated) labelling of feature groups has received little attention so far. This is at least partially caused by the lack of cartographic principles that can be found in the literature on this subject. Though



Figure 2.14 Different placement strategies: (a) Ionische In. Bézier curve, shape-connecting. Source: Apenninen- und Südosteuropäische Halbinsel, 1:5,000,000. In: Schandl, H. (Ed.) (1982) Ed. Hölzel Österreichischer Oberstufen-Atlas, p. 45. (b) Kleine Sunda In. Circular Arc, grid-aligned, through the Archipelago. Source: Australien und Neuseeland, 1:30,000,000. In: Imhof, E. (1976) Schweizerischer Mittelschulatlas, 17th Ed., p. 128, Orell Füssli. (c) Nördl. Sporaden circular arc, shape-aligned, connecting; Kykladen circular arc, shape-aligned, through. Source: Östliche Mittelmeerland (1978), 1:5,000,000. In: Große, G. and Kötter, H. (Ed.) List Großer Weltatlas - Mensch und Erde, p. 88, List Verlag.



Figure 2.15 Different placement strategies: (a) Dj. el Djelf Straight-line, shape-aligned. Source: International Map of the World (Aviation edition) 1:1,000,000, N-G-38, Sheet Er-Riyad, Sonderausgabe Nr. 2 Stand VI.1942, German General Staff. (b) Straight-line, shape-aligned, through. Source: International Map of the World 1:1,000,000, Sheet N-G-37 Medina, Sonderausgabe Nr. 2 Stand VI.1942, German General Staff. (c) Gebel el Gardeba circular arc, shape-aligned, through for linear elements. Source: Croquis de L'Afrique au 1:1,000,000 (Aviation edition), N-G-34, 1939, French Army Geographical Service. (d) Hebriden circular arc, shape-aligned, alongside; St. Kilda straight line, grid-aligned, accompanying. Source: Britische Inseln und Nordsee, 1:4,000,000. In: Imhof, E. (1976) Schweizerischer Mittelschulatlas, 17th Ed., p.66, Orell Füssli.

extensive guidelines for map labelling have been given in seminal works by [36, 149, 316], information on the labelling of feature groups is surprisingly sparse. Wood [316] suggests that, to label island groups:

[...] the group name should be on a curve following the general shape of the group or positioned so that the name balances the overall shape of the group.

No further guidelines for the labelling of feature groups are known.

Contribution. We provide an overview of the possible strategies for labelling feature groups as can be observed in manually labelled maps. We then define a framework of feasible labelling algorithms. Finally we compare existing, manual labels, replicated from printed atlases, to a subset of the different optimal algorithmic solutions. To the best of our knowledge this is the first attempt to analyse the techniques used by skilled cartographers in a formal quantitative way. Furthermore, the framework allows us to define precise algorithmic questions pertaining to the automated labelling of feature groups which can readily be investigated in future algorithmic work.

Cartographic design of feature labelling. Bertin [28] noted that the cartographic representation of groups of features across scales is one of the most difficult and error-prone tasks within cartography. As he shows in his example of a group of lakes, the problems of emphasis and visual grouping become multidimensional: shape, orientation, Gestalt properties, and non-geometric attributes all compete for the attention of the mapmaker. This has also been recognized as a hard problem in automated generalization [265]. As with all classifications, grouping geometric objects always keeps some elements of arbitrariness. This puts more pressure on the label: The string *Liverpool*, for example, should identify a single point feature on the map representing the town and nothing else. *Spitsbergen*, by contrast, should have a clear relationship to all parts of the Archipelago. Following Imhof [149], the fundamental function of any label is disambiguation. This function is naturally harder to achieve for object groups, which are potentially close to other object groups, than for the simple object-label pairs in point labelling. A single label might even be all that ties the objects together visually. Group labels hence have a constructive function in addition to the descriptive function that all labels carry. Manually labelled maps show a much greater variety of placements for group labels than for point labels. Instead of a clear hierarchy of 6 – 8 preferred positions, we find curved labels, axis-aligned straight lines, rotated straight lines, who all might or might not overlap the constituent features, placed outside or within the group, and so forth. This greater variety is due to the higher degrees of freedom for both the arrangement and shape of the feature, as well as the position of the label. It is often even unclear which placement strategy (each in turn warranting its own algorithm) is required under which circumstances. Many non-geometric determinants appear to play a role. One example are administrative peculiarities, especially regarding international borders, that heavily use the constructive role of the label. But also authoring and reproduction techniques influence placement. Copper engraving and the growing virtuosity some engravers achieved led to toponym densities above 700 toponyms per 10cm^2 , which could still be reproduced by lithographic processes. Off-set printing paired with manual labelling via rub-off letters or similar

techniques lead to lower densities, and thus more degrees of freedom, which were used differently by different cartographers.

Table 2.1 Strategies for label placement.

| Types | Position | Overprinting |
|-----------------------------|------------|-----------------|
| <i>Straight line</i> | | |
| grid aligned | Accompany | seldom/touching |
| | Through | Common |
| shape aligned | Alongside | seldom/touching |
| | Through | seldom/touching |
| <i>Circular arc</i> | | |
| grid aligned | Accompany | seldom/touching |
| | Through | seldom/touching |
| shape aligned | Alongside | No |
| | Through | seldom/touching |
| <i>Bézier curve</i> | | |
| shape aligned | Alongside | seldom/touching |
| | Through | seldom/touching |
| | Connecting | No |

Colour usage is another non-geometric determinant, especially regarding the visual impact of, and tolerance for, overprinting. Light background colours paired with a full black are much more forgiving of small overprints than on-screen rasterised maps. As a consequence, we distinguish between small overprints which are of no harm in offset-printing and are limited to the outline of constituent polygons. We call this *touching* (see Kykladen in Fig. 2.14(c)) in contrast to a full overprint such as found in Fig. 2.14(b).

Algorithmic framework. The input to a group labelling problem is a set S of k features, which are given as simple polygons P_1, \dots, P_k with n vertices in total. The label to be computed is a shape as well, and depending on the label type, has a baseline that is either straight, circular, or a Bézier curve. The label shape itself is the baseline offset along the perpendicular by the text height. We first define a space of possible label designs. We include four different characteristics that may affect the labelling: label shape, point of measure, distance measure, and overlap. These characteristics are independent and, thus, our framework covers all 54 possibilities that result from the Cartesian product of these characteristics (see Tab. 2.2).

The first characteristic is shape. We consider straight lines, circular arcs (being the simplest type of curves), and the commonly used cubic Bézier curves as baselines for the labels. The second characteristic is the point of measure used to define the distance between a label and a single feature. The simplest representation of a feature is a single point, namely the centroid. The centroid, however, need not be representative of the feature. Alternatively, we can use the point of the feature that is closest to the label. If the label intersects the feature, the distance would hence be zero. Lastly, it may be the

Table 2.2 The characteristics for labelling within our framework.

| Shape | Point of measure | | Distance measure | | Overlap | |
|---------------|------------------|---------------|------------------|---------|-------------------|-------------|
| Straight Line | Centroid | | Min-Max | | Intersection-free | |
| Bézier curve | × | Closest point | × | Min-Sum | × | Overlapping |
| Circular arc | Area | | Min-Sum-Squares | | | |

case that the label is close to the complete island, so we can also use the complete area of the island to compute the distance. This definition gives rise to an integral. Thirdly we consider the distance measure being optimized. Different distance measures are in use in cartography [322]. We use three common ones, namely, the min-max, min-sum, and min-sum-of-squares distance measures. The min-max distance captures the largest distance between the label and the features. This measure is a measure of the point of worst fit. By contrast the min-sum distance computes the sum over all distances from the label to the features. As such, the min-sum distance is a measure of average fit between shapes. A few features may be far removed from the label, however. The min-sum-of-squares distance resolves this by using the squared distance between the label and the features. The min-sum-of-squares distance finds an average fit that is reasonably good at any point. Finally, we take the overlap with the features into account. Labels should generally not overlap their respective features. For the inverse problem of labelling a group of lakes (the Great Lakes, the Finger Lakes in New York State,...), overlapping the label with the lakes may be less of a problem.

Techniques. We first briefly discuss some computational issues involved when determining optimal labels as well as suitable simplifications to overcome these. Then we sketch techniques which are suitable to solve the simplified problems. Algorithmic details are beyond the scope of this study. First, measuring distance using area is more complicated than using single points as there are an infinite number of points involved. We will simplify our problem by using a suitable finite sampling of all points of each feature, thereby discretising the input to sets of points for every labelling setting. Second, instead of computing a label that optimizes a measure, we will compute a center line that optimizes the measure. The center line is halfway between the baseline and the top of the label. We can extend the optimal center line to a label afterwards.

Third, we require labels that span the full extent of the feature group. We make the simplifying assumption that the width of a label can be controlled, to some degree, by changing the letter spacing. As a consequence, we consider label positions that do not need a left and a right extreme side. For straight line labels this implies that we can assume that the label length is long enough to measure all distances using perpendicular distances to the label Fig. 2.16. Similarly, for circular arc labels we assume that the distance from any point to the label is a perpendicular distance to a circle. In several settings these simplifications allow us to use known algorithms from different fields for optimal labels.

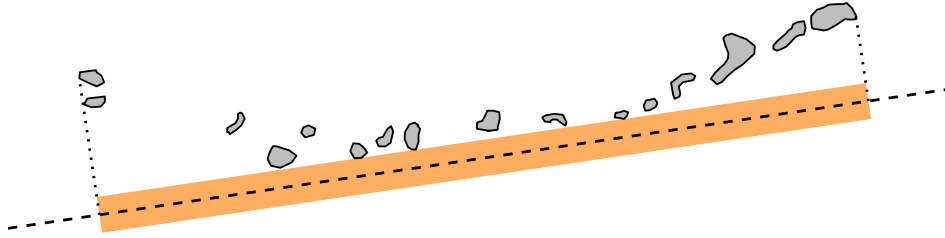


Figure 2.16 The label for a group of islands is assumed long enough to measure distance perpendicular to the center line for any point of the islands.

Moreover, computing an optimal full line or circle, rather than an optimal line segment respectively a circular arc, reduces the number of degrees of freedom in placing the label by two. Often the number of degrees of freedom has a direct influence on the efficiency of the resulting algorithm, and may show up in the some form in the exponent of the running time bound. After computing an optimal line or an optimal circle, we can still choose the most suitable placement of the letters along the line or circle to ensure the extent is indeed fitting for the group, allowing optimality for line segments and circular arcs as well. For cubic Bézier curves we cannot use a corresponding simplification to reduce the number of degrees of freedom. Instead, we observe that we have to deal with eight degrees of freedom, two coordinates for each of the four points that defines the curve.

Overlapping labels. When we dissect the possible combinations within the framework the simplest group of settings are the centroid overlapping measures. These measures do not need the fact that features are polygons. Instead we can just consider a point set for which we desire an optimal placement. Algorithms to optimize these measures over all placements are already known within the areas of computational geometry and computational statistics. For the min-max measure, we can compute the convex hull of the centroids and then apply a rotating calipers algorithm [254] to find two parallel lines that have all points in between and are closest together. The optimal line is exactly in the middle of these parallel lines. Using standard computational geometry techniques, the running time is $O(n + k \log(k))$. For the min-sum measure, we observe that a line can only be optimal if it is a halving line: no side of the line can contain more than half of the points. Hence, the optimal line can be computed using geometric dualisation ([73, Ch. 8]). In dual space we can compute the median level or levels in the arrangement of lines. Using various known results [38, 81, 96], we obtain an $O(n + k^{\frac{4}{3}} \log(k))$ time algorithm. The optimisation of the min-sum-of-squares measure is equal to regression with the error in variables equally likely to be caused by the x- and y-values. Deming regression, also known as the error-in-variables model, computes the optimal line minimizing the sum of squared distances in $O(n)$ time. When considering the area versions of the problem the algorithms remain the same, although the number of points will be considerably higher due to the sampling of the polygons. Note that the min-max setting in combination with

area minimizes the distance to the overall furthest point.

To measure distances to the closest points, we first replace every island by its convex hull, in $O(n)$ time [190], as this does not alter the result. For the min-max measure we use an algorithm that rotates two parallel lines, akin to rotating calipers, to find the optimal line in $O((n + k^2) \log(n))$ time. A variation of this algorithm solves the min-sum and min-sum-of-squares versions: there are $O(n + k^2)$ combinatorially distinct orientations and for each, we can optimize the corresponding function. We also mention one specific result for circles that follows immediately from known results, namely the settings where the circle can overlap the islands and minimizes the maximum distance to the centroid or to the area. This computational problem is equivalent to computing the smallest width annulus that contains a set of points; a quadratic time solution is well-known [73, Ch. 7].

Non-overlapping labels. There are two different approaches to obtain algorithms for computing optimal lines in the non-overlapping settings. First, we can represent the space of all lines that do not intersect any island by using the dual plane again. The total complexity of these lines in the dual is $O(n + k^2)$. We can subdivide the dual space further until we can optimize a single function. Second, we can study the geometry of the situation and derive properties that an optimal solution must have. These properties will limit the search space for the optimal label, and thus restrict the number of required computations. An example is the non-overlapping line (given our set of features) having the optimal min-sum distance to a set of points. By proving that the optimal line always passes through at least two points (of the point set or the feature points) we can develop a more efficient algorithm. Both approaches also work to determine optimal circles. But the running time will increase and not all properties carry over from lines to circles.

Comparison. We explore the applicability of the algorithmic framework described above by testing a subset of optimal algorithmic solutions (circular arc baselines) against digitised, manual labels. We digitised 30 circular arc labels from a variety of different Austrian, Swiss and German atlases. We then compared the labels to the automatically generated optimal labels.

We compared the manual labels with the *circular-arc — area — min-max — non-overlapping* labels resulting from our framework. Within the set of 30 labels, we found 7 instances where the resulting label was similar to the manual label. In some examples an offset of the island group was required for the label to match the manual label. Fig. 2.17a) shows an example including both the manual and computed label for the Ryukyu islands. While several manual labels fit the min-max distance measure well, our exploration indicates that the min-max measure is not the main criterion applied by cartographers. It may lead to situations where the descriptive function of the label is sacrificed for the benefit of a single outlier of the group (Fig. 2.17b). Using an alternative geometric measure may solve this problem. For example, the min-sum-of-squares measure takes the average distance of all features into account. Unfortunately, we do not yet have optimal algorithms for min-sum-of-squares circular arc labels and, hence, cannot test this hypothesis. A better circular arc label would also be possible if we do not require the label to be on the outside of the group of islands. Unfortunately, we do not yet know how to find such labels optimally. We believe in *objectivity through optimality* and hence will test these settings once

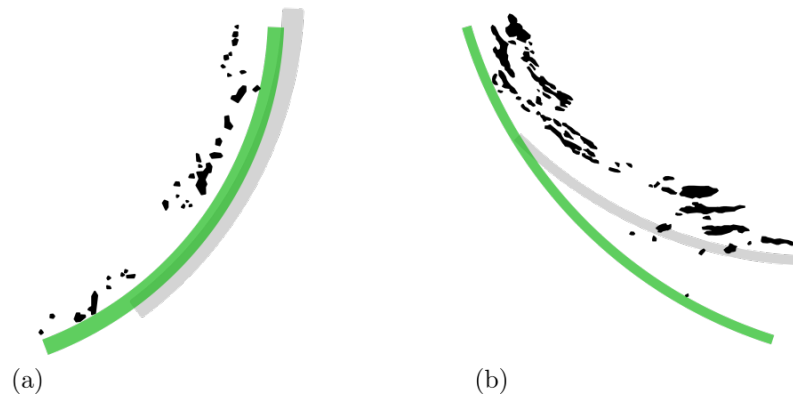


Figure 2.17 Manual (grey) and computed (green) labels for different island groups. (a) The Ryukyu islands. The automatically generated label matches reasonably well, but requires an offset from the group. Digitised from Asien (1976), 1:30,000,000. In: Imhof, E. Schweizerischer Mittelschulatlant, 17th Ed., p. 87, Orell Füssli. (b) The Dalmatian islands. Two problems interfere with automated labelling. The min-max measure focusses only on the point of worst fit and the label can be only on the outside of the group of features. Digitised from Westliche Mittelmeerländer (1978), 1:5,000,000. In: Große, G and Kötter, H. (Ed.) List Großer Weltatlas - Mensch und Erde, p. 87, List Verlag.

we or others succeeded in developing optimal algorithms. Our current framework takes into account the distance to features only, but does not yet consider the shape and extent of the whitespace around the group. As already mentioned by [316], labels may either follow the general shape of the group or complete its overall shape. The second option is mainly tied to the whitespace around the feature group (Fig. 2.18). The label does not necessarily optimize the geometric distance to the group of features, but completes the geometric shape of the group. Labels may also be used to balance the visual weight of the feature group. During our comparisons, it became apparent that several label positions could be reproduced with the framework but with an inverted curvature.

The manual samples nearly always prefer to tie the features together like a pincer or enclose them like a bracket. This is in contrast with the actual curvature of the boundary of the group which might bend away (Fig. 2.19a). As expected, small overlaps with the features are frequently used in manually placed labels and hence such an option should be included in our framework.

Conclusion. We outlined an approach to quantitatively study the labelling of feature groups by comparing manually generated labels to a set of formally defined, algorithmically optimal placements. In the absence of cartographic guidelines for this important



Figure 2.18 Antilles. The manual label (grey) completes the group and is less likely to be captured by a geometric distance measure. Digitised from: from *Mittelamerika: physisch* (1988), 1:15,000,000. In: Thauer, W and Norkowski, T (Eds.) *Seydlitz Weltatlas*, p. 146, Cornelsen.

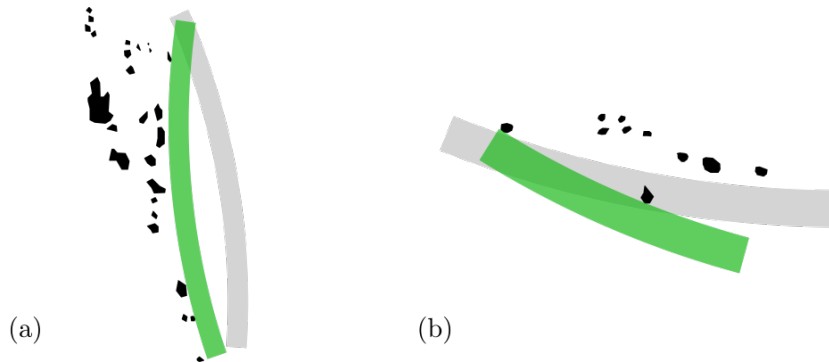


Figure 2.19 a) New Hebrides. Manual labels (grey) are often concave towards the island groups, the computed label has a lower distance to the islands. Digitised from *Australien* (1978), 1:30,000,000. In: Große, G and Kötter, H. (Ed.) *List Großer Weltatlas - Mensch und Erde*, p. 120, List Verlag. (b) Society Islands. Requiring non-overlapping labels may be overly restrictive. Digitised from *Pazifischer Ozean* (1978), 1:60,000,000. In: Große, G and Kötter, H. (Ed.) *List Großer Weltatlas - Mensch und Erde*, p. 123, List Verlag.

labelling problem, we believe that our systematic study will eventually lead to a set of clear specifications which are suitable for automated construction of high-quality labels that match best manual practices. First results are encouraging, but clearly extensive future work is needed to develop optimal algorithms and similarity measures, extend the framework, and hopefully finally validate our approach.

Chapter 3

Schematisation in the Context of Cartographic Generalisation

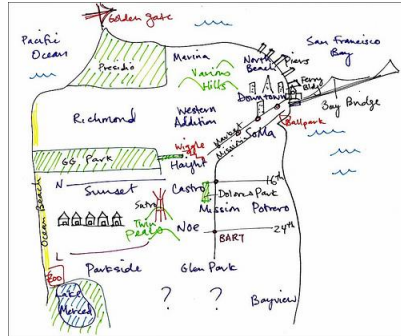
In the last decade schematised maps have garnered substantial research interest from disciplines such as cartography, computational geometry and spatial cognition. More often than not, the individual disciplines have been following their own specific goals, leaving the question of what they have in common relatively open. Substantial algorithmic research has had metro maps and their automated creation as its focus. In this chapter we seek a more systematic treatment of what constitutes schematised maps. This chapter organises and differentiates the understanding of what schematisation is and how it relates to generalisation. To underscore the relation, we close this chapter with an approach for generating caricatures of urban areas for a medium scale map product lying at the intersection point of schematisation and generalisation.

3.1 Generalisation research and schematisation

3.1.1 A classification of schematised maps

We have identified seven types of schematised maps; these include mental maps and sketch maps, educational, propaganda, mass media info-graphics, and schematic maps. There is some overlap between schematised maps and what Muehlenhaus [202] calls *persuasive maps*. While educational, propaganda and mass media schematised maps surely could be categorised as persuasive, not all persuasive maps are actually schematised in the sense of the above definition.

Mental maps. These are, for the sake of our classification, artefacts resulting from attempts at drawing a mental model of space. Such drawings usually abstract greatly from real-world geometries and show only small selections of objects [123, 163], Fig. 3.1a. Schematised maps in general themselves are supposed to communicate the mental model



(a) Mental/sketch map



(b) Schematic (Metro) Map

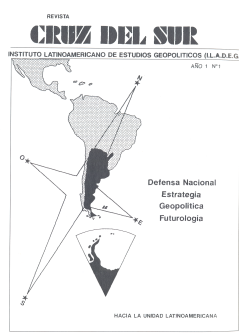
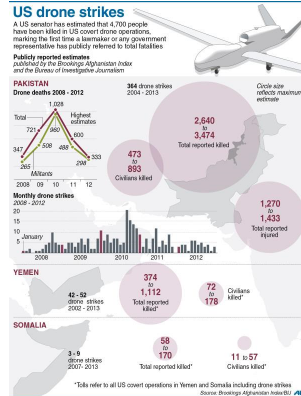
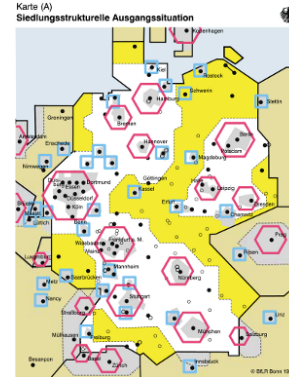


Figure 7.3 Cartographic map of an continental Argentina
 Source: *Revista Cruz del Sur, Argentina: geopolítica y futuro*

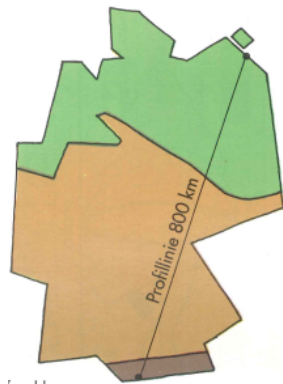
(c) Propaganda Map



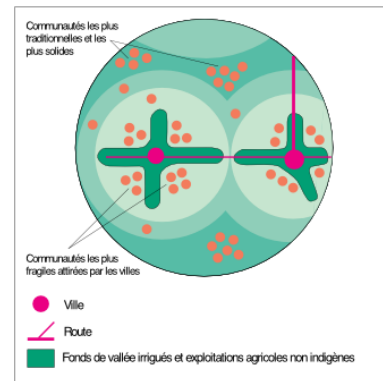
(d) Mass-media Map



(e) Geodesign Map



(f) Educational Schematised Map



(g) Chorematic Map

Figure 3.1 Examples for schematised maps [182].

somebody knowledgeable constructed for a region. Seen as such, schematised maps in general are artefacts derived from a mental map too, but constructed and drawn in a professional manner.

Chorematic maps. Chorematic diagrams are all those maps and map-like diagrams (for example Fig. 3.1g) that use one or more graphical embodiments of the choremes as introduced by Roger Brunet (explored in greater detail in Chapters 4 and 5).

Geodesign maps. Inspired by GIP-RECLUS's spatial planning cartography (i.e. the Blue Banana), some EU member organisations (German and Dutch planning institutions, for example) developed an approach for a synthesizing map style for spatial planning cartography. It is an amalgam of chorematic concepts and more traditional techniques of planning cartography, like using intricate systems of hachures and colours on top of subdued topographical maps (Fig. 3.1e). They are perceived as being especially useful for communicating strategic political scenarios and high level policy guidelines that lack precise localisations [90, 221, 266]. In recent years, a homogenisation of EU planning cartography can be witnessed in which geodesign and chorematic concepts are toned down and retained at the same time [90, 246]).

Educational schematised maps. The two most common schematised map types in education are French croquis and German Faustskizzen.

Croquis. The word describes sketches in general, but here the specific sketches are meant that French pupils are supposed to be able to construct when graduating from high school in geography (geo-bac) since the late 1990s. These croquis are synthetic thematic depictions of continents or countries, constructed on a non-distorted but emptied base map, using a specific symbol set. They are directly influenced by the chorématique. Closely related are the schémas, which are indistinguishable from chorematic diagrams, save that they are (re-)produced by students. The introduction of this graduation task was supposed to strengthen analytical thought and map competence. Many pupils seem to solve the task rather by memorizing samples from preparatory books or the internet instead of actually constructing the croquis, which has been criticised [45, 93, 191]. Poignant examples and further sources can be found in [223].

Faustskizzen. This German word means rough sketch, but shall be understood as those sketches, which were used as a learning tool in German pre-war geography classes. Pupils had to memorize a set of instructions from which sketches of the topography (which sets them apart in aim from the French croquis) of a continent or a country would then be reconstructed, including rivers and mountain ranges (Fig. 3.1f). These sketches were drawn on the blackboard, with pencil, or even on sand in the outdoors. Their simplified depictions of countries are a precursor to the depiction of space in the chorématique. Ludwig Barth further developed their use for school education in the GDR with his publications aimed at geography teachers. He renamed them *Merkbilder* (lit. mnemonic diagrams) and put them into a theoretical context of didactic methodology [19, 20].

Schematic maps. Schematic maps such as topograms or metro maps depict (mostly in linear form) geographical entities with emphasis on the correct topology but locationally distorted in order to achieve greater clarity (Fig. 3.1b). The most famous example is the

London Tube Map. Reviews of algorithmic solutions to the automated production of such maps are considered in [182, 205, 312].

Propaganda maps. Propoganda maps are suggestive maps that are created specifically to reinforce and emphasise how spatial processes and situations mirror ideological pre-conceptions about the world and how it works. They too require instant comprehension and typically use simple geometries, high contrast colours and striking symbols, Fig. 3.1c [208, 245]. Also included under this heading are *geopolitical maps* [33, 208].

Mass media maps. Of growing importance are mass media maps and infographics. Their nature is decidedly ephemeral with short production cycles and low exposure times. The ambition is highly schematised depictions with low cartographic complexity and a symbology of high iconicity Fig. 3.1d. This is different from Web-maps which afford means of interaction and are not constrained by limited exposure time.

3.2 Defining schematisation

We define schematisation in cartography as a process that uses cartographic generalisation operators in such a way as to produce diagrams of a lower graphical complexity compared to maps of the same scale; the process aims to maximize task-adequacy while minimizing non-functional detail. In contrast, traditional cartographic generalisation can be understood as trying to maximize functional detail with task-adequacy (in the form of legibility) as a constraint. A detailed substantiation of this definition and differentiation follows below, as does a discussion of complexity and scale in cartography.

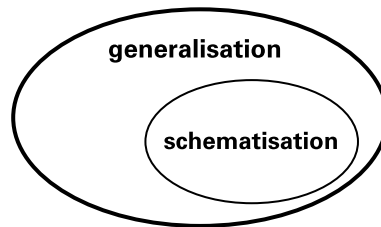


Figure 3.2 Generalisation and Schematisation.

3.2.1 What is cartographic schematisation?

Schematisation as a general term obviously encompasses a wide range of meanings. Starting with the question whether one talks about *a* schematisation, the result of some process, or the process of schematisation itself, the word itself can be synonymous with colloquial concepts like simplification, aggregation, generalisation, reduction, abstraction, representation, diagramming and so forth. As cartography and especially cartographic generalisation research regularly deal with graphical modelling, a language for precise

differentiation between concepts and operations has been established and can be viewed as a baseline consensus [126, 222]. For example, simplification and aggregation as concepts are well established in cartography as being disjunct operations that might come up when a map is either compiled from data or generalised to a different scale. While this difference between a body of differentiating and precise technical terms of a scientific discipline and a semantically broader colloquial terminology seems obvious, confusion may easily arise by conflating the two. Especially when specific problems are addressed by several disciplines at the same time, switching between precise and colloquial terminology can hamper productivity and insight. In the case of cartographic schematisation, some semantic confusion can be witnessed, for example:

To maintain good legibility of small geographic features, certain characteristics (e.g. the width of a road) must be exaggerated. As a consequence, the representation must be simplified to fit all important features onto the representational medium. Simplifications of this kind can be considered as schematizations, as certain aspects are summarized in these maps. For example, on a hiking map the width of the trails is not depicted to scale; their width is exaggerated. Therefore, not all curves of a serpentine might fit on the map. However, curviness of a trail is a very important feature that should not be eliminated by smoothing the curve; thus, on some hiking maps serpentine are depicted with fewer turns, falsifying the number of turns but maintaining the general character of the trail. The shape of the trail has been schematized due to spatial constraints on the map. As simplifications of this kind are generally applied to cartographic maps, cartographers rarely speak of schematic maps. [165]

Following the quote from top to bottom Klippel et al. can be read to say that the generalisation operator exaggeration needs a simplification. Then Klippel et al. say that simplifications of that kind, which would by their own logic be exaggerations, are indeed schematisations. From the context it becomes clear that they cannot be talking about simplification as the generalisation operator, but rather as “simplification” a stand-in for cartographic generalisation. This does their argument a disservice: while trying to separate schematisation from generalisation they exchange generalisation operators with “simplifications” and say some operators are schematisation, but smoothing is not.¹ This is at odds with the first remark though, that exaggeration operations need simplifications.

To a cartographic audience, any separation between schematisation and generalisation thus becomes meaningless, as all maps are generalised and by their logic simplified and schematised. Klippel et al. recognize this and write:

So far, there has been no definition of schematisation and schematic map in cartographic terms and some cartographers reject the notion of a special class of maps that is called schematic.* Although cartographic maps are

¹It is noteworthy that one algorithm for preserving the impression of curvature for roads is in fact called “schematisation” and subsumed as an example of the generalisation operator of caricature [172, 222] in cartographic literature.

highly schematic, it is not clear, (1) whether cartography considers schematic maps as regular instances of one of the classical cartographic maps (and if so: what schematisation by cognitive principles means in cartographic terms) and (2) to what extent cognitive considerations and notions can be expressed in terms of classical cartographic language. We argue for using the term schematic map for a certain type of maps those that are intentionally schematised beyond the requirements of the representational medium.[...]

*D. R. Montello and S. Fabrikant pointed out that especially thematic maps are (highly) schematic. In fact, naming a map schematic is regarded as a pleonasm (pers. comm. Dec 2003).

Their resulting definition, refined to encompass cognitive adequacy:

We define schematisation to be the process of intentionally simplifying a representation beyond technical needs to achieve cognitive adequacy

has been applied in subsequent works, such as [212] or [135]. It also was underlying earlier works on schematisation such as [112]. The differentiation between schematisation and generalisation is still not accomplished. This is easy to show in theory and practice: generalisation is definitely also a process of intentionally simplifying a representation to achieve cognitive adequacy. Any differentiation must then lie within the notion of ‘beyond technical needs’, which remain undefined, although crucial. This gap is narrowed by Haunert and Sering, who write:

More generally, we use the term schematic map for any map whose distortions result from some design principle applied and exceed those distortions commonly found in geographic maps - here distortions are mainly due to the projection of a sphere (the globe) onto the map plane and due to cartographic displacement.

The question what ‘geographic’ maps are arises, and is only partially answered by naming projection and displacement as hints to their nature. If geographic maps include thematic maps, their statement regarding common distortions is wrong. Thematic maps commonly show a great variety of design principles with distortions different from the two explicitly named ones. If one exchanges ‘geographic map’ with topographic map, on the other hand, the statement rings true. The ‘technical needs’ of Klippel et al.’s definition also make much more sense when topographic maps are referenced. It appears that none of the extant definitions can separate schematisations from thematic maps. The main question for differentiating generalisation and schematisation then, is to differentiate between thematic maps and schematic maps. To my knowledge, no definition has explicitly tackled this question until now.

Besides theoretical concerns, one can find real consequences of the lack of differentiation between generalisation and schematisation. For example Barkowsky et al. [16], who propose a form of line simplification without providing stopping criteria. If, as the discussion has shown, schematisation can indeed be viewed as using generalisation operators

beyond a certain point, this certain point is indeed the key to understanding the nature of schematisation. We postulate that this *certain point* of differentiation can be identified by examining map complexity. As the cited examples have illustrated, such a differentiation is crucial for conducting actual schematisation tasks, if only to inform stopping criteria.

3.3 Governing the generalisation process in schematisation

Maps are graphical models of a geographical region and the phenomena included therein. Any modelling task involves a priori decisions: a decision upon the level at which modelling happens and upon the extent of the model. These decisions can only be made with a clear understanding of the intended use of the model [35]. Graphical models mainly aim at visual interaction, and as such the main limits of the scope of a graphical model are the limits of the human visual system. For maps in particular, the fundamental modelling questions therefore come down to: What phenomena are going to be displayed? How are the phenomena going to be displayed?

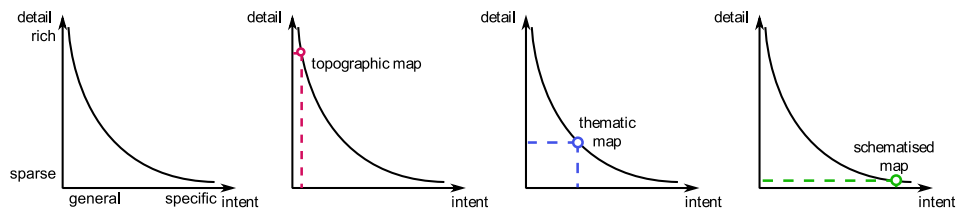


Figure 3.3 Differentiating topographic, thematic and schematised maps.

Cartographic generalisation research has immensely profited from the fact that these questions have been pre-decided upon in the realm of topographic mapping. Certain sets of a priori decisions have crystallised into the traditional range of cartographic scales. The governmental and private practice of producing topographic paper maps to regulated and well-defined specifications is at least three hundred years in the making. This historical process of production and usage has coalesced into the firm understanding of scale in topographic mapping. This makes cartographic scale the lynchpin of generalisation. The level of modelling, the number of depicted objects and even their symbolisation are all defined by the cartographic scale for which a map is produced. By that reasoning, we can see that cartographic scale has for most practical means been used as a stand-in for the intent of the model. Generally speaking, the intent of producing a 1:50 000 map is succinctly answered by saying a 1:50 000 topographic maps is being produced. While such practice has yielded great results in topographic generalisation (most notably full automatised for deriving OS VectorMap District [234]), it obviously does not apply to thematic mapping (cp. [181, 183]). The differences in intent produce differences in the answer to the a priori modelling questions. A map can be intended to serve general

or specific purposes. In general parlance as well as in concept, the general purpose map is a topographic map. From the place in the continuum between general intent and specific intent flows a stark consequence for map compilation: a general purpose map must show as much detail as can be fit in, whereas a specific map must show the pertinent phenomena in the best possible way. As has been alluded to, the specificity of intent is a continuum, and maximising content is not a zero-sum antagonist to maximising message. The interplay between amount of detail and specificity of intent define the nature and type of generalisation problems. For topographic maps, the overwhelming majority of generalisation operations are concerned with resolving conflicts for drawing space. In such drawing space conflicts, the problems generated by ramping up detail overshadow all other concerns [186]. The majority of graphical conflicts in thematic maps arise from the interplay of visually adequate data portrayal and faithful geographic context. Under the proposed differentiation, thematic maps are naturally the widest category; on the more general end of the intent spectrum (e. g. 1:25k soil maps), the cartographic conflicts are nearly as much informed by scale as those found in topographic generalisation, whereas on the specific side of the spectrum (e. g. election maps) communication and aesthetic questions rise to the forefront. Finally, schematised maps are so supremely governed by their specificity of intent, that they intentionally distort and eliminate non-functional detail in excess of what a thematic map would warrant (e. g. election maps of U.S.-election results would always strive to keep overseas territories or the District of Columbia in a visually decodable manner). If we say that the amount of detail in maps of the same scale is a function of the specificity of intent, we must find a way to quantify this amount of detail. As we need a scale-independent perspective, we examine map complexity.

Map complexity. The subject of map complexity has several facets that we will briefly outline here. Our interest, as elucidated above, is to find complexity measures that allow to differentiate between different classes of maps regardless of scale. Narrowing it down further, we seek for a scale-independent measure to tell schematisations from other kinds of maps. Due to this goal, we keep the general discussion on complexity and its possible semantic interpretations and use cases short. We point to [102] and [132] for more detailed discussions of the majority of related work.

While many more complex information density and diversity indices and measures are known, some more straightforward ones encountered in the related work appear to suit our purpose. Following [102], we can use loss-free compression rates, for example from bmp to png-8 at a constant resolution of 300 dpi as an indicator for visual complexity with just as much explanative power as more complex ones. This map-level complexity measure can be augmented with simple measures for complexity such as total object number (ON), the absolute object line length (OLL), following [131]. The number of objects (NO) and the summed length of all object lines (OLL) have been found to correspond best with human-perceived complexity and amount of information [131]. In Reimer 2010 [223] we first suggested to introduce a normalisation over the drawing area in map units (OLLpA), i. e. $\frac{mm}{mm^2} = \frac{1}{mm}$. This allows comparison of information density between different types of maps, on contrast to OLL which is a measure of absolute information content. Using drawing space millimetres as the dimension for OLLpA is convenient as it produces num-

bers interpretable for cartographic practice due to its relation to staples of generalisation like minimum size and minimum distance. We define the measure as:

$$OLLpA = \frac{\sum_{i=1}^n \sum_{j=1}^m l_{ij}}{ab} \quad (3.1)$$

where l_{ij} is the line length of object o_{ij} of object type i , and a, b are the long and short side of the bounding box around all map objects. The variable i stands for the number of different object types and j for the number of objects of that type i .

Structurally this is the cartographic line frequency, related to Bertin's density concept of sign per minimum visible distance, which is why we suggest the name Bertin [Bt] for this unit of measurement. The cartographic line frequency has several desirable properties that makes it a most practical measure for our purpose.

It is:

- (1) human interpretable via concepts from cartographic drawing such as drawing space millimeters, minimal dimensions and so forth
- (2) based on empirical legibility research such as [131]
- (3) congruent with cartographic theory and especially Bertin's density concept
- (4) in consequence of (3) also congruent with Tufte's re-imagined concept of the data-ink ratio [287]
- (5) congruent with information theory [255]:
 - (1) greater line length means more entropy
 - (2) results match up with run length encoding and other data compression techniques for raster images [102]
- (6) based on an absolute zero [0 = no map content] and absolute maximum [5 = parallel lines become visually inseparable as per minimal dimensions]
- (7) vector based and thereby independent of technical resolution concerns, unlike raster based measures
- (8) in linear relation with the computational input complexity; an increasing number of edges beyond the size of the minimal dimensions will mean a linear increase in the measure
- (9) in radical relation to the drawing space
- (10) ignoring non-textured area fills
- (11) resistant to degenerate cases such as parallelism of lines and cartographically necessary variations of line thickness
- (12) more expressive than map load or the amount-of-ink-used

In the following, we will shortly illustrate some of the desirable properties of our measure. Traditionally, map load has been the most popular complexity measure in cartography that was actually used to inform map production. Map load K basically is the percentage of the map that is covered by symbols, that is the inverse of remaining white space. It was defined by TÖPFER as:

$$P[\%] = \frac{\sum f[mm^2]}{f_G[mm^2]} \cdot 100 \quad (3.2)$$

where P is the percentage of the graphical map load K and where $\sum f$ is the amount of drawn elements in mm^2 and f_G the cartometrically measured area in the drawing space, also in mm^2 (see [281], pp. 81).

As long as the same amount of map area is covered, the map load remains constant. Figure 3.4 shows that effect and provides the cartographic line frequency in comparison. Clearly, the intuitive notion of visual complexity matches well with our measure and the constant map load in percent has no power to express such perceivable differences, corroborating our claim (12).

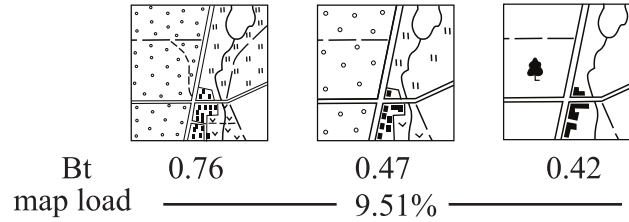


Figure 3.4 Map Load in comparison to cartographic line frequency in Bt as complexity measures. Figure redrawn and amended from [281], p.79

Figure 3.5 shows the gamut of the cartographic line frequency. The absolute maximum value Bt_{max} is the maximum possible number n of lines with minimal thickness t_{min} that can be fitted in a one by one millimetre square keeping the minimum distance between lines $dist_{min}$. As $dist_{min} = 0.15mm$ and $t_{min} = 0.05mm$ [126], it follows that each line occupies $0.2mm$ total. Thus we get a theoretical maximum value of $Bt_{max} = n = \frac{1mm}{0.2mm} = 5$. On the more practical extremes, topographic maps typically yield values between 0.9 and $1.5Bt$ and schematic (metro) maps consistently yield values below $0.1Bt$. As we will show in Chapter 4, spot samples of thematic maps range between 0.7 and $1.2Bt$. Most importantly we can show that the mean values of certain schematised map classes (chorematic diagrams) are indeed a statistically highly significant differentiation measure.

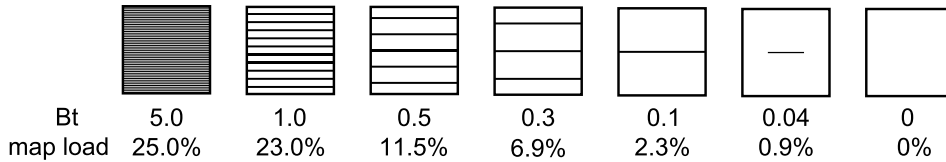


Figure 3.5 Gamut of the cartographic line frequency, exemplified by parallel lines in a $1cm^2$ box.

With this measure, we now have a tool to differentiate between thematic maps and schematisations, which was the snare for preceding definitions. Let us revisit the definition we provided at the beginning of this chapter:

We define schematisation in cartography as a process that uses cartographic generalisation operators in such a way as to produce diagrams of a lower graphical complexity compared to maps of the same scale; the process aims to maximize task-adequacy while minimizing non-functional detail.

Not only have we now the yardstick against which to measure. We also can interpret the generalisation-schematisation gamut itself as a continuum, within which it is safe to say that certain thematic maps are nearly schematised or nearly as detailed as topographic maps and so on. Furthermore it is possible to compare the amount of schematisation that results from several distinct generalisation operations.

3.4 Schematisation operators

As elucidated above, the processes of schematisation can be understood as being a subset of the generalisation operators. Their goals emphasise different aspects making it worthwhile to discuss and group the most common processes. We group the operators according to their cartographic and semantic purposes. We identify six forms of schematisation and discuss the individual operators using the agreed-upon terminology of the generalisation operators as laid down for example in [126, 222]. Note that from an algorithmic geometry perspective the nomenclature might differ, so we provide links back to that terminology where possible.

3.4.1 Forms of schematisation

Extant schematised maps might make use of any or all forms of schematisation. They can be employed in isolation or in conjunction, with some combinations being very common such as caricature and smoothing.

Strong reduction of detail. Although reduction of detail is the baseline operation in cartographic generalisation, in schematisation it is applied way beyond any necessities of geometric scale as calculable by the radical law (basis for automated map generalisation, see [282, 283]) as we have seen. The number of objects and distinguishable classes are usually reduced beyond visual constraints and thereby need other metrics to be guided by than the traditional constraints in map generalisation. The most common schematisation operators for that form of schematisation are amalgamation, elimination and synthesis.

Amalgamation. Due to the low number of classes in the target schematisation, very strong amalgamation usually takes place, especially for area-class data. Often, smaller patches of non-matching objects are reclassified and amalgamated to provide a low number of contiguous objects. The geometric meso-structures governing the choice for contiguous objects to grow and emphasise via amalgamation must be identified, which at heart is a semantic, that is model generalisation question.

Elimination. Elimination is an extreme case of selection where all non-functional detail is omitted. This includes eliminating features and objects that technically could be shown in the available drawing space without visual clutter. The aim is to reduce the

cognitive workload and concentrate on very few (or just one) main message(s). In turn, the guiding metric must be the pre-set number of objects in the target diagram.

Synthesis. Some of the most striking schematisations such as the Blue Banana [51] represent not only a geometric reduction in detail. Instead they present in a single synthetic cartographic symbol or arrangement thereof as an intellectual synthesis that shows the geographic as well as the geometric essence of an answer to a spatial inquiry. Synthesis is a model generalisation operation; it presupposes a thorough understanding of the subject matter. The result should have high visual selectivity in Bertinian terms, that is it should be recognizable pre-attentively. The visual variable colour is traditionally employed to ensure this, but the schematisation operation itself remains an (for the general case) unsolved modelling question.

Smoothing. Line and area objects undergoing smoothing are changed to provide more visual harmony to the end result. For schematisations that might even mean to present natural, flowing lines like rivers with a set of straight lines, or to depict man-made serrated borders with gentle Beziér-curves. The resulting visual representations usually remain closer to their input geometry than is the case with stylisation (below) and can be considered more ideographic. As discussed by Meulemans [192], a merely simplified object might give the appearance of lacklustre generalisation, and the visual impression generated by the introduction of some form of harmony or smoothness underlines the wilful act of schematisation. How we can measure this harmony has been quite elusive, and a part of our work concentrates on finding ways to understand and measure exactly that. So far, we have found out that some but not total *parallelism* for straight lines is used in several extant schematisation examples, see Subsection 5.5.1. Other smoothing operations can be accomplished by redrawing parts of polylines with low number of *cubic Beziér-curves*. All three are discussed in detail using chorematic diagrams as example in Chapter 5. How to measure or even define parallelism for segments of curves has remained a hard task. A tentative solution using map-wide fields of normals has been proposed and tested by Hemmer et al. [137], but has not been developed further since.

Geometric stylisation. The results of geometric stylisation are shapes that field a rigid, structured and abstract look, underlining the nomothetic character of the object. Due to harshly restricted allowed outputs, their automated construction is especially popular as an interesting geometric puzzle that can be solved and optimised in fields like graph drawing or computational geometry. In these fields, further optimisation tasks might include the minimisation of line crossings or guaranteeing area-preservation.

Strict angular restriction. Early metro map algorithms and naïve interpretations of spatial planning maps (compare [90]) postulate a limited number of angles that are to be employed. Limitations to increments of 45° , 60° and 90° are the most common, leading to octilinearisation, hexagonal or orthogonal shapes respectively. This form of schematisation is the easiest to express algorithmically. As a consequence, strict angular restriction is sometimes and erroneously equated with schematisation *in toto*. As Roberts discusses thoroughly in his seminal work on the design rules of schematic (metro) maps *Underground Maps Unravelling* [236] not even the deceivingly simple transport network depictions are served well by arbitrary angular restrictions. For a thorough investigation

of the algorithmic aspects of such \mathcal{C} -oriented schematisations especially for polygons we point the reader to recent work by Meulemans [192].

Circular arcs. Using only circular arcs can provide either a comic-book like quality for smaller circle radii or be almost indistinguishable from gentle curvatures when large radii are employed. As circular arcs are only defined by a single parameter, it is relatively easy to guarantee a conformal transformation, that is, keep the schematisation area-preserving regarding the input. There are several precedents in extant schematised maps and graph drawings, for example network drawings by the artist M. Lombardi or certain chorematic diagrams. They inspired several algorithmic advances such as [290, 292] (also see Chapter 5) for polygons and [91, 92, 98] for graph drawing. More fundamental questions regarding the cognitive dimension of what circular arcs actually accomplish in visual communication have been raised [217, 293], but their appeal is not yet fully understood.

Aesthetic stylisation. Aesthetic stylisation aims at adding some external quality to any other form of schematisation by changing the drawing style from plain vector depictions to some mimicked form. The emotional quality of the mimicked or alluded style is thereby added to the map elements. The link between chosen algorithm to underlying aesthetic and set of tonalities and values remains under-explored as of this writing.

Sketchy. Sketchy aesthetics are conjectured to convey qualities like irreverence, imprecision, transience, intentionalism and should therefore be used accordingly to frame a schematisation's narrative. Several automated techniques that emulate hand-drawn design elements have been developed, for example Wood et al. [317], Fig. 3.6a.

Non-photorealistic rendering. In the wider field of geovisualisation and 3D-models, non-photorealistic computer graphics techniques have been suggested for illustrative, artistic and informal information display [85], Fig. 3.6b.

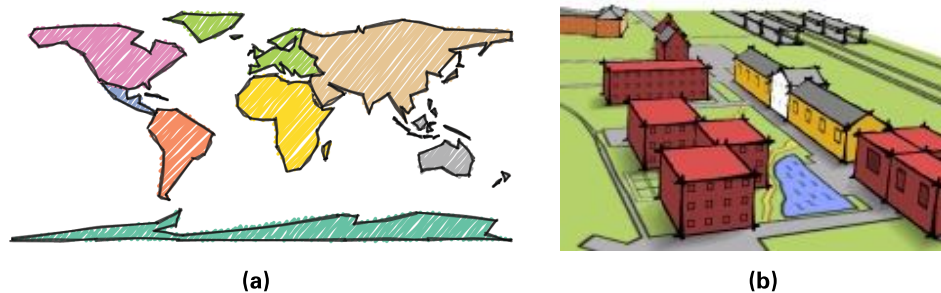


Figure 3.6 (a) Sketchy rendering [317] (b) Non-photorealistic rendering [85].

Collapse. This common generalisation operator denoting the move from a higher dimensional object to a lower dimensional object, for example from polygon to point in the case of churches or whole cities is also a common schematisation operator. Here it can be applied even more radically.

Iconisation. In schematised maps, whole concepts and configurations can be collapsed into a point symbol, just like religious buildings in topographic maps. In schematisation

though, it is not obvious how to automatically derive a high-iconicity point symbol from an arbitrary input instead of simply replacing a footprint with a pre-defined symbol.

Glyphs. Collapsing road polygons to their centreline is a proven technique in topographic mapping. There are some schematisations depicting the very general lay of the land, where mountain ranges are collapsed into glyph-like linework. Taking examples like these as inspiration, we have developed a technique to create schematised maps using glyphs for all polygons that remain effective communication artefacts [294]. This is fully discussed in Chapter 6.

Caricature. In schematisation, caricature encompasses techniques where certain visual characteristics of a single object are emphasised over other parts of the same object or objects. It results in an uneven degree of schematisation for the object as a whole and has no justification from the input geometry alone. Such semantically motivated uneven emphasis is regularly put on elements via:

- (1) highlighting/ignoring certain shape elements such as estuaries
- (2) arrows
- (3) colour variation
- (4) attribute based polygon size variation (resulting in cartograms)
- (5) non-uniform scale (cp. ‘vario-scale in [251] and focus-and-context techniques such as [135, 289])

As the list shows, the algorithmic problems are very different for each of these cases, but our grouping is conceptually motivated, as mentioned above.

The preceding sections have highlighted the conceptual relations between schematisation and cartographic generalisation. In our view, schematisation research can indeed be one way to approach the excluded middle of thematic map generation. In the following section, we provide a real-world example that meshes modelling approaches from schematisation with generalisation approaches successfully producing medium-scale urban areas from real-world data.

3.5 Efficient derivation and caricature of urban settlement boundaries for 1:250k

Urban areas are classical examples of entities that only exist on a certain level of aggregation and detail, that is, scale. Although numerous efforts from several disciplines have been undertaken, the automated derivation of urban settlement boundaries remains an active topic of interest in production as well as research. We present a computationally efficient method for deriving urban areas from authoritative large-scale data and a caricature algorithm aimed at 1:250k maps using a form of angular schematisation.

3.5.1 Introduction and related work

The last decade saw great advances in automated map generalisation for topographic maps, with a strong concentration on scales up to 1:100k [10]. Urban areas, on the other hand, are higher-order geographic phenomena really coming into focus for medium scales starting around 1:200k and smaller. While generating boundaries for urban agglomerations as higher-order phenomena have been researched from different perspectives such as spatial analysis [280] as well as multiple representation [65, 179], their efficient generation still poses problems [129]. Besides efficiency issues during the model generalisation step, the cartographic generalisation for medium-scale urban area polygons has seen little attention so far. Like many other NMAs, Ordnance Survey (OS) produces medium-scale products, namely the Strategi vector dataset and map series that are generated and maintained independently from the most detailed base data. In NATO aligned countries, the JOG as a precursor to vmap level 1 products are an example of these duplicate, legacy efforts [284]. In order to streamline and harmonise production, it is recognised that medium-scale products should be derived from the same base data as the large-scale products in the future. We derive urban area polygons from OS MasterMap data for the use with the Strategi vector dataset.

3.5.2 Approach

Our approach was to first analyse the existing built-up area polygons ($N = 24772$) in the current Strategi dataset (manually generated) and compare them to the available OS MasterMap data. From that analysis, we generated both the potential model of partonomic relationships [65] as well as the constraints for the cartographic generalisation. Our approach to investigate the design principles the human cartographers heeded is similar to our investigation of schematised maps. The insights into the design inform the caricature stage. Before we can caricature, that is schematise, some polygon, we first must build these polygons from the very detailed mosaic of OS MasterMap data.

Analysis

The analysis showed that the feature types comprising urban settlements are buildings, land plots connected to buildings and sealed non-road surfaces. Figure 3.7 shows an example of sealed non-road surfaces in bright red. They are often but not always close to industrial buildings and can be interpreted as a mixture of parking lots, private roads and so forth. A certain part of these surfaces consists of more or less rectangular areas such as parking lots, truck loading zones or manoeuvring areas within non-public compounds. Others are just non-public road-like structures that are very elongated. Whereas the other mentioned feature classes are fully components of what constitutes urban areas, the non-road sealed surfaces must be differentiated in order to avoid the unwanted connection of outlying areas into a more homogeneous built-up area. The example in Fig. 3.7 shows such a case.



Figure 3.7 OS MasterMap data, sealed non-road areas in red. Ordnance Survey Crown Copyright. All rights reserved.

The potential advantages of deriving urban areas directly from small scale data are exemplified by Figure 3.8. The Strategi representation of Halkyn was produced from older material with a different basemap and spatial reference and from already generalised data. It is quite natural that the resulting shapes both show a non-systemic positional offset (i.e. low positional accuracy) and little relation to the current general appearance of the settlement. The cartographic style of the urban regions in the 1:250k product was revealed

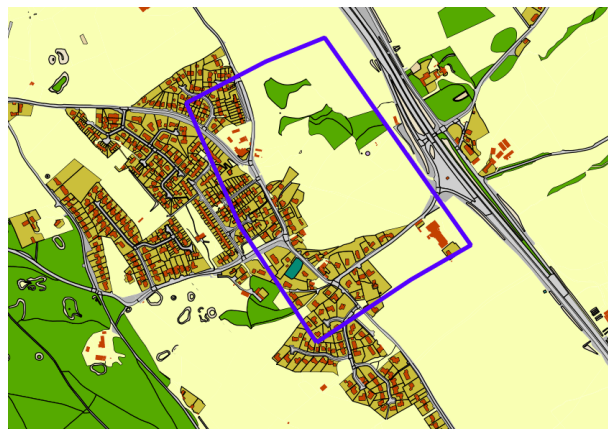


Figure 3.8 OS MasterMap polygons for the Halkyn area, near Liverpool. Current 1:250k Strategi representation of Halkyn in blue. Ordnance Survey Crown Copyright. All rights reserved.

to be very consistent. The measures chosen to constrain the caricature process after model generalisation were the vertex frequency measured in drawing space millimetres (cp. [94], Figure 3.9) and the observed small range of interior angles, see Table 3.1.

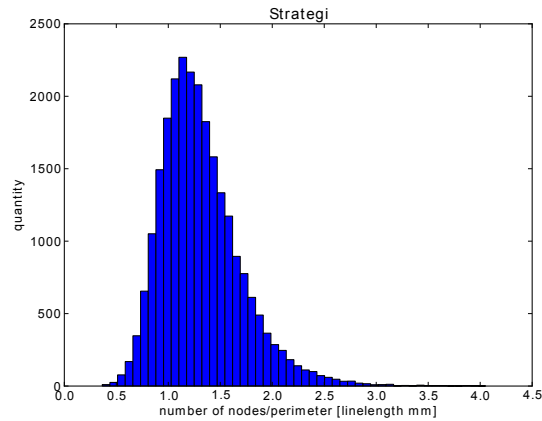


Figure 3.9 Vertex frequency distribution for the current Strategi dataset. Ordnance Survey Crown Copyright. All rights reserved.

Table 3.1 Selected measures for Strategi urban polygons; v/circ is shorthand for vertices over circumference and r^2 is the coefficient of determination between two variables in a linear model.

| N=24772 | min. angle | vert. | circ. | v/circ. |
|---------|------------|-------|--------|---------|
| mean | 74.67 | 16.8 | 13.6 | 1.31 |
| median | 78.53 | 12.00 | 9.57 | 1.26 |
| min | 5.29 | 3.00 | 2.12 | 0.36 |
| max | 129.81 | 2711 | 2840.5 | 4.05 |
| stddev | 13.82 | 26.45 | 25.54 | 0.39 |
| r^2 | - | - | - | 0.96 |

Algorithm

The process is divided into a model generalisation and a cartographic generalisation phase.

Model generalisation. Visual inspection and the quantitative analysis showed the feature types that were most representative of urban regions. These are simply selected from the full data set (Fig. 3.11a and 3.11b). To successfully select the non-road sealed surfaces,

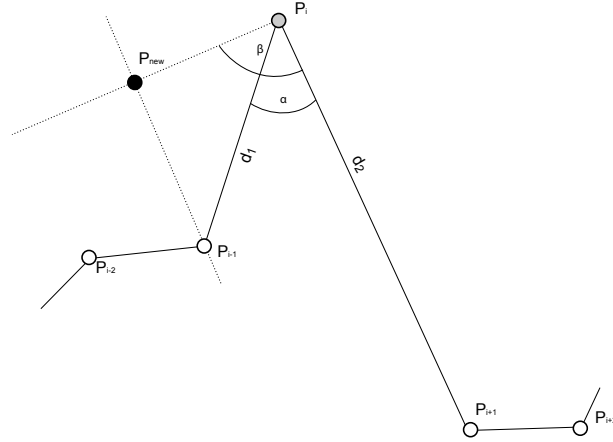


Figure 3.10 Exemplification of the caricature process. With interior angle $\alpha < 70^\circ$, distances to pre- and antecedent vertices are compared. Here, d_1 is shorter and defines the insertion point for P_{New} at $\beta = 90^\circ$ to $\overline{P_i P_{i+1}}$.

the algorithm checks the aspect ratio of the bounding box of each object and compares the bounding boxes area to the polygonal area of the selected object. As a result, we eliminate private roads and similar features but retain the sealed surfaces especially in industrial areas that so much contribute to conceptions of built-up areas. We simply used axis-aligned bounding boxes so that narrow roads are even penalized further compared to a tight-fitting rotated bounding box. The aspect ratio rule is in fact added to catch the road-like surfaces that run parallel to the coordinate axes, that is N-S and E-W (see the long, narrow red shape connecting the eastward settlement and the westward industrial area in Fig. 3.7). All adjacent polygons of the selection are then joined (Fig. 3.11c). While this is a potentially costly operation, we made use of the very efficient `ST_Union` PostGIS function. As the function generates a giant single polygon before we separate the non-adjacent ones, it runs into hard-coded size limitations within the DBMS for a whole Master Map tile. To circumvent these limitations, the tile is cut into four quadratic pieces and joined afterwards. A 15m buffer is applied to join city blocks across streets and close cul-de-sacs (Fig. 3.11d). The polygons above the threshold sizes are then selected as seen in Fig. 3.11e.

Cartographic generalisation. The remaining polygons are now of the correct size and approximate the built-up areas relatively well, but at a much larger scale, i.e. are much too detailed. The governing measure for the scale of urban polygons has been empirically derived to be vertices per millimetre of circumference at the target scale. The need for simplification, that is, removal of vertices, is answered by a self-intersection-free implementation of the Visvalingam-Whyatt algorithm [301]. The algorithm stops when the target complexity, i.e. number of vertices over circumference, has been reached. For

our Rhosesmor example that number was the minimum of eight vertices (Fig. 3.11f). After a maintenance step, the simplified polygons are handed to the caricature algorithm (Fig. 3.11g and 3.11h). This is needed to provide the proper appearance for the visual product. It has been determined that manually created urban areas seldom field interior angles below 70° , whereas the V-W algorithm has the tendency to create rather pointy polygons with acute interior angles. Nevertheless, our V-W implementation produces better input for the caricature step compared to Douglas-Peucker that has a tendency to overreact to elongated shapes. Such elongated shapes are common in urban polygons and the overreaction of D-P was one of the motivations of developing other line simplification algorithms such as V-W for urban areas [302].

The angular schematisation itself detects acute interior angles that need to be replaced. When an acute angle below the chosen threshold is recognized, the algorithm adds a new point to orthogonalize the acute outcrop, see Figure 3.10. The new point's position is constructed via constructing a line through a precedent or antecedent point that runs parallel to the polygon segment connecting the acute point with its antecedent or precedent point, respectively. The choice whether to move backwards or forwards is made based upon which distance is shorter. After each such operation the polygon is checked for validity and repaired if necessary. The algorithm thus is self-intersection free. The newly introduced angles are always orthogonal and thus cannot produce infinite loops. Some clean-up is necessary in post-processing as there are corner-cases which produce very small forms beyond any visibility threshold that need to be removed via a blow and shrink.

Computational complexity

In the following we will discuss asymptotic complexity. The computational complexities of the PostGIS functions that are used would be very laborious to verify, so we work from the general descriptions of their workings to evaluate their asymptotic complexity.

Model generalisation. The selection of the relevant feature classes without using any index has complexity $O(N)$, where N is the number of objects within the database ($> 30,000,000$ for the test dataset). As the construction of an index (for example a B-tree) on the attribute that the selection was based upon is also $O(N \log N)$ and the following selection of k results would take another $O(\log N + k)$ time, we omit indexing the full dataset. With a fully indexed database, that step would thus be possible in $O(\log N + k)$. Cutting up the set into four quadrants currently takes $O(3N)$ time. The quadrants are spatially indexed, which takes $O(N \log N)$ time. Dissolving the polygons that are adjacent is accomplished by using the `ST_Union` function. The current implementation works on geometries without existing topology information. It internally structures the data into an STR-Tree [174] ($O(N \log N)$) and then unions the tree from the bottom up taking $O(N)$ [219]. It is practically the most resource intensive operation of the approach. Buffering adds another $O(N)$ in time complexity as well as the selection of all polygons of a certain size. Uniting the buffered polygons takes $O(N \log N + s)$ time, with s being the number of intersections. The dataset has been so drastically reduced that the further

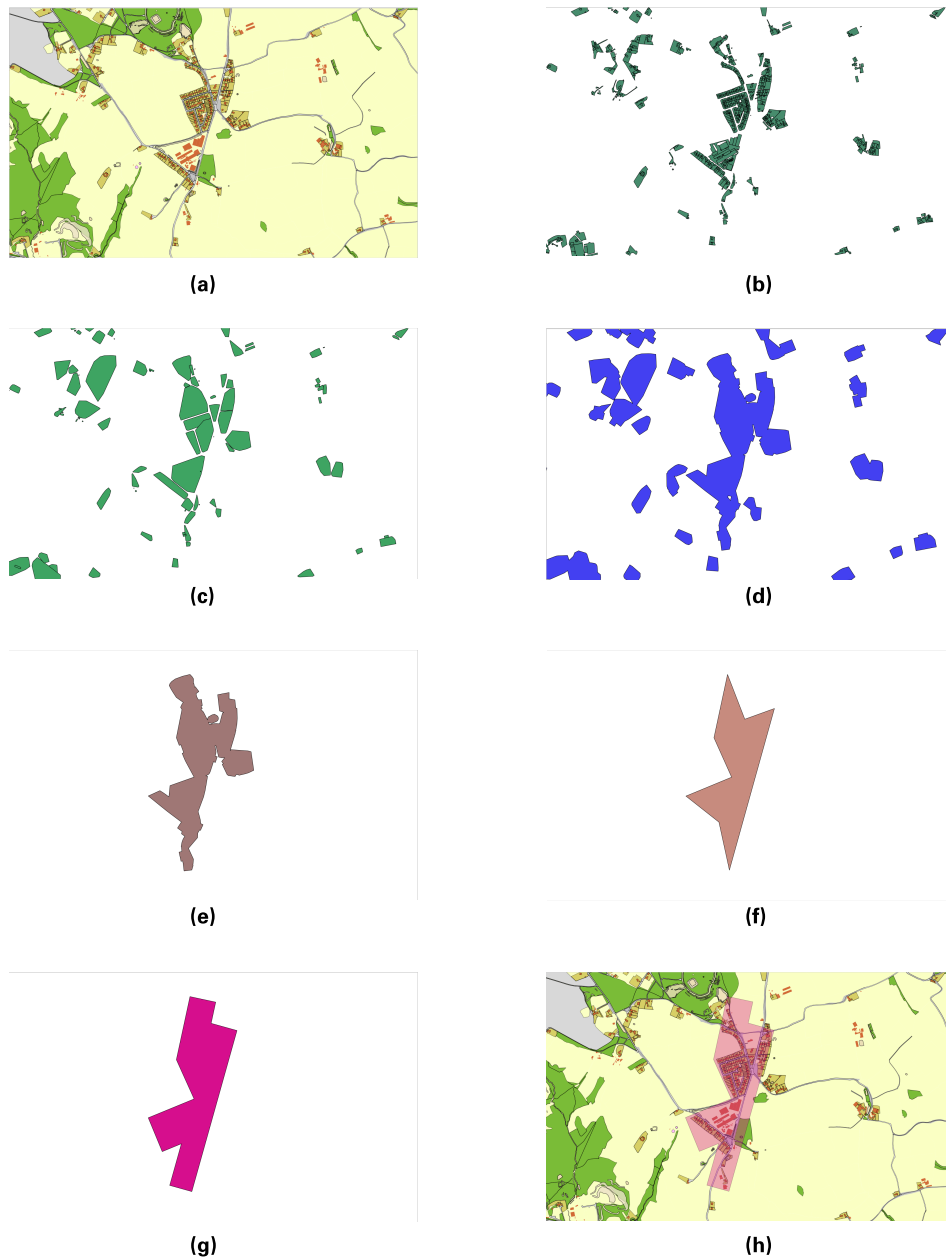


Figure 3.11 (a) OS MasterMap polygons, Rhosesmor area. (b) Selected polygon types. Note the sealed non-road surfaces surrounding the industrial area in the middle triangle. (c) Rhosesmor area after the union steps. (d) Roads are closed and buffered polygons joined. (e) After the selection per minimum size step. (f) Result of the simplification step. (g) Result of the schematisation step. (h) Comparison of output (transparent magenta) with input data. Ordnance Survey Crown Copyright. All rights reserved.

algorithms shall be noted as being dependant on input n representing the vertices of the remaining polygons from the area filter step onwards.

Cartographic generalisation. Our self-intersection free Visvalingam-Whyatt implementation is hard-coded to never decrease the size of a polygon below 8 vertices. It uses the `ST_IsValid` function after each change c for $O((n \cdot c) \cdot n \log n)$ and a PostGIS zero-distance-buffer ($O(n)$) to repair self intersections if needed. The angular schematisation changes each acute angle below the threshold up to the theoretical maximum for the number of possible acute angles of $\frac{n}{2} + 2$. Checking topology and repairing it can happen just as many times and involve manipulation of all vertices of the polygon, i.e. $O((\frac{n}{2} + 2) \cdot n \log n)$. Further repair functions such as shrink and blow and zero-distance-buffer all run in linear time i.e. $O(n)$ and a potential alignment step via the `ST_Snap` function would add $O(n^2)$ time complexity.

The consolidated asymptotic time complexity for the model generalisation step is then:

$$\begin{aligned} O(N) + O(3N) + O(N \log N) + O(N \log N) + O(N) \\ + O(N) + O(N \log N + s) \approx O(N \log N + s) \end{aligned} \quad (3.3)$$

where N is the size of the original input.

The consolidated asymptotic time complexity for cartographic generalisation is then:

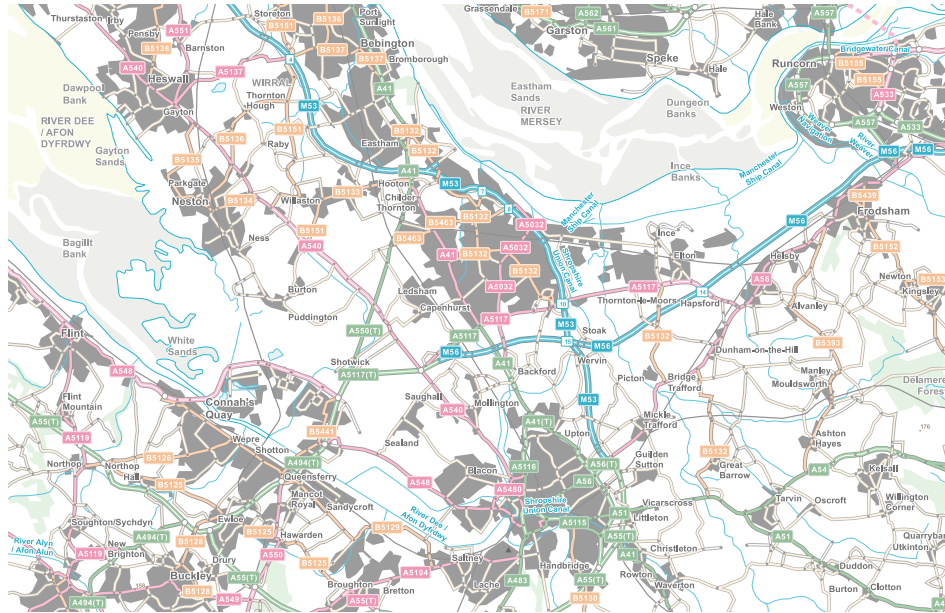
$$\begin{aligned} O(c \cdot n^2 \log n) + O((\frac{n}{2} + 2) \cdot n \log n) \\ + O(n) + O(n^2) \approx O(c \cdot n^2 \log n) \end{aligned} \quad (3.4)$$

where n the much reduced size after model generalisation.

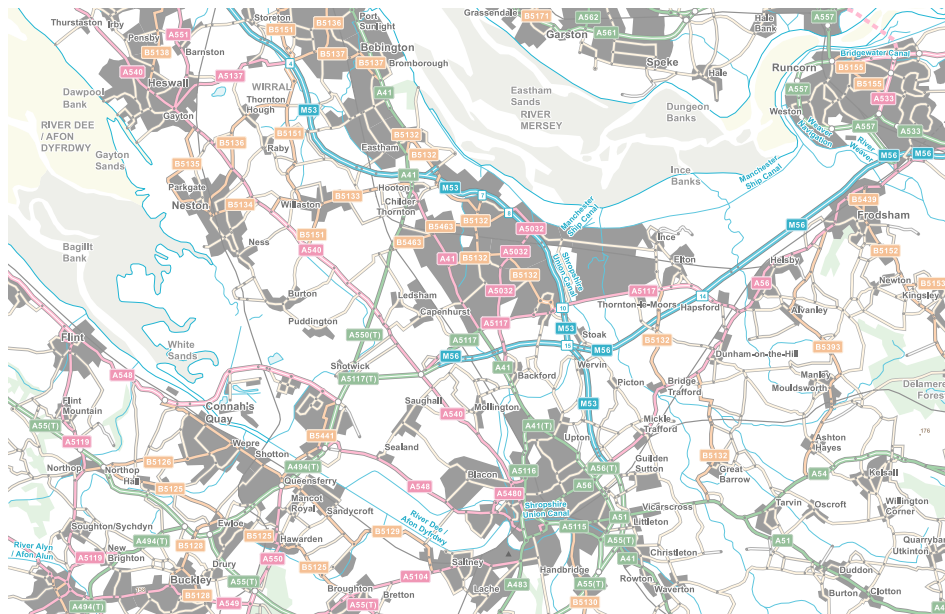
3.5.3 Results

Figure 3.12a shows part of the SJ tile and the resulting urban regions. The depicted urban areas cling closer to built-up areas and are slightly more detailed, especially in regards of what is left out compared to the current Strategi dataset (Fig. 3.12b). To allow a more detailed review of the algorithm's behaviour, we have provided Fig. 3.13. A visual comparison to aerial imagery indicate the resulting shapes are in our opinion indeed good representations of the settlements of the region. As described above, the algorithms can easily be tuned for the desired complexity and inclusion or exclusion of feature classes.

The implemented version of the approach needs 196 minutes on 64bit machines with 8GB of RAM to run the whole process. More than 75% of the time is taken up by the initial data selection and union operations. Afterwards the data size is reduced radically which allows quick repetition of the cartographic generalisation steps to tune the parameters if so desired. The overbearing influence on runtime of the model generalisation is not unexpected. The sheer traversal of the millions of entries of the input compares very unfavourably to the hundreds of polygons handled in the cartographic generalisation stage.



(a)



(b)

Figure 3.12 (a) Urban regions as generated by our approach visualised with ArcGIS in the supplied Strategi style at 1:200000. (b) Current Strategi dataset visualised for comparison. Ordnance Survey Crown Copyright. All rights reserved.

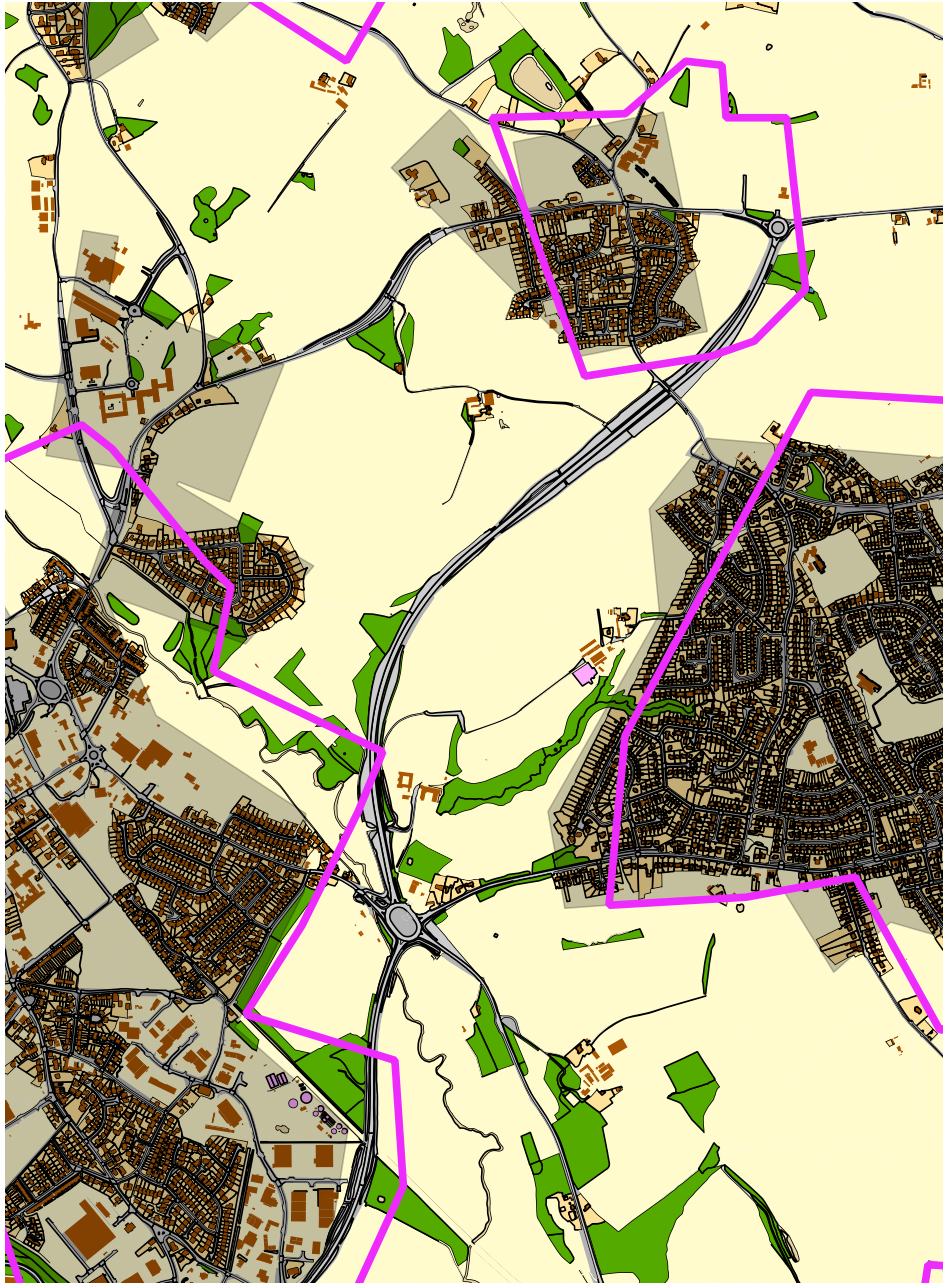


Figure 3.13 Legacy Strategi urban areas in magenta, our results as transparencies at $\approx 1 : 15000$. Ordnance Survey Crown Copyright. All rights reserved.

3.5.4 Summary and outlook

The approach is able to derive visually scale-appropriate urban regions for a 100km Master Map tile within hours. No proprietary software or expensive hardware is needed for that task. The problems of data alignment and settlement subdivision indicate that fresh derivation of relevant features directly from MasterMap data to the Strategi scale is very desirable in the future. Beyond this individual problem, we could show how schematisation and generalisation combine to move forward automated map generation. Furthermore, the use-case shows that with proper analysis and modelling of the cartographic goals, simple modifications of known algorithms can suffice in producing highly functional results.

Chapter 4

Chorematic Diagrams

In August 1980 a French geographer and cartographer published a paper on spatial modelling in geography. He freely mixed and matched structuralist, Marxist, cybernetic and semiologic ideas of the French left's intellectual tradition with quantitative and analytical geographic thoughts from the English speaking world, rightwing geopolitics as well as positivist and landscape-oriented influences from early 20th century geography. In the wake of Francois Mitterand's rise to power, his ideas found institutional and intellectual backing and were instrumental in creating new journals, thousands of maps and dozens of books. These books included a new critical dictionary of geography, several atlases and a re-imagined ten volume *Geographié Universelle* as an homage to Vidal de la Blache. His name is Roger Brunet and his school of thought became known as the *chorématique*. Besides his intellectual influence he was a highly skilled cartographer and created a visual tradition of its own with deep links to his school of thought that even changed EU policy. The resulting cartographic artefacts, the chorematic diagrams, are the subject of investigation of the following two chapters, where we investigate and model them to enable their automated construction.

The scientific background, usage practice, and symbolisation dimension of printed chorematic diagrams are only known superficially and anecdotally. In this chapter, we lay the groundwork for a more complete understanding of chorematic diagrams by examining the institutional and scientific background in which they were developed. We then present a taxonomy of chorematic diagrams, combining findings from the examination of the scientific background with a quantitative analysis and observations on usage practice. The taxonomy is validated in Section 4.3. This taxonomy crucially informs any attempt at automated generation, as different chorematic diagram classes suggest different modes of construction and different degrees of generalisation. The underlying methodology is explained and justified in detail in Section 4.6.

4.1 Chorematic diagrams defined

Roger Brunet developed classes for spatial structures and processes along with a specific way of rendering them graphically [42, 43]. He called them *chorèmes* (eng. *choremes*), a neologism composed of the Greek word $\chi\acute{\omega}\rho\alpha$, meaning space, territory, place and the suffix -ème from theoretical linguistics [43]. The term is to be understood as an analogue to words such as morpheme, phoneme or grapheme, which refer to the smallest linguistic (audible and written respectively) units that carry (semantic) meaning. They were popularized by the work done within the Groupement d'Intérêt Public (GIP) RECLUS, which was founded in 1984 under Brunet's leadership [210]. Their output included many thematic maps, partly or entirely made from chorèmes. Because it were these chorematic diagrams and maps that garnered attention, the term *chorème* became synonymous with a certain style of graphic depiction of geographic space.

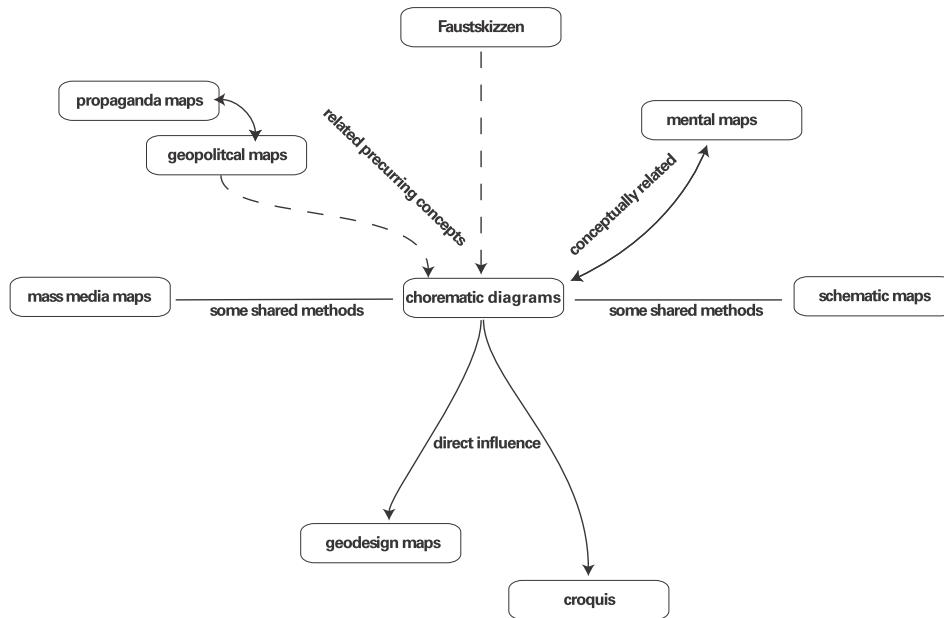


Figure 4.1 Relationships between chorematic diagrams and other schematised maps. Entries are sorted from top to bottom by age.

In order to disentangle the choremes proper from the images containing them, we have adopted the following definition for our objects of interest:

Chorematic diagrams are all those maps and map-like diagrams that use one or more graphical embodiments of the choremes as introduced by Roger Brunet.

The question arises what these choremes then are, which we will answer with a definition provided by Tainz, 2001:

Chorèmes are a tool for the structural and iconic representation of complex geospatial situations. They consist of terms and graphics that largely abstract from actual objects and precise cartographic symbols. Brunet differentiates between seven classes of basic spatial configurations that take different forms for point, line, area or network-based embodiments of these configurations. Each one is linked to an associative and indexical sign for the respective structure or process (Fig. 4.2). Chorematic diagrams can either be maps with additional, highly aggregated layers or map related representations that abstract from the precise topographic and thematic spatial structure. By doing this, the latter enable a high-level comparison of the structures between different regions (abbreviated from [274]).

They are, as per Chapter 3, also specific kind of schematised map. As has been alluded to earlier, chorematic diagrams sit on the crossroads of schematised maps and thematic maps. Their peculiar position within the realm of schematised maps is depicted in Fig. 4.1.¹ Research into chorematic diagrams is as such a very promising endeavour, not only for its own sake, but also in order to produce further insight into the vast expanse of yet unexplored cartographic products between large-scale topographic maps and metro maps.

4.2 Chorematic diagrams explained

As integral part of the analysis of a map series in accordance with Section 4.6, we begin with a discussion of the history of ideas behind the *chorématique* as well as institutional backing and reception. All three definitely influence the goals and make-up of extant chorematic diagrams. As we will later see this is not only crucial for general interpretation, but it provides valuable clues for the unlocking of some of the tacit knowledge underlying the cartographic design (Chapter 5).

Roger Brunet's *chorématique*. Brunet's attempt to map specific graphical expressions to a limited number of recurring geographical structures and dynamics is built upon several influences. The foundation lies in the general belief that geographic space and the human endeavours within it can be modelled at all. In this, Brunet follows Bunge's statement that a purely ideographic approach in geography based on the concept of the uniqueness is a scientific dead-end [47, 58]. Bunge's main inspirations, Thünen and Christaller are main influences in Brunet's view on geography as a science, and so are Hagget and Chorley, who have in turn themselves be inspired by Bunge [40, 41, 42, 46, 47, 121]. A parallel line of inspiration stems from traditions of explaining the world following the *École des Annales* in Braudel's writing and Marxist ideas filtered through Wallerstein's World System Theory [52]. While these influences helped to shape Brunet's view

¹For a tentative comparison of chorematic diagrams with geopolitical and propaganda maps, please see [127]


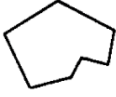






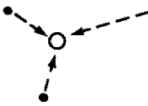



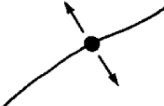

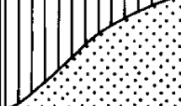

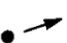

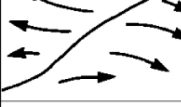

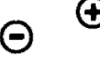







| | Point | Line | Area | Network |
|--|--|---|--|--|
| models of the manner in which a region is subdivided |  chief towns 1 |  adm. boundary 2 |  state, region 3 |  centers, boundaries and polygons 4 |
| models of a region's infrastructure |  node vertex 5 |  lines of communication 6 |  service, irrigation drainage area 7 |  network 8 |
| models of gravity |  satellite points 9 |  lines of gravity 10 |  attraction area 11 |  preferred relationships 12 |
| models of fronts of communication |  passage point 13 |  rupture, interface 14 |  contact areas 15 |  "port" coast base abutment of a bridge 16 |
| models of unilaterally biased movements |  directed movement 17 |  division line 18 |  tendency surfaces 19 |  dissemmetry 20 |
| models of conquest diffusion |  point evolutions 21 |  axes of propagation 22 |  areas of extension 23 |  tissue of change 24 |
| models of hierarchies |  urban pattern 25 |  dependency relationship administrative boundaries 26 |  subset 27 |  linked network 28 |

Figure 4.2 Table of the choremes changed from Brunet [43], english translation from [291]

on models in geography, he was not a strong believer in the superiority of quantitative methods in order to actually find and formulate the governing structures and models of space [41]. His research methods to construct spatial models are strongly influenced by French structuralism and constructivism, systems theory, cybernetics and semiotics, the Chicago school as well as geomorphologic reasoning. Therefore, it might be said that Brunet saw himself as promoting a qualitative and linguistic approach instead of the quantitative and mathematical approaches put forth by Bunge, Haggett and Chorley, but in a complementary rather than renunciative way [47, 50]. In fact, Brunet went on to describe the chorématique he was about to develop as a mediating method between ideographic and nomothetic approaches in geography [42]. While his geographical works were built around his ideas of modelling space and spatial models (cf. [41]), the year 1980 saw the combination of his geographical analysis techniques with a structured graphical sign system (then called chorèmes) in the seminal article *La composition des modèles dans l'analyse spatiale* [42]. This article served as reference and starting point for a stronger emphasis on cartography in French geography, which in turn revitalized geographic research itself [25, 210]. The idea of creating a rigorous sign system for the graphical description of systems is akin to the systemographie approach as laid down by French constructivist and systems theorist Jean-Loius Le Moigne in *La théorie du système général. Théorie de la modélisation* [46, 99]. This sign system (Fig. 4.2) was built and conceptually refined along the lines of Bertin's Semiology of Graphics [28], which is the last major influence leading to the development of choremes that we have identified [43]. In sum, we would like to highlight the fact that Brunet did not create his choremes in a vacuum. They are related to and partially correspond to the taxonomies of spatial processes that have become commonplace in human geography. The prime example being [125] on the geographical side. On the cartographic side he built upon the widely accepted semiology of graphics. Still, we can only make this argument for the outer form of the chorématique. The epistemological dimension of Brunet's modelling approach is idiosyncratic due to its multiple components, as we have shown above. Whether this specific mixture actually is yielding sound results for human geography, is beyond the realm of automated cartography to decide. It is important though, to know these foundations, if we want to understand how existing chorematic diagrams were created. The scepticism towards a dominance of quantitative modelling and the linguistic mindset has direct repercussions for the cartographic representations as we will later see.

GIP-RECLUS and the production of chorematic diagrams. The successful dissemination of chorematic maps throughout French science, administration and schools, is closely linked to the institutional backing Brunet enjoyed in the form of GIP-RECLUS. This Groupement d'intérêt public (Public Interest Group) was christened RECLUS (Réseau d'études des changements dans les localisations et les unités spatiales, Network for the Study of Changes in Localities and Spatial Structure), alluding to Élisée Reclus (1830-1905) himself one of the founding fathers of French geography and main author of the *Nouvelle Géographie universelle* [25]. Before GIP-RECLUS was installed at the Maison de Géographie in Montpellier, France, in 1984, Brunet had worked closely with government institutions. From his chair in Reims, where he had founded the Journal *l'Espace*

géographique in 1972, he was called to become a research director in the CNRS, the French National Committee for Scientific Research in 1976. He left this position to work as scientific councillor for the Ministry of Science and Technology in the Mitterand Administration after Mitterand's election in 1981. With the new administration, new paradigms for spatial planning became relevant, and Brunet proposed the formation of a dedicated and high profile public research institution for human geography, not in Paris, but in southern France. Financing for the six million Francs budget came from CNRS, DATAR (national organisation for spatial planning, re-named DIACT in 2005), ORSTOM (national research organisation for overseas territories, now IRD), IGN (National Geographic Institute), ministries, universities as well as local and regional governments. All this in addition to income generated from government contracts. At its height, more than 50 researchers on-site and 200 collaborators worked for GIP-RECLUS and it was one of the largest research institutions for social sciences in all of France at the time [25, 117, 210]. These resources were used to work on large projects, of which a national atlas of France, a new 10-volume edition of a *Géographie Universelle* (GU) and a new critical Dictionary for geography (*Le Mots de la géographie, dictionnaire critique* 1992 by Brunet, Farras and Théry) left maybe the most lasting impact on French geography and cartography. Brunet was at the centre of most of the projects and saw to it that his particular ideas of modelling and graphic presentation, i.e., the *chorématique*, are presented and used throughout (with some notable exceptions like France in the GU). The full-colour journal *Mappemonde* was established in 1986 with the main purpose of being a vehicle for this marriage of regional analysis and modelling to graphical presentation. Alongside the big projects and the journals *Mappemonde* and *l'Espace géographique* were newsletters, regional and statistical atlases, research documents and spatial strategy papers for government institutions. It was this combination of fundamental research, applied geography, cartographic products, textbooks and government contract work that greatly spread the importance and fame of the *chorématique*, GIP-RECLUS and ultimately Roger Brunet. As the CEO, main visionary as well as researcher, he was in turn propelled to the position of one of the doyens of contemporary French geography. Coinciding with shifting political majorities and ultimately with the end of the Mitterand administration in 1995, funding for GIP-RECLUS was cut prematurely and the organisation disbanded in 1997. Former Members founded the 'Association RECLUS' as a follow-up organisation, the national atlas being finalized in 1999 with legacy funding. The journals continue to be published, with *Mappemonde* switching to pure web publishing in 2004 (since then renamed *M@ppemonde*), and *l'Espace géographique* still in printed form [117].

Reception and debate. The great successes for Brunet, GIP-RECLUS and the *chorématique* were not unilaterally lauded in France. At the height of popularity in the mid-1990s, fundamental criticism was expressed in the geopolitical journal *Hérodote*. The debate took the form of a duel between the journal *Hérodote* and GIP-RECLUS with their central figures Yves Lacoste and Roger Brunet as their respective champions [303]. Regarding the peculiar nature of French geographical journals, Benko and Strohmayr [25] wrote:

The majority of French geographical journals, in other words, functions like a club; quite often the same academic personalities are authors and judges of

articles at the same time. The rate at which members of an editorial board publish in their own journals is consequently rather high;[...].

Such a structure intrinsically favours the personalisation of debates, and it did so in the case of the *chorématique*. Yves Lacoste decided and proclaimed that *Hérodote* as a journal will and does

oppose this dangerous and damaging aberration of geography [169].

The whole debate shall not be re-told here, but several noteworthy points of critique were raised against the *chorématique*.

While these criticisms were aimed at the method in general, a lot of attacks were made at specific maps. Especially the great success of Brunet's work on the spatial structure of France for DATAR, summed up in the famed 'Blue Banana' (for a discussion, see [90, 178], Fig. 1.5), drew criticism from *Hérodote*'s authors. His visions supposedly were that of a 'doom sayer', 'alarmist', brought forth in 'spatial planning lyrics' that implied inevitability, the 'game' of an 'illusionist' [116]. Yves Lacoste's criticism also was approaching the point of calling Brunet a charlatan and pseudo-scientist on grounds of diagnosing an unhealthy urge to oversimplify [168]. This was in line with Lacoste's general disillusionment with and critique of all theoretical models in the social sciences, especially those with an orthodox Marxist foundation [70]. It should be noted, however, that Lacoste himself had the will and plan to reform (French) geography as a scientific discipline and to change geography's role in society via his own geopolitical school of thought. He postulated that geography should face the challenge of interacting more with politics to prepare decision making processes. He also diagnosed the existence, and postulated to make more use of, 'geographic logics'. He saw geographic thought inescapably linked to maps, which should in turn be re-emphasized again, alongside a renaissance of dedicated spatial analysis [167]. Both Brunet and Lacoste also tried to modify the way geography was taught in the French secondary school system and vied for the same audience (geography teachers and non-specialists) with their publications *Mappemonde* and *Hérodote* [70]. Lacoste also was greatly inspired by Élisée Reclus (1830-1905) (the same as that served as a namesake for Brunet's GIP-RECLUS), and saw himself as having continued and systemised Reclus's work [138, 170]. Noting the overlapping ambitions between Brunet and Lacoste makes it plausible to suspect that the methodological debate over *choremes* might have been interwoven with a contest for sovereignty of interpretation in French geography and for the succession to E. Reclus. Returning to *Hérodote*'s critique on Brunet's 'Blue Banana', we can see that the graphical model was successful in conveying the essence of Brunet's analysis. Brunet's analysis indeed became the master narrative for France's elites across the political spectrum [178]. The particular success story of the 'Blue Banana' did not end there. Even after GIP-RECLUS was closed down, the idea remained strong in European spatial planning [90, 103], and via the European Spatial Planning Observation Network of which DIACT is a member, a toned down version of chorematic cartography remains in circulation to this day in EU documents, trickling down into national planning documents. Lacoste's *Hérodote* did not uncover any instances of failed communication via chorematic diagrams. In fact, they

mostly criticised the chorematic map as being too effective in spreading those ideas, because they felt that the analysis itself was wrong or that it was unethical, not so much the mode of presentation. This pattern matches the general undercurrent of the critique: neither the general idea of modelling space, nor the concept of presenting results in high-concept maps was renounced, but the specifics of Brunet's epistemological approach and practice. As such, the debate was mostly one about epistemology in geography rather than cartography. Below we have provided a tabular collection of the main criticism raised, sorted into epistemic, procedural, moral and cartographic criticisms([223, 303]):

Epistemic criticism

- The excessive simplification can lead to a situation in which arguments are not build upon the convergence of facts and observations, but are constructed with arguments pleasing the authorities [116]
- The risk of being caught in a closed system that limits thought and expression [260]
- Pointing to *laws of space* for explanation is as dangerous as invoking *laws of history* in order to push certain viewpoints and derive authority from [168]
- Although it claims to be hypothetic-deductive in nature, many maps are as if they were just automatically generated from statistical data [260]

Procedural criticism

- The terminology surrounding the chorématique is in constant flux, so that one cannot be sure which word means what: *chorème*, *modèle*, *carte-modèle*, *iconic model* have all been used, sometimes for the same things, sometimes for differentiation [303]
- Often, research questions, hypothesis and choice of modelling methods are not discussed satisfactorily [303]
- Sometimes, *model-maps* are not based or related to any *real map*, for example in official documents for spatial planning [260]
- Choremes are called *the alphabet of geography*, but the *alphabets* actually used are inconsistent with each other [260]

Moral criticism

- A pedagogically undesirable development that ignores social questions; *an abstract geometry of lines and points without climate or topography or landscapes...humans are degraded to lowly elementary particles...* [185]
 - Prognoses are alarmistic [116]
-

Cartographic criticism

- Bizarre forms like potatoes, arrows, models, and interfaces are hard to discern and hard to translate into *spatial logic* [168]
 - Chorematic maps work much better and leave little to be desired when used in direct conjunction and comparison with regular maps [260, 303]
 - The chorematic maps themselves are useful tools only as long as the symbols remain decodable and the analysis methods leading to their formulation are transparent [77]
 - Semantic decoding is sometimes hard and needs backing by empirical cartography [274]
-

A sample article. A short example of the typical usage of existing chorematic diagrams is now given. In an article for the GIP-RECLUS journal *Mappemonde*, Didelon [82] examines the actual and projected effects of the Indian government's *Unigauge* railway renovation program on regional disparities in north-western India. Didelon presents the argument, that while there are backwater regions that profit from the program, there are others that are left out of that development. This argument is backed up by a successive row of chorematic diagrams highlighting the salient geographic facts (Fig. 4.3). The first diagram two poles (+ one) introduces the dominant urban centres (Delhi, Bombay and to a lesser degree Ahmedabad) with their respective spheres of influence. The diagram uses the lines of gravity-choreme (Fig. 4.2.10). The second diagram (Fig. 4.3) divides the region into three landscapes with the area-class-choreme (Fig 4.2.3). The railway network hierarchy between national, electrified railway and secondary, regional lines is shown in Fig. 4.3.c, using the network-choreme (Fig 4.2.8). These three diagrams are drawn at the same scale ($\sim 1 : 20,000,000$), and with the same highly generalised territorial outline used as base map, or rather spatial container. In a preceding inset map, the region of interest was introduced to provide the needed spatial context for the reader. The fourth diagram (Fig. 4.3.d) uses an idiosyncratic method to depict some arguments presented at greater length in the article itself, namely, the differences between regions of similar economic development and administrative regions. Administrative information is given via labelling, whereas area-class information is given via exploded-areas and labelling coupled with annotations that need the legend to be understood. As an overlay, the choreme axes of propagation (Fig 4.2.22) communicates that only western Rajasthan receives growth impulses resulting from flow of goods and railway renovation.

4.3 Taxonomy

In this section, we present the compiled results of the analysis of existing chorematic diagrams. Informed by the academic underpinnings of the chorématique as revealed and discussed in chapter 4.2, we first describe the diagrams textually before we delve into the results of the graphical and geometric analysis. We conclude with tests of the presented

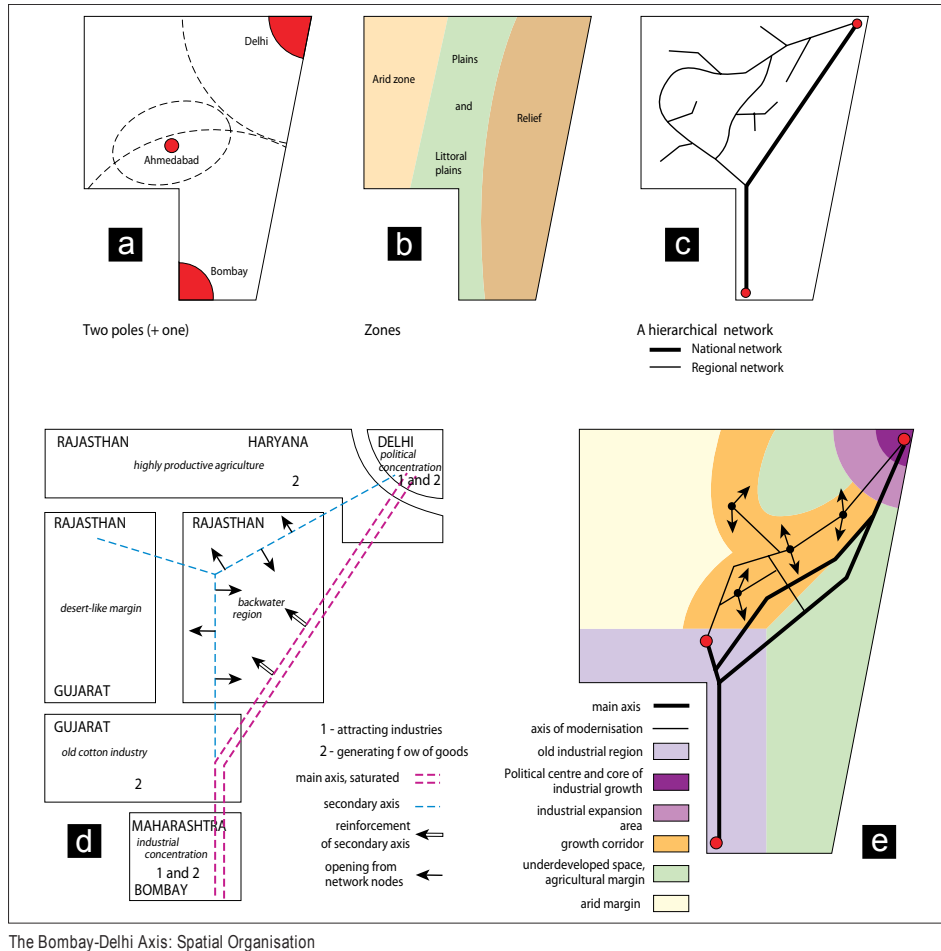


Figure 4.3 A series of chorematic diagrams depicting the development of the railway line in Western Rajasthan. Redrawn and translated from [82].

taxonomy. The individual design rules and necessary sub analyses are exemplified in Chapter 5.

4.3.1 Descriptive analysis

To provide some guidance to the more statistical side of the analysis, we provide a textual description of the taxonomy of chorematic diagrams that was developed according to the methods laid down in Section 4.6. We start with some contextualising general information

on the production and publication environment in which chorematic diagrams dwelled. The last segment in this section presents the taxonomy of chorematic diagrams, being a refined version of the preliminary taxonomy presented in [223].

Publication environment

Chorematic diagrams were published in four major distinctive forms:

- (1) Mappemonde (Journal) cf. Fig. 4.4a
- (2) Atlases cf. Fig. 4.4b
- (3) Monographs cf. Fig. 4.4c and d
- (4) M@ppemonde (Web-Journal).

A complete catalogue of all GIP-RECLUS publications is available under <http://www.mgm.fr/Catalogue.pdf>. In the following we provide some detail about the publications that include chorematic diagrams.



Figure 4.4 Exemplary cover images for the major outlets for chorematic diagrams (a) Mappemonde journal (b) Atlas of China (c) Géographie Universelle d) Monographs.

Mappemonde. The GIP-RECLUS journal Mappemonde was subtitled '*Revue Trimestrielle sur l'Image Géographique et les Formes du Territoire*' which translates to 'Quarterly Journal on Geographic Images and Shapes'. This was their main vehicle for popularisation of the chorématique. It was printed in full colour throughout its publication run and had a non-standard format of $20 \times 26\text{cm}$, slightly smaller than A4.² Articles ran lengths from two to eight pages in average and were each heavily illustrated, not always but often with chorematic diagrams. The Mappemonde articles that include chorematic diagrams are the main object of investigation in this chapter.

Atlases. Starting 1986 GIP-RECLUS set out to publish a series of Atlases using chorematic techniques in varying forms and in cooperation with several publishing houses. The first

²inspection of the originals with cartographic magnifier suggest a standard four-colour CMYK offset print for the majority of volumes

was the multilingual 'Brazil: A chorematical atlas' [277]. The maps and diagrams were solely produced with early map construction software and produced in greytone with a single full red colour tone. The main contents are thematic maps showing quantitative data, accompanied by chorematic diagrams in smaller size to explain processes and configurations in space and time that govern the geography of Brazil. The second in this series of Atlases concentrating on a single country was the *Atlas of Spain* [104]. Fielding the same basic concept, it showed much improved graphical quality, using vector and manual cartographic tools, two colours for most plates as well as several full colour plates. The third atlas produced together with Fayard, the *Atlas on China* [115] shifted emphasis to the conventional thematic maps and only included some chorematic diagrams in order to highlight major spatial structures. The atlases of the series 'Dynamiques du territoire'³ were produced in a similar style to the China atlas, with a higher page count and increasingly sophisticated and complex thematic maps in addition to synoptical chorematic diagrams. Generally speaking, the cartographic traits of the chorematic diagrams in these works are congruent with the general chorematic diagram population.

Monographs. Starting with [43] Brunet irregularly published a loose series of monographs on his own views on cartography and especially geography, for example [46, 50]. Most of these works include a modified version of the basic choreme table and the associated spatial grammar and some exemplary chorematic diagrams. These outings are cartographically unremarkable in the sense that they do not differ too much from the style as is to be encountered in Mappemonde. The pragmatic dimension sometimes did enforce slight changes as for example the restriction to blue, grey and black as colours for [50], Fig. 4.5. Choremes and with them chorematic diagrams became an integral part of the multi volume Brunet-version of the *Géographie Universelle* (GU). Most of the chorematic diagrams encountered in the GU appeared in some form elsewhere, too. Some were mere photographic reproductions, others were redrawn or re-coloured to match the printing process of the GU. As no digital versions were available, they were not analysed further but the results can be safely assumed to be representative of them, too.

M@ppemonde. With the move to an online-only publication, the reprographic pragmatics changed (see Section 4.6) drastically. The chorematic diagrams published since 2004 in M@ppemonde are outside of the scope of this Chapter.

³covering Iran, Russia, Greece, Romania, Brazil, Laos, Thailand and Vietnam in single publications each



Figure 4.5 Example diagram from [50]. Note the use of blue and a colour gradient.

Production environment

Early issues up to 1990 fielded maps and chorematic diagrams created with traditional analogue cartographic techniques. From 1990 onwards that was nearly fully replaced with maps visibly created with vector drawing programs such as Adobe Illustrator. The offering of product specific add-ons [118] suggest indeed that Adobe Illustrator was the software of choice at GIP-RECLUS in the '90s. Even though many new functions and filters are available nowadays, some of which had influence on map aesthetics in general, the style was kept until today, so it seems to be stable since that time.

4.3.2 Taxonomy

One of the core conjectures of our work on chorematic diagrams is the existence of distinct classes of diagrams. Each class is conjectured to have its own purpose and design rules for some or all of its elements. The differences in diagram classes are presented in the form of a taxonomy. A preliminary version of a taxonomy was presented in [223]. The taxonomy as presented below was developed in the iterative procedure described in Section 4.6.

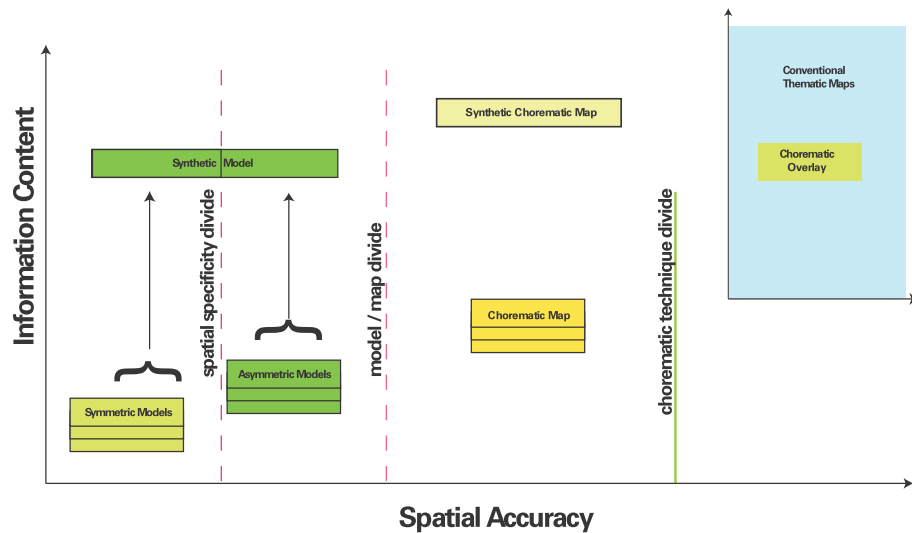


Figure 4.6 Information content and spatial accuracy of the chorematic diagram classes.

The identified classes are:

- (1) Symmetric Chorematic Models = SM
- (2) Asymmetric Chorematic Models = AM
- (3) Synthetic Chorematic Models = SYM
- (4) Chorematic Maps = CM

- (5) Synthetic Chorematic Maps = SCM
- (6) Chorematic Overlays = OV
- (7) Chorotypes
- (8) Chrono-choremes

The general relationship between the classes 1.-6. on the information content-spatial fidelity plane is shown by Fig. 4.6. In the following you can find a concise description of each class.

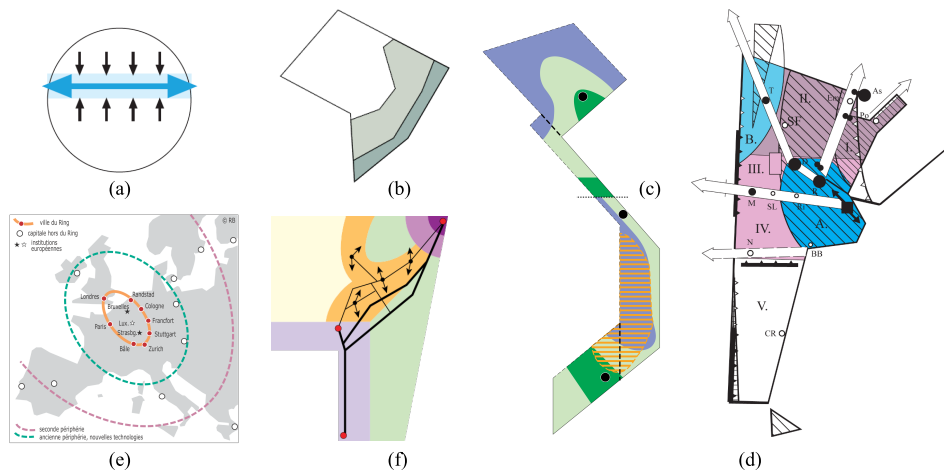


Figure 4.7 (a) Symmetric Model for the Loire basin from [197] (b) Asymmetric Model for Brazil from [277] (c) Chorematic Map for Vietnam from [272] (d) Synthetic Chorematic Map of Argentina from [124] (e) Chorematic Overlay from [48] (f) Synthetic Model for Western Rajasthan from [82].

Symmetric models. Symmetric models are symmetric, undirected simple forms, like a rectangle a circle or a hexagon, with very few thematic layers, often just one (Fig. 4.7a). The simple form is a place holder for the territory under discussion, and the thematic information is arranged in a manner so that the proportional localisation of the phenomenon is shown, i.e. cardinal directions can be discerned. Often, these sparsely layered diagrams are used to introduce the salient components of a regional analysis one by one (similar to Fig.4.3). They are the building blocks of, and lead up to, synthetic models. Deciphering them is of varying difficulty, strongly depending on the connection to the referred geographic space a user is able to make. Only very few symmetric models stand or could stand on their own. For French readers, the hexagon will almost immediately be recognized as representing mainland France, and their knowledge about France topography helps contextualizing the presented information. Nearly all other symmetric models need and are given more context information by additional text and graphics, and are viewed as

being effective communication tools if used in such a manner [260]. Usually the depicted area is highly distorted, and choropleth information is only proportional. They are sometimes used to compare geographic phenomena of areas that have no comparable geometries, all South East Asian countries as hexagons, for example. This highlights their model character. Such comparisons might even violate neighbourhood topology (Fig.5.12).

Asymmetric models. Asymmetric models are diagrams with few thematic layers, and a simple but irregular (directed) polygon as a basemap. They are used nearly interchangeably with symmetric models. Sometimes they are compared to them to highlight how real space is transforming conceptual symmetry (for example Chile as a square versus Chile as an elongated rectangle). Elements are placed with greater accordance to reality. Asymmetric models are not used for the comparison of different regions and are the first degree of spatial specificity in chorematic diagrams (Fig. 4.6).

Synthetic models. Usually the end-result of a regional analysis, synthetic models include all salient geographical phenomena introduced previously during the analysis in the form of single models. They highlight the interaction of the phenomena. Most of the time, the synthetic model is drawn at a larger scale than the preceding models. Their synoptic nature leads to rather busy looking diagrams, which often need a key to be decoded. They have been attacked the most as being arbitrary or indecipherable [168, 274]. Synthetic models are most effective with the single models they are comprised of and the spatial reference made clear. They exist in symmetric as well as asymmetric form (Fig. 4.6).

Chorematic maps. More complex irregular polygons are used as basemaps for this category. The regions are depicted in a manner that allows unambiguous identification for someone who is familiar with their shape. These kinds of maps are also characterized by a thinned out amount of thematic content, compared to regular thematic maps of the same scale. In fact, they are often used as synopses of conventional thematic maps. Chorematic maps are sometimes used in a stand-alone fashion, without accompanying other chorematic diagrams.

Synthetic chorematic maps. They are in principle very much like Synthetic Models, but using the more specific geometries of chorematic maps.

Chorematic overlays. Chorematic Overlays are these kinds of chorematic diagrams, that are formed by placing a chorematic design element, usually some area shape, on a regular thematic base map. As such, they represent the intrusion of chorematic analysis and design into the wider geographic debate. The most famous chorematic diagram, the Blue Banana, belongs to this class.

Chorotype. Chorotypes are those graphical products that abscond the idiographic elements of chorematic diagrams. In a nutshell, they are indistinguishable from general graphical depictions of models in geography. They are so general that they are not maps or diagrams of one particular place anymore. They are outside the scope of this work.

Chorematic icons. Chorematic icons are comparable to the two model classes Symmetric Maps (SM) and Asymmetric Maps (AM), but in a miniaturised form. They were especially used by Théry and Waniez in their works on Brazil [277, 303]. Both works postulate

general spatial patterns, mapped to choremes, which govern a multitude of phenomena in their spatial distribution and dynamism. These patterns are presented as a catalogue of chorematic diagram models (asymmetric in [277], and symmetric in [303]) in the introduction section. The conventional thematic maps in the main body of both works are accompanied by small model icons. The icon models of the patterns that are relevant for the specific spatial distribution depicted in the thematic map appear highlighted. This represents the inverse approach to the mentioned (a)symmetric models being used to display partial analysis results; the quantitative data are checked against choremes, instead of the choremes being presented as a qualitative reduction form of the quantitative data. As only three of the sampled diagrams show chorematic icons and those available in monographs are tied to only two authors and one region of interest, icons were not studied further in this research.

Chrono-choremes. Archaeologist Christophe Batardy [21] is an example for the continued application of the regional analysis and chorematic modelling along Brunets lines, but transposed from geography to modelling the past condition and development in time of a region. Such approaches are subsumed under the labels paleo- or chrono-chorematique [278]. Especially the subject of modelling the development of urban structures across time has gained some interest by a working group of French archaeologists in conjunction with geographers with links to GIP-RECLUS. Several round table meetings have occurred and a special issue of *M@ppemonde* (#100, 4-2010) was dedicated to this area. The cartographic outputs are not unlike those encountered in other areas such as transport or economic geography, where a series of schematisations depict the different development stages of a pertinent spatial system. The urban chrono-choremes specifically attempt to find a common key which is used to depict the different urban regions in a standardised manner [83]. This falls into the time-frame of *M@ppemonde*, many animations and symbols that are very peculiar to urban development are used. Chrono-choremes lie outside the scope of this research.

4.4 Graphical and geometric analysis

For the thorough graphical and geometric analysis, 681 chorematic diagrams from *Mappemonde* were considered. The distribution of diagram classes within that set is documented in table 4.1. It can easily be seen that the Symmetric and Asymmetric classes are the most numerous, accounting for $\sim 76\%$ of all measured diagrams. As has been mentioned, their numerical preponderance is closely linked to their usage as mono-thematic or single-factor depictions. In turn, the other diagram classes are more interesting, as they so far have been more elusive to describe, as well as being those that bear the burden of communicating results instead of intermediate steps in a spatial analysis. We note that a statistically sound number of Synthetic Chorematic Models ($N = 43$) and Chorematic Maps ($N = 88$) is available. In turn, the analysis of the remaining classes leaves some more room for interpretation due to lower sample sizes. In the following we will provide an overview across all classes first, and provide the detail for each individual class later.



Figure 4.8 Example for a common key for urban chrono-choremes [83].

Table 4.1 Distribution of diagram classes within the analysed set.

| Class | Frequency |
|---------------------------|-----------|
| Symmetric Models | 319 |
| Asymmetric Models | 202 |
| Synthetic Models | 43 |
| Chorematic Maps | 88 |
| Synthetic Chorematic Maps | 12 |
| Chorematic Overlays | 14 |
| Unique | 3 |
| Sum | 681 |

4.4.1 Across classes

The summary statistics in table 4.2 provide a first overview of the metric variables that were measured. They present the backdrop against which individual classes can be measured against. Preliminarily, the 'average' chorematic diagram roughly has an Atlas-like

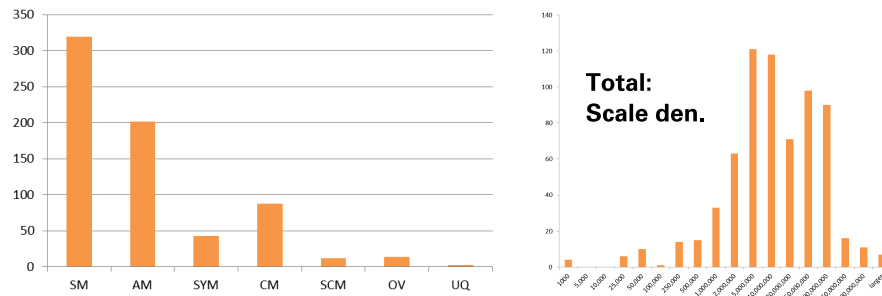


Figure 4.9 Histograms of the distribution of diagram classes and scale denominators within the analysed set.

scale of 1 : 8,000,000, is about 4 by 4 cm in size, features 40cm of linework, yielding a .26Bt complexity rating and is either a rectangle or a polygon with about 6 control points.

Scale. As Table 4.2 indicates, the scale denominator has a very wide range and a large standard deviation. A closer look on the last column of the comprehensive table 4.3 reveals that more than a third (35.25%) of all diagrams fall into the 1:5-10,000,000 scale range, a range typical of Atlases with a much larger mapsize. This scale range is a natural consequence of the chorématique, steering the geographic analysis to larger regions and whole countries, as it is especially common in human geography. That being said, the diagrams are definitely not restricted to such chorographic-geographic subject matters. They are used across all scale ranges from classroom plans to miniature world maps at scales smaller than one to half a billion (Table 4.10).

Lettering. The lettering in chorematic diagrams is usually sparse or non-existent at all. In case of point features, very often only abbreviations are used and neither primitive nor advanced techniques for *Freistellung* (see definitions in Chapter 1) are used. Often special

Table 4.2 Summary statistics for the ratio scaled attributes of all measured diagrams. Abbreviation used are: den. for denominator, w for width, h for height, OLL for object line length, Bt for cartographic line frequency measured in Bertin, cp for control points and col. for colours.

| | scale den. | w[mm] | h[mm] | OLL | Bt | cp | col. |
|---------|-------------|-------|-------|--------|------|------|-------|
| median | 7927350.00 | 38.89 | 37.10 | 391.75 | 0.26 | 4.00 | 6.00 |
| mean | 34339227.69 | 46.87 | 45.17 | 708.72 | 0.32 | 5.14 | 7.91 |
| meandev | 40275777.39 | 23.25 | 21.44 | 578.56 | 0.14 | 2.60 | 4.28 |
| stddev | 80936868.33 | 28.94 | 26.21 | 844.42 | 0.23 | 4.74 | 15.62 |
| cv | 2.36 | 0.62 | 0.58 | 1.19 | 0.72 | 0.92 | 1.97 |

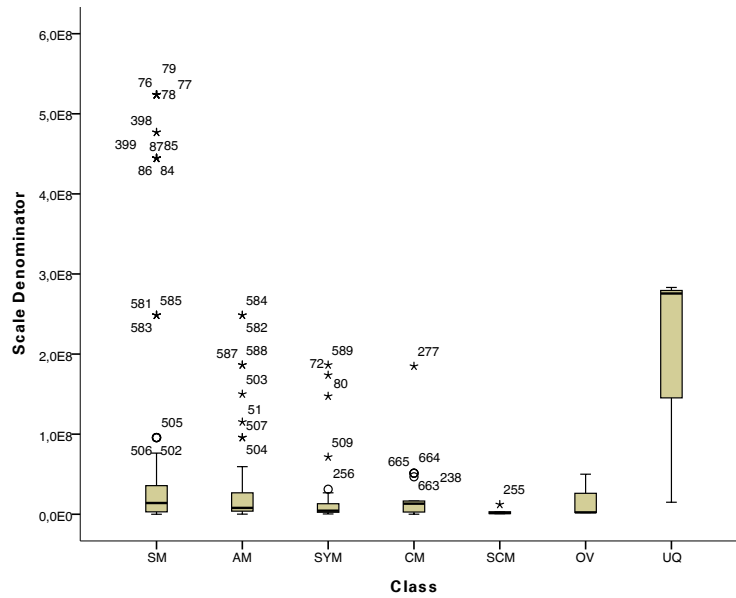


Figure 4.10 Boxplots of the scale denominators.

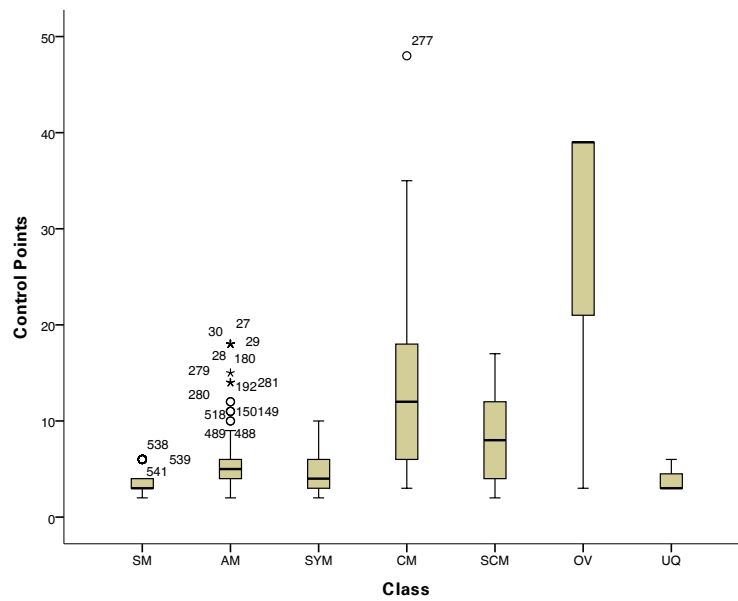


Figure 4.11 Boxplots of the Control Points.

Table 4.3 Absolute and relative occurrence of scales.

| Scale class | SM | | AM | | SYM | | CM | | SCM | | OV | | Total | |
|--------------------|--------------|-------|--------------|-------|--------------|-------|--------------|-------|--------------|-------|--------------|-------|--------------|-------|
| <i>denominator</i> | <i>freq.</i> | % | <i>freq.</i> | % | <i>freq.</i> | % | <i>freq.</i> | % | <i>freq.</i> | % | <i>freq.</i> | % | <i>freq.</i> | % |
| 1,000 | 4 | 1.25 | 0 | 0.00 | 0 | 0.00 | 0 | 0.00 | 0 | 0.00 | 0 | 0.00 | 4 | 0.59 |
| 5,000 | 0 | 0.00 | 0 | 0.00 | 0 | 0.00 | 0 | 0.00 | 0 | 0.00 | 0 | 0.00 | 0 | 0.00 |
| 10,000 | 0 | 0.00 | 0 | 0.00 | 0 | 0.00 | 0 | 0.00 | 0 | 0.00 | 0 | 0.00 | 0 | 0.00 |
| 25,000 | 0 | 0.00 | 0 | 0.00 | 0 | 0.00 | 6 | 6.82 | 0 | 0.00 | 0 | 0.00 | 6 | 0.88 |
| 50,000 | 3 | 0.94 | 0 | 0.00 | 0 | 0.00 | 7 | 7.95 | 0 | 0.00 | 0 | 0.00 | 10 | 1.47 |
| 100,000 | 0 | 0.00 | 0 | 0.00 | 0 | 0.00 | 1 | 1.14 | 0 | 0.00 | 0 | 0.00 | 1 | 0.15 |
| 250,000 | 3 | 0.94 | 8 | 3.96 | 0 | 0.00 | 3 | 3.41 | 0 | 0.00 | 0 | 0.00 | 14 | 2.06 |
| 500,000 | 4 | 1.25 | 4 | 1.98 | 2 | 4.65 | 3 | 3.41 | 2 | 16.67 | 0 | 0.00 | 15 | 2.21 |
| 1,000,000 | 8 | 2.51 | 8 | 3.96 | 4 | 9.30 | 9 | 10.23 | 3 | 25.00 | 1 | 7.14 | 33 | 4.87 |
| 2,000,000 | 30 | 9.40 | 17 | 8.42 | 6 | 13.95 | 5 | 5.68 | 3 | 25.00 | 2 | 14.29 | 63 | 9.29 |
| 5,000,000 | 47 | 14.73 | 50 | 24.75 | 12 | 27.91 | 7 | 7.95 | 2 | 16.67 | 3 | 21.43 | 121 | 17.85 |
| 10,000,000 | 54 | 16.93 | 46 | 22.77 | 8 | 18.60 | 9 | 10.23 | 0 | 0.00 | 1 | 7.14 | 118 | 17.40 |
| 20,000,000 | 37 | 11.60 | 15 | 7.43 | 3 | 6.98 | 15 | 17.05 | 1 | 8.33 | 0 | 0.00 | 71 | 10.47 |
| 50,000,000 | 67 | 21.00 | 21 | 10.40 | 4 | 9.30 | 1 | 1.14 | 0 | 0.00 | 5 | 35.71 | 98 | 14.45 |
| 100,000,000 | 42 | 13.17 | 27 | 13.37 | 1 | 2.33 | 19 | 21.59 | 1 | 8.33 | 0 | 0.00 | 90 | 13.27 |
| 250,000,000 | 4 | 1.25 | 6 | 2.97 | 3 | 6.98 | 1 | 1.14 | 0 | 0.00 | 2 | 14.29 | 16 | 2.36 |
| 500,000,000 | 9 | 2.82 | 0 | 0.00 | 0 | 0.00 | 2 | 2.27 | 0 | 0.00 | 0 | 0.00 | 11 | 1.62 |
| and larger | 7 | 2.19 | 0 | 0.00 | 0 | 0.00 | 0 | 0.00 | 0 | 0.00 | 0 | 0.00 | 7 | 1.03 |
| Sum | 319 | 100 | 202 | 100 | 43 | 100 | 88 | 100 | 12 | 100 | 14 | 100 | 678 | 100 |

Table 4.4 Lettering prevalence among chorematic diagrams.

| Lettering | Frequency | Percent |
|-----------|-----------|---------|
| yes | 313 | 45.96 |
| numbers | 1 | 0.15 |
| no | 367 | 53.98 |

processes, regions or development axes are labelled only. One instance was observed that had a numbered key, a very unusual technique in professional cartography. In total (see table 4.4.1), roughly half of the analysed diagrams show any lettering, whereas the rest is not labelled.

Size. The measured drawing space sizes are testament of the usage nature of chorematic diagrams. The measurements are provided separately for width (Fig. 4.13) and height (Fig 4.14) in millimetres with area available as derivation. While the two dimensions show some variation, there is no clear attributable effect at work beyond the mentioned confinements to an embedding into text or with conventional maps which take up the larger part of the page. The statistics show clearly that chorematic diagrams are never used on their own and consequently never cover a full page in the sampled data. The largest measured size was 188.42cm^2 , comprising 30% of an A4 page's 623.7cm^2 and 36% of a Mappemonde page's 520cm^2 . An informal examination of diagrams that were not included in this stage of measurement suggest they adhere to this principle too. A to-scale visualisation of the encountered dimensions is shown in Fig. 4.12. Also note that there is a tendency for an $\frac{\text{width}}{\text{height}}$ aspect ratio slightly below 1.0, presumably an artefact of the portrait orientation of Mappemonde and all other evaluated GIP-RECLUS sources.

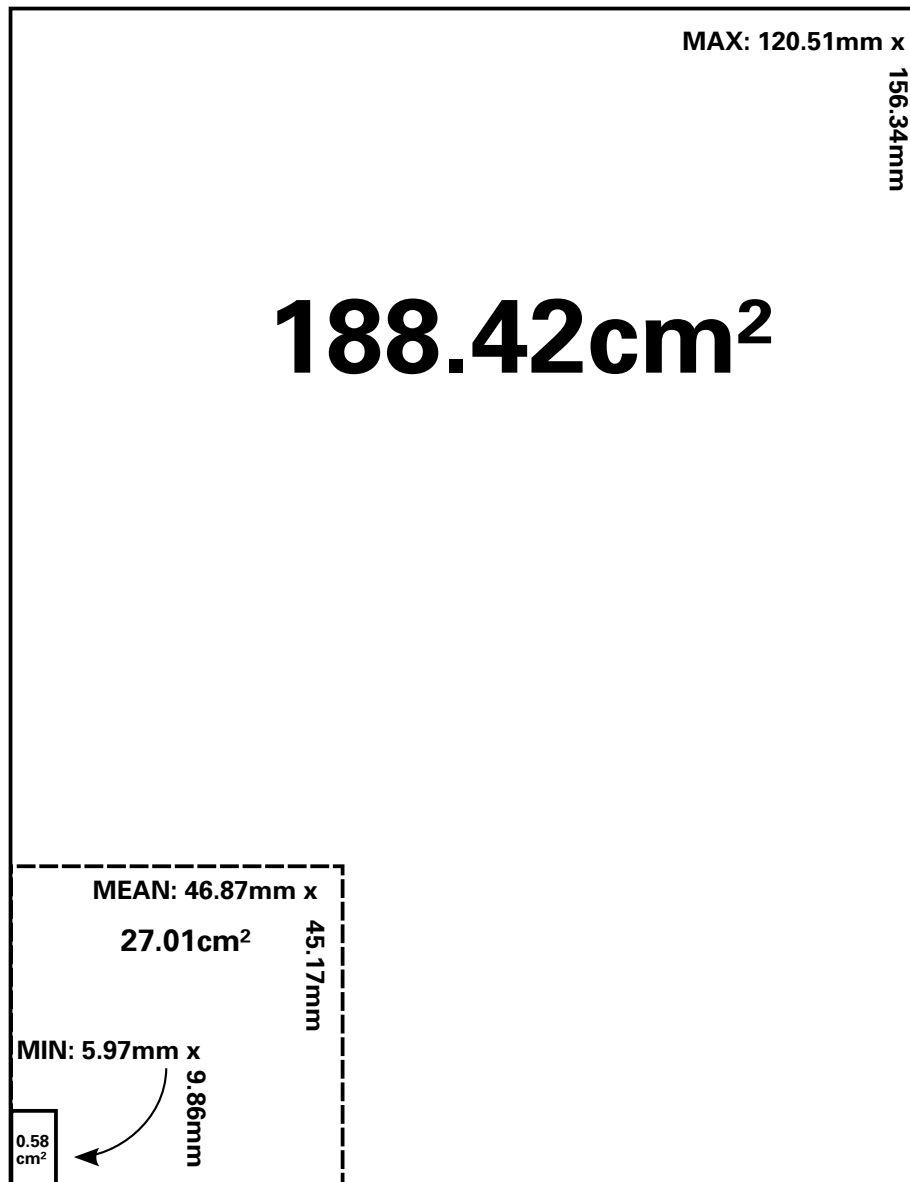


Figure 4.12 Maximum, minimum area values and mean width and height visualised.

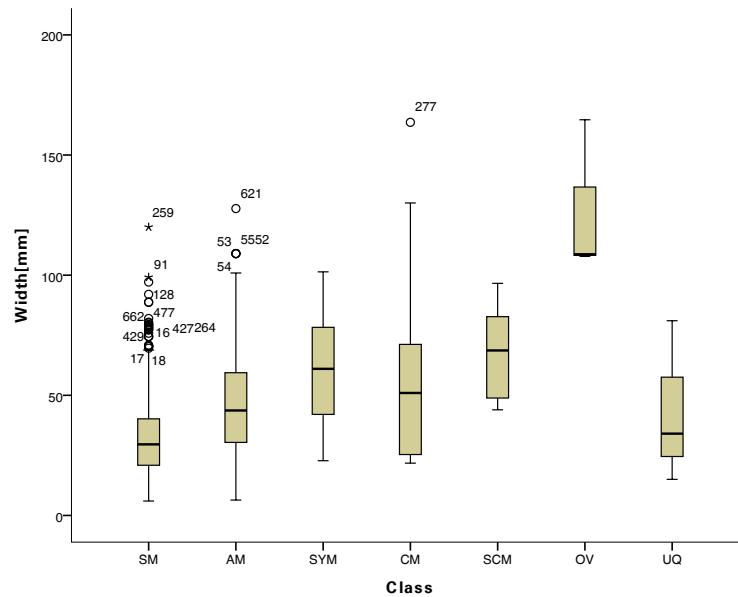


Figure 4.13 Boxplots of the widths.

Complexity. The complexity was measured both by absolute information content in Object Line Length (OLL) (Table 4.17) as well as the complexity measure Bertin [Bt] (Table 4.16) as explained in Chapter 3. The sampled diagrams show great similarity in their Bt score, exemplified by the narrow coefficient of variation of 0.72. This is testament to their nature as schematisations. The mean value of $0.32Bt$ together with the stddev of $0.23Bt$ characterise chorematic diagrams as being of general lower complexity than both topographic maps as well as thematic maps with a regular, non-schematised base map. The total OLL-values vary slightly more, with a coefficient of variation of 1.19 from the mean of $708.72mm$ and a stddev of $844.42mm$. This OLL length is directly interpretable as amount of cartographic vector graphic elements in chorematic diagrams being very light in comparison to regular maps. The bigger spread of OLL is a function of the variation in absolute size and the split between the analytic and the synthetic diagram classes, as will be discussed for the individual classes. The classes 1.-6. have a monotonously rising mean in absolute information content as measured in OLL.

Outline types. The unorthodox presentation of geometries is one of the most peculiar visual characteristics of chorematic diagrams. Here, the biggest attention is drawn to the strongly schematised representation of territorial outlines. As has been mentioned before, the literature so far has only provided anecdotal evidence about this element of cartographic design. Table 4.5 shows the absolute and relative distribution of outline types respectively. The most commonly occurring outline types in *Inselkarten* are circles ($n = 76 \rightarrow 11\%$), polygons ($n = 128 \rightarrow 19\%$) and rectangles ($n = 154 \rightarrow 23\%$),

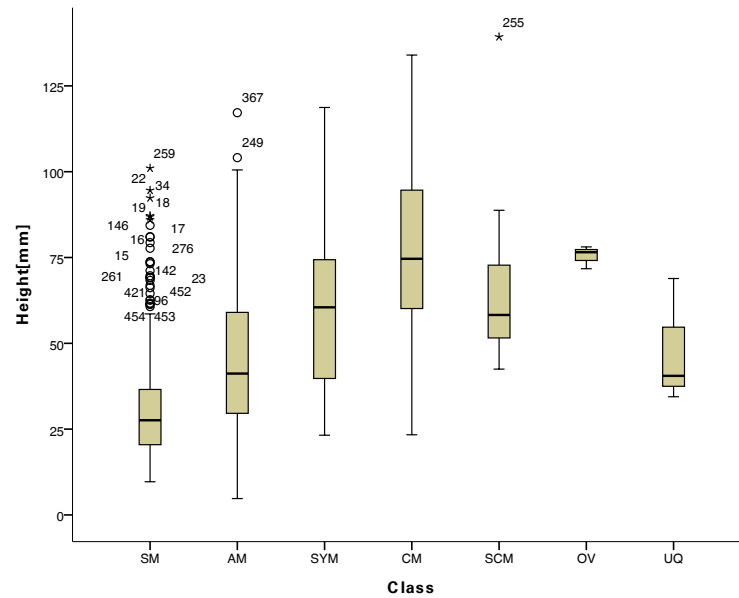


Figure 4.14 Boxplots of the heights.

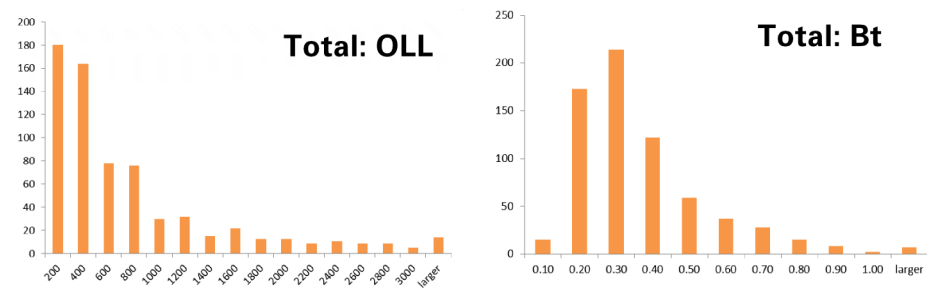


Figure 4.15 Histograms of the object line length and cartographic line frequency over all classes.

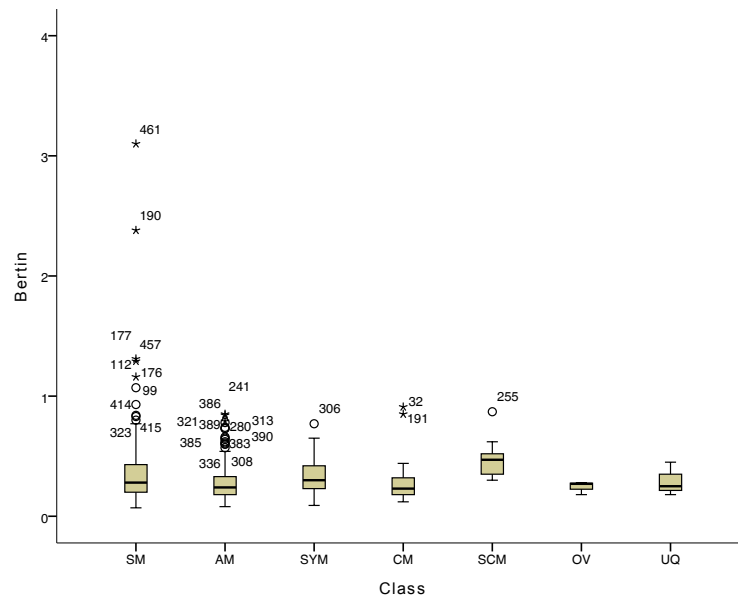


Figure 4.16 Boxplots of the complexity measure Bertin.

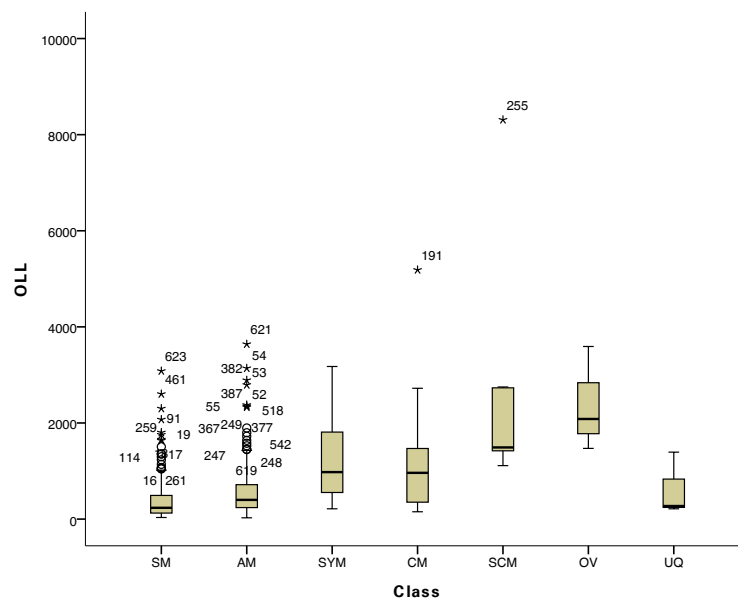


Figure 4.17 Boxplots of the information content measure OLL.

Table 4.5 Absolute and relative frequency of outline types.

| Class | SM | AM | SYM | CM | SCM | OV | Total |
|--------------------|--------------|--------------|--------------|--------------|--------------|--------------|--------------|
| Circle | 60 | 7 | 6 | 1 | 2 | | 76 |
| Ellipse | 30 | 2 | 1 | | | 1 | 34 |
| Square | 19 | | 1 | | | | 20 |
| Rectangle | 138 | 1 | 10 | 1 | 2 | | 154 |
| Triangle | 10 | 6 | 5 | | | | 21 |
| Hexagon | 38 | | 3 | | | | 42 |
| Polygon | | 92 | 6 | 26 | 1 | 3 | 128 |
| Circular arc | | 24 | 1 | | | | 25 |
| Curved | | 26 | 5 | 9 | 4 | | 44 |
| Overlay | | | | | | 2 | 2 |
| <i>Rahmenkarte</i> | 24 | 44 | 5 | 51 | 3 | 8 | 135 |
| Sum | 319 | 202 | 43 | 88 | 12 | 14 | 681 |
| | % | % | % | % | % | % | % |
| Circle | 18.81 | 3.47 | 13.95 | 1.14 | 16.67 | | 11.16 |
| Ellipse | 9.40 | 0.99 | 2.33 | | | 7.14 | 4.99 |
| Square | 5.96 | | 2.33 | | | | 2.94 |
| Rectangle | 43.26 | 0.50 | 23.26 | 1.14 | 16.67 | | 22.61 |
| Triangle | 3.13 | 2.97 | 11.63 | | | | 3.08 |
| Hexagon | 11.91 | | 6.98 | | | | 6.17 |
| Polygon | | 45.54 | 13.95 | 29.55 | 8.33 | 21.43 | 18.80 |
| Circular arc | | 11.88 | 2.33 | | | | 3.67 |
| Curved | | 12.87 | 11.63 | 10.23 | 33.33 | | 6.46 |
| Overlay | | | | | | 14.29 | 0.29 |
| <i>Rahmenkarte</i> | 7.52 | 21.78 | 11.63 | 57.95 | 25.00 | 57.14 | 19.82 |
| Sum | 100.00 | 100.00 | 100.00 | 100.00 | 100.00 | 100.00 | 100.00 |

comprising a total of more than half ($n = 358 \rightarrow 53\%$) of the sampled diagrams. Roughly a fifth ($n = 135 \rightarrow 20\%$) of the diagrams are *Rahmenkarten*.

The substantive differences in outline choice also reflect back on the number of control points used per outline, as Table 4.11 shows.

Symbolisation. The choice of cartographic symbols used for chorematic diagrams appears to be relatively limited. Table 4.6 shows the absolute occurrence and table 4.7 the relative frequencies of symbol types used. The most profound overall observation though, is the utter lack of any kind of symbols with a high *iconicity* [32] as well as quantitative symbolisation, both of which are staples of regular maps. Instead, the same basic geometric figures are used for the wide variety of subject matters encountered. Of these basic geometric symbols, a point symbolisation by circles is the single most common element of chorematic diagrams with 60% of all diagrams using them. The most important linear

elements are PAT L (pattern variations on lines) (37%) for static elements and the usage of arrows for many kinds of dynamism (56%).

Table 4.6 Absolute frequencies of symbolisation types. Not that the sums are larger than the number of maps per class, as maps often field multiple symbolisations. The Abbreviations are explained in Tab. 4.26

| | Symbology | SM | AM | SYM | CM | SCM | OV | Total |
|--------------|-------------------|------|------|------|------|------|------|-------|
| Point | +- | 38 | 10 | 9 | 11 | 2 | 1 | 71 |
| | <i>circles</i> | 171 | 118 | 33 | 63 | 12 | 10 | 407 |
| | <i>FO P</i> | 23 | 18 | 9 | 21 | 4 | 5 | 80 |
| | <i>squares</i> | 23 | 18 | 9 | 7 | | 3 | 60 |
| | <i>hexagon</i> | 2 | 1 | | | | | 3 |
| | <i>triangles</i> | 4 | 7 | 2 | 7 | 2 | | 22 |
| | | | | | | | | |
| Line | <i>CA L</i> | 1 | | 1 | 1 | | | 3 |
| | <i>curved L</i> | 29 | 24 | 4 | 7 | 4 | | 68 |
| | <i>FO L</i> | 23 | 13 | 9 | 7 | 5 | 1 | 58 |
| | <i>L</i> | 30 | 37 | 5 | 19 | 4 | 3 | 98 |
| | <i>PAT L</i> | 103 | 65 | 27 | 36 | 9 | 8 | 248 |
| | <i>poly L</i> | | 9 | | | | | 9 |
| | <i>arrow</i> | 157 | 111 | 38 | 57 | 10 | 7 | 380 |
| Area | <i>PAT A</i> | 33 | 27 | 15 | 1 | 7 | 6 | 89 |
| | <i>FO A</i> | 1 | 5 | 2 | | | 1 | 9 |
| | <i>ellipse</i> | 49 | 21 | 9 | 19 | 1 | 5 | 104 |
| | <i>rectangles</i> | 29 | 3 | 1 | | | | 33 |
| | <i>gradient</i> | 4 | 6 | 2 | 1 | | | 13 |
| Subd. | <i>hexali.SD</i> | | 7 | | | | | 7 |
| | <i>L SD</i> | 3 | 3 | | | | | 6 |
| | <i>curved SD</i> | | 50 | 19 | 19 | 7 | 8 | 103 |
| | <i>CA SD</i> | 25 | 15 | 3 | 4 | | | 47 |
| | <i>poly SD</i> | 38 | 26 | 8 | 27 | | 3 | 102 |
| | <i>rect SD</i> | 31 | | 4 | 17 | 1 | | 53 |
| Misc. | <i>icons</i> | 2 | | 1 | | | | 3 |
| | \sum | 817 | 594 | 209 | 324 | 68 | 61 | 2073 |
| | \emptyset | 2.56 | 2.94 | 4.86 | 3.68 | 5.67 | 4.36 | 3.06 |

4.4.2 Symmetric chorematic models

As a consequence of how the diagrams were assigned to their classes, the most characteristic feature of SM is the predominance on symmetric simple geometric forms used as

Table 4.7 Relative frequency of occurring symbolisations. Note that the relative frequencies add up to more than 100% per class, as a single map can field multiple symbolisation types. The numbers are relative to the number of maps in each class, i.e. 58% of all Assymmetric Models use circles as part of their point symbols.

| Symbology | | SM | AM | SYM | CM | SCM | OV | Total |
|--------------|-------------------|--------------|--------------|--------------|--------------|---------------|--------------|--------------|
| Point | + - | 11.91 | 4.95 | 20.93 | 12.50 | 16.67 | 7.14 | 10.47 |
| | <i>circles</i> | 53.61 | 58.42 | 76.74 | 71.59 | 100.00 | 71.43 | 60.03 |
| | <i>FO P</i> | 7.21 | 8.91 | 20.93 | 23.86 | 33.33 | 35.71 | 11.80 |
| | <i>squares</i> | 7.21 | 8.91 | 20.93 | 7.95 | | 21.43 | 8.85 |
| | <i>hexagon</i> | 0.63 | 0.50 | | | | | 0.44 |
| | <i>triangles</i> | 1.25 | 3.47 | 4.65 | 7.95 | 16.67 | | 3.24 |
| | | | | | | | | |
| Line | <i>CA L</i> | 0.31 | | 2.33 | 1.14 | | | 0.44 |
| | <i>curved L</i> | 9.09 | 11.88 | 9.30 | 7.95 | 33.33 | | 10.03 |
| | <i>FO L</i> | 7.21 | 6.44 | 20.93 | 7.95 | 41.67 | 7.14 | 8.55 |
| | <i>L</i> | 9.40 | 18.32 | 11.63 | 21.59 | 33.33 | 21.43 | 14.45 |
| | <i>PAT L</i> | 32.29 | 32.18 | 62.79 | 40.91 | 75.00 | 57.14 | 36.58 |
| | <i>poly L</i> | | 4.46 | | | | | 1.33 |
| | <i>arrow</i> | 49.22 | 54.95 | 88.37 | 64.77 | 83.33 | 50.00 | 56.05 |
| Area | <i>PAT A</i> | 10.34 | 13.37 | 34.88 | 1.14 | 58.33 | 42.86 | 13.13 |
| | <i>FO A</i> | 0.31 | 2.48 | 4.65 | | | 7.14 | 1.33 |
| | <i>ellipse</i> | 15.36 | 10.40 | 20.93 | 21.59 | 8.33 | 35.71 | 15.34 |
| | <i>rectangles</i> | 9.09 | 1.49 | 2.33 | | | | 4.87 |
| | <i>gradient</i> | 1.25 | 2.97 | 4.65 | 1.14 | | | 1.92 |
| Subd. | <i>hexali. SD</i> | | 3.47 | | | | | 1.03 |
| | <i>L SD</i> | 0.94 | 1.49 | | | | | 0.88 |
| | <i>curved SD</i> | | 24.75 | 44.19 | 21.59 | 58.33 | 57.14 | 15.19 |
| | <i>CA SD</i> | 7.84 | 7.43 | 6.98 | 4.55 | | | 6.93 |
| | <i>poly SD</i> | 11.91 | 12.87 | 18.60 | 30.68 | | 21.43 | 15.04 |
| | <i>rect SD</i> | 9.72 | | 9.30 | 19.32 | 8.33 | | 7.82 |
| | | | | | | | | |
| Misc. | <i>icons</i> | 0.63 | | 2.33 | | | | 0.44 |

territorial outlines. Circles (19%) and rectangles (43%) alone comprise 62% of all observed SM outlines as shown by Table 4.5. In fact, 138 of the grand total of 154 observed occurrences (= 87%) of rectangles used as outlines are found with SM-class diagrams. Succinctly, the mean number of control points measured as (3.47) is the lowest of any class (Table 4.8). They also have the lowest mean size and the lowest mean information content of all measured classes. These observations correspond with the general description and their usage situation as single factor elements leading up to a synthetic map. In the same way we can interpret the under representation of arrows (*SM* : 49% vs.

Total : 56%). Following the chorématique, arrows are used to describe more complex processes and dynamisms that are often shown at later stages of the geographic argument. Their mono-thematic usage is further documented in the negligible use of subdivisions ($< \frac{1}{3}$), see Table 4.7. Moreover, the subdivision symbolisations that are more spatially specific such as curved subdivisions are sparingly used, if at all. Symmetric chorematic models do show a relatively high mean of cartographic complexity ($0.36Bt$) and the highest stddev ($0.29Bt$) of all classes. This corresponds to notions that SM are perceived as being the hardest to decode.

Table 4.8 Summary statistics for Symmetric Models

| $N = 319$ | scale den. | w[mm] | h[mm] | OLL | Bt | cp | col. |
|-----------|--------------|-------|-------|--------|------|------|------|
| median | 11268938.00 | 28.27 | 26.99 | 228.54 | 0.28 | 3.00 | 5.00 |
| mean | 46296385.87 | 33.16 | 31.74 | 365.56 | 0.36 | 3.47 | 5.49 |
| meandev | 54687458.22 | 14.04 | 12.72 | 271.51 | 0.17 | 0.97 | 2.28 |
| stddev | 106285269.02 | 19.20 | 17.51 | 417.61 | 0.29 | 1.20 | 3.54 |
| cv | 2.30 | 0.58 | 0.55 | 1.14 | 0.81 | 0.35 | 0.64 |

4.4.3 Asymmetric chorematic models

Asymmetric chorematic models derive their name from their predominant outline type, namely irregular polygons without axis of symmetry in the plane. A total of 70% ($n = 142$) AMs use some form of polygon, be it straight-line (46%) or composed from circular arcs (11.88%) or Bézier curves (13%). The higher spatial specificity warrants a higher mean value (5.92) for control points compared to SMs. The slight increase in spatial specificity manifests itself in the increased usage of more complex subdivision symbolisation. A total of 45% of all AMs use either Bézier (25%), circular arc (7%) or straight-line (13%) curves for demarcation of subdivisions. In general, the AM classed diagrams are mostly as sparse in symbol usage as SMs ($\emptyset 2.94$ symbol types per diagram, see Table 4.6) and succinctly show mostly sub-average relative occurrences per symbol type (Table 4.7). The extreme schematisation that allow SMs to display the whole world at scales smaller than 1 : 250000000 was not recorded for AMs (Table 4.3). The lower mean value of 1 : 200000000 is a function of this lack of outliers that are uniquely present with SMs (Fig. 4.10 and Table 4.9).

4.4.4 Synthetic chorematic models

Synthetic chorematic models usually share their territorial outlines with the SMs or AMs they are a synopsis of. Thus the relative frequencies of outline types is a function of the union of the distributions of SMs and AMs and unremarkable different from the total distributions (Table 4.5). Succinctly, the mean number of control points of 4.42 is close to being the average of the CPs recorded for SM and AM classed diagrams. Their main characteristics are the increased mean size and significantly increased absolute information

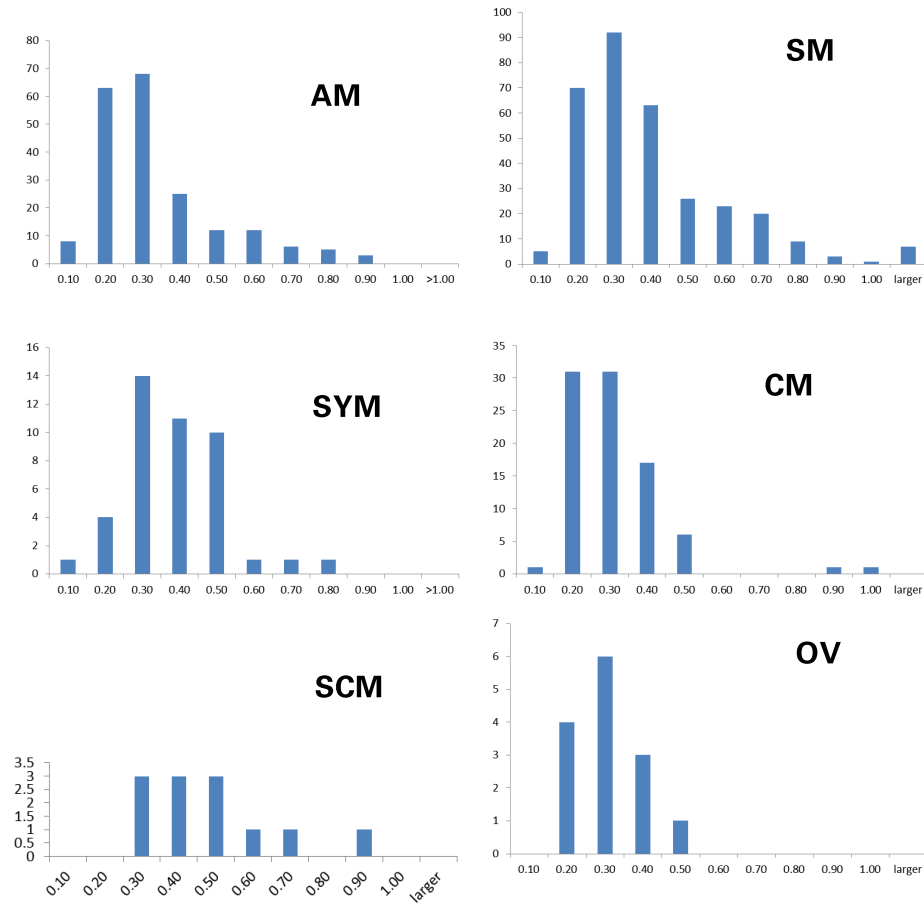


Figure 4.18 Histograms of the measured cartographic line frequency in Bt for the six discussed diagram classes.

Table 4.9 Summary statistics for Asymmetric Models.

| $N = 202$ | scale den. | w[mm] | h[mm] | OLL | Bt | cp | col. |
|-----------|-------------|-------|-------|--------|------|------|------|
| median | 7883675.00 | 44.78 | 42.78 | 431.64 | 0.24 | 5.00 | 6.00 |
| mean | 21021143.12 | 47.74 | 45.44 | 597.99 | 0.28 | 5.92 | 6.43 |
| meandev | 23041190.46 | 19.77 | 16.88 | 386.25 | 0.12 | 2.32 | 2.57 |
| stddev | 36762491.48 | 24.76 | 21.63 | 578.46 | 0.16 | 3.52 | 3.50 |
| cv | 1.75 | 0.52 | 0.48 | 0.97 | 0.57 | 0.59 | 0.54 |

content OLL of $1225.9mm$ (Table 4.10), a positive change of $\Delta = 627.3mm$ compared to AMs which constitutes more than double the mean OLL value Table 4.17. The size

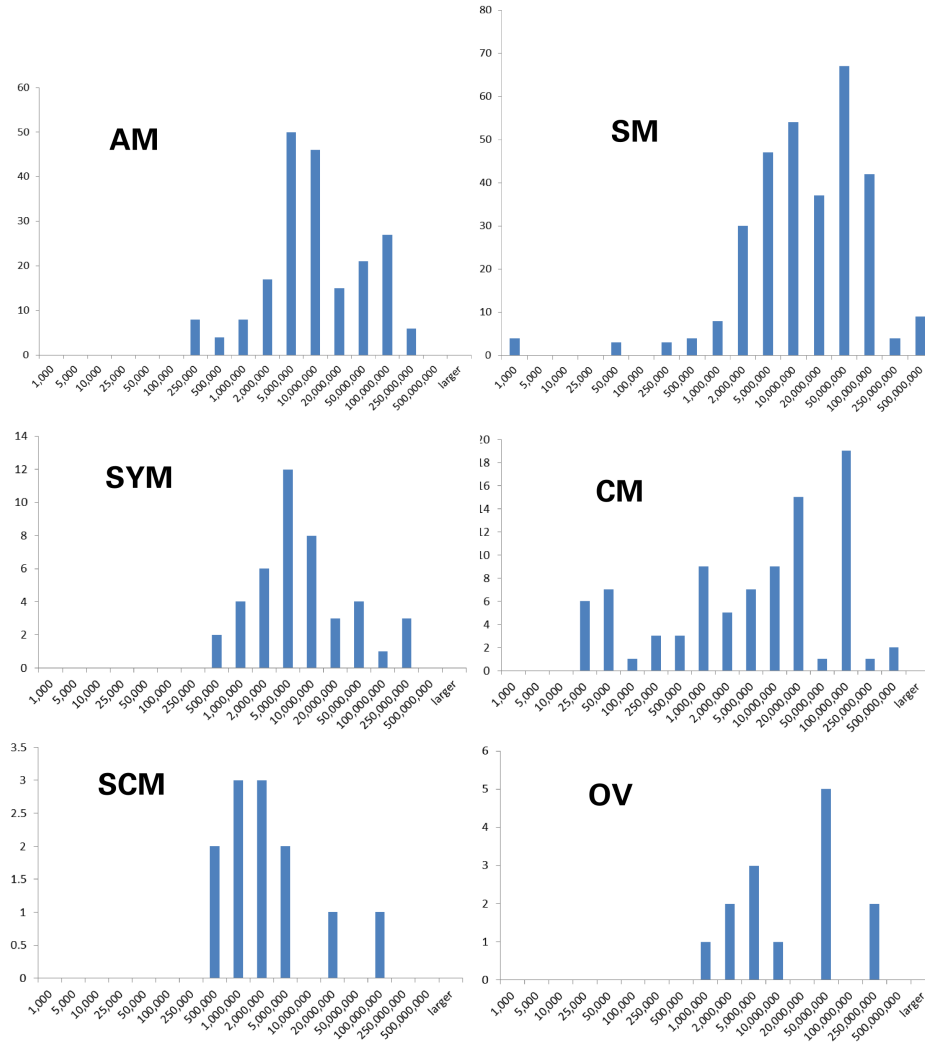


Figure 4.19 Histograms of the measured scale denominators for the six discussed diagram classes.

increase for depicting the same regions of interest as the other Chorematic Models leads naturally to a decrease in mean scale denominator. In conjunction with more than doubling the information content, the complexity is slightly higher at $0.33Bt$. The absolute increase in content is also accompanied by a more than two-fold increase in colour usage

with a mean of 12.33 colours used, as well as the second highest ($\varnothing 4.86$) average number of symbology types used per diagram. In being visual depictions of results of a geographic analysis, SYMs need to distinguish significantly more features and feature classes within the same diagram compared to the more mono-thematic SMs and AMs. Succinctly, variations of the form of point and line symbols are used more often alongside an above average occurrence of complex patterns for area features as Table 4.7 shows. Especially curved subdivisions are present in 44% of the observed diagrams, which underlines that constructing a smooth geographic region in the vein of the Blue Banana (see Fig. 1.5) is a common result in chorematic analysis. SYM-classed diagrams show the highest percentage with 88% of arrow usage, a testament to their synthetic nature with the need to show multiple processes and dynamisms with arrow-based choremes in a single diagram.

Table 4.10 Summary statistics for Synthetic Chorematic Models.

| $N = 43$ | scale | den. | w[mm] | h[mm] | OLL | Bt | cp | col. |
|----------|--------|-------|-------|-------|---------|------|------|-------|
| median | 44144 | 14.00 | 63.20 | 60.76 | 1013.91 | 0.30 | 4.00 | 11.00 |
| mean | 194645 | 58.98 | 62.11 | 60.79 | 1225.29 | 0.33 | 4.44 | 12.33 |
| meandev | 245453 | 94.66 | 19.33 | 20.06 | 678.23 | 0.11 | 1.81 | 4.16 |
| stddev | 429707 | 71.33 | 22.31 | 24.95 | 782.04 | 0.14 | 2.19 | 5.64 |
| cv | | 2.21 | 0.36 | 0.41 | 0.64 | 0.42 | 0.49 | 0.46 |

4.4.5 Chorematic maps

Chorematic maps are the first class to have a geometric precision that show a unique connection to existing geodata, that is to the shape of geographic features. For *Inselkarten*, the outlines use on average 14.39 control points (Table 4.11) either with straight-line or curved polygons. *Rahmenkarten* on the other hand, are found most often in this class both in absolute ($n = 51$) as well as relative (58%) terms (Table 4.5). The mean sizes are increased over SM, AM and SYM-classed diagrams, as is their information content of 1406.86mm (Table 4.11). The increased OLL value is signifying that they are often used in a stand-alone fashion. Succinctly, there is less need for visual differentiation than in SYMs, leading to a lesser mean value for colour usage (10.28) and average symbolisations per map ($\varnothing 3.68$) (Table 4.6). The net result of the increased size with lesser pressure to show multiple thematic layers compared to the Synthetic classes SYM and SCM regarding complexity is a mean of 0.28Bt. This constitutes the second lowest class, complexity-wise.

4.4.6 Synthetic chorematic maps

Although CMs generally are used in a stand-alone fashion, 12 instances were observed where a cartographic-geographic synthesis was created from them. They share the outline characteristics with the constituent CMs but with a much higher information content

Table 4.11 Summary statistics for Chorematic Maps.

| <i>N</i> = 88 | scale den. | w[mm] | h[mm] | OLL | Bt | cp | col. |
|---------------|-------------|-------|-------|---------|------|-------|-------|
| median | 6294643.00 | 70.00 | 76.72 | 1248.03 | 0.28 | 12.00 | 9.00 |
| mean | 25825509.49 | 72.47 | 74.83 | 1406.86 | 0.28 | 14.39 | 10.28 |
| meandev | 30613506.95 | 24.70 | 17.20 | 761.19 | 0.09 | 7.19 | 3.82 |
| stddev | 49552932.94 | 31.44 | 24.50 | 954.43 | 0.10 | 9.83 | 6.07 |
| cv | 1.92 | 0.43 | 0.33 | 0.68 | 0.36 | 0.68 | 0.59 |

of OLL 2299.47mm (Table 4.12). Due to the similar mean drawing space dimensions, their mean cartographic complexity is the highest of all the diagram classes at 0.43Bt. Such a high graphical density arising from the synthetic nature warrants the highest average of symbolization types at Ø5.67 per diagram (Table 4.6). As with the SYM-classified diagrams, the high need for differentiation between feature classes of the same geometry type manifests itself in the heavy use of pattern and form manipulation (Table 4.7). They also share the preponderance of arrows, with 83% of all SCMs using them. The high documented mean value for colours (58) stem from only two diagrams with gradients, which present an impasse to the method of counting colours. Discounting these two cases would yield a mean value of 13.20 colours used per diagram.

Table 4.12 Summary statistics for Synthetic Chorematic Maps.

| <i>N</i> = 12 | scale den. | w[mm] | h[mm] | OLL | Bt | cp | col. |
|---------------|-------------|-------|-------|---------|------|------|--------|
| median | 1477443.50 | 81.32 | 67.35 | 1563.55 | 0.39 | 8.00 | 13.50 |
| mean | 6812110.75 | 75.19 | 70.65 | 2299.47 | 0.43 | 8.22 | 57.92 |
| meandev | 9041441.08 | 18.07 | 17.95 | 1148.51 | 0.14 | 4.74 | 74.53 |
| stddev | 15064334.65 | 20.54 | 24.71 | 1879.43 | 0.18 | 5.59 | 100.07 |
| cv | 2.21 | 0.27 | 0.35 | 0.82 | 0.42 | 0.68 | 1.73 |

4.4.7 Chorematic overlays

By their nature as choremes overlaid on top of a regular base map, the outlines documented for the sampled diagrams actually represent areas on that base map. In case of non-area choremes such as processes or lines of attraction, no outline at all is present. As such, the outline types as well as number of control points are more or less immaterial. Expectedly, regular base maps are much more precise in the geometric information they depict, resulting in the highest measured information content for any of the discussed classes at a mean OLL value of 2846.44mm (Table 4.13). The diagram dimensions governing size are also the highest, approaching half a page. The OV-classified diagrams are by definition mono-thematic and succinctly warrant fewer symbolisation types and less need to differentiate between feature classes by colour or form and pattern variations. The ex-

act mean and percentage values of these elements are of lesser explanatory power for OV's due to both the small sample size ($N = 14$) and especially the method of measurement that measures the base map alongside the few chorematic elements.

Table 4.13 Summary statistics for Chorematic Overlays.

| $N = 14$ | scale den. | w[mm] | h[mm] | OLL | Bt | cp | col. |
|----------|-------------|--------|-------|---------|------|-------|-------|
| median | 5909091.00 | 110.33 | 82.66 | 2283.29 | 0.27 | 39.00 | 14.00 |
| mean | 45125318.33 | 118.32 | 90.24 | 2846.44 | 0.27 | 27.00 | 14.42 |
| meandev | 51533843.44 | 20.54 | 17.35 | 1120.92 | 0.07 | 16.00 | 3.75 |
| stddev | 69471975.22 | 25.79 | 22.54 | 1384.59 | 0.09 | 16.97 | 4.31 |
| cv | 1.54 | 0.22 | 0.25 | 0.49 | 0.33 | 0.63 | 0.30 |

4.5 Validation of the taxonomy

The proposed taxonomy as a refinement of the preliminary taxonomy presented in [223] was developed in the iterative procedure described in Section 4.6. Viewing only the sampled diagrams as they were discussed above, the description of differences in both measurements and observations is valid upon itself. To answer the question though, whether the observed mean value differences can statistically be interpreted as originating from true differences in the base population of the diagram classes, we conducted an Analysis of Variance (ANOVA) (for a detailed explanation, see Section 4.6). An ANOVA was conducted for all ratio scaled measurements, namely scale denominator, width, height, information content (OLL) cartographic complexity (Bt), number of control points and number of colours. Table 4.14 shows the results regarding the ANOVA for the scale denominator. We can reject H_0 for the F-value of 4.76 with an error likelihood of <0.00 , that is with almost certainty. We thus adopt H_A : At least one class' mean value for scale denominator is representing a different population than the others. At least 4% of the variation of scale is explainable by membership in a given class.

Table 4.14 ANOVA results for scale denominator.

| | SS | df | MS | F | Sig. |
|----------------|----------------------|-----|----------------------|------|---------|
| Between Groups | $1.81 \cdot 10^{17}$ | 6 | $3.02 \cdot 10^{16}$ | 4.76 | <0.00 |
| Within Groups | $4.28 \cdot 10^{18}$ | 674 | $6.34 \cdot 10^{15}$ | | |
| Total | $4.46 \cdot 10^{18}$ | 680 | | | |
| R^2 | 0.04 | | | | |

Table 4.15 shows the results regarding the ANOVA for the diagram width in *mm*. We can reject H_0 for the F-value of 18.50 with an error likelihood of <0.00 , that is with almost certainty. We thus adopt H_A : At least one class' mean value for width is

representing a different population than the others. At least 14% of the variation of width is explainable by membership in a given class.

Table 4.15 ANOVA results for width.

| | SS | df | MS | F | Sig. |
|----------------|------------|-----|----------|-------|-------|
| Between Groups | 230181.29 | 6 | 38363.55 | 18.50 | <0.00 |
| Within Groups | 1397458.52 | 674 | 2073.38 | | |
| Total | 1627639.80 | 680 | | | |
| R^2 | 0.14 | | | | |

Table 4.16 shows the results regarding the ANOVA for the diagram height in *mm*. We can reject H_0 for the F-value of 14.21 with an error likelihood of <0.00, that is with almost certainty. We thus adopt H_A : At least one class' mean value for height is representing a different population than the others. At least 11% of the variation of height is explainable by membership in a given class.

Table 4.16 ANOVA results for height.

| | SS | df | MS | F | Sig. |
|----------------|------------|-----|----------|-------|-------|
| Between Groups | 292433.85 | 6 | 48738.97 | 14.21 | <0.00 |
| Within Groups | 2311438.74 | 674 | 3429.43 | | |
| Total | 2603872.58 | 680 | | | |
| R^2 | 0.11 | | | | |

Table 4.17 shows the results regarding the ANOVA for the information content OLL in *mm*. We can reject H_0 for the F-value of 69.93 with an error likelihood of <0.00, that is, with almost certainty. We thus adopt H_A : At least one class' mean value for OLL is representing a different population than the others. At least 38% of the variation of OLL is explainable by membership in a given class.

Table 4.17 ANOVA results for OLL.

| | SS | df | MS | F | Sig. |
|----------------|--------------|-----|-------------|-------|-------|
| Between Groups | 186307267.99 | 6 | 31051211.33 | 69.93 | <0.00 |
| Within Groups | 299275862.62 | 674 | 444029.47 | | |
| Total | 485583130.61 | 680 | | | |
| R^2 | 0.38 | | | | |

Table 4.18 shows the results regarding the ANOVA for the cartographic complexity in Bt. We can reject H_0 for the F-value of 4.26 with an error likelihood of <0.00, that is, with almost certainty. We thus adopt H_A : At least one class' mean value for complexity

is representing a different population than the others. At least 4% of the variation of complexity is explainable by membership in a given class.

Table 4.18 Analysis of variance for map complexity in measured in Bertin.

| | SS | df | MS | F | Sig. |
|----------------|-------|-----|------|------|-------|
| Between Groups | 1.31 | 6 | 0.22 | 4.26 | <0.00 |
| Within Groups | 34.59 | 674 | 0.05 | | |
| Total | 35.90 | 680 | | | |
| R^2 | 0.04 | | | | |

Table 4.19 shows the results regarding the ANOVA for the number of control points. We can reject H_0 for the F-value of 68.13 with an error likelihood of <0.00, that is, with almost certainty. We thus adopt H_A : At least one class' mean value for number of control points is representing a different population than the others. At least 43% of the variation of control points is explainable by membership in a given class.

Table 4.19 ANOVA results for control points.

| | SS | df | MS | F | Sig. |
|----------------|----------|-----|--------|-------|-------|
| Between Groups | 5296.04 | 6 | 882.67 | 68.13 | <0.00 |
| Within Groups | 6970.64 | 538 | 12.96 | | |
| Total | 12266.68 | 544 | | | |
| R^2 | 0.43 | | | | |

Table 4.20 shows the results regarding the ANOVA for the number of colours. We can reject H_0 for the F-value of 29.04 with an error likelihood of <0.00, that is, with almost certainty. We thus adopt H_A : At least one class' mean value for number of colours is representing a different population than the others. At least 21% of the variation of the number of colours is explainable by membership in a given class.

Table 4.20 ANOVA results for colours.

| | SS | df | MS | F | Sig. |
|----------------|-----------|-----|---------|-------|-------|
| Between Groups | 34094.02 | 6 | 5682.34 | 29.04 | <0.00 |
| Within Groups | 131479.03 | 672 | 195.65 | | |
| Total | 165573.05 | 678 | | | |
| R^2 | 0.21 | | | | |

The ANOVA-results can be summed up as being of overwhelming evidentiary value for the notion that the proposed taxonomy catches at least one fundamental difference for each measure. Still, we do not know which classes significantly differ from each other in

which measure. This question is explored by a post-hoc analysis that compares all classes and all measures against each other and checks for statistical significances.

Table 4.21 Overview over the Tamhane post-hoc test. Rows without significant test results have been left out.

| | Measure | SM | AM | SYM | CM | SCM | OV | UQ |
|------------|--------------|----|----|-----|----|-----|----|----|
| SM | Scale den. | | ✓ | | | ✓ | | |
| | OLL | | ✓ | ✓ | ✓ | | ✓ | |
| | Bertin | | ✓ | | ✓ | | | |
| | Control Pts. | | ✓ | | ✓ | | | |
| | Colours | | | ✓ | ✓ | | ✓ | |
| | Width | | ✓ | ✓ | ✓ | ✓ | ✓ | ✓ |
| | Heigth | | ✓ | | ✓ | ✓ | ✓ | |
| AM | Scale den. | ✓ | | | | | | |
| | OLL | ✓ | | ✓ | ✓ | | ✓ | |
| | Bertin | ✓ | | | | | | |
| | Control Pts. | ✓ | | ✓ | ✓ | | | |
| | Colours | | | ✓ | ✓ | | ✓ | |
| | Width | ✓ | | | ✓ | ✓ | ✓ | |
| | Heigth | ✓ | | | ✓ | | ✓ | |
| SYM | OLL | ✓ | ✓ | | | | ✓ | |
| | Control Pts. | | ✓ | | ✓ | | | |
| | Colours | ✓ | ✓ | | | | | ✓ |
| | Width | ✓ | | | | | ✓ | |
| CM | OLL | ✓ | ✓ | | | | | |
| | Bertin | ✓ | | | | | | |
| | Control Pts. | ✓ | ✓ | ✓ | | | | ✓ |
| | Colours | ✓ | ✓ | | | | | ✓ |
| | Width | ✓ | ✓ | | | | | |
| | Heigth | ✓ | ✓ | | | | | |
| SCM | Scale den. | ✓ | | | | | | |
| | Width | ✓ | ✓ | | | | ✓ | |
| | Heigth | ✓ | | | | | | |
| OV | OLL | ✓ | ✓ | ✓ | | | | |
| | Colours | ✓ | ✓ | | | | | ✓ |
| | Width | ✓ | ✓ | ✓ | ✓ | ✓ | | |
| | Heigth | ✓ | ✓ | | | | | |

As has been discussed in Section 4.6, the variances of the measures for each class are not equal and the sample sizes vary strongly among classes. This precludes the use of standard post-hoc tests such as the Scheffé test. Instead we use the Tamhane T2 post-hoc test, which is adjusted to account for unequal variances and unequal sample sizes. It is known to be conservative, meaning it has a low chance of Type I errors also known as false positives. For the sake of brevity, we do not reproduce all details of the results. Instead we provide a summary in Table 4.21. Every checkmark (✓) denotes that the comparison between means of the two classes tested as being statistically significantly different from each other for the given measure at 95% level of confidence. The UQ-class was included for completeness and to show that there is no measure that is only significantly different for UQ. Otherwise we ignore the UQ-diagrams as by definition no generalizable insight can be derived from them. The remaining test results depicted in Table 4.21 prove that each of the classes are measurably different from more than one other class in more than one attribute. A more detailed inspection reveals that the classes SM, AM and CM test to be different from each other in the most attributes. Furthermore, the class pairs of CM-SCM and SYM-SCM did not test for any significant pairwise differences at the 95%-level. The question whether the SCM-class is superfluous and could be rolled into one of the other classes is not settled by the test. A close inspection of the Tamhane-T2 test results show significance levels of approx. 85% for the CM-SCM pairwise comparisons. We interpret the lack of conclusive evidence as a function of the low number ($N = 12$) of measured SCMs and maintain the class.

4.5.1 Non-parametric tests

We note again (see Section 4.6) that the data violate some of the Prerequisites (standard distribution and homogeneity of variances) for parametric tests like an ANOVA. The very high significance of the results, coupled with the known robustness of ANOVA against violation of the standard deviation Prerequisite lead us to use ANOVA as confirmation of our H_A . By doing that we can use the more informative ANOVA results as help for interpreting the size of the effect of class on each measure. Nevertheless we conducted some additional non-parametric tests as corroboration of our results.

Comparison of means. To corroborate the rejection of the individual H_0 s, we additionally conducted a non-parametric Kruskal-Wallis test. Our data meets all Prerequisites for that test. The results are summed up in Table 4.22 and confirm the adoption of all H_A s with the same overwhelming nigh certainty. This is further proof that we were correct in moving forward to the post-hoc analysis above.

Correlations. While describing the observed characteristics of each class, we repeatedly made connections between, for example, a rise in content and an accompanying rise in colour usage and symbolisations. In order to gain a notion on the parallelism of effects, we measured the correlation between attributes with the non-parametric Spearman's rank correlation coefficient ρ [61].

The correlation coefficients as documented in Table 4.23 do generally show the expected pattern. Height and width are of course strongly correlated as are both to the OLL

Table 4.22 Results of the non-parametric Kruskal-Wallis test.

| | Scale | OLL | Bertin | CPs | Colours | Width | Height |
|----------|-------|--------|--------|--------|---------|--------|--------|
| χ^2 | 30.95 | 238.31 | 34.05 | 165.39 | 199.34 | 200.92 | 246.45 |
| df | 6 | 6 | 6 | 6 | 6 | 6 | 6 |
| sign. | .000 | .000 | .000 | .000 | .000 | .000 | .000 |

Table 4.23 Results of the Spearman test.

| | | Scale | OLL | Bertin | CPs | Colours | Width | Height |
|---------|--------|-------|-------|--------|-------|---------|-------|--------|
| Scale | ρ | 1.000 | -0.27 | 0.16 | 0.05 | -0.26 | -0.32 | -0.30 |
| | sig. | | .000 | .000 | .288 | .000 | .000 | .000 |
| | N | | 681 | 681 | 544 | 679 | 681 | 681 |
| OLL | ρ | | 1.000 | -0.01 | 0.21 | 0.65 | 0.71 | 0.73 |
| | sig. | | | .816 | .000 | .000 | .000 | .000 |
| | N | | | 681 | 544 | 679 | 681 | 681 |
| Bertin | ρ | | | 1.000 | -0.15 | 0.10 | -0.37 | -0.37 |
| | sig. | | | | .000 | .013 | .000 | .000 |
| | N | | | | 544 | 679 | 681 | 681 |
| CPs | ρ | | | | 1.000 | 0.20 | 0.29 | 0.32 |
| | sig. | | | | | .000 | .000 | .000 |
| | N | | | | | 542 | 544 | 544 |
| Colours | ρ | | | | | 1.000 | 0.58 | 0.63 |
| | sig. | | | | | | .000 | .000 |
| | N | | | | | | 679 | 679 |
| Width | ρ | | | | | | 1.000 | 0.82 |
| | sig. | | | | | | | .000 |
| | N | | | | | | | 681 |
| Height | ρ | | | | | | | 1.000 |
| | sig. | | | | | | | |
| | N | | | | | | | |

value which in turn is positively linked with the number of used colours. Complexity in Bertin is negatively correlated to a size increase, but is independent from the total amount of information.

4.6 Methodology

For the research on chorematic diagrams, we are partially thrown back to a point comparable to the situation before the first topographic map was even digitised, i.e. without any measurements, algorithms or documentation. In other words, we are not only lacking a cartographic model, we are even lacking the data to base any modelling on. Topographic map generation via generalisation informed by proper modelling has so far been attacked by using certain knowledge acquisition techniques [305]. These are summed up in table 4.24

Table 4.24 Suitability of established knowledge acquisition techniques for investigating chorematic diagrams.

| Method | Problems and Limitations | Suitability |
|------------------------------------|---|---------------|
| Conventional Knowledge Engineering | chorematic cartographers not available for interviews | none |
| Analysis of text | Texts on the chorématique concentrate on the geographic side, not on the cartographic side; next to no procedural knowledge | very low |
| Reverse engineering | traditionally assumes input as well as output; for chorematic diagrams, input is unavailable | medium |
| Machine learning | presupposes a very narrow question | low |
| Amplified intelligence | has not yet been implemented [133] | none |

As we can see, the state of the art of knowledge acquisition in generalisation research is not directly applicable to chorematic diagrams. The most suitable route, analysis of maps for reverse engineering is not directly applicable due to the unattainable input data. Rather, a more fundamental and broader knowledge base needs to be acquired first. The high level of sophistication the knowledge base for topographic mapping has reached serves as a guidance augmenting, but not governing our modelling effort. Instead we have chosen to pursue an analysis of maps guided by the Cartographic Methodology as presented by [209] and originating with [27].

Methods. During the last thirty years of generalisation research there seems to have been relatively little need to ask fundamental epistemic questions. This is surely explainable not in spite of, but to a large part because of the successes that did not challenge the governing paradigm meaningfully. Basic epistemic investigations would include questions like: What is knowledge itself? How can we hope to learn? What can we learn at all? ⁴

⁴While pursuing technological and algorithmic improvements, it is easy to discount such undertakings. But to pause a moment and ask oneself the question: What has humanity actually learned from someone being able to produce a 1:50k scale map fully automatically? That somebody translated a man-made language transformation (maps to maps) into another man-made language transformation (data to data)?

For cartography, such fundamental epistemic investigations were especially carried out in the Eastern Block countries, among other areas, during the 60s, 70s and 80s of the 20th century. These investigations led from very basic theoretic questions to a whole body of epistemically rigorous theories for the whole of cartography as a scientific and technical endeavour of mankind. From firm foundations in the philosophy of science, A. M. Berlyant developed a comprehensive methodology of cartographic investigation, published in 1978 [27]. To a German language audience this methodology was opened up by Rudi Ogrissek's seminal work on theoretical cartography *Theoretische Kartographie* in 1987 [209]. In its essence the Ogrissek-Berlyant-methodology provides not only a systematic ordering of possible methods and their outcome for cartographic investigation but also an sequential ordered approach with which to investigate a map series.

Table 4.25 Cartographic methodology after Berlyant, changed from [209].

| Category | Methods | Results |
|--------------------|--|--|
| Description | Qualitative visual analysis, not automated | General descriptive text, overview, classification |
| Grapho-analytic | Qualitative and quantitative collection of graphical traits, not automated/semi-automated | Colour, number and type of symbols used, polygon characteristics, visual variables, etc. |
| Geometric | Mathematical modelling of coordinate transformation, semi-automated | Spatial accuracy measures, transformations |
| Statistical | Collection and analysis of traits for many diagrams, comparison, semi-automated | Classification, clustering, similarity and dissimilarity |
| Information theory | Calculation of measures for complexity and information content from vector and raster data; comparison, semi-automated | Complexity metrics |

4.6.1 Collection of base data

At the outset of this research, a literature review was conducted aiming at getting an overview about where and how chorematic maps were published. It quickly became apparent, that the huge majority of chorematic maps was produced and published under the auspices of GIP-RECLUS. Using web-accessible library catalogues and the websites of *Maison de la Géographie* as well as the library catalogues of the map collection of the Prussian State Library a list of publications potentially containing chorematic diagrams was created and

periodically updated. The main source of published chorematic diagrams was identified as the journal *Mappemonde*, which describes itself thus:

This quarterly review, in colour, about maps and images of territory, launched in 1986, with an international editorial advisory committee, aims at bringing the latest finds of graphic and iconographic research on space and locations to a wide-ranging readership that consists of consultants, firms or local authorities as well as the whole of the teaching profession. [117]

66 of the 72 issues in 18 Volumes (1986-2003) were available as free download via the mgm website at the start of this research. Four issues were available as hardcopies at the Prussian State Library. As with other sources from libraries, the included chorematic diagrams were xeroxed and scanned or directly scanned. As a sidenote, the missing issues were later added to the website, the last in July 2013 by the mgm website hosts. As was mentioned above, the journal was moved from print to web publication starting in 2004 and renamed M@ppemonde to signify that change. All issues of M@ppemonde were inspected online and the automatically generated pdfs of those articles that contained chorematic diagrams were downloaded. From the list of potentially choreme-yielding monographs, several were procured through private means when not available via the German library system. Those unavailable were periodically searched for via Amazon and antiquarian channels. In the case of the Reclus Atlases of Romania, Laos and Vietnam unsuccessfully or prohibitively expensively so. Periodical web-image and text searches were executed to find web-only sources for chorematic diagrams, such as thesis documents, grey literature and the like. This continuous collection effort was accompanied by a continuous visual inspection as a propaedeutic step of the analysis. Starting with the Nr. 3 issue of Vol. 5 (1990), the freely available Mappemonde pdf-files include vector graphics, with all preceding issues being available as scanned raster images only. In order to collect vector data at least for the full set of Mappemonde journal, an effort was undertaken to manually digitize the scanned raster images. After several weeks, this effort led to equipment failure [tenosynovitis] and had to be abandoned. Nevertheless, the efforts resulted in enough vectorisations to make an informed decision on whether the diagrams available only in raster form were measurably different from the others. The continuous inspection of the M@ppemonde journal highlighted that the online-diagrams were different enough from the rest of the materiel to exclude them from the formal quantitative analysis. The main reason being that they are produced for inclusion into html, sometimes including animations, and thus cannot be directly compared via the methods explained below. The switch from Mappemonde to M@ppemonde thus marks a convenient as well as logical delimitation of the base data for the quantitative analysis.

4.6.2 Analysis methods

In the following we present which and how individual methods were used to what particular end. We direct the reader to the fact that insight was gained by the process of interacting with the body of existing diagrams in addition to the rigorous examination of the numeric results of the more formal methods.

Qualitative description. The qualitative description is based on traditional techniques of literature review and semi-formal comparison with the gathered material. In addition, text critique methods and categorisations from theoretical human geography were employed (cf. Section 4.2), especially regarding the ideological underpinnings of the chorématique and its critics. Furthermore, contact with other researchers into the field was sought to ensure no duplicate efforts were being undertaken, resulting in affirmation that the analysis approach was unique.⁵ The results are textual descriptions of the observations and findings. These have been discussed with the scientific community at several occasions.

Visual analysis. Visual inspection was used throughout the research as a steering method to generate hypotheses and conjectures on a case-by-case basis. A more thorough visual analysis was carried out after collecting the majority of analysed chorematic diagrams in order to generate an overview about the problem dimensions. This was conducted as follows: noticing that on-screen inspection was inadequate, not the least due to scale and colour issues, all available articles were printed in colour with a high quality laser printer. Spot tests were conducted with printouts and Xeroxes with the original printed journals at the Prussian State Library to ensure no systemic size or colour error was present. The printouts were then individually ascertained and spread across the floor of a large room at the German Research Centre for Geosciences GFZ. In an iterative process spanning several days, similar looking diagrams were grouped and notes were taken, resulting in a first taxonomy. During the course of this research, this manual spatial sorting by visual inspection was repeated several times to accommodate newly available sources and conceptual changes. We then compared the groups to each other and made adjustments, until a workable taxonomy was created that was robust enough to be able to categorise all chorematic diagrams known so far. The governing attributes used for grouping were:

- apparent visual complexity
- apparent spatial fidelity informed by territorial outline choice
- publication environment.

One arising difficulty was the fact that the sub-sorting by published article or monograph did not lend itself to articles with numerous noticeably different chorematic diagrams. A third stage taxonomic visual inspection was carried out while individually inspecting the diagrams on-screen and assigning each diagram to one of the chorematic diagram classes and noting the result in a spreadsheet. Each diagram was consecutively assigned an identification number, sorted by publication date and position within the publication assuming western reading direction, i.e. from upper left to lower right. When there was a numbering scheme employed by the individual author, that was used instead.

Capturing regions of interest. The geographical regions that are represented by each diagram were noted in the spreadsheet in textform. In a second step, the textual descriptions were vectorised and thus geo-located manually⁶ in the form of a point shapefile. In order to gain a visual impression of the spatial distribution of covered regions, the results were displayed in a map (Fig. 4.20).

⁵personal communication V. Del Fatto 2008 and R. Laurini 2008 and 2011

⁶With the help of student assistant Sarah Lohr.

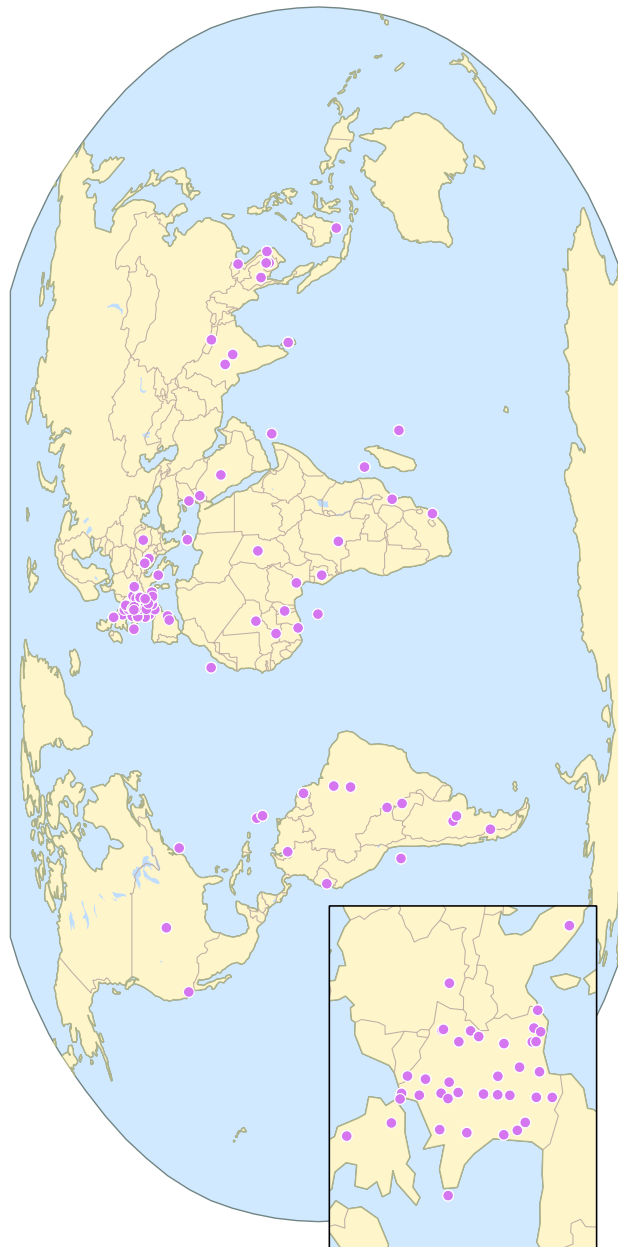


Figure 4.20 Point symbol map of the regions of interest for the analysed chorematic diagram fielding Mappemonde articles.

Measuring scale. The cartographic scale of each diagram was measured by choosing two clearly identifiable geographic objects in the diagram, if possibly cities, and measuring the distance between them in millimetres with a vector drawing program. To ensure no scaling issues arose, spot tests were conducted with the printouts, which had been checked against the originals earlier. In the relatively rare case of a provided scale bar, the distance could directly be related to real world distances and the scale denominator calculated. More often, the real-world distance had to be procured by manual measurement in an Atlas map in an appropriate projection, and in some cases for obscure villages via the online tool WebMapService of the World provided by the GIScience group at the University of Heidelberg [119]. The Atlases used were the National Geographic Atlas of the World, the Schweizerischer Mittelschulatlas and a German Edition of the Times World Atlas [150, 259, 298]. The calculated scale denominator was entered into the spreadsheet. This process doubled as an informal investigation into the questions regarding projection usage in chorematic diagrams.

Measuring sizes. The effective width and height of each diagram were measured by interactively drawing a bounding box including all spatially located content in the Inkscape vector drawing program and copying the millimetre values to the spreadsheet. Being unable to automatically export bounding box values is a known issue with the Inkscape program. As the bounding box needed to be manually selected to make sure oversized legends and design artifacts did not skew the results, this was still the most efficient process.

Measuring information content. We kept the same selection box used for size measurement for the measurement of information content. As explained in Chapter 3, the cartographic line frequency is the most expressive complexity measure for the purposes of this research. As it is based on the sum of the length of all lines and outlines, the content within the box had to be measured for that combined OLL value. We wrote an extension for Inkscape in Python that automatically calculated and returned the OLL value for each selection. The returned value was copied and pasted to the spreadsheet where it was automatically normalised over the drawing space area calculated from the dimensions of the selection box. This step too could not be further automatised, as the line length calculations presume that no object groupings within the vector drawing exists. These groupings had to be removed manually for each diagram but were not present all of the time. A more profound reason for the impossibility of further automation was the manual nature of the vector originals: Many diagrams used cartographic short cuts and tricks like covering unwanted areas with large white rectangles or "smart" layer arrangements to produce the wanted effect. These and other peculiarities had to be recognised and removed on a case-by-case basis. The semi-automated method described has a shortcoming regarding hachures, as each hachured line will contribute its full length to the OLL value. Chorematic diagrams with hachures (coded PAT A later on) potentially have a slightly higher OLL and succinctly complexity value than might be visually warranted.

Symbology analysis. In order to analyse symbolisation usage, a list of expected classes of symbolisations was created and a shorthand notation developed informed by the iterative

visual analysis. They were roughly grouped by point, line, area and subdivision symbols. Each diagram was inspected on-screen and the matching shorthand for an observed symbolisation entered as text into a single spreadsheet cell, with semi-colons as delimiters. When an unforeseen symbolisation arose, a shorthand was created on the spot and added to the master list, to be used from that point on. Table 4.26 shows the abbreviations used in the rest of the thesis for symbolisation.

The batches of symbol shorthands were later exported and grouped by chorematic diagram class. A python script was written that removed typos and white spaces and counted occurrences per class, returning a csv-File with said content.

Territorial outline measurement. The data for the outline types was documented in the spreadsheet in two ways, via visual classification and measurement of control points.

Table 4.26 Abbreviations for the encountered symbology types.

| | Abbrev. | Explanation |
|--------------|-------------------|--|
| Point | <i>+-</i> | Plus and/or minus as point symbols |
| | <i>circles</i> | filled or unfilled circles of various sizes |
| | <i>FO P</i> | variation of the form variable for point symbols such as stars |
| | <i>squares</i> | same usage as circles |
| | <i>hexagon</i> | same usage as circles |
| | <i>triangles</i> | same usage as circles |
| Line | <i>CA L</i> | circular arc line symbol |
| | <i>curved L</i> | line symbol using Bezier curves |
| | <i>FO L</i> | form variation of line symbols |
| | <i>L</i> | nondescript straight line symbol, usually black |
| | <i>PAT L</i> | variation of pattern over a line |
| | <i>poly L</i> | polyline symbol |
| Area | <i>arrow</i> | arrows, often in the form of cubic Bezier curves |
| | <i>PAT A</i> | pattern variation such as hachure over an area |
| | <i>FO A</i> | form variation over an area |
| | <i>ellipse</i> | ellipses used to form areas |
| | <i>rectangles</i> | rectangles used to form areas |
| Subd. | <i>gradient</i> | a colour gradient applied over an area |
| | <i>hexali SD</i> | hexalinear subdivision, i.e. one that only uses 60 angles |
| | <i>L SD</i> | straight line subdivision |
| | <i>curved SD</i> | a subdivision using Bezier curves |
| | <i>CA SD</i> | circular arc subdivision |
| | <i>poly SD</i> | polyline subdivision |
| Misc. | <i>rect SD</i> | rectilinear subdivision |
| | <i>icons</i> | miniature chorematic diagram |

During visual appraisal, the following territorial outline types were encountered for *Inselkarten*: Circle, Ellipse, Square, Rectangle, Triangle, Hexagon, Polygon, Circular Arc and Curved. *Rahmenkarten* were assigned to their own category. A special outline type is actually mostly devoid of an outline, this type is called Overlay. Overlays are chorematic layers put atop conventional base maps. The number of control points could only be usefully derived for *Inselkarten*, and was interactively counted within Inkscape. The number of control points in the strict sense of this measure is the minimal number of points that is needed to uniquely define the present shape, for example 2 for a circle, 3 for a square and four per cubic Bézier curve. Although conceivably automatable, the peculiarities of the manual vector drawings forced a close interactive inspection again, as some polygons and curves were over-defined or an outline that was visually coherent was in fact created from several disjunct line elements.

Collecting colour and lettering information. In order to collect information on colour usage, we wrote a python extension for Inkscape that returns all colours within a selection box as hexadecimally coded RGB colours as well as their total number. Note that black and white were counted as colours in this survey, that is a purely black and white diagram might be appraised with one or two colours, depending on whether a white background element and / or frame was used or not. Further computational investigations into colour usage such as placement and distances of selected colours in a common colour space were considered, but were deemed to lie outside the scope of this research. Lettering information was collected by marking diagrams that had lettering on the map face with 'yes', those without with 'no' and those that used numbers and a numbered key in the legend with 'numbers' in the spreadsheet.

4.6.3 Taxonomy validation methods

As noted above, the taxonomy acted as a guide for the more detailed collection of data as well as an ordering and ideation device regarding design rules. As such it was a substantial part of the modelling itself. As the preliminary classification was done by iterative visual analysis as described above, the question arose as to whether the visually identified classes could be corroborated with the appraised traits of the individual diagrams. Apart from descriptive statistics and correlation tests, an analysis of variance (ANOVA) was conducted for each of the ratio-scaled measures against the taxonomic classes to test the measured differences between classes for statistical significance. As some of the value of the modelling part in this research hinges on the classes being convincing and relevant as well as measurable, we will briefly recapitulate the ANOVA analysis principles. The following is strongly based on [11, 248] and was cross-checked for English standard terminology with [61, 307].

Analysis of variance. The analysis of variance is a very popular and robust multivariate statistical method that is applied when there are ratio-scaled dependent variables and nominal to ordinal-scaled independent variables, i.e. categories. When there is only one independent variable, a one-way analysis of variance is used, as is appropriate for the case of chorematic diagram classes. When values such as the mean of an observed variable var-

ies for the sub-populations, in our case diagram classes, the question arises whether the variation in means is statistically significant or not. Informally, the question is whether there is any statistical indication that the classes belong to the same base population or not. More formally: Let $x_i(1, \dots, q)$ be the q discrete categories of variable X . Let the arithmetic mean value of variable y belonging to category x_i be μ_i and the grand mean of variable Y over the whole sample across categories be μ . Let the j th observed value of Y in the i th category be y_{ij} . From that we can express y_{ij} as:

$$y_{ij} = \mu_i + \epsilon_{ij}$$

with ϵ_{ij} = residual of value y_{ij} from μ_i .

When we denote the difference between μ and μ_i with δ_i we get:

$$y_{ij} = \mu + \delta_i + \epsilon_{ij}. \quad (4.1)$$

This is known as the means model for a one-way ANOVA analysis. The means model thus assumes that every measured value y_{ij} for a given category results from the addition of two terms to the grand mean μ . The effect of the category is δ_i and ϵ_{ij} are the residuals from measurement errors and/or non-measured effects. For our concrete case, X is the nominal-scaled chorematic diagram class with x_i with $q = 7$ and $i \in SM, AM, SYM, CM, SCM, OV, UQ$. The null hypothesis is that Y and X are independent, that is, the grand mean of a measure described above such as the number of control points is independent no matter which chorematic diagram class a given diagram belongs to:

$$H_0 : \mu_{SM} = \mu_{AM} = \mu_{SYM} = \mu_{CM} = \mu_{SCM} = \mu_{OV} = \mu_{UQ} = \mu. \quad (4.2)$$

The corresponding alternative hypothesis is: H_1 : at least two chorematic diagram classes have different μ_i values. Assuming the summary statistics as estimations of the means are available and hint at structural differences, the null hypothesis can be tested by a decomposition of all variations of values into systematic and residual parts. This decomposition is done by calculating the sum of squared differences (sum of squares; SS) between individual measurements and the grand mean of the respective measure and the individual category means as well as the sum of squares between category means and the grand mean itself:

$$\underbrace{\sum_{i=1}^q \sum_{j=1}^{n_i} (y_{ij} - \bar{Y})^2}_{\text{total Sum of Squares}} = \underbrace{\sum_{i=1}^q \sum_{j=1}^{n_i} (y_{ij} - \bar{Y}_i)^2}_{\text{Sum of Squares within groups}} + \underbrace{\sum_{i=1}^q n_i (\bar{Y}_i - \bar{Y})^2}_{\text{Sum of Squares between groups}}. \quad (4.3)$$

In this decomposition, the SS_{betw} + (Sum of Squares between groups) is interpreted as the systematic influence of X (diagram classes). In order to test the null hypothesis, this systematic influence is tested for being significantly larger than the overall error with an F-test. By taking into consideration the respective degrees of freedom (df), mean square values (MS) are calculated a ratio of which is the F-value for the F-test. The critical

F-value that defines the level of significance is calculated from the pairwise degrees of freedom among and between groups. The result is a p -value interpretable as the level of confidence for the correctness of the null hypothesis from $p = 0$, null hypothesis is wrong to $p = 1$, the null hypothesis is correct. The coefficient of determination R^2 between measurement and diagram class is derived by the ratio of the Sum of Squares between groups and the total Sum of Squares. It can be directly interpreted as a percentage value for the amount of variation directly explainable by membership of a certain diagram class. The ANOVA result-tables in Section 4.3 present the analysis in the following form:

Table 4.27 Sample table highlighting the relationship of ANOVA results and their generation.

| | SS | df | MS | F | Sig. |
|----------------|--|---------|-------------------------------|------------------------------|------|
| Between Groups | $\sum_{i=1}^q n_i (\bar{Y}_i - \bar{Y})^2$ | $q - 1$ | $\frac{SS_{betw}}{df_{betw}}$ | $\frac{MS_{bet}}{MS_{with}}$ | p |
| Within Groups | $\sum_{i=1}^q \sum_{j=1}^{n_i} (y_{ij} - \bar{Y}_i)^2$ | $N - q$ | $\frac{SS_{with}}{df_{with}}$ | | |
| Total | $\sum_{j=1}^{n_i} (y_{ij} - \bar{Y})^2$ | $N - 1$ | | | |
| R^2 | $\frac{SS_{betw}}{SS_{total}}$ | | | | |

Prerequisites. The analysis of variance always has some descriptive value via the calculated effect decomposition. In order to generate statistically sound interpretations regarding the null hypothesis however, certain prerequisites must be considered, namely:

- (1) variable Y_i should follow a normal distribution around its mean μ_i with a standard deviation of $\sigma\epsilon$.
- (2) variances σ^2 should be equal
- (3) samples should be independent
- (4) sample sizes should be roughly equal

ANOVA is known for robustness against violations of Prerequisite 1 and is often used (successfully) on sample sizes below the threshold needed to formally test for normal distribution [11]. The robustness of ANOVA against non-normality stems from asymptotic theory and is applicable for large sample sizes. It can still only be assumed to be robust for the comparison of means, most other inferences are not applicable [252]. For our analysis, we judged the distributions by visual inspection of the respective histograms for each class and a Kolmogorow-Smirnow goodness of fit test. The measurements for the collected data do not follow (and could not be fitted by the K-S test) an obvious standard distribution, but show very similar looking distributions for each metric. For Prerequisite 2, the variances ($= \sigma^2$) for each measure and class were compared amongst classes in Table 4.28. The variances for Scale denominator, OLL, Control Points and Colours comprise several orders of magnitude and can thus not be assumed to be homogeneous. While ANOVA is often applied even for unequal variances, care must be taken with the selection of the post-hoc analysis [79].

Table 4.28 Variances comparison.

| | Scale den. | width | height | OLL | Bertin | CPs. | Colours |
|-----|------------------------|-------|--------|---------|--------|--------|---------|
| SM | $1133.2 \cdot 10^{13}$ | 367 | 307 | 174943 | 0.08 | 1.46 | 13 |
| AM | $135.8 \cdot 10^{13}$ | 616 | 470 | 336287 | 0.03 | 12.48 | 12 |
| SYM | $189.0 \cdot 10^{13}$ | 510 | 638 | 626142 | 0.02 | 4.94 | 33 |
| CM | $248.4 \cdot 10^{13}$ | 1000 | 607 | 921406 | 0.02 | 99.75 | 37 |
| SCM | $24.8 \cdot 10^{13}$ | 460 | 666 | 3853352 | 0.03 | 35.19 | 10924 |
| OV | $448.0 \cdot 10^{13}$ | 719 | 481 | 2024572 | 0.01 | 432.00 | 21 |

Prerequisite 3 is fulfilled with the described methodology of chorematic diagram selection. The sample size for diagram classes varies, especially for SCM, OV and UQ classes. As such, we cannot fully assume Prerequisite 4 to be fulfilled. Again, ANOVA is known to be generally robust against class size differences, but the consequences for the choice of post-hoc analysis must be considered [79]. As corroboration of the rejection of H_0 leading up to the post-hoc analysis, we also conducted a non-parametric Kruskal-Wallis test that does not have demands on normality or equality of variances [61, 307].

Post-hoc analysis. For the cases where the ANOVA analysis led us to reject the null hypothesis, we only know that H_1 has to be adopted, saying that at least one diagram class is different from the others. For these cases a post-hoc analysis was carried out to analyse which classes are significantly different from each other. Conceptually these post-hoc analyses perform individual tests in all possible permutations. A conservative approach like the popular Scheffé method [307] had to be rejected due to the violations of Prerequisites 2 and especially 4 [79]. Instead of eliminating heterogeneity of variances by adjusting them away ([53]), we used the Tamhane T2 post-hoc method [276] for multiple comparisons. Not all results are presented in this thesis, due to length considerations.⁷ Instead all the conducted post-hoc analyses were checked for significant results. We prepared a synoptic table 4.21 without providing the individual measures for mean difference, std error, significance and lower and upper confidence interval bounds and so forth.

⁷These can easily be reproduced from the data that will be made available online.

Chapter 5

Modelling Chorematic Diagrams

The preceding Chapter 4 was concerned with widening the knowledge base in a positivist manner. This Chapter presents the cartographic design principles that are observably driving the look and feel of published chorematic diagrams. Such aesthetic as well as artisanal qualities are commonly understood to be difficult to formalise by positivist analysis methods and are also known as *tacit knowledge*. Following the literature, it is only by experience and practice that tacit knowledge can ever be hoped to be gained before it is further formalised. Our experience with chorematic diagrams design stems from the processes described in the preceding Chapter 4. In the following, we will move from very general observations in Section 5.1 towards a more formal constraint-based model of chorematic diagrams in Sections 5.2 and 5.3. In the closing Section 5.5 we present two studies that are concerned with validating and parametrising individual constraints.

5.1 Design principles

It is long recognised in generalisation research, that knowledge acquisition for automated map production is as crucial as it is difficult (see Chapter 1). Especially the fact that “[...] cartographic knowledge [...] is essentially encoded graphically and thus hard to describe by words.” [306, p. 142].

Knowledge that is included in artefacts only is not idiosyncratic to cartography. Such cases arise in various circumstances. In Artificial Intelligence (AI) research often encounters this problem when trying to devise expert systems. In an article on tacit knowledge in AI research, Johannessen [156] identifies that non-codified knowledge can be encountered especially in “[...] the case of the vocational and aesthetic world.”. While several techniques to tackle this problem have been proposed for cartography (see Table 4.24 and [161]), neither has made wide inroads [133]. The difficulty in describing tacit know-

ledge formally has long been recognized in philosophy. The philosopher Wittgenstein and subsequent authors hold the view, though, that tacit procedural knowledge “[...] can be communicated directly via examples and general hints.” [156]. That is exactly what was done most famously by Eduard Imhof and later Wood [316] for label placement. One of the most cited works in automated label placement is [149], which represents general verbal guidelines and copious graphical examples on how to position text on maps. For an example, see figure 5.1. For the case of label placement, Imhof’s presentation of tacit knowledge forms the foundational source of information to the present day, for example [238, 271]. Following Johannessen, it is possible to transform broad guidelines and detailed examples into operationalisable knowledge within a given scientific context.

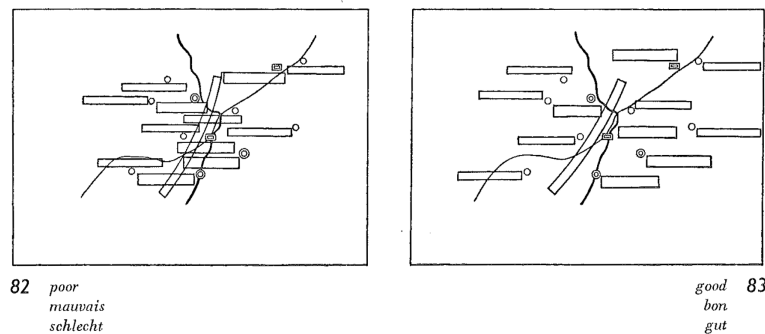


Figure 5.1 Visual examples of poor and good label placement solutions from Imhof [149].

Succinctly, we present the design principles of chorematic diagrams by description and example. We start with the general design goals that chorematic diagrams seem to strive for and review more detailed examples roughly ordered by the concepts of composition, thematic encoding and shape.

5.1.1 Overarching design goals

As we have shown with the statistical analysis (Chapter 4), chorematic diagrams come in different types and field quite a few different symbolisation strategies. Still, an astute observer can recognise a common look and feel, a common aesthetic at work. The fact alone that researchers from different disciplines accept and talk about the existence of “the choremes” when addressing chorematic diagrams as a unity is testament to the existence of overarching design goals at work.

In the following we will argue, that the overarching and characteristic visual design goals of chorematic diagrams are *clarity*, *abstractness* and *harmony*. They are present in nearly all chorematic diagrams, with only few counterexamples, which can safely be interpreted as atypical. In a sense they are efforts gone awry, such as Fig. 5.2. The three mentioned visual design goals are the driving forces that are governing individual

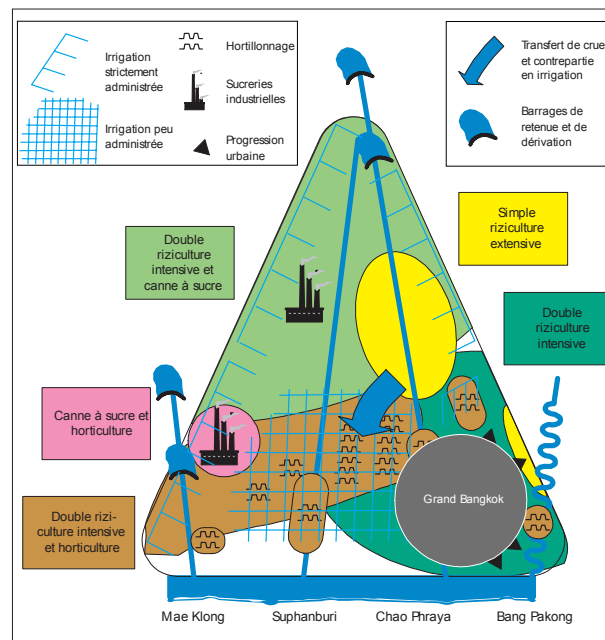


Figure 5.2 Example of misemployed chorematic design principles [199].

graphic procedures and lower level tasks. They represent the visual design philosophy of chorematic diagrams.

Lucidity. Chorematic diagrams are portraying complex geographic situations in intellectually controllable ways. That chorematic designers aim for that goal is not surprising *per se*. As shown previously, the ideology behind Brunet's chorematique is about finding relevant and recurring patterns in spite of a deluge of detail (see Chapter 4). Turned upon its head, Brunet's goal becomes a conjecture with wide ranging epistemic ramifications: the world's complexity can be reduced to very simple cartographic expressions for certain (many) geographic purposes. Beyond the measurable reduction of detail, chorematic diagrams are neatly tidied-up models of reality. They take the form of map-like diagrams that strive for clarity and controllability, and with it intellectual safety and affirmation to potentially messy and confusing situations. A quite literal example of a chaotic, messy, violent and confusing situation is the Los Angeles Riot of 1992. Fig. 5.4 is a press pho-

tograph from the time exemplifying these qualities and Fig. 5.5 is a chorematic diagram that accompanies a two-page article discussing the course and causes of the riot.

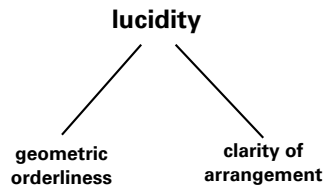


Figure 5.3



Figure 5.4 Impression from the Los Angeles 1992 Riots [309].

As can be seen, the photograph is a rhetoric appeal to emotion first, and reason second with the reverse being true for maps. The longing for geometric orderliness as a road to intellectual controllability is much stronger in chorematic diagrams (Fig. 5.5) than in thematic maps such as Fig. 5.6. Whereas the thematic map shown follows the aim of quantitative and geometrically precise data portrayal, the chorematic diagram aims for the portrayal of the overarching structures and processes by placing the elements into neatly shaped spatial 'bins' that coincide with structural categories: All blacks are in the banana shape of South Central, ocean and land are separated by a smooth curve, hispanics are 'collected' and put into two circles that are conveniently sized and a third larger expanse that is in visual contrast to all other spatial bins; the processes are depicted as magenta coloured fronts and eruptions tying back to the 'social volcano'-imagery that is conjured

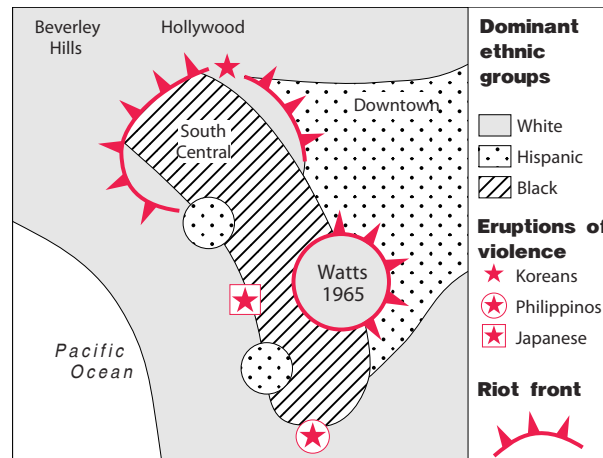


Figure 5.5 Geometric orderliness: Map from a Mappemonde publication on the Los Angeles Riots. Translated from [14].

in the accompanying article [14]. The two main strategies with which lucidity is reached are geometric orderliness and clarity of arrangement.

Abstractness. The symbols used in chorematic diagrams consistently show a big visual distance to the material or immaterial phenomena that are depicted. As explained in Chapter 4 (table 4.7), only 12% of the examined chorematic diagrams use point symbols different from simple forms like circles or squares. All these can safely be understood to be symbols of low iconicity in carto-semiotic terms [88].

The choice for a high degree of abstraction for the outer, visual form is rooted in the theory of the chorématique at the junction of the ideographic and the nomothetic (see Chapter 4). The claim to universal applicability of the choremes laid down by Brunet is visually reinforced by using a limited set of symbols for nearly all geographic phenomena. Visual display of spatial arrangement and structure are highlighted, while the actual subject matter is often only discernible by consulting the legend and accompanying texts. Strong abstraction is not only carried out for point symbols, but for linear and area elements, too. Especially area pattern fills use a low number of linear hatches varied by frequency and direction. In contrast, conventional thematic cartography often uses area pattern fills to visually reinforce the phenomenon such as land-use or land cover.

Fig. 5.8 shows an example for an economic map from a school atlas fielding point symbols of a high iconicity such as stylised bananas, palm trees, rubber plantation and cocoa beans over highly texturised land use/land cover area fills. The colours for the more abstract point symbols as well as the land use/land cover areas attempt to provide cues to their meaning via an associative colour choice. Examples are yellow diamonds for gold mining or grey for aluminium mines and industries.

Fig. 5.9 is an example for the abstractness of symbolisation in chorematic diagrams.

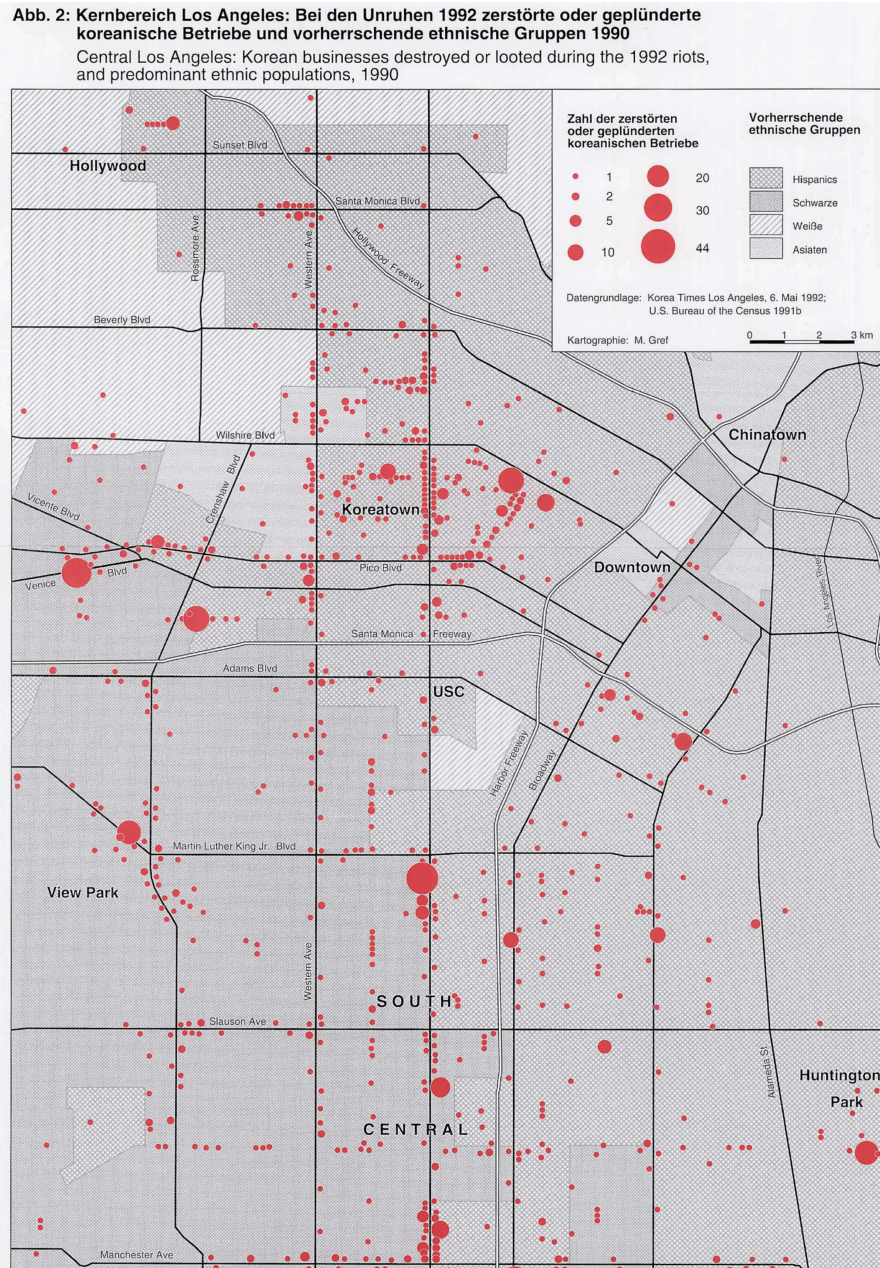


Figure 5.6 Map from a journal publication on the Los Angeles Riots [279].

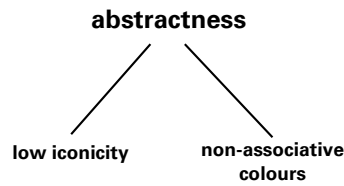


Figure 5.7



Figure 5.8 Section of an economic map of Africa,¹ 160000000, centered on Abidjan [321].

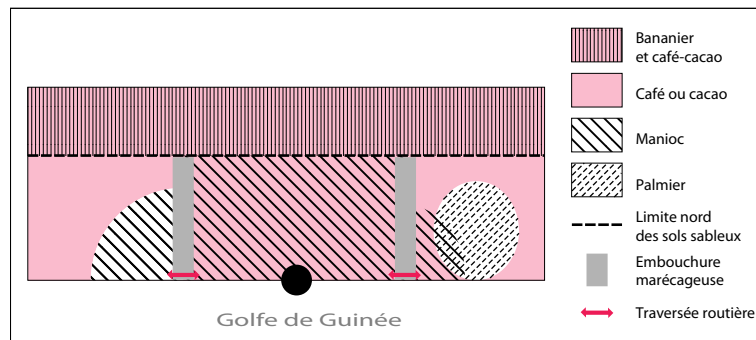


Figure 5.9 Chorematic diagram on crops around Abidjan, source [198].

It portrays thematically similar elements such as banana, cocoa, palm trees and manioc plantations and crops around Abidjan. Colours and patterns are decidedly arbitrary and unrelated to any notion of western-african vegetation. The abstraction in colour usage does even eschew the usage of a blue ocean, so that out of context, the ivory coast appears as an island. In subtle ways, choosing colour, point symbol and hatching schemes based on visual distinctiveness without any consideration for connotations helps in creating a neutral, scientific look on a subject matter. The potentially contentious subject of race

and ethnicity in Fig. 5.5 avoids naive associations, with 'white' having the highest grey-value and so forth. The two main strategies with which abstractness is reached are using low-iconicity symbols and non-associative colours (Fig. 5.7).

Harmony.

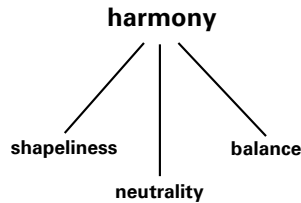


Figure 5.10

While the word harmony has a wide range of meanings, under it we here subsume a specific range of aesthetic qualities that drive the look or feel of chorematic diagrams. The chorematic harmony comprises a neutral and scientific appearance, balanced layouts as well as the peculiar style of geometric shapes found in chorematic diagrams. The quest for a harmonious visual appearance permeates many of the individual design choices and is the driving force behind the unique style of geometric schematisation that arguably make chorematic diagrams so memorable. One of the early definitions of chorematic diagrams in English goes on to say:

[...] kind of powerful diagram (*choréme*) that Brunet has perfected and which manage to convey the essential message of a complex argument with a few carefully chosen pen strokes, symbols and shading [71].

The quest to find out the details of chorematic shapeliness has thus been one of the areas of a more detailed investigation. In contrast to persuasive maps [202], the inherent poignancy of the schematised representation is tempered by subdued colours as well as smooth and gentle geometries. While repetition and a reduced set of angles and directions are definitely part of chorematic shapeliness and thus harmony, overbearing patterns are carefully avoided. The regularity and strict form of, say a hexagonal outline is mellowed by a non-hexagonal subdivision as in Fig. 5.12. Whereas a thematic map such as Fig. 5.6 dutifully repeats the grid pattern of Los Angeles streets further reinforced by the rectangular *Rahmenkarte*-layout, Fig. 5.5 harmoniously contrasts the smooth shapes of ethnic regions with its own *Rahmenkarte*-layout. The three main aesthetical qualities by which harmony is reached are shapeliness, neutrality and balance.

Subsumption. The three overarching design goals interact with varying prominence in all chorematic diagrams to produce the unique chorematic design space. That is to say that while many other maps and diagrams follow aesthetic principles like harmony or abstraction, the specific embodiments these principles find in chorematic diagrams is unique in their mixture and underlying goals. The following three sections roughly group the more

specific observations by the map compilation tasks composition, thematic encoding and drafting the shapes.

5.1.2 Composition

Composition here encompasses observable conscious and subconscious editorial decisions that govern the chorematic diagram as a whole or as diagram group.

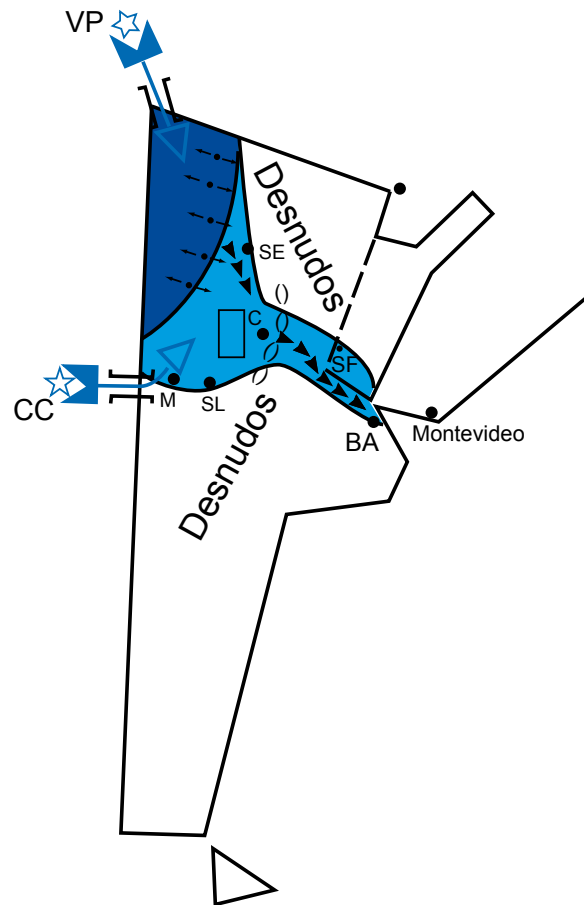
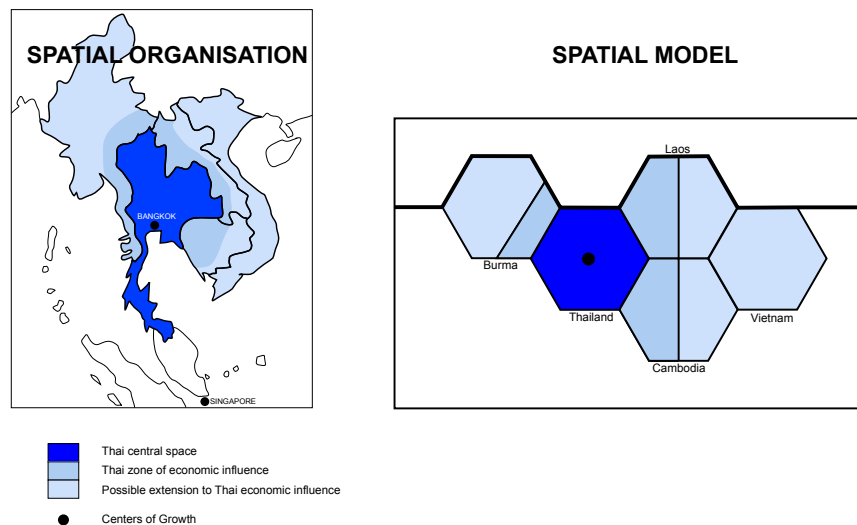


Figure 5.11 Influx of *criollo* settlers into Argentina. Redrawn from [124].

As has been established in Chapter 4, chorematic diagrams are always part of a wider geographical argument that is being made. The diagrams themselves highlight the spatial part of the argument, whereas the texts discuss causes, processes and effects. In light of the rationalist-materialist epistemic approach of the *chorématique* it follows naturally that the geometric form of a diagram is carefully matched to the geographic argument

that is being made. If the region of interest is framed as being a container of the discussed geographical phenomena, the boundaries of the region become the visual containers for the chorematic symbolisation. A quite literal example is Fig. 5.11, where settlers of the *criollo* caste are depicted as a blue *flow* filling up parts of the "empty bottle" of Argentina. The influx happens at two specified entry points signified each by a filler plug-like symbol. All instances of chorematic diagrams being framed as *Inselkarten* highlight the notion of the region of interest being such a container, for the argument being made in that specific instance. The instances (20%, see table 4.5) where *Rahmenkarten* are presented highlight the embeddedness of the phenomena within the continuum of geographic space, such as the Los Angeles riots example in Fig. 5.5. These decisions are of even greater importance when different regions of interest are being juxtaposed or compared. Consider Fig. 5.12, where the diverse geometries of South-East Asian nations are all reduced to hexagons of the very same size. Here visual similarity emphasises the nomothetic geographic elements in an otherwise highly idiographic environment.



The Thai Dream

Figure 5.12 The economic influence of Bangkok and Thailand in S-E Asia as thematic map and chorematic diagram. Note the wilful topology violation of Burma in the Spatial Model. Redrawn from [39].

Conscious use of such a kind of specificity matching allows subtle relations and juxtapositions to be emphasised, as has been done effectively in Fig. 5.13. Three chorematic diagrams show the three French overseas départements in the Americas. By layout alone, they are displayed as a unit. Their overseas nature is emphasised by including the ocean in all three, with Martinique and Guadeloupe as proper Islands and Guyane as classical case of a coastal entrepôt. Geometrically, Guadeloupe is shown as a 'double' Martinique

at the same scale via two and one circle respectively. Thus, both unifying and differentiating spatial properties of said regions are highlighted at the same time. The geometries have been tidied up in support of the overarching goal of lucidity.

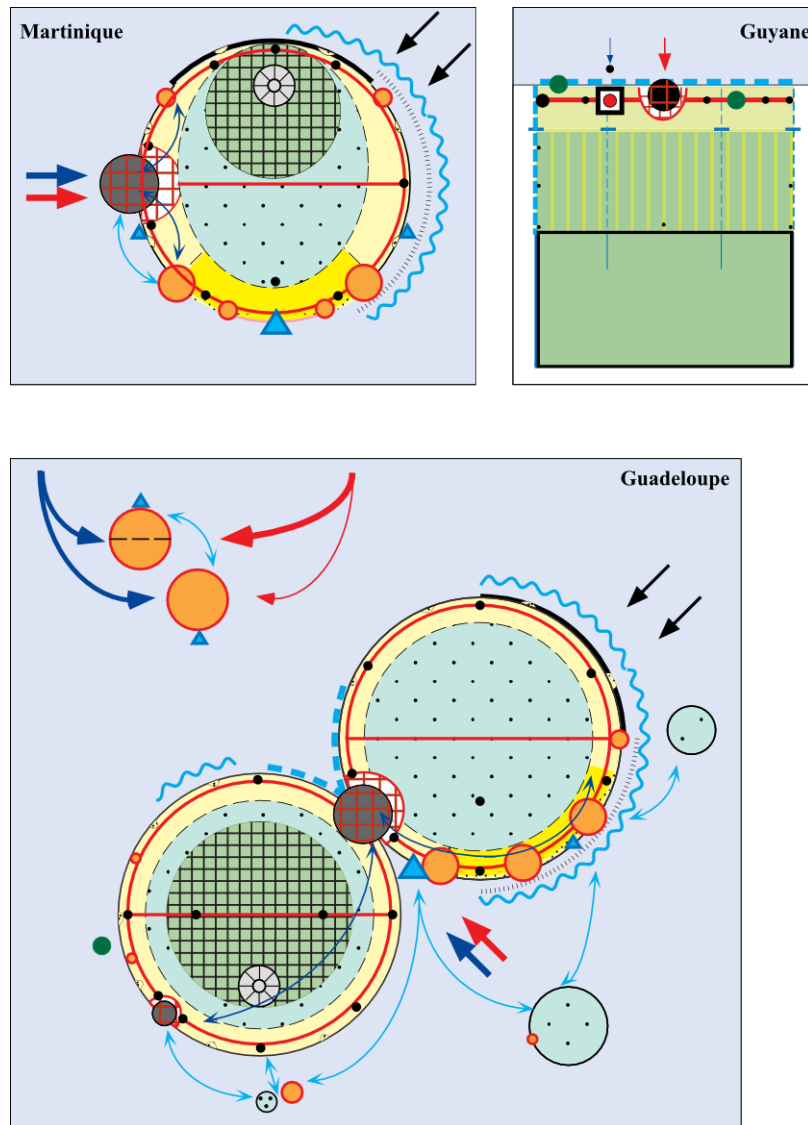


Figure 5.13 Arrangement of chorematic diagrams of French overseas territories highlighting various external and internal similarities and differences. Source [134].

Assuming we could somehow measure the spatial structure S of a given region, the compositional decisions in Fig. 5.13 show the set of external relations E :

$$E = S_{Martinique} \propto S_{Martinique} > S_{Guyane} \gg S_{World} \quad (5.1)$$

This is to say that compositional decisions regarding layout and outline choice are partially made in order to express those exterior relations that strengthen the geographic argument being pursued. For regular maps, the geometries as material exponents of spatial structure are expected to express their relations implicitly (if considered at all). Chorematic design can even go so far as to willingly ignore topological relations without being technically forced to do so by any orthodox cartographic constraint. An example here is Fig. 5.12, positioning Burma in a way that it becomes separated from Laos, although in this case Burma could safely be placed in a topology-preserving arrangement at the empty spot above Thailand.

5.1.3 Thematic encoding

From the wealth of available mapping techniques for thematic data (for example [166, 261]), only few are encountered. Although never made explicit by Brunet himself, the simple reason is that chorematic design eschews the display of quantitative data altogether. With less than a handful of counterexamples to be found (most notably [139, Fig. 6]), the lack of quantitative mapping techniques can safely be understood as the main determinant of chorematic thematic encoding. Following Bertin, quantities can only be encoded via the retinal variable size. In its essence, chorematic encodings do not use size as retinal variable, but instead solely concentrate on using size within the two dimensions of the plane. Chorematic diagrams thus always concentrate on the visual task of showing the spatial extent and location of a given phenomenon. With the focus firmly on the question what is where? and taking into account the goal of abstractness, carefully choosing the number and shape of the phenomena to be displayed is the logical main encoding strategy for thematic entities.

Area-class paradigm. Extant thematic cartography abundantly makes use of the choropleth technique. Categorical maps, also known as area-class maps, have been identified as being the more truthful and expressive solution [187], but still require a high degree of manual interpolation and intervention [54]. Chorematic diagrams, by their very nature as schematised representation of some geographical phenomenon's geometry, follow what we call the area-class paradigm. Instead of using administrative subdivisions, the thematic polygon's extents are drawn so as to coincide with the phenomenon. A striking example is given in Fig. 5.14. The upper left shows a chorematic area-class depiction of the basic structure of migratory and natural population change in Romania, the rest of the diagram shows an orthodox choropleth depiction and colour-coded histograms illustrating the different change patterns. The main generalisation operations at play here are aggregation and selection, followed by a schematised redrawing of the geometries. All three operations are undertaken in the spirit of bringing neatness and tidiness into the displayed geometries. The example also provides a good impression of the amount of

schematisation that has happened, from seven distinct classes and hundreds of administrative polygons to just three distinct areas. The compositional choices further serve to emphasise the area-class paradigm: where the mosaic of the choropleth elements suggest containment, as it is backed up by the Inselkarten layout, the chorematic diagram opposes the rectangular outline of chorematised Romania with the naturally curving interior subdivision of the area-class depiction. By doing that, the viewer intuitively expects the areas to continue into a wider, European population change landscape especially in the west where the Gestalt properties of the used curves hint at closed yellow shapes just behind the border.

For the more analytic diagram classes that concentrate on very few phenomena (i.e. AM, SM, OV and partially CM), a shape is a thing-in-itself. For the synthetic cases (SYM and SCM) the visual problem of displaying overlapping and thematically interacting phenomena comes to the forefront. Extant diagrams attempt to maximise differentiation and separability of individual layers by employing highly separable colours and hachures. The hachures use only a few variations of the retinal variables direction and texture/grain, namely 45°-steps and not more than three line/dot spacing schemes (e.g. Fig. 5.5, 5.9). These are usually in accordance with the suggestions and conjectures regarding high separability of direction and texture/grain from Bertin.

Colours. It was already established that the analytic diagram classes of AM and SM use a lower number of colours than the synthetic classes (Chapter 4). The concrete colour choices follow two different general strategies as logical outcomes of the area-class paradigm and the overarching goal of harmony, especially balance and neutrality. The goal of abstractness with its demand for non-associative colours serves not so much as a constraint, but as an enhanced degree of freedom for colour choice.

The first strategy is to use black and shades of grey in addition to a single main colour, which we call *austere guide-colour technique*. The guide-colour technique as exemplified by Fig. 5.15 and 5.5 contrasts the conceptual basic situation in shades of grey with the more salient and active phenomena and processes in the fully saturated guide-colours green and magenta, respectively. Such colour usage makes the division between base-map and thematic layer obvious and harkens back to the traditional cartographic technique of using a greyed out version of a topographic map as base-map. The choice of the guide-colour itself is more or less arbitrary, but extant diagrams sometimes appear in groups in the examined MappedMonde sources. That is to say that there are groups of articles in individual issues, for example on agriculture, that make use of the very same guide-colour. This is a cue to unity of modelling and geographic approach more than any direct connotation or material association of phenomenon to colour impression. Generally speaking, the austere guide-colour technique serves the general goal of lucidity well by putting emphasis on some phenomena in contrast to others in a visually obvious way with the potentially highest degree of selectivity. As there is little room for variation of a single colour, the austere technique is most often encountered in the analytic diagram classes SM, AM.

The second strategy that can be observed is the usage of a wide colour palette in order to provide visual separability for a multitude of phenomena within the same diagram.

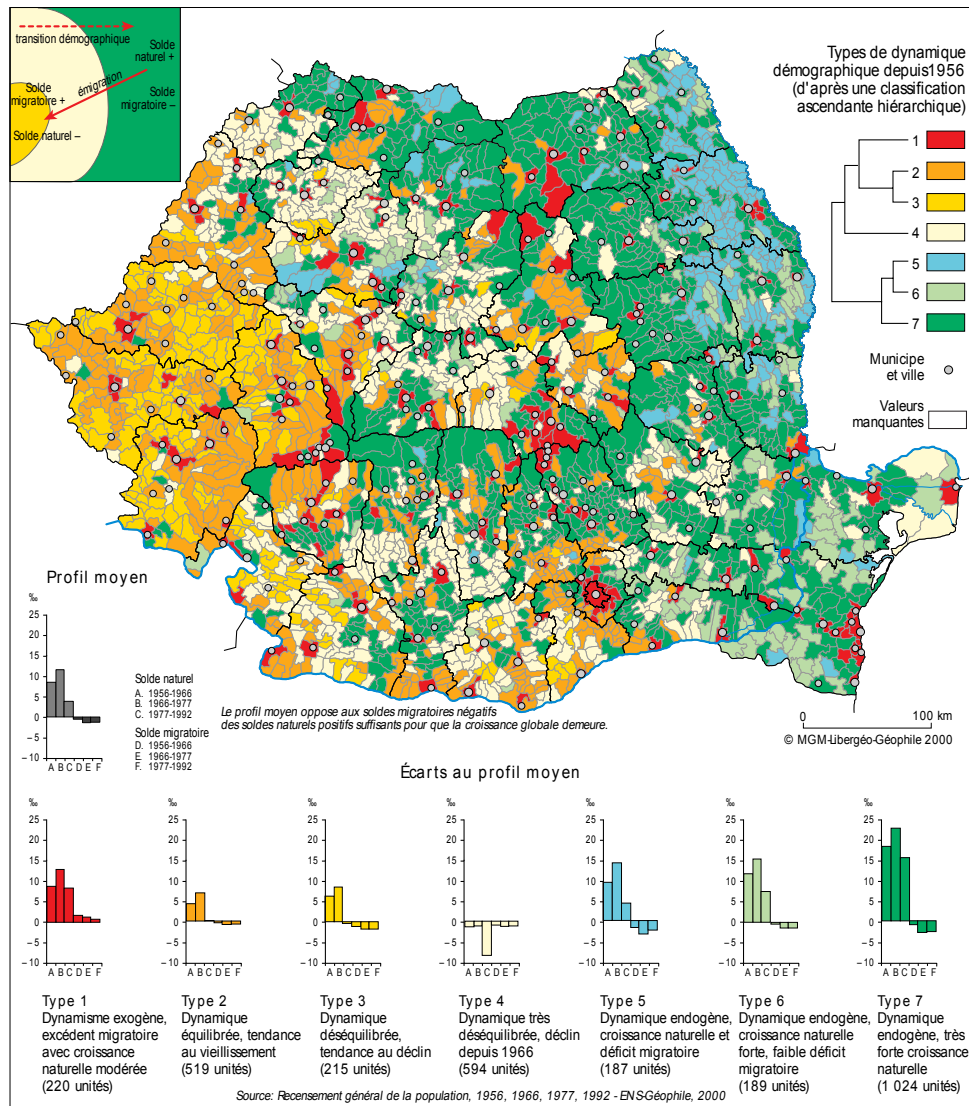


Figure 5.14 Population dynamism map from the *Atlas de Roumanie* [235].
Source: from the Atlases review [114].

we call this the *pastel-technique*: The demand for high visual separability as it is being mellowed by the notions of neutrality and a scientific look lead to the use of muted, low saturation pastel colours for polygons comparable to those used in political maps in atlases. Line features and point features are then coloured in fully saturated, highly

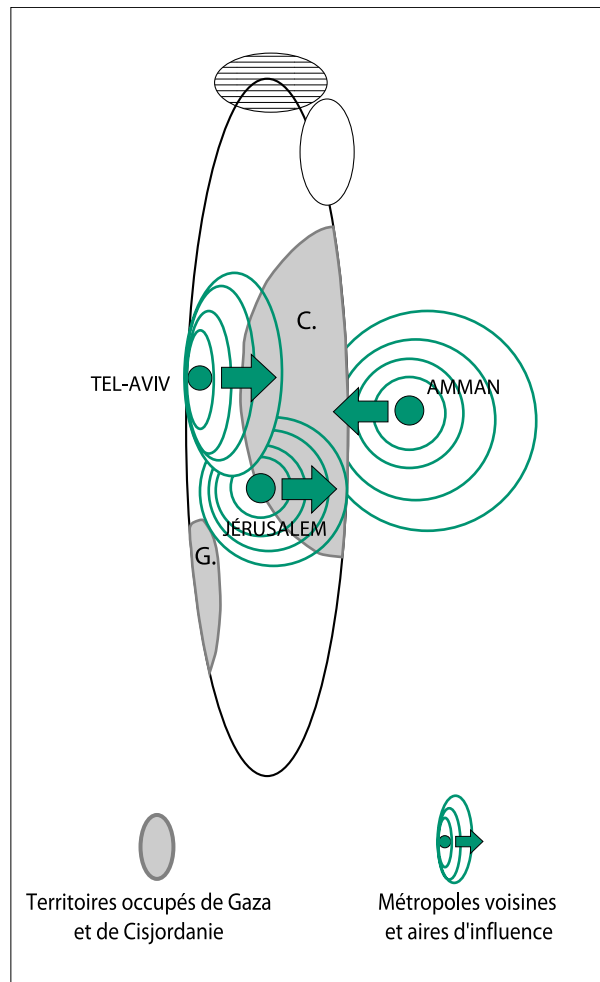


Figure 5.15 Example for the guide-colour technique, where black, grey and a single hue are varied used producing a neutral look for a potentially contentious subject. The diagram shows the influence of selected cities in the region. Source [143].

salient colours (such as black, red and dark blue) avoiding the yellow tones. An example of skillful application of these criteria is observable in Fig. 5.13. Such colour choices for line and point features are congruent with best practices in thematic cartography as laid down by [148], for example. It follows naturally that the pastel-technique is most often used for the synthetic diagram classes SYM and SCM.

As mentioned above, chorematic diagrams concentrate on showing qualitative data.

While eschewing quantitative data they do sometimes display ordinal relations of areal phenomena. Usually not more than three gradations are used, signified by colour value variations. As can be witnessed in Figs 4.3[e], 5.12 and 5.14, these ordinal relations are often based on a more general ordering of phenomena instead of a straightforward reclassification of some otherwise ratio-scaled variable. We call the tendency to display a low number of thematic gradations the *weak ordinal concept* in contrast to the full range of ordinal encodings partial to colour-gradient usage in conventional thematic maps.

5.1.4 Shape

The geometric shape of geographic line, area and network features found in chorematic diagrams presents the biggest departure from regular cartographic practice. From a generalisation viewpoint, the transformations the shapes undergo, would have to be characterised as a form of the generalisation operation caricature or viewed as operations specific to schematisation (see Chapter 3). It is important to note, that not all features of the same geometry type are treated equally: subdivisions are treated differently from territorial outlines, arrows differently from other linear, and network-forming elements differently from all others.

Territorial outlines. The shape of territorial outlines comes to the forefront in all *Inselkarten* layouts. They come in three different basic varieties (percentages from Table 4.5):

- symmetric shapes without clear elongation (circles, squares, hexagons) [20%],
- symmetric shapes with one clearly elongated axis (ellipses, rectangles and triangles) [31%] and
- asymmetric polygonal shapes constructed from either straight lines, circular arcs or Bézier curves [29%].

The Subsection on composition already discussed how the intended geographic message influences the choice of map type and arrangement to highlight the set of relevant external relations of the region of interest. The choice between displaying Guyane, for example, as a square or as rectangle on the other hand, is based upon the interior relations that are to be emphasised:

These choices themselves are not arbitrary: the circle implies that no direction is privileged and the periphery is everywhere at the same distance from the centre, while a square in this regard has four blind spots, an elongated rectangle already implies strong hypothesis on the structure of space, with a preferred direction; and so on. [43]

Whereas the symmetric outlines are driven by geographic intent, the asymmetric polygonal shapes are indeed schematised versions of their input geometries. The input geometries can be assumed to be the territorial outlines as they would be found at the cartographic scale of the projected chorematic diagram. They are first simplified beyond the conventional needs of the target scale and then get smoothed to fulfil one of the embodiments of chorematic harmony, i.e. harmonious curves or angularly adjusted straight

lines. The specific chorematic understanding of harmony for asymmetric shapes does not blindly enforce the design rules. Instead of forcing all segments of an outline to follow some *a priori* design rule, a certain amount of variation and individuality is maintained. The outline in Fig. 4.3 could easily have been orthogonalised fully, but purposefully was not. Such slight irregularity amidst radical geometric tidiness underlines the individuality and uniqueness of the region of interest. This mirrors the concept of *Fukinsei* (lit. "without symmetry") in Japanese aesthetics which by balancing symmetry with asymmetry expresses a form of natural harmony [78]. The enso circle in Zen Buddhism (Fig. 5.16) is probably the most famous expression of the Fukinsei concept.



Figure 5.16 Zazen bell with Enso in Background. Source: wikimedia commons.

The asymmetric outlines also achieve harmony by presenting no grossly protruding elements, overly acute angles and/or inflexions in the case of curves.

Ancillary topographic data. Brunet decidedly states that pure simplification based on geometry alone is anathema to chorematic design. Rather, other considerations have to inform the transformation:

One should not summarise at random or make diagrams without guiding principles, or be content to draw a straight line where reality is vague and sinuous, and a circle where it is roughly potato-shaped: that would be mutilation, not representation. – [44, p.120]

In a very lively reaction to a contentious article on a supposedly objective geometric process to derive the territorial outline of Australia [216], Brunet reinforces the notion that geometric operations need to be informed by topographic knowledge, which one can understand as ancillary data [49].

Recurring topographical situations that need to be considered are estuaries and vertices where an administrative boundary and a body of water meet (Fig. 5.27).

Subdivisions. Subdivisions lie at the heart of the chorematic area-class paradigm. The visual saliency of the smallest shown area is usually well above the minimal dimensions ensuring visibility. Conceptually, a subdivision is always a full tessellation of the parent polygon, but chorematic diagrams strive to avoid the whole to become unglued. This is especially true for *Inselkarten* which usually contrast the style of the outline with the style of the shapes governing the subdivision as for example in Fig. 5.14. Fig. 5.22 shows how not heeding such a design principle can create an unglued outline that looks like it does not form a whole. The visual contrast needed for cohesion is reached, for example, by choosing a straight-line polygon outline with a curved subdivision on the interior as also employed in Fig. 4.3. Another strategy against unglued outlines is to use symmetric shapes such as circles and ellipses which visually appear to lie on top of the region of interest. The same effect is used when hachures are employed, for both see Fig. 5.11.

For the case of *Inselkarten*, the individual polygons of a subdivision are usually of a lower complexity compared to the outline. This restriction does not apply where areal dynamism is encoded as a form of a conceptual wavefront spreading over or into another area such as in Fig. 5.17.

Network-forming elements. Network-forming elements [297] play a recurring and constituent role within the *chorématique* as one of the four major geometry types. Consequently they are often encountered in chorematic diagrams, although rarely take visual precedence. The example in Fig. 4.3 shows both visual strategies employed for network-forming elements: subfigure c) shows a strongly generalised transportation network that still includes sinuous edges between vertices and subfigures d) and e) show schematised topological networks with all edges being straight lines.

The former strategy is mostly applied to streets and where locality still is informative, whereas the latter takes precedence for conceptual networks where topological structure is at the forefront. The latter strategy can be likened to the metro map metaphor of schematised maps (cf. Chapter 3). These schematised networks are either strongly reduced to octolinearity or not angularly changed at all.

5.1.5 Chorematic design principles and cartographic merit

The sum of the observations elucidated above inform us on the properties of chorematic maps. Many of the properties are aesthetic qualities, some others are basic, observable facts. We already partially hinted and noted on connections between aesthetic qualities and some of the basic properties. The question arises though, whether there is a greater scheme, or system of aesthetic qualities these relations can be brought into. And more importantly: How do these relations themselves relate to what the community understands

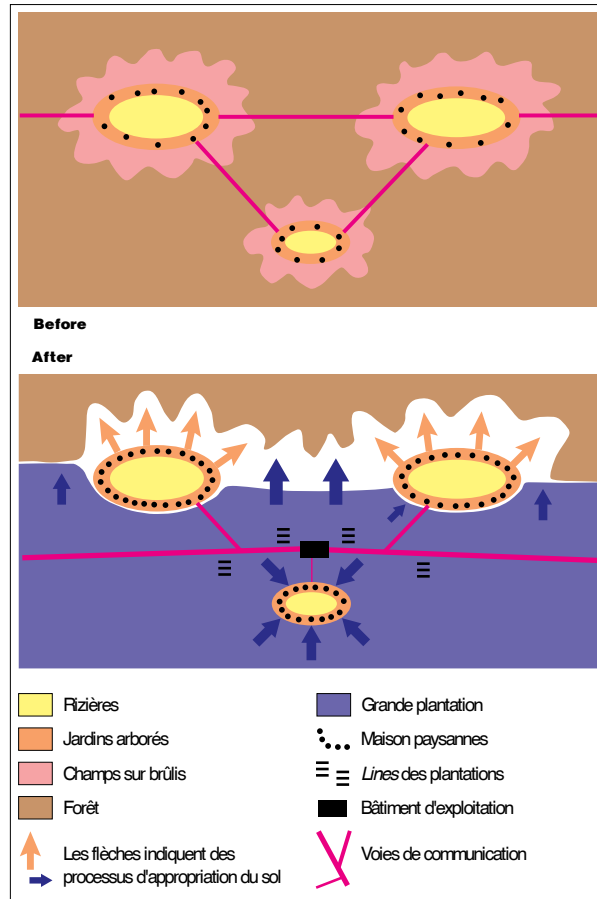


Figure 5.17 Land use changes in rural villages and plantations of Sri-Lanka, example for a chorematic wavefront. Note the high sinuosity and use of cubic Bézier splines. Source [194].

as good cartographic practice? In other words: Are chorematic diagrams any good? This question can of course only be answered under the presumption of an available general model of cartographic merit. In the following, we will sketch a general model of cartographic merit and link the chorematic design principles to them.

A theory of cartographic merit. Cartography has long been thought of as being at the crossroads of technique, science and aesthetics. One of the most widely accepted definitions of cartography reads:

cartography: The art, science and technology of making maps, together with their study as scientific documents and works of art. [195, 1.1]

If we understand aesthetics as being part of art, it is only fitting to look into the study of aesthetics, a branch of the philosophy of art, for some direction. In his article "Aesthetic Qualities and Aesthetic Value" [120], Alan Goldman develops a model for the relation of basic objective properties and artistic merit via the relations of some aesthetic qualities. He divides the properties of a work of art hierarchically into supervening evaluative aesthetic qualities, middle level evaluative aesthetic qualities and objective basic properties. The most important supervening evaluative aesthetic qualities are positively evaluated concepts like beauty (pleasing form), power of expression and originality. The middle level evaluative aesthetic qualities are then more detailed concepts, gracefulness or vividness of colour tying back into beauty, for example. It is important to note that the first two levels remain fully evaluative, that is to say that one observers vivid colour might look garish to another person. In other words, the moment an observer attributes a work with any of the evaluative qualities, *he has already judged it*. Goldman then goes on to state that it will remain impossible to tie observable, measurable facts into some evaluation function for artistic merit as a whole. One of the most profound reasons being that some evaluative qualities can supervene others without being necessitated by observable facts. This is especially the case for originality, which, if it becomes zero, will leave a work of art without any artistic merit whatsoever. It is exactly here where we can draw a firm line between art and cartography: for a map to be of value, it is utterly irrelevant whether any element of the map as aesthetic product is original.

We can thus go on and define a tentative high-level model for cartographic merit based on the fundamental supervening evaluative qualities of accuracy, expressiveness and beauty. A map that is to possess any cartographic merit must possess some amount of all three, with originality as an optional modification:

$$Merit = (Accuracy \cdot Expressiveness \cdot Beauty) \cdot (1 + Originality) \quad (5.2)$$

The three essential supervening aesthetic qualities do mirror the three dimensions of cartography from the definition above, with accuracy matching the scientific, expressiveness the technique and beauty the art part of said definition. Where it does not matter whether a certain map is original or not, the evaluative part of judging the other criteria is dependent on a certain task at hand, i.e. cartographic merit is ultimately also relative to outside context.

Chorematic merit. In Fig. 5.18, we have joined cartographic merit as described above with the chorematic design goals. The middle level evaluative qualities are mere examples, and many others might play a role for the general case of cartographic merit. The diagram does show, that the chorematic design goals can be understood as specific instances of aesthetic qualities essential for the expressiveness and beauty of a map in general. Good chorematic diagrams following the principles and constraints explored in the preceding sections thus fulfil at least two of the three essential qualities of a map. As we joined the chorematic design goals into a tentative model of chorematic merit, we can identify a bad chorematic design. The example shown in Fig. 5.2 violates many of the objective basic properties: The colours used for subdivisions are all fully saturated,

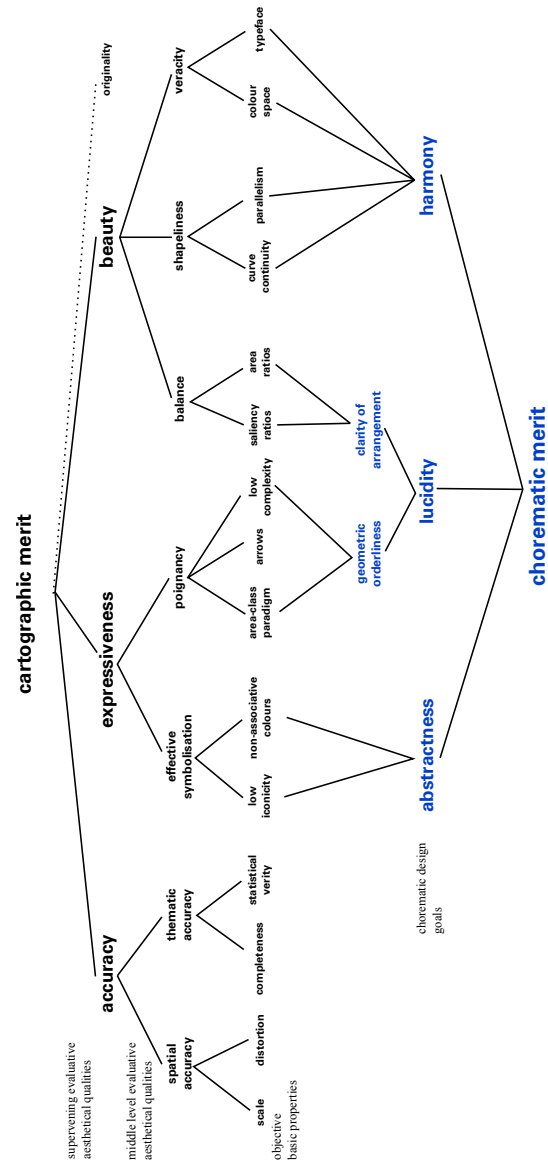


Figure 5.18 Our model of chorematic merit as instantiation of cartographic merit.

it uses high-iconicity symbolisation, has an unbalanced layout as well as a confusing, uneven subdivision structure bringing untidiness such as undefined white spaces and an overlap in the lower right corner. While not being totally without cartographic merit, the

chorematic is the lowest we could find among the sampled diagrams. It fails at providing a high amount of abstractness, lucidity and partially harmony. This is a first proof of concept to show that the insight gained so far can already serve qualitative judgement within the chorematic design space as well as in the wider concepts of aesthetics in of cartography.

5.2 Modelling for automation

Creating exactly the map that a person needs without any further information except some geodata is of course a logical impossibility. It has been proven possible though, to automatically create some maps provided that *a priori* knowledge about what the map is supposed to accomplish is available. In this section we propose a general model for the automated generation of chorematic diagrams. The model is general in the sense that it specifies what one needs to know and how these facts interrelate, but does not tie itself to a specific implementation or method. Nevertheless, we provide cues to existing or trivially attainable techniques for solving individual problems as well as to applicable data-structures. We begin with the examination of the necessary input, i.e. the information one needs and how to store said input. We then go into a more formal review of the chorematic constraints identified in the preceding Section 5.1. Section 5.4 presents the model of a procedure that connects the preceding elements into a construction strategy.

5.2.1 Necessary input

What we here call necessary input is structurally equivalent to what is called user requirements in the realm of on-demand mapping (well-discussed in [15]). Calling them necessary input highlights the fact that we attempt to identify those bits of information that are of *logical* necessity. At its most basic, we must need to know something about the purpose of the map. Chapter 3 has shown that schematised maps are almost entirely driven by their purpose compared to topographic, in other words, general purpose maps. A different way of expressing the purpose of a map is to ask which task it is useful for, or which task shall it support. Let t be a single task from the set of all tasks T . Noting that some models and taxonomies for tasks exist, they are still so general that we currently cannot assume a complete task model for all $t \in T$. What is especially missing is the matching function m to schematisation operation O . Instead we will identify what one needs to know first. Currently, user requirements are either only known and modelled in a relatively coarse, exemplary way (for example [106]) or are collected via very specific interactive processes such as design wizards [15]. With the minimum requirements as elucidated in the following, such an interactive process can conceivably be created.

5.2.2 Task definition

A useful task definition must answer the most basic questions of *what?* *where?* and *how?*. In the case of construction from data stored in some form of geodatabase, the *what?* is

also a *where?* question on its own. The task model must remain quite general as current research is lacking a well-formed 'atomic' interpretation of map-use task. Any task t can be matched to an ordered array of information known as the Task Definition Vector \hat{t} . This means the function:

$$f(t) = \hat{t} \quad (5.3)$$

is surjective ($f : T \twoheadrightarrow \hat{T}$), as it is true that

$$\forall t \in T, \exists \hat{t} \in \hat{T}, f(t) = \hat{t}. \quad (5.4)$$

Surjectivity of tasks and realized maps is in fact a cornerstone of why making maps is useful: one map is potentially helpful for several tasks. The informations necessary to generate a chorematic diagram are the region of interest R , the set of relevant external relations E , the set of relevant internal relations I , the layer hierarchy H and the list of relevant geographic processes P . The Task Definition Vector can thus be written as:

$$\hat{t} = \begin{pmatrix} R \\ E \\ I \\ H \\ P \end{pmatrix} \quad (5.5)$$

Region of interest. The regions of interest can be conveniently encoded by a bounding box *bbox* or a toponym *top*:

$$R := \{(bbox_1, top_1), \dots, (bbox_n, top_n)\} \quad (5.6)$$

where $bbox = [x_1, y_1], [x_2, y_2], [x_3, y_3], [x_4, y_4]$ and *top* is a string of characters that can be geocoded via existing gazetteers. Either can take no value, indicating implicitly whether embeddedness or container characteristics are more warranted for that region. The number of regions n is usually 1 but in the case of comparative approaches several can be included in the same diagram.

While it is conceivable to have non-rectangular *Rahmenkarten*-layouts, current geodata-base technology nevertheless would create a *bbox* for the spatial query.

External relations. The external relations can be understood as the set of all relations E that provide relative and or absolute information on the similarities between the n regions of interest. This includes information on the relation to the outside world. The input would be in the form of a symmetric matrix E considering at least all n regions of interest plus the outside world and plus specific entities k which might be important for peculiar geographic arguments. This yields an $m \times m$ matrix where $m = n + 1 + k$, $k \in \mathbb{N}_0$. To illustrate the concept, we will continue the example in Fig. 5.13 from Section 5.1. Here, we have the three regions of interest of Martinique, Guadeloupe and Guyane who are all in the same explicitly spelled out relation to France, namely overseas *Départements*. They also are in some relation to the world, with two common factors being situated in

the Americas as well as bordering the Atlantic Ocean. Both relations are made explicit in the paper and are thus assumed to be part of the geographic argument at hand. Our external relation matrix E_{ameri} thus has $n = 3$ regions of interest and $k = 1 = \text{France}$ entities peculiar to the argument of the article, yielding a 5×5 matrix as per:

$$m = n + 1 + k = 3 + 1 + 1 = 5. \quad (5.7)$$

Each entry $s_{ij}, s \in \{0, \dots, 1\}$ in the matrix is then some normalised structural similarity measure, with $i, j = \{\text{Martinique, Guadeloupe, Guyane, World, France}\}$. One can clearly see the symmetry of the matrix and perfect similarity between each entity and itself:

$$\mathbf{E}_{ameri} = \begin{bmatrix} 1 & 0.5 & 0.2 & 0.1 & 0.3 \\ 0.5 & 1 & 0.2 & 0.1 & 0.3 \\ 0.2 & 0.2 & 1 & 0.1 & 0.3 \\ 0.1 & 0.1 & 0.1 & 1 & 0 \\ 0.3 & 0.3 & 0.3 & 0 & 1 \end{bmatrix}. \quad (5.8)$$

Note that France and the World have zero similarity in that matrix. This is to say that the chorematic diagram does not in any way relate France and the world. This is in contrast to the unity of all three regions of interest being expressed both in their relation to the world (ocean) as well as especially their selection for comparison to begin with, which is entirely based on their common relation as parts of France. In essence, these are weights that express which relations to highlight and which to subdue for the geographic argument being pursued. We remind the reader that the schematisation operations for chorematic diagrams can be utterly radical so as to display any arbitrary collections of regions as circles of the same size, which would be indicated by the matrix being filled with 1's, for example.

Internal relations. The information on the relevant internal relations are needed especially for the shape-related decisions regarding individual regions of interest. The entry I for the task definition vector \hat{t} is constructed in the form of an ordered array itself. The necessary pieces of information are the number of relevant principal geometric axes $a \in \mathbb{N}$ defaulting to 1, their emphasis weights w_i ordered by length of axis and a list L of coordinate pairs $c = (x, y)$ of geographic characteristic points which are not already covered by the available geodata G , including ancillary data $A \subset G$. The entry thus takes the form:

$$I = \begin{pmatrix} a \\ w_1, \dots, w_a \\ L = c_1, \dots, c_i | c \notin G \end{pmatrix} \quad (5.9)$$

To provide an example, imagine a chorematic diagram is to be drawn for the country of Chile. The diagram is supposed to show vegetation differences between coastal areas and the Chilean Andes but should also show differentiation by climate zones. Two differentiating principal spatial axes (N-S and E-W) would be needed, with a slight overem-

phasis put on the E-W axis which would be too narrow otherwise. Assuming no otherwise critical points need to be considered, the encoding would look like:

$$i_{Ch\acute{u}leVeget} = \begin{pmatrix} a = 2 \\ w_1 = 1, w_2 = 2 \\ L = \{\} \end{pmatrix} \quad (5.10)$$

Thematic hierarchy. The thematic hierarchy H is encoded as an ordered list of pointers p to elements of the input geodata G and their corresponding importance weights w_i with i being equal to the number of layers. The ordering of the pointers indicates the drawing hierarchy and the corresponding weights regulate the emphasis they have for the geographic argument.

Processes. Of the 28 basic choremes as established by Brunet [43], 16 are concerned with processes with the remaining 12 mostly being concerned with static spatial structure (see Fig.4.2). In order to encode which of these 16 processes are to be displayed where in entry P of the task definition vector \hat{t} , a pointer p to the pertinent process from the set of chorematic processes $Ch \in [9 - 24]$ is needed. In addition each process needs to be supplied with a point, line, area or network-forming geometry as its origin o and corresponding points lines or areas as sinks s . The basic set of choremes can be substituted or supplemented by more specific sets of processes, such as those developed for agricultural processes in [66].

Topology. We established in Section 5.1 that chorematic diagrams may allow some topology violations if it serves the geographic argument and harmonious appearance. Technically, one could demand the user to provide a weighting matrix T_w for all topological relations of the input. Conceivably, the matrix could be generated in an interactive fashion with the user graphically indicating violable topologies. As topology violation is very seldom encountered in the diagrams the gains pale in comparison to the effort and overhead involved. There is also no general harmony function which to parametrise against, so we omit to forcibly include special topology variations. In a sense, for automated construction we assume the topology weighting matrix to be filled with 1's as default. Should a user have a graphical and geographical idea he absolutely must express then it is the most economical to allow manual post-hoc manipulation. Should a general harmony function become available, T_w could be added to the task definition vector \hat{t} .

5.3 Chorematic constraint modelling

It is common in automated map-labelling to formalize precepts on cartographic design in declarative sentences and call those "Rules". The nomenclature developed in automated generalisation distinguishes between rules and constraints in the following manner:

[...] rules state what is to be done in a process, while constraints stress what results should be obtained. [133, p. 73]

In the following we adopt the usage from generalisation research and present a consolidated list of chorematic design constraints. The observations are all justified in the running text above but are here isolated from their context as the first step of formalisation. We will briefly discuss each individual constraint that has been identified in Section 5.1 in light of further formalisation for computational construction.

5.3.1 General guidelines

GG1. *Chorematic diagrams should be of low cartographic complexity.* The cartographic line frequency $OLLpA[Bt]$ as explained in Chapter 3 is a suitable measure for cartographic complexity. The insights from the preceding Chapter 4 allow us to assign mean values and upper bounds for the complexity measure depending on the intended chorematic diagram class $c \in C = SM, AM, SYM, CM, SCM, OV$. The mean cartographic complexity C is then:

$$C_{mean} = f(c) = \begin{cases} 0.36Bt & \text{for } c = SM \\ 0.28Bt & \text{for } c = AM \\ 0.33Bt & \text{for } c = SYM \\ 0.28Bt & \text{for } c = CM \\ 0.43Bt & \text{for } c = SCM \\ 0.27Bt & \text{for } c = OV \end{cases} \quad (5.11)$$

For further differentiation the upper and lower bounds and other dispersion measures can be determined for each diagram class accordingly as simple lookup functions $f(c)$.

GG2. *Chorematic Diagrams should be abstract.* What we generally mean by calling a diagram abstract is that its geometric symbols provide very few visual cues to the non-geometric attributes of the geographic objects and phenomena they stand for. While we cannot hope to develop a generic measure for abstraction in graphics soon, the discussions in Subsection 5.1.1 revealed two determinants of how chorematic diagrams are abstract. Namely, low iconicity (see EC2) and avoidance of symbolic colour association (see EC3). For the time being, the degree to which EC2 and EC3 are fulfilled can stand in as a measure for abstraction. As degree of iconicity and symbolic colour association are values that go up as abstractness goes down, abstractness can be expressed as:

$$A_{chorem} = f(EC2, EC3) = \frac{1}{(w_1 \cdot EC2 + w_2 \cdot EC3)^\alpha}. \quad (5.12)$$

The α denotes a potentially penalty factor and the w s are weights. A simple negative linear relation seems unlikely, but the exact degree and nature of the exponential drop-off remains unknown. With our current knowledge we can recognise safe choices that are abstract enough.

GG3. *Chorematic diagrams should aim for a lucid display of their message.* Such clarity of presentation can conceivably be measured by balance measures B_i such as the range of

beneficial size ratios between area objects B_{areas} , the range of beneficial saliency differences $B_{saliency}$ and the amount of geometric orderliness of all objects B_{order} . These are all relative phenomena in that they look at interrelations between objects and groups of objects. Measuring the balance of the overall layout B_{layout} would be done in a similar vein. As has been shown for map labelling (cf. disambiguation in Chapter 2) and in multi-agent generalisation systems, such measures are attainable but require great effort for each individual type of group phenomenon. By definition, each such group phenomenon is independent of the others, meaning that should two group phenomena interact, they would warrant another meta-group measure. For the case of chorematic diagrams, the low general number of objects counter this potentially exploding problem space. A measure for the lucidity L can thus take the simple form of a weighted sum:

$$L = w_1 \cdot B_{areas} + w_2 \cdot B_{saliency} + w_3 \cdot B_{order} + w_4 \cdot B_{layout}. \quad (5.13)$$

GG4. *Chorematic diagrams should strive for harmony in the geometries they display.* A general harmony function would need to take into account how good each individual shape matches the geometric constraints regarding shapeliness. Depending on the type of object, type of geometry and drawing style, individual functions come into play. For example, curve continuity as one sub-element of shape-harmony, follows utterly different measurements than angular restrictions and so on. Such a weighted sum of individual shape evaluations seems much more attainable in the near future than, for example, a general function of abstractness. More formally, harmony H :

$$H = \sum_{i=1}^n w_i \cdot \sum_{j=1}^m h_{ij} \quad (5.14)$$

where h_{ij} is the harmony value for $object_{ij}$ of object type i . The variable n stands for the number of different object types with different harmony functions and m for the number of objects of such a type; w_i denotes the weight for object type i .

GG5. *Chorematic diagrams should aim for a veracious look by employing neutral fonts and a scientific look & feel.* It is quite obvious that this is the most relative of the general guidelines. It is definitely feasible to observe what fonts, colours and other design elements can be found in the contemporary scientific mainstream and emulate that. But the mapping of material characteristics of a diagram to notions of "science" and "neutrality" are changing over time in a non-linear and fundamentally unpredictable manner. One cannot predict at what point and due to which reason a certain font or colour range stops being "scientific" and starts looking quaint or even repulsive. An example might be the well-known changes the value judgements attached to fonts change depending on former usage. After widespread adoption by corporate America in the '60s and '70s and again in the age of the desktop publishing, the font Helvetica has, for some, become the face of Capitalism, the Vietnam war and the state [144]. In other words, anything but neutral. As usage of design elements and the advance of scientific publishing and its attached look & feel over time are unpredictable, we abstain from further modelling of GG5.

5.3.2 Composition constraints

CC1. *Chorematic diagrams should use Rahmenkarten-layouts to highlight embeddedness.* As indicated by the input, if a *Rahmenkarte* is warranted, the diagram should be constructed as one. The algorithm/procedure is simply triggered, cutting out the geodata from the database in a rectangular fashion. For purposes of further reprojection, this bounding rectangle takes the place of the territorial outlines. The constraint measure thus is simply a boolean variable $x \in \{false, true\}$ taking the value *true* in the case of a *Rahmenkarte*. It can be directly derived from the Region of Interest R that is part of the input vector \hat{t} .

An evaluation of the necessary input R thus already is sufficient to decide which value constraint CC1 takes:

$$x_{CC1} = f(R) = \begin{cases} true & \text{for } [x_1, y_1] \neq [x_2, y_2] \neq [x_3, y_3] \neq [x_4, y_4] \\ false & \text{for } top \neq \{\} \end{cases} \quad (5.15)$$

CC2. *Chorematic diagrams should use Inselkarten-layouts to highlight a spatial container.* Very similar to CC1, the value for CC2 can directly be derived from the input vector \hat{t} :

$$x_{CC2} = f(R) = \begin{cases} false & \text{for } [x_1, y_1] \neq [x_2, y_2] \neq [x_3, y_3] \neq [x_4, y_4] \\ true & \text{for } top \neq \{\}. \end{cases} \quad (5.16)$$

CC3. *Chorematic diagrams should arrange multiple regions such as to highlight external geographic relations important for the argument.* The external geographic relations are stored as part of the input vector \hat{t} in the form of the $m \times m$ matrix E . Presupposing the existence of some structural similarity measure, the realised structural similarity in the form of E_{out} could be compared to the intended structural similarity E_{in} . Measuring the adherence to CC3 can then be accomplished calculating the Frobenius norm $\|\cdot\|_F$ [29] of the difference between input and output matrices:

$$Measure_{CC3} = \|E_{\Delta}\|_F \quad (5.17)$$

where $E_{\Delta} = E_{out} - E_{in}$.

The Frobenius norm is generally defined as the square root of the sum of squares of the absolute value of all matrix elements, so that the Measure for CC3 becomes:

$$\|E_{\Delta}\|_F = \sqrt{\sum_{i=1}^m \sum_{j=1}^n (a_{ij} - b_{ij})^2} \quad (5.18)$$

where $a_{ij} \in E_{out}$ and $b_{ij} \in E_{in}$.

A measure for structural similarity to populate the matrices remains the missing piece to determine the beneficial values for $CC3$.

CC4. *Labelling and annotation are optional.* The choice is left to the user, formally making the constraint a binary variable with $value_{CC4} = \{0, 1\}$. Note that this is only true for observed chorematic diagrams that were all placed inside a larger context of accompanying text.

CC5. *Chorematic diagrams should have an exhaustive legend.* This represents mostly a constraint on all other degrees of graphical freedom, as $value_{CC5} = true$ leaves no choice, graphical real estate must be set aside and an exhaustive legend generated.

CC6. *Scale information is optional.* The choice is left up to the user, formally making the constraint a binary variable with $value_{CC6} = \{0, 1\}$.

CC7. *Some topology violation might be allowed.* Topology violations have only been observed in cases where the violation serves $GG3$ and $CC3$ at the same time. See also the arguments in section 5.2 regarding the harmony function.

CC8. *Overbearing patterns should be avoided.* It is currently unclear how the visual weight of emergent phenomena like patterns (in the sense of section 5.1) could be measured in maps.

5.3.3 Encoding constraints

Note: in the following we use parts of the Bertinian terminology [28] to formalize encoding constraints.

EC1. *Chorematic diagrams should only show qualitative or ordinal scaled data.* Formally, the set of legal target scale levels SL at which components are displayed should not include Quantity Q :

$$SL = \{\equiv, \neq, O\} \quad (5.19)$$

EC1a. *Ordinal phenomena should have about three intensities.* In other words, the ordered components C should not have a Length $L_C > 3$. We call this the weak ordinal concept.

EC2. *Chorematic Diagrams should only use low-iconicity symbolisations.* It is unclear how to measure iconicity, but if one had an approach then no symbol should have iconicity higher than a certain threshold. So long as the symbolisation choices are within the established acceptable list of examples, EC2 can be fulfilled automatically. Formally:

$$I = \{i | i \in \mathbb{R}^+ \text{ is iconicity value for each unique symbol } s \in S\} \quad (5.20)$$

$$measure_{EC2} = \sup I \quad (5.21)$$

$$value_{EC2} \in [0, x), x \in \mathbb{R}^+ \quad (5.22)$$

The generic iconicity function $I = f(s)$ as well as x are unknown. For the set of realised point symbols $S_p \subset S$ identified in Chapter 4

$$S_p = \{s_p | s_p \in \{+-, \text{circles}, \text{stars}, \text{squares}, \text{hexagons}, \text{triangles}\}\} \quad (5.23)$$

it is known that

$$I = f(s_p) < x, \forall s_p \in S_p. \quad (5.24)$$

In turn they (the members of S_p) can be safely used.

EC3. *Chorematic diagrams should mostly use colours with a low semantic connotation to the subject matter.* Following Imhof [148], colours can have inner, outer or no semantic association to the objects they reference. In his sense, outer associations are visible colour similarities between map symbol and geo-object, with the prime example being green for woodland. Inner associations are culturally contingent concept-colour mappings such as (love, red). There is currently no automated way to reliably assign a semantic category to arbitrary input geo-data, although suggestions for common cases have been made [262]. There also is no model for generating prevalent colours based on a known semantic category suitable for outer associations. Both factors currently prevent any further quantification or formalisation of this constraint. There are lookup-tables for culturally contingent (concept, colour) pairings which could be used in the future.

EC4. *Analytic diagrams may just use a single hue in addition to black and white (austere-guide-colour technique).* The choice seems to be unrelated to subject matter and thus arbitrary. Once positively decided for, it can be fulfilled, by simply choosing a hue value x which is then fixed so that only lightness and saturation may be varied.

EC5. *Synthetic diagrams should use muted and desaturated colours for areas.* We call this the pastel-technique. Technically limiting the colour choice to pastels is implementation and colour-model dependent. One feasible strategy is to randomly generate roughly perceptually equidistant colours and using only those that match the saturation and lightness conditions of pastel colours in the respective colour model. In the HCL (Hue-Chroma-Lightness; $H \in [0, 360]$ and $C, L \in [0, 10]$) model, pastel colours live in the space between the values [152]:

$$H : \{0 - 360^\circ\} \ C : \{0 - 0.9\} \ L : \{1 - 1.5\} \quad (5.25)$$

EC6. *Line and point symbols should use fully saturated colours and avoid yellow hues.* In the HCL model this limits the range of values for the colour C of line and point symbols to:

$$C_{P,L} = H : \{0 - 50; 70 - 360^\circ\} \wedge C : \{> 3\} \quad (5.26)$$

EC7. *Analytic diagrams should strive for a high separability of visual elements/components.* Such separability \neq can be achieved by several variations V of the visual variables:

$$V_{\neq} = \{2PD(IM), SI, VA, TE, CO, OR^-\} \quad (5.27)$$

In cartography the highest selective power is attributed to variations of implantation IM as a sub-element of the 2 dimensions of the drawing plane PD and colour CO . Whereas implantation can only take three variations of selective power ($IM \in [P, L, A]$), colour space is much larger. Several colours spaces such as CIELAB attempt to provide perceptually equidistant coordinates, so that computed distances equal perceptive distances. Let the perceptual distance between two colours a and b be ΔE_{ab}^* , then the partial measure for EC7 concerning colour $measure_{CO}$ is the set of all pairwise distances $D \in |Lab|$. The partial constraint is fulfilled when:

$$\min(D) > \Delta E^*_{mid} \quad (5.28)$$

where ΔE^*_{mid} is the threshold value after which perceptual distances are classified as 'high'.

EC8. *Processes should be displayed by a variation of the symbolisation suggestions from the table of choremes.* Given the set of processes $p \in P$ from the task definition vector \hat{t} , an associative array in the form:

$$A = ("Process" : "Choreme") \quad (5.29)$$

can be created. This map of concrete process to abstract chorematic process lies at the heart of the chorématique. As mentioned above, we can only cover the cartographic and geometric aspects in this work. The cartographic embodiment D of a chorematic process $ch \in CH$; $CH = \{ch | ch \in 8 < \mathbb{N} < 25\}$ is a function of that process ch coupled to origin(s) o and sink(s) s .

$$D = f(ch) = \begin{cases} n \cdot \text{arrow}_i \text{ for } ch = 9 \text{ (satellite points)} \\ n \cdot \text{cascading circles, ellipses for } ch = 10 \text{ (orbits)} \\ \text{polygon for } ch = 11 \text{ (attraction area)} \\ n \cdot \text{lines for } ch = 12 \text{ (preferred relationships)} \\ 2 \cdot \text{arrow}_o \text{ for } ch = 13 \text{ (passage point)} \\ \text{polyline for } ch = 14 \text{ (rupture)} \\ 2 \cdot \text{hachured band for } ch = 15 \text{ (contact areas)} \\ n \cdot \text{arrow}_i + m \cdot \text{arrow}_o \text{ for } ch = 16 \text{ (base, abutment)} \\ \text{arrow}_o \text{ for } ch = 17 \text{ (directed movement)} \\ k \cdot \text{arrow}_o + \text{line for } ch = 18 \text{ (division line)} \\ \text{arrow}_f + \text{polygon for } ch = 19 \text{ (tendency surfaces)} \\ n \cdot \text{arrow}_i + \text{subdivision for } ch = 20 \text{ (asymmetry)} \\ n \cdot ' + ' + m \cdot ' - ' \text{ for } ch = 21 \text{ (point evolutions)} \\ \text{arrow}_l \text{ for } ch = 22 \text{ (axes of propagation)} \\ \text{isopleth for } ch = 23 \text{ (areas of extension)} \\ l \cdot \text{arrow}_o + \text{wavefront for } ch = 24 \text{ (tissue of change)} \end{cases} \quad (5.30)$$

Due to the importance and variety of arrows in the source material, we differentiate them further:

- (1) arrow_i denotes inbound arrows, they all share the same destination sink s and need n specified origins o , where n is equal to the number of arrows.
- (2) arrow_o denotes outbound arrows, the n arrows all share the same origin o and need $n \cdot s$ destinations. For $ch = 24$ the number of arrows is equal to the number of expanding network elements l , that is $n = l$.
- (3) arrow_l denotes a line-feature with an arrow head.
- (4) arrow_f denotes a field of arrows filling a polygon

Note that the peculiar geometric definition of origins and sinks can vary, most likely is that they can be assigned to some existing or constructed object.

EC9. *Hachures and patterns should be simple variations of spacing dots or lines.* This constraint can be fulfilled by generally following Bertin's suggestions and examples for texture variation (TE) [28]. The set of allowed variations is reduced by only allowing lines and circles as basic shapes.

EC10. *Line Hachures should use few variations of direction and maximise their angular difference.* This constraint amounts to limiting the combined realised Length L :

$$TE + OR \rightarrow L_{\neq} \approx 3$$

5.3.4 Shape constraints

SC1. *The choice of the type of territorial outline for Inselkarten should reflect the interior geographic relations important for the argument.* As we presuppose that the interior geographic relations $I = (a, w_1 \cdots w_i, L)$ have been handed over alongside the task definition vector \hat{t} , we can formally interpret the choice of outline type O as a function of I :

$$O = f(I) = \begin{cases} \text{circle} \vee \text{square} & \text{for } a = 1 \wedge L = \{\} \\ \text{ellipse} \vee \text{rectangle} & \text{for } a = 2 \wedge L = \{\} \\ \text{triangle} & \text{for } a = 1 \wedge |L| = 3 \\ \text{hexagon} & \text{for } a = 3 \wedge L = \{\} \\ \text{polygon} & \text{for } a > 3 \vee |L| > 3 \end{cases} \quad (5.31)$$

Note that there is currently no firm understanding about when, why and for which subsets a polygon should employ curved segments, straight lines or circular arcs.

SC2. *Symmetric outlines should heed the aspect ratio of the minimum bounding rectangle of the input geometry if and only if this is in accordance with I .* This constraint is measured by comparing the resulting aspect ratio to the prospected aspect ratio derived by multiplication of the axes with their respective weights w_i from I .

SC3. *Asymmetric outlines should have a low number of control points.*

$$|CP_{asym}| \in [5 - 40] \quad (5.32)$$

The legal number of control points can be narrowed down further if we have information about the target chorematic diagram class.

SC4. *The resulting shape should be within a certain threshold distance to corresponding points on the input polygon.* The threshold distance value $dist$ was empirically determined to be:

$$dist = 0.03 \cdot diamP \quad (5.33)$$

SC5. *Some, but not all, segments in straight-line polygons should be parallel to each other.* The amount of parallelism Q can be measured as explained in detail below (Section 5.5).

$$Q(S) = \begin{cases} \frac{\sum_{e \in S} q(e)}{2 \cdot \sum_{e \in S} |e|} & \text{if } S \text{ is valid} \\ 0 & \text{if } S \text{ is invalid} \end{cases}$$

The constraint values should be within the range:

$$value_{SC4} \in [0.2 - 0.8] \quad (5.34)$$

Note that this soft constraint is subject to a hard constraint based on the chorematic diagram class c :

$$Q = f(c) = \begin{cases} [e, f[:= \{p \in \mathbb{R} | e \leq p \leq f\} & \text{for } c \in \{SM, SYM\} \\ [e, f] := \{p \in \mathbb{R} | e \leq p < f\} & \text{for } c \in \{AM, CM, SCM, OV\} \end{cases} \quad (5.35)$$

where $e = 0$ and $f = 1$, signifying the absolute bounds.

SC6. *Curved outlines should show some continuity between adjacent curve segments.* For a discussion of and heuristic approaches to continuity in curved outlines see Chapter 6 and [292]. The beneficial degree and type of continuity for a given connecting vertex depends on the general shape of the territorial outline. Both the location as well as the mapping to a desired continuity are related to the general problem of outline segmentation, which remains an open problem.

SC7. *Curve segments should show some, but not total, similarity in curvature.* This map-wide measure seeks to capture self-similarity over the whole map akin to SC5. As we are still lacking a parallelism measure for cartographic Bézier - curves (see Chapter 3, Subsection 3.4.1), the range of values is not precisely known.

SC7a. *Circular arcs should have similar but not necessarily equal radii.* The extant diagrams suggest that $\approx 30\%$ of the circular arcs should use similar radii. Note that the statistical basis needs to be broadened for more general insight.

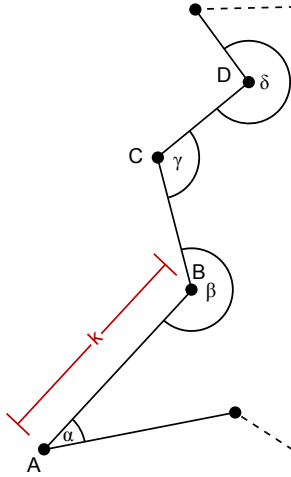


Figure 5.19 Exemplary chain of a polygon with inner angles $\alpha - \gamma$.

SC8. *Outline segments of any kind should not be too long or too short.* Formally, the length k (cf. Fig. 5.19) should lie within a certain range D :

$$D = [c, d] := \{k \in \mathbb{R} | c \leq k \leq d\} \quad (5.36)$$

where c and d are the empirically derived lower and upper thresholds, respectively. Note that we assume all segments to be cartographically simplified to exclude any variations beyond the well-known minimal dimensions of visibility.

SC9. *Outline segments should not show angles or inflections that are too steep or acute.* Formally, the angle a (cf. Fig. 5.19) should lie within a certain range A :

$$A = [a, b] := \{\alpha \in \mathbb{R} | a \leq \alpha \leq b\} \quad (5.37)$$

where a is the lower allowed steep and b the upper acute angle.

SC10. *Topographically important points should be geometrically exaggerated.* This constraint can be fulfilled by including geographic characteristic points L from the internal relations vector I in addition to those derived geometrically.

SC11. *Estuaries and lagoons in the input geometry should be ignored.* As with geographic characteristic points, the identification of estuaries and lagoons presupposes some kind of ancillary data source A allowing the identification of the relevant chains C of the input polygon P . While identification only based on outline geometry is impossible, extant gazetteers might provide already enough disambiguation to inform otherwise geometric detection procedures.

SC12. *Multi-part outlines should only show parts above a certain size.* Due to the considerable variety of sizes of chorematic diagrams, the lower size bound (L) should be expressed as relative value m , except where the absolute limits of visibility would be violated:

$$L = f(A) = \begin{cases} m \cdot A & \text{if } m \cdot A \geq \dim_{min} \\ \dim_{min} & \text{if } m \cdot A < \dim_{min} \end{cases} \quad (5.38)$$

where A is the area of the largest part of the multi part outline and \dim_{min} the applicable cartographic minimal dimension, both in drawing space mm^2 .

SC13. *Arrows should be represented with curves with not more than two inflexion points.* The basic notion can be further specified for different kind of arrows. In cartography, arrows are drawn with Bézier curves. The degree of the Bézier curve naturally limits the number of possible inflection points. The upper bound on the Bézier curve's degree d is a function of the chorematic arrow class $a \in [inbound, outbound, line, field]$:

$$d = f(a) = \begin{cases} 2 & \text{for } a = inbound \vee outbound \vee field \\ 3 & \text{for } a = line. \end{cases} \quad (5.39)$$

Note that in case of $a = line$, the base feature might need to be represented with a cubic Bézier spline, that is a set of C^0 -continuous cubic curves, in lieu of a single cubic curve.

SC14. *Subdivisions should be visually different from the outline.* In the realised chorematic diagrams this is often achieved by choosing different schematisation operations Sc (cf. Chapter 3) for territorial outline O and subdivision Sc respectively. Formally: $Sc_O \neq Sc_S$, where:

$$Sc_x \in [\textit{straight}, \textit{parallelism}, \textit{Bézier}, \textit{C - oriented}, \textit{circulararcs}]. \quad (5.40)$$

SC15. *Subdividing curve segments that start and end on the territorial outline should not have more than one inflexion point.* This constraint can be fulfilled by only fitting a cubic Bézier curve in the mentioned case. Formally, let be the chain C be a maximal series of consecutive edges of degree 2 from the planar subdivision S of the area defined by the outline shape O . Then C is replaced by a fitted cubic Bézier curve C_{bez} if:

$$c_1 \wedge c_n \in O \wedge [c_2 - c_{n-1}] \notin O \quad (5.41)$$

where c denotes a vertex of the Chain C with c_n being the last vertex. Note that this rule obviously only applies to cases where a decision has been made to use a curved subdivision. In the case of straight line subdivision, a simplification to 4 vertices would fulfil the constraint. See Subsection 5.5.2 for further elaboration and a simple implementation.

SC16. *Elements of a subdivision that are fully contained within the territorial outline or in a Rahmenkarte should follow SC1-12.*

SC17. *Wavefront subdivisions should have a higher sinuosity than all other area elements.* Let cartographic sinuosity y be the ratio of actual path length over the direct connection between start and end point (this is known in computational geometry as *detour sinuosity*, cf. [56]). Then:

$$y_{wavefront} \gg \max[y_{area}] \quad (5.42)$$

must hold. For practical purposes that often can be achieved allowing wavefronts to be created with more than twice the number of Bézier curves compared to other area elements.

SC18. *Network-forming elements should be planar.* Theoretically, planarity could be checked with the Kuratowski theorem etc. [142]. More practically, edge crossings in geodata usually have a well-defined semantic meaning, for example a bridge. This constraint thus is mostly a constraint on model generalisation.

SC19. *Network-forming elements should be of very low complexity.* As network forming elements are planar graphs with an upper bound on the number of edges of $e \leq 3v - 6$ their complexity can simply be measured by the number of vertices v . During our analysis, we have not encountered a chorematic network with $v > 50$. For comparison the London Tube Map, the poster child of low complexity maps, currently depicts 270 stations [107].

SC20. *Angular schematisation of network-forming elements is optional.* Although often interpreted as the cornerstone of schematisation especially for transportation maps,

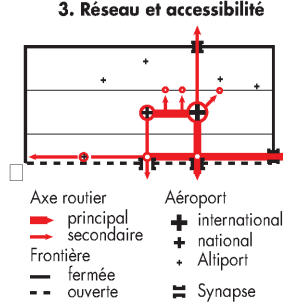


Figure 5.20 Example for an octilinear chorematic transport network.
Source [243]

generating *mathcalC*-oriented transformations of the input [193] is rarely encountered (Fig. 5.20). From what we gather the decision is as such arbitrary and in doubt no *mathcalC*-oriented transformation should be conducted for networks.

SC21. *Transportation networks may retain some sinuosity of edges.* Edges in the above sense are chains C maximal series of consecutive edges of degree 2. The upper bound U of the detour sinuosity y (cf. SC17) for transportation networks is 1.5.

5.4 Procedural model

Any attempt at automated schematisation needs to be governed by the pairing of desired output complexity and generalisation operators. Generating the desired output complexity/design rule pairing from an input task can be interpreted as a function of the form:

$$f(n) = \sum_{i=1}^n (W_i s_i) \quad (5.43)$$

with $s \in S$; $W_i \in [0, 1]$ and $W_i + W_j = 1$; where W_i denotes the weight attributed to s_i , the chorematic class from the set of all classes S from an input task t . Currently there are no available automated methods that model this function, so we treat it as a black box, that means we presuppose this decision has been made a priori. The degree to which we must apply these techniques depends largely on the complexity of the underlying data and the number of objects we wish to visualise. The classification and complexity measures that result from investigations into chorematic diagrams have the advantage of allowing us to transform the black-box problem into a matching problem.

Let T be the set of tasks and S be the set of chorematic diagram classes. Then the matching $m : T \times S \rightarrow \mathbb{B}$ is a Boolean function that decides whether a chorematic class in S matches the given task in T . The set $M_s(t) : T \rightarrow \mathcal{P}(S)$ gives for any task $t \in T$ the subset of S that matches t . That is,

$$M_s(t) = \{s | s \in S \wedge m(t, s)\} \quad (5.44)$$

Such a matching from task to the minimally allowable chorematic diagram classes expressed as $sup/f(s) : s \in S/$ seems more tractable than a possibly AI-complete black-box function of the general case. Instead of the complete function $f(t)$, we only need to know the minimum required information for a given task to select from the known and well-described set of chorematic diagram classes. Assuming we are given a task-derived chorematic diagram class and a layer hierarchy derived from datasets associated with the task, we can envisage the compilation stages as: the reduction in complexity of each layer, the application of various design rules, and their evaluation (Fig. 5.21). Depending on the outcome of the evaluation, the preceding step needs to be repeated or adjusted. The layers are hierarchically inserted into the first layer (always the territorial outline) via a mapping utilising anchor points that preserve desirable topological relations (cf. Saalfeld 2001 [242]). This hierarchical model mimics a process often used in manual chorematic diagram creation, in which layers are created and fused to the schematised basemap with different design principles applied to different layers.

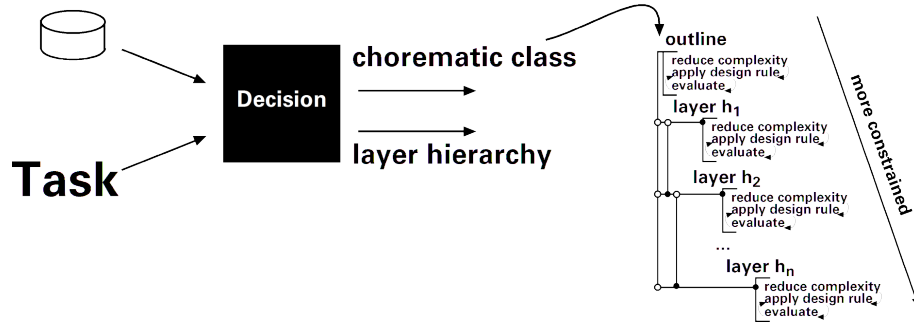


Figure 5.21 Modelling the design of chorematic diagrams.

5.5 Exemplary validation

To move from very general observations to measurable properties is naturally a labour-intensive endeavour. In the following section we present two explorations of individual constraints, namely *SC3*, *SC4*, *SC5* (low number of control points, threshold distance to input and some parallelism) in the first subsection on outline parallelism. The second subsection dealing with *SC14* (visual difference between outline and internal subdivision) and *SC15* (limited number of inflection points) is one of the few approaches for bringing Bézier curves into automated map generation.

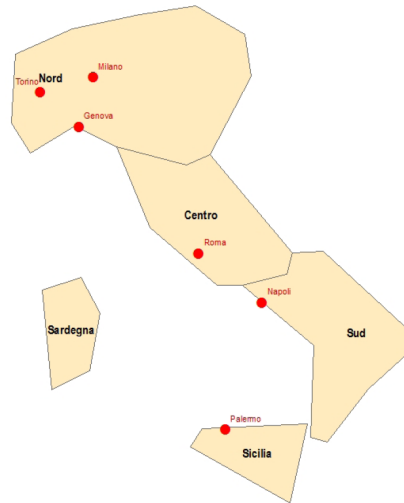


Figure 5.22 Automatically drawn diagram of Italy [80].

5.5.1 Parallelism in chorematic diagrams

Introduction. In Section 5.3 we claim that the outlines of chorematic diagrams use some but not total parallelism as part of their design principles. We test this hypothesis by automatically generating outlines of high parallelity and comparing these to manually drawn chorematic outlines from our collection. The outlines are computed by selecting characteristic points of a given territorial outline and using these as input for a simulated annealing process on the vertices and edges that attempts to maximise parallelity.

Related work. Published chorematic diagrams indicate that strict adherence to octilinearity or another C -orientation is not suitable for chorematic diagrams. An approach that does not consider angles as horizontal geometric relations [264] has been proposed by Del Fatto [80]. Del Fatto’s method does not differentiate between the schematisation of the territorial outline and the thematic subdivision (i.e. area-class map [187]), and generalises them in the same step, approaching a convex hull for every face (see Fig. 5.22).

In a follow-up publication, Chiara *et al.* [67] do not let the outlines approach convex hulls, but equate line-simplification with producing chorematic maps. They use the following techniques for visual representation: line simplification with a topology-preserving Douglas-Peucker algorithm, on-map label placement and flow-mapping for visualising quantitative flow information and a geographic projection (see Fig. 5.23 and Fig. 5.24). As no detailed information on the method is provided, we cannot compare directly. However, our own findings [223] indicate that published chorematic diagrams do not display quantitative information, very rarely use on-map labels—if at all, then as abbreviations—use very low numbers of vertices for territorial outlines and use the cartesian or conformal projections appropriate for the area of interest. Hence, their ap-

proach does not seem to follow the cartographic design rules of chorematic diagrams. Instead, they are concerned with the concept of chorematic diagrams as inspiration for interactive data exploration, making their research only orthogonally related to our work.

Our method to generate outlines uses the notion of characteristic points. Choosing the most characteristic points from a polyline or polygon is closely related to the wider area of (line) simplification. Line simplification has been researched widely and has several well-known algorithms including Douglas-Peucker [87] and Imai-Iri [146]. Nonetheless, several known problems exist. These problems include starting point dependency [176], parametrization to specific scales [177, 220] and the lack of a universally applicable validation (distance) measure. Chorematic diagrams depict geometries of wildly varying scale at the same level of visual complexity. For example, a city's outline in one instance is drawn with the same low number of points as that of a continent in another diagram. in

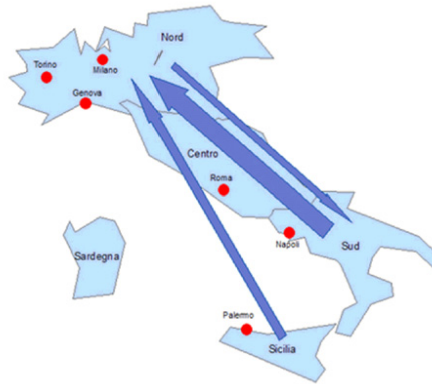


Figure 5.23 Automatically drawn diagram of Italy [67].

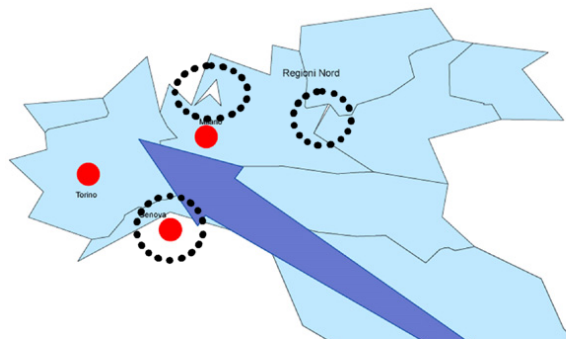


Figure 5.24 Detail of Northern Italy of Chiara *et al.* [67]. The position of Genova and two simplified lakes (encircled) give the impression of topology violations.

generalization, algorithms are often parametrised to some target scale. In contrast, this scale has no influence in chorematic diagrams. Therefore, algorithms have to be parametrised to the desired visual style.

Hypothesis. Based on the inspection of manually drawn chorematic diagrams, we conjecture that an important design rule for chorematic outlines is *parallelity*. A high number of edges should be parallel. Preferably, parallel edges should “face” each other. By this, we mean that (part of) the orthogonal projection of one edge coincides with (part of) the other edge. This concept is illustrated in Fig. 5.25. However, to preserve the shape of the outline, vertices are constrained to stay within a certain range of their original position. These two properties are used to develop a simulated annealing algorithm to generate outlines with high parallelity. This method assumes that the outline already has few vertices. Therefore, we pre-process shapes by selecting characteristic points as described below. In the paragraph on results, we verify our hypothesis by visually inspecting generated outlines. Where possible, we compare it to the angular structure of a comparable manually drawn outline, which we consider to be the “ground truth”.

Characteristic point selection. One of the salient visual characteristics of chorematic diagrams is their minimalist, schematised design. The complexity (number of vertices) of a chorematic territorial outline typically ranges from five to fifteen. These few points bear the burden of forming a shape that is recognizable as a representation of the area of interest: they should be *characteristic points*, sometimes also referred to as critical points. For a chorematic outline, they should also be such that the outline is aesthetically pleasing. Our simulated annealing method, described in the paragraph on simulated annealing, assumes that the input has the desired complexity and that the vertices are characteristic. Hence, we require an algorithm to extract characteristic points from a polygon or subdivision.

Selection algorithm. The selection of characteristic points is closely related to line simplification. Therefore, our method builds on existing line simplification algorithms. Common algorithms such as Douglas-Peucker [87] and Imai-Iri [146] are threshold-based methods for polylines: a simplification is found such that the distance between input and output is at most the threshold ε . To find a simplification with a given number of vertices, say k , we perform a binary search to find the minimal value of ε for which the Imai-Iri algorithm produces an output with complexity at most k . Solutions with less than k points may be desirable in some cases, as adding another characteristic point actually increases the distance to the original shape. A simple example is given Fig. 5.26.

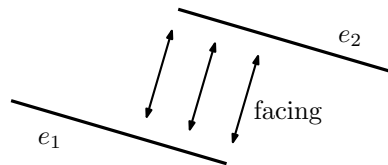


Figure 5.25 Edges e_1 and e_2 partially face each other.

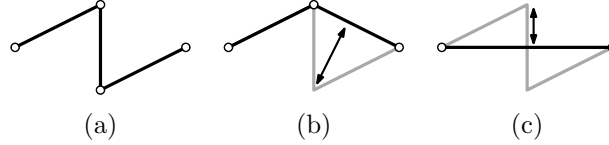


Figure 5.26 (a) A polyline with 4 points. (b) Simplification with 3 vertices; distance is $\frac{4}{\sqrt{11}} \approx 1.79$. (c) Simplification with 2 vertices; distance is 1.

The Imai-Iri algorithm is defined for polylines instead of polygons or subdivisions. Therefore, we must split the outline into polylines and execute the algorithm on each polyline separately. For subdivisions we cut at every vertex of degree three or higher. Now the input consists of a set of polylines and polygons. Polygons also have to be converted to a polyline by cutting at some vertex. This vertex automatically becomes a characteristic point. When a high number of vertices is used, this starting point dependency may not be much of an issue. However, since we aim for a very low complexity, the issues caused may be quite severe. An obvious solution is to try all vertices as starting point and use the best one (for example the starting point that yields the least number of vertices in the output). However, this incurs a rather large overhead, increasingly so if there are multiple polygons to be simplified simultaneously. Therefore, we use a heuristic that cuts a polygon at one of its diametrical points. This corresponds to the heuristic applied by the Douglas-Peucker algorithm which considers distant points to be characteristic for a shape.

Discussion. Strictly speaking, a requirement of the method is that the result does not intersect itself. That is, it must still be a simple polygon or subdivision after simplification. This ensures that the annealing process starts with a valid solution. The Imai-Iri method cannot guarantee that the result is free of intersections. However, due to the low target complexity, this is unlikely to occur and did not occur in our experiments. More advanced methods exist, such as the one of De Berg *et al.* [75]. This method guarantees that the result does not intersect itself. It cannot guarantee though, that a certain complexity can be achieved, as intersections are tested with the original shape of nearby polylines, rather than the simplified version.

Since the final shape is represented by few points, it is important to also consider geographic characteristic points in addition to geometric characteristic points [154]. This differentiation is often overlooked [220], but cannot be ignored in cartography. While geometric characteristic points are obtainable from the shape itself, geographic characteristic points typically require some auxiliary information. An example is the Danish-German border (Fig. 5.27), which a viewer expects to be represented by at least two points. Purely geometric threshold-based methods consistently fail to detect this significant feature and create a triangular shape at low complexity. Using auxiliary information, our method would be able to deal with such geographic characteristic points by cutting any polyline at these points as well. However, we did not include this in our experiments.

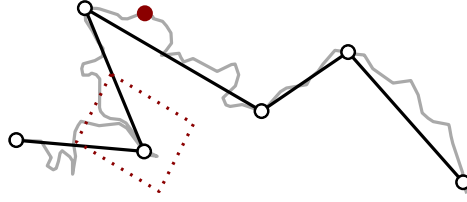


Figure 5.27 Northern border of Germany. The solid vertex is important to represent the Denmark-Germany border, but goes undetected by geometry-based methods when aiming at a low complexity. The Estuary of the Elbe, marked by a dotted rectangle, creates an unwanted concavity.

Simulated annealing. Simulated annealing is a generic framework, often applied for optimisation problems [162]. It has been used in generalisation and especially schematisation research [4, 7, 8]. We use the method to generate chorematic territorial outlines. Simulated annealing finds a good solution to the problem by using a heuristic local search in the solution space. Such local searches are at risk of getting stuck in local optima. The idea of simulated annealing is to have a lot of flexibility initially to escape these local optima. This flexibility is then decreased over time. Simulated annealing starts with some valid solution and tries to transform it into another solution, one which is hopefully better. A “temperature” is used to indicate and control the flexibility of the process. Based on the temperature and a random factor, it is possible to force the acceptance of a new solution,

Algorithm 5.1 FindChorematicOutline(\mathcal{G}, Δ, dt)

Require: \mathcal{G} is a planar graph, Δ is the threshold distance, dt is the temperature decrease

```

1:  $C \leftarrow \mathcal{G}$ 
2:  $O \leftarrow C$ 
3:  $T \leftarrow 1$ 
4: while  $T > 0$  do
5:    $r \leftarrow$  A random number between 0 and 1
6:   Modify  $C$  into  $C'$ 
7:   if  $Q(C) < Q(C')$  or  $r < T$  then
8:      $C \leftarrow C'$ 
9:   if  $Q(O) < Q(C)$  then
10:     $O \leftarrow C$ 
11:    $T \leftarrow T - dt$ 
12: while a modification is made do
13:   Modify  $O$ 
14: return  $O$ 

```

even if it is considered to be worse than the old one. If the temperature reaches zero, the annealing process stops, returning the best solution found so far. Since every vertex is not allowed to move arbitrarily far away from its original position, our solution space is guaranteed to have some maximal value, thus, after reaching temperature zero, the optimal solution so far is still modified, as long as it in fact improves the result. Algorithm 5.1 presents a high-level overview of the method. Simulated annealing requires two main ingredients: a quality measure for solutions, and a method to obtain a new solution from an existing solution. The quality measure Q is based on parallelity and is described below.

Parallelity as a quality measure. The hypothesis states that parallel lines should be encouraged in chorematic diagrams. Therefore, the quality measure Q for our simulated annealing approach is based on parallelity. Every edge in the solution has its quality, $q(e)$, which lies between 0 and twice its own length. The quality of a solution is then the sum over all edges, divided by twice the total perimeter length. This normalizes the score to the interval $[0; 1]$ and ensures that solutions with a longer or shorter perimeter are not preferred by default. We also wish to enforce a valid solution, one where edges do not cross and where every vertex of the solution is within a threshold distance of its original position. The threshold distance we used is 0.03 times the diameter of the shape. This corresponds approximately to what seems to be used in various manually drawn chorematic diagrams. If a solution is invalid, its quality is 0. Summarizing, the quality of a solution S is defined as follows:

$$Q(S) = \begin{cases} \frac{\sum_{e \in S} q(e)}{2 \cdot \sum_{e \in S} |e|} & , \text{ if } S \text{ is valid} \\ 0 & , \text{ if } S \text{ is invalid} \end{cases}$$

What remains is to define the quality of a single edge. As stated, $0 \leq q(e) \leq 2 \cdot |e|$ must hold, for the normalisation to work. The quality of a single edge consists of two parts, $q_1(e)$ and $q_2(e)$. The first part, $q_1(e)$, is the pure parallelity score. if e is parallel to another edge, then $q_1(e)$ equals $|e|$, it is zero otherwise. Adjacent edges, that share a vertex of degree two, are not taken into account. This is because we assume all the vertices to be significant: when two such adjacent edges are parallel, the shared vertex visually disappears and is no longer significant. The second part, $q_2(e)$, is the “facing bonus”. For every edge e' parallel to e , the overlap of e and the orthogonal projection of e' onto e is computed and added to the facing bonus, up to a maximum of $|e|$. These two parts are added to obtain $q(e)$. However, this poses a problem for the simulated annealing: if an edge is not parallel to another edge, its quality is zero. Hence, the quality measure is not strong enough to distinguish between two similar solutions, where an edge is “more parallel” to another edge in one solution compared to the other. In order to steer the annealing process to better solutions, we multiply the length of the edge with the result of a Gaussian function on the minimal angle of e with any other edge, rather than giving it a binary contribution based on the existence of a parallel edge. This Gaussian function (illustrated in Fig. 5.28) is centred at 0, has a height of 1, and a width of 0.05: $\text{Gauss}(\alpha) = e^{-200 \cdot \alpha^2}$. That is, only edges that have a small minimal angle have a significant factor. Let $\alpha(e, e')$ denote the smallest angle between two edges (with a value of ∞ for two adjacent edges) and let $\phi(e, e')$ denote the length of the overlap of the orthogonal projection of e'

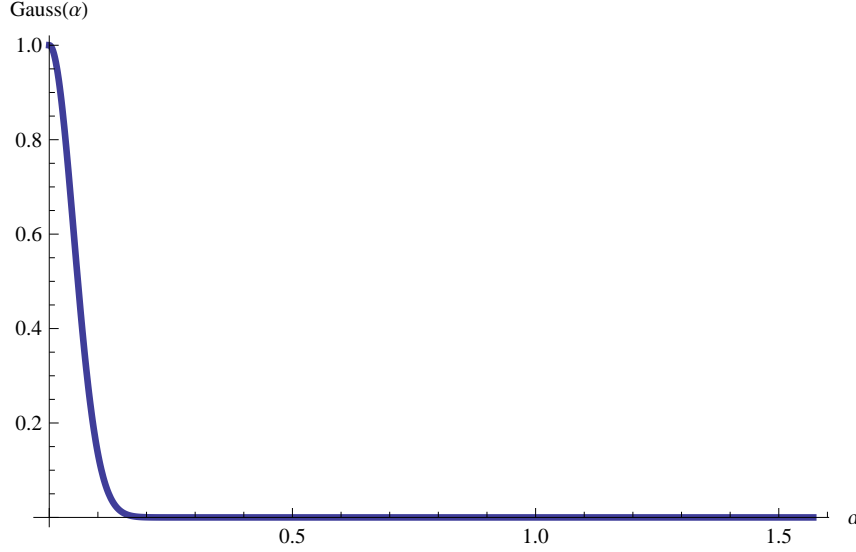


Figure 5.28 The Gaussian function for angles α in radians. It is positive for any α and strictly decreasing.

onto e if e and e' are parallel, it is zero otherwise. We can then summarize the above as follows:

$$\begin{aligned} q(e) &= q_1(e) + q_2(e) \\ q_1(e) &= |e| \cdot \text{Gauss}(\min_{e' \in S \setminus \{e\}} \alpha(e, e')) \\ q_2(e) &= \min \left(|e|, \sum_{e' \in S \setminus \{e\}} \phi(e, e') \right) \end{aligned}$$

Modifying a solution. To modify a solution, we move each vertex separately. For this we require a set of candidate moves for a vertex v . These candidate moves are generated by observing that moving v can have three effects on an adjacent edge: the orientation remains unchanged, the orientation is rotated clockwise, or the orientation is rotated counter clockwise. When the orientation remains unchanged, there are only two options left, either the edge shrinks or grows, meaning vertex v moves along the edge (or an extension of it). For each edge, these moves become candidate moves. Additional candidate moves are obtained by combining effects (e.g. rotating both edges clockwise). Every edge has two perpendicular vectors, representing a clockwise and counter clockwise rotation. The additional candidate moves are now generated by combining each such perpendicular vector of one edge with a perpendicular vector of another. Finally, not moving the vertex is also added as a candidate move. Any duplicate candidate moves are eliminated. Except for the move that keeps v in place, all candidate moves are given the same length, $\frac{1}{200}$ times the threshold distance. This results in at most $1 + 2 \cdot (|e| + |e|^2)$ candidate moves, where $|e|$ is the number of edges incident to the vertex v . For a vertex of degree two,

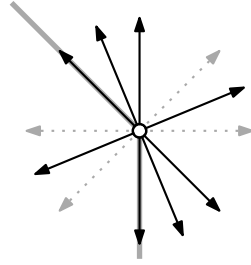


Figure 5.29 Candidate moves (solid black arrows) for a vertex of degree two. The dotted gray arrows indicate the perpendicular vectors used to combine effects.

this means nine candidate moves, combining each effect of both edges. An example of candidate moves is given in Fig. 5.29.

For each vertex, we select a random candidate move. However, these are not applied, until a candidate move has been determined for each vertex. All these candidate moves are then applied simultaneously to obtain the new solution.

Recall that the simulated annealing process uses two variables, r and T , that express the flexibility of the process. With a small chance ($r < \frac{T}{10}$), we also allow that the entire solution is reset, to be able to escape local maxima more often. Every vertex is then set to a random position within the threshold distance of its original location.

Computation time. The actual computation time to reach the results shown here is several minutes per polygon. More formally, the number of steps is determined by the search for the diametrical points, taking $O(n^2)$ in a naive implementation, which is dominated by the repeated simplification to find the wanted number of vertices with a time complexity of $O(n^2(\log n)^2)$ [146, Theorem 3.2], where n is the number of input vertices of the polygon. The calculation of our measure takes $O(m^2)$ time and is repeated for each of the k simulated annealing steps. In total our approach thus needs $O(n^2(\log n)^2) \cdot O(k \cdot m^2)$ steps, where m is the (low) number of target vertices for the chorematic outline type.

Discussion. Another method to tackle an optimisation problem is *least-squares adjustment* (LSA), a method that has been applied in generalization as well (see Sester [250]). Intuitively though, our hypothesis lends itself more for simulated annealing as we desire to reinforce good properties (parallelity), rather than weaken the bad properties: a line segment that is not parallel to any other is not necessarily a bad segment. LSA may cause edges that should be parallel to be not parallel, in order to make another edge “more parallel”.

Also, there are many possible variants for simulated annealing in this context. The quality measure we propose favours long edges being parallel over short edges. With some small changes, the quality measure can be adapted such that short and long edges are weighed equally. However, we suspect that long edges are more salient than the shorter ones, the parallelity of longer edges is more important. Also, it may be desirable to incorporate into the quality measure how many edges are considered parallel to

another. The effect of four edges having the same orientation is stronger than two pairs having the same orientation. This becomes mainly a concern for outlines that have a high number of (characteristic) points. In our quality measure, the problem is partially dealt with by the facing bonus. Finally, other ways of modifying a solution are possible as well. For example, one could move only a single vertex each iteration, rather than moving all simultaneously. Whether this actually improves the effectiveness of the annealing process is unclear and left as future work.

The simulated annealing process assumes that characteristic points have been selected beforehand, and that these points have been selected reasonably well. Any solution has its vertices close to their original locations. It may be possible to reduce the impact of the characteristic-point selection. Instead of requiring that each vertex stays within a threshold distance of their original location, we could for example require that the entire chorematic diagram has a Hausdorff or Fréchet distance of at most some threshold distance in comparison to the original subdivision. However, this leads to a greatly increased complexity of the algorithm. Furthermore, since the simulated annealing process requires an initialization with a valid solution, a valid solution has to be found first: for some given threshold and complexity, these are not guaranteed to exist. By decoupling the characteristic-point selection from the simulated annealing process, we guarantee the existence of a valid solution.

Results. In this section, we compare chorematic outlines we obtained using our algorithm to those found in the literature and discuss our findings. First, we discuss results in comparison to manually drawn outlines. After, we discuss results for subdivisions and compare it to an automatically generated outline.

Comparison to manually drawn outlines. Figs 5.30 to 5.36 show the result of our method applied to territorial outlines in comparison to manually drawn chorematic diagrams (modified to emphasise the outline). Results are shown for Argentina, Brazil, Cambodia, Guyane (twice), Spain, and Vietnam. The number of characteristic points used and the parallelity of these chorematic outlines are given in Table 5.1. Note that to measure parallelity in diagrams found in the literature, a certain margin of error has been

Table 5.1 The parallelity quality measure between our result (SA) and manually drawn outlines.

| Case Territory | Points | Parallelity | |
|-----------------------|--------|-------------|--------|
| | | SA | Manual |
| Argentina (Fig. 5.30) | 13 | 0.730 | 0.206 |
| Brazil (Fig. 5.31) | 6 | 0.631 | 0.316 |
| Cambodia (Fig. 5.32) | 9 | 0.542 | 0.307 |
| Guyane (Fig. 5.33) | 11 | 0.733 | 0.301 |
| Guyane (Fig. 5.34) | 11 | 0.726 | 0.301 |
| Spain (Fig. 5.35) | 8 | 0.369 | 0.450 |
| Vietnam (Fig. 5.36) | 12 | 0.780 | 0.762 |

introduced. This is not only due to the accuracy of the manual work. It is a known phenomenon in perception research that angles within ensembles of other line segments and angles are systematically misperceived, appearing larger or smaller depending on context [206]. This implies that the parallelity score may be slightly lower (or higher) due to lines that appear parallel to the viewer (and perhaps even the cartographer) are in fact not parallel.

We think that, for example, our results for Argentina, Brazil, Guyane, Spain and Vietnam are valid and aesthetically pleasing schematisations of their regions. To a lesser extent, this also holds for the outline produced for Cambodia. Trying to fit the method to deliver the exact same results is in danger of overfitting the process to the few examples where a ground truth is available.

Except for Argentina, the manually drawn chorematic outlines have a moderate to high parallelity measure, supporting our hypothesis that parallelity is an important design rule for territorial outlines in chorematic diagrams. We observe also that the parallelity obtained by our method is typically higher than the parallelity of the manually drawn outline. Visual inspection indicates that the manually drawn outlines are better, implying that parallelity is not the only design rule at play here. Some distortions made by our method are too significant. For example, the northern part of Vietnam (Fig. 5.36) is compressed too much.

A major difference in the Guyane example (Fig. 5.33) is the indent at the mouth of the Approuague river. It is kept in our version, but eliminated in the manually drawn version. Using a different input, we obtain a chorematic outline that corresponds more closely to the manually drawn outline (see Fig. 5.34). The problem is a result of the method used for characteristic-point selection. Nearly all problems with characteristic points for the considered outlines can be categorized as belonging to one of three cases:

- Estuaries and large rivers
- Memorable national or regional boundaries
- Narrow territorial extrusions

Especially at the national scale, estuaries are ignored in the manual examples, if both banks belong to the region of interest depicted in the outline. On the other hand, if the estuary (or river) coincides with a boundary to a neighbouring entity, the point at which boundary and river bank meet becomes an important visual anchor, as it happens with the Rio de la Plata and the Argentine-Uruguayan border. Narrow territorial extrusions, such as the Texas Panhandle, Schleswig-Holstein in northern Germany, Svay Rieng province in southeastern Cambodia or Misiones province in north-western Argentina are cartographically important, but are consistently not detected by our point-selection method. Instead of two, only one characteristic point is selected, and a triangular shape with an acute angle is the result.

We observe that for Brazil (after forcing one characteristic point, see Fig. 5.31) and Vietnam (see Fig. 5.36) the selected characteristic points in our result correspond approximately to those used by the manually drawn outline. These two cases have the same visual structure: the result shares approximate angles and facing sides with the manually

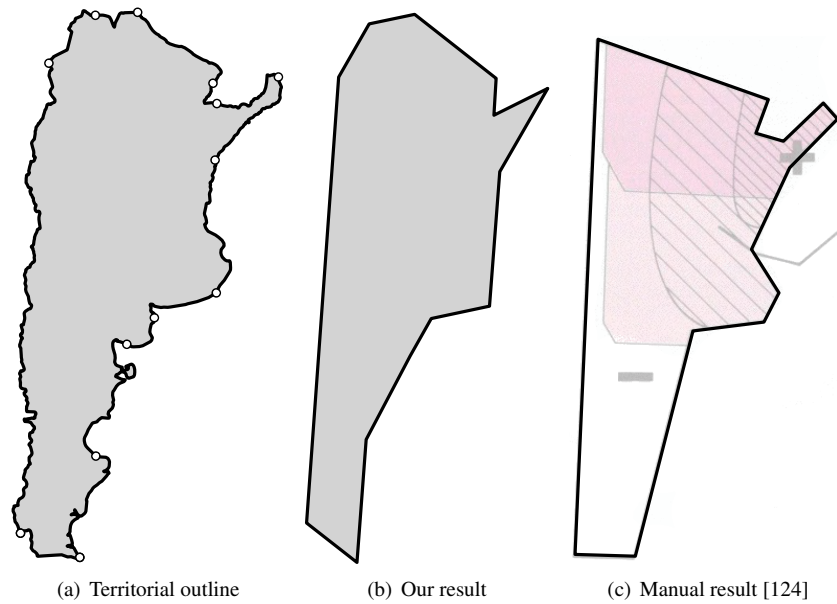


Figure 5.30 Chorematic outlines for Argentina.

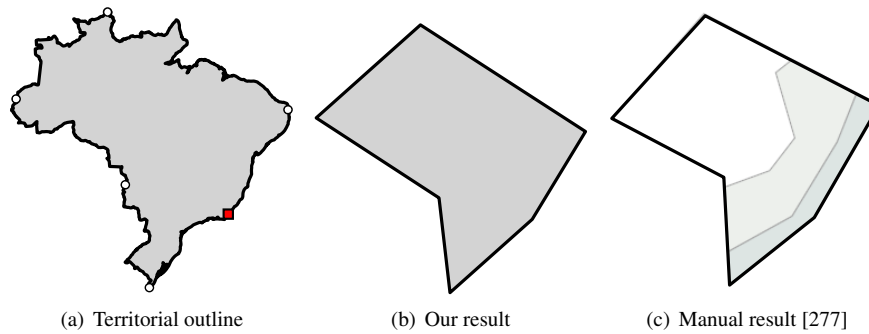


Figure 5.31 Chorematic outlines for Brazil. One geographic characteristic point (square) at Rio de Janeiro is placed manually to obtain structural correspondence with the manual result.

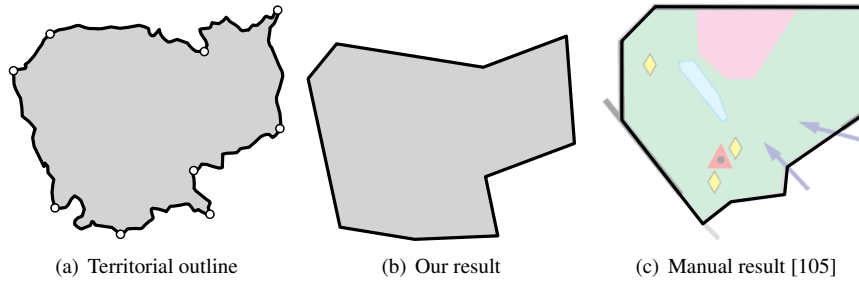


Figure 5.32 Chorematic outlines for Cambodia.

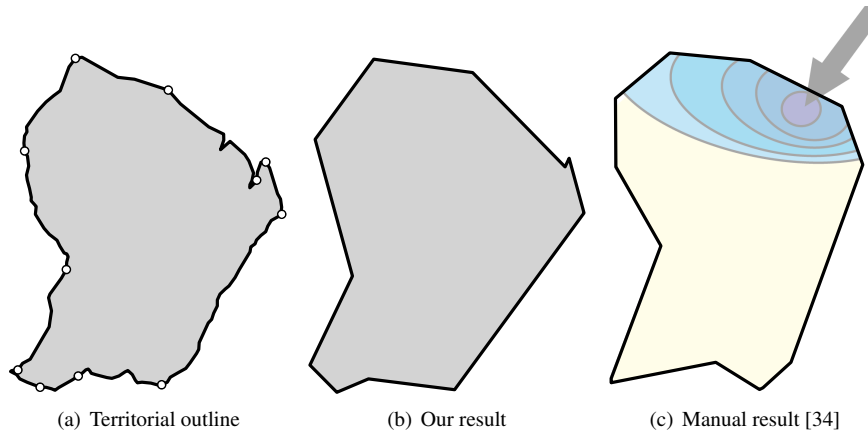


Figure 5.33 Chorematic outlines for Guyane.

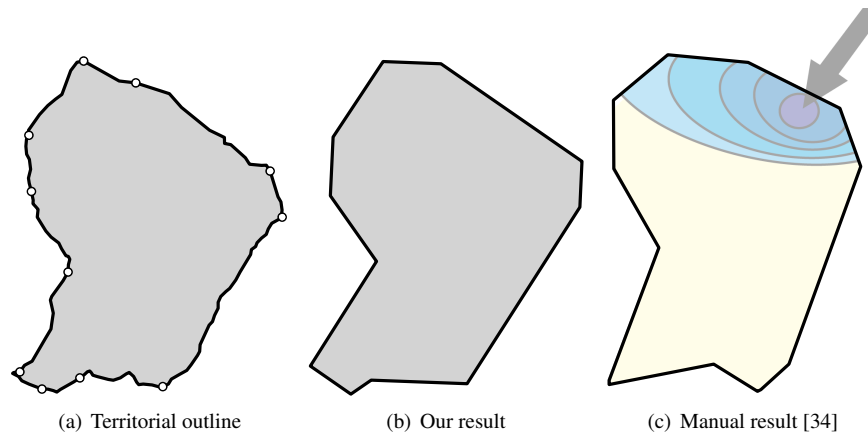


Figure 5.34 Chorematic outlines for Guyane. In the input, the Approuague estuary is merged with the mainland.

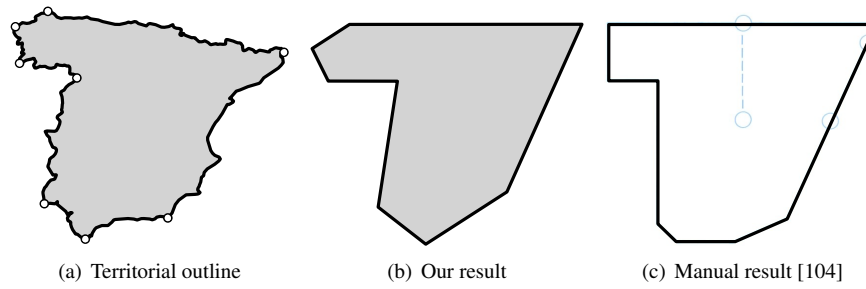


Figure 5.35 Chorematic outlines for Spain.

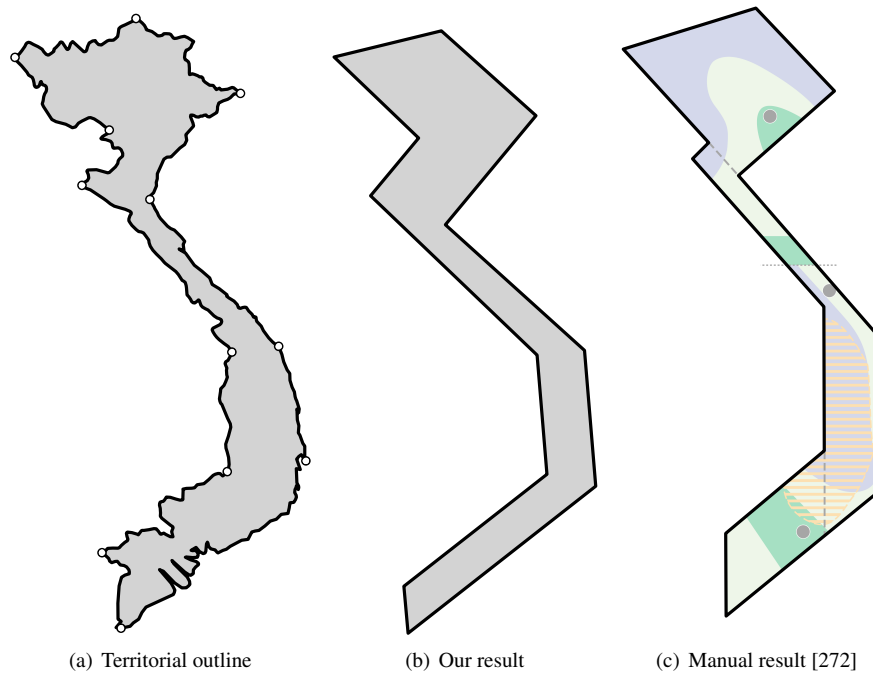


Figure 5.36 Chorematic outlines for Vietnam.

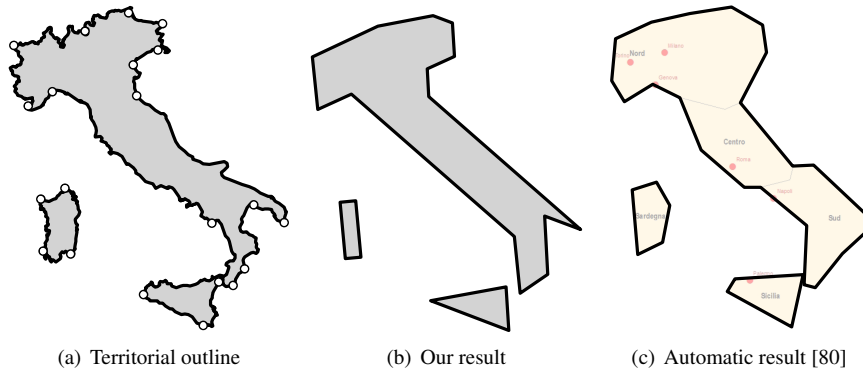


Figure 5.37 Chorematic outlines for Italy. Our result has been obtained by treating Italy as a whole.

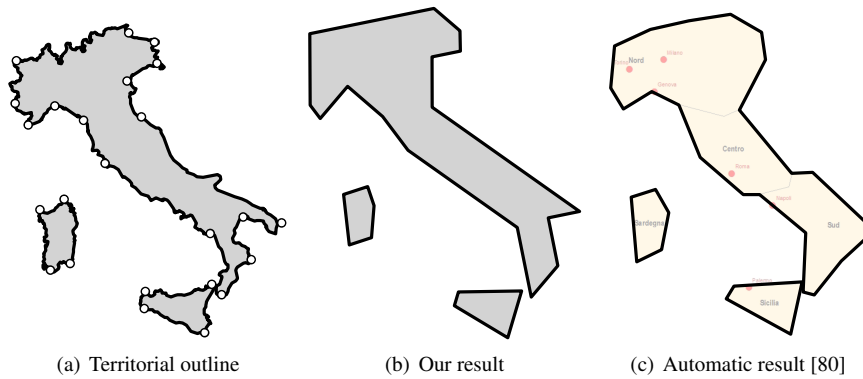


Figure 5.38 Chorematic outlines for Italy. Our result has been achieved by treating islands individually.

Table 5.2 The angular deviation of the characteristic points (CP) and our result (SA) in comparison to the manually drawn outlines. Values are mean and standard deviation in degrees.

| Territory | CP | SA |
|---------------------|-------------|-------------|
| Brazil (Fig. 5.31) | 5.6° / 6.9° | 4.5° / 4.6° |
| Vietnam (Fig. 5.36) | 7.3° / 7.4° | 3.3° / 3.0° |

drawn version. To support this claim, Table 5.2 shows for these two cases the average angular deviation between our result and the manually drawn chorematic outline, as well as between the selected characteristic points and the manually drawn outline. The average angular deviation is computed as $\frac{1}{N} \sum_{e \in S} \alpha(e)$, where $\alpha(e)$ indicates the smallest angle between an edge e and the corresponding edge in the manually drawn outline. This measure decreases from characteristic points to our result, indicating that the simulated annealing process moves the edges such that the used orientations are more similar to the outline found in the literature. For the other cases, at least one detected characteristic point is significantly different from the ones used in the manually drawn diagram. Therefore, this measure has no great explanatory power and thus these values have been omitted.

Results for subdivisions. Fig. 5.37 shows our result for Italy in comparison to an chorematic outline that was automatically generated by Del Fatto [80]. Here, Italy is treated as a subdivision consisting of three polygons. Table 5.3 shows the parallelity measure for these outlines. It also indicates the parallelity of each of the islands in isolation. Note that, even though the parallelity of Sicily is 0, the edges of Sicily are parallel to edges of the mainland, affecting the score of the whole. The distribution of characteristic points plays an important role here. Getting a fourth point on Sicily and a fifth on Sardinia requires quite a lot of extra characteristic points on the mainland first. Therefore, we also created an outline where each island is treated separately from the mainland. This result is shown in Fig. 5.38; Table 5.4 shows the parallelity scores. Note that in these results, there is no parallelity between the islands as they were treated individually.

This comparison with Del Fatto's approach [80] further hints that parallelity plays a salient role in the design of chorematic territorial outlines. The low scores for Del Fatto's results prove that parallelity was not considered there; the visual comparison between both solutions suggests that our result is a better chorematic schematization for Italy. Therefore, the hypothesis of the importance of parallelity for chorematic outline schematization seems vindicated.

Conclusions. The results are supporting our hypothesis: while parallelity alone is not sufficient to obtain a good chorematic diagram, our results indicate that ignoring parallelity is likely to lead to unsatisfactory results. It must be noted that it is important that suitable characteristic points are selected. Hence, a study of the relation between the selection and quality of the resulting chorematic outline may be worthwhile. Also, better algorithms for selecting characteristic points can be used. Since our simulated annealing algorithm does not depend on how the characteristic points are selected, our method is

Table 5.3 A comparison of parallelity between our approach and Del Fatto's outlines [80] for Italy as a whole. Also see Fig. 5.37.

| Case | | Parallelity | |
|-----------|--------|-------------|-------------|
| Territory | Points | SA | Del Fatto |
| italy | 21/31 | 0.805 | 0.333 |
| Mainland | 14/22 | 0.724 | 0.245 |
| Sicily | 3/4 | 0 | $\ll 0.001$ |
| Sardinia | 4/5 | 0.997 | 0.003 |

Table 5.4 A comparison of parallelity between our results and Del Fatto's outlines [80] for Italy, where islands are treated separately. Also see Fig. 5.38.

| Case | | Parallelity | |
|-----------|--------|-------------|-------------|
| Territory | Points | SA | Del Fatto |
| italy | 25/31 | 0.699 | 0.333 |
| Mainland | 16/22 | 0.801 | 0.245 |
| Sicily | 4/4 | 0.243 | $\ll 0.001$ |
| Sardinia | 5/5 | 0.249 | 0.003 |

easily interchanged for another.

Though it is less obvious how to define parallelity for curved segments, the use of such elements would increase the flexibility of the chorematic dramatically, allowing for a wider range of solutions. Manually drawn chorematic diagrams often combine polygonal with curved representations. However, such a mixed approach hints at a design choice separate from how to represent a particular outline.

For a more complete automated generation of chorematic diagrams, we need not only a territorial outline, but also ways to generate its content, such as the curvy subdivision shown inside Vietnam in Fig. 4.7c. Besides generating such highly abstracted subdivision from actual data, one would need to morph the subdivision from the original outline to the chorematic outline. One could consider the points where the subdivision touches the outline as “anchor points” that can be mapped relatively straightforwardly to the chorematic outline. However, this does not account for all distortion that occurs. Ideally, one would have a continuous mapping from the interior of the original to the interior of the chorematic diagram, thereby respecting cartographic consistency.

5.5.2 Curved subdivisions for chorematic diagrams

Introduction. In this study, we examine if and how we can schematise a thematic subdivision given only a certain, low, number of cubic Bézier-curves. We present this as a further feasibility study for some of the shape constraints of the constraint model.

Related work. The problem we address can be described as: Automatically schematise a categorical map with BCs according to design-rules found in chorematic diagrams. In our running example, the pertinent design rules derived from our process investigating chorematic diagrams:

- (1) To emphasize the container aspect of a given region of interest, the territorial outline should be depicted differently from the internal subdivision and presented as free-standing entity that is as an *Inselkarte*.
- (2) Subdivision boundaries should be drawn with cubic Bézier splines consisting of one (most common) up to three (seldom) cubic BCs. Some cubic BCs might have two identical control points, effectively representing quadratic BCs.
- (3) Territorial outlines should have between 8-15 vertices and a high amount of parallelity.

Below we provide a short overview of the related work regarding the mentioned sub-problems.

Territorial outlines. The territorial outline for Italy that is used in our running example has been generated with the method presented above (see subsection 5.5.1). Here, outlines are computed by selecting characteristic points of a given territorial outline. These inputs are used for a simulated annealing process on the vertices and edges that attempts to maximize parallelity. As with preceding work, it is here applied to a national outline.

Categorical maps. The general problems concerning choropleth maps as opposed to categorical or area-class maps are well known [187], but often the actual generalisation of categorical geometries remains the realm of manual generalisation (for example Bucher and Schlömer 2006 [54], see also Fig. 5.39).

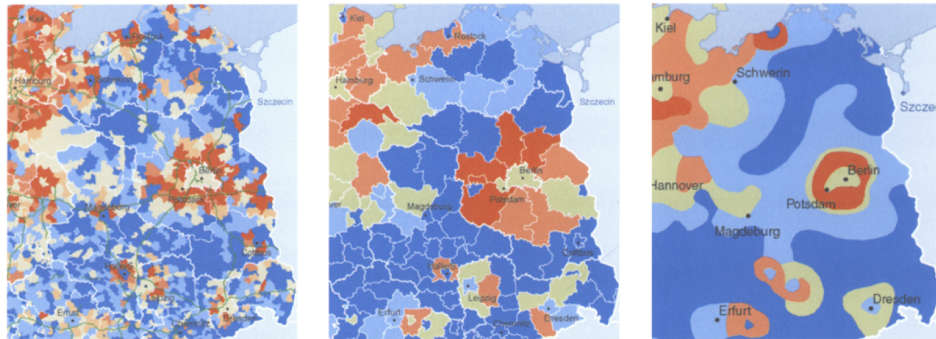


Figure 5.39 Illustration of the generalisation problems with choropleth vs area-class maps; from left to right historical data, choropleth of prognosis data and manually generalised prognosis for east German population (from [54]).

For the case of a changing base-map or territorial outline, this problem is even heightened. As the general approach in this study is to treat the internal subdivision different from the

outline, we indeed need to map the interior of one area into the interior of another with a schematised shape. Saalfeld [242] provided an existence proof for area-preserving affine mappings. In essence he proved that a continuous mapping from one polygonal subdivision to another one that preserves area and topology is always possible. Saalfeld does underline the fact that his procedure is computationally very expensive and basically impractical. He suggests that alternative methods should be developed. To our knowledge, no follow-up work has been presented since. Galanda has provided a framework for constraint formulation for polygonal generalization [113]. Steiniger and Weibel's work on horizontal and vertical relations in categorical maps form the basis for considerations leading to our insertion strategies [264].

Bézier curves. Computer graphics research, especially in CAD and font/sketch recognition has an ample array of algorithms concerned with BCs. The properties of Bézier curves that our approach makes use of are convex hull, variation diminishing, affine invariance and pseudo local control. Although there is also a considerable amount of curve fitting techniques, nearly all algorithms fitting BCs to some input line work with piecewise techniques. That is to say that once a cubic curve is found to be unable to match the target polyline a new cubic BC is added, usually while keeping some form of continuity (for example Schneider [247]). Our aim is to find a suitable fit to a given boundary polyline with just a single cubic BC, a task which only few algorithms (for example [189]) concern themselves with. While this is known to be difficult [256], our goal of schematisations allows for a greater degree of geometric error than other applications. While some manual schematisations sometimes use splines of up to three chained BCs, for this study we only allow a single cubic curve. This provides the starkest schematisation and has to our knowledge not been addressed so far. While it is naturally easier to fit a spline to a polyline than just fitting a single curve, this would dilute the purpose of minimizing output complexity. The addition of extraneous bends into schematisations has been established as being bad design [236]. By limiting ourselves to single cubic BCs, we constrain the number of bends to a maximum of two. In lack of other constraints for curve schematisation and because of the danger of overfitting the splines to polylines, we chose this route.

Approach. The general idea of this approach is to schematise the subdivision by isolating the boundaries between categorically different areas and extract them as polylines. A cubic BC is fitted to each polyline separately which is then projected to the already schematised new outline. The order of insertion of the fitted BCs is crucial for preserving topology. This insertion order is obtained by data preparation and inclusion of some ancillary data and modelled via different classes of anchor points. This general strategy is illustrated by an example of a categorical map of Italy's regional differences in natural and migratory population change.

Data preparation. The provided example is concerned with the cartographical part of schematisation. Thus we assume the most important parts of model generalisation to have happened already. Using EUROSTAT/ESPON data on the level of NUTS-3 regions (Fig. 5.40), these regions were dissolved based on their migratory type. This migratory

type already is a strong model generalization provided by the EU as a regional planning device. Administrative enclaves and exclaves were eliminated and the dataset reprojected to cartetic UTM coordinates. All islands below a threshold of the smallest mainland NUTS-3 region were eliminated. The topological holes created by the Vatican and San Marino were kept at this time with their centroids later to be reprojected into the schematised outline as anchors for point symbolisation.

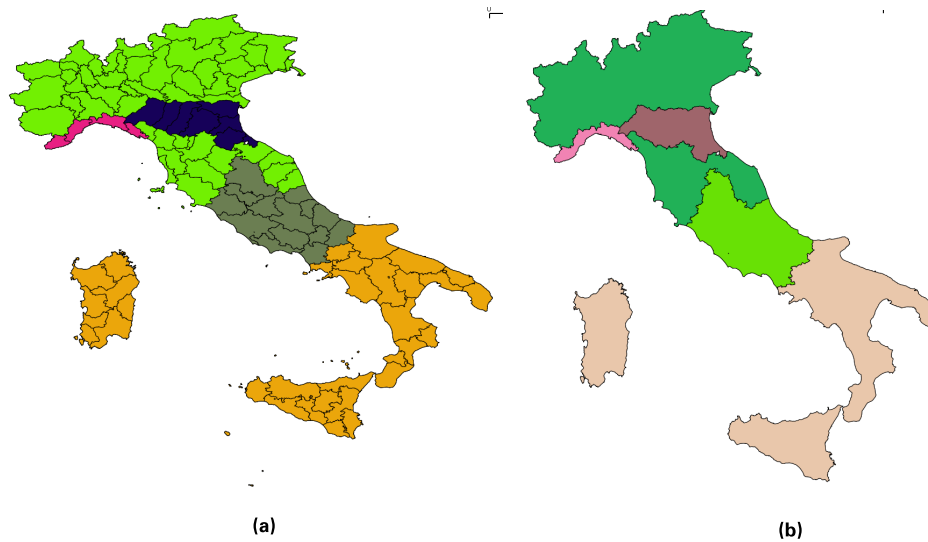


Figure 5.40 (a) The input data. (b) Input after reprojection and after union of adjacent polygons of the same class.

Anchor points for topology preservation. For approaches that schematise a whole categorical map at the same time, traditional topology preservation techniques and algorithms can be applied during the process. As our approach treats the territorial outline and interior subdivision differently, we use so-called anchor points that inform the reinsertion of schematised boundary lines.

In our example, we have two degrees of anchor points that inform the internal schematisation (Fig. 5.41). First order internal anchor points are those points that lie on the original territorial outline and are topologically connected to two categorically different areas. Second order anchor points are those points that are connected to three categorically different areas but not the original territorial outline. Assuming the reinserted schematised boundaries do not intersect with the outline, themselves or other boundaries, these anchor points ensure that the internal topology is preserved. Keeping the topology consistent for other neighbourhood considerations needs the introduction of ancillary data. For the depiction of countries, we already observed that the points where a national boundary and an ocean meet are interpreted as being crucial for recognition (Section 5.5.1). For the



Figure 5.41 First (square) and second (diamond) order internal anchor points.

example of Italy, we considered the adjacency to other nations and surrounding areas of the Mediterranean as depicted in Fig. 5.42 .

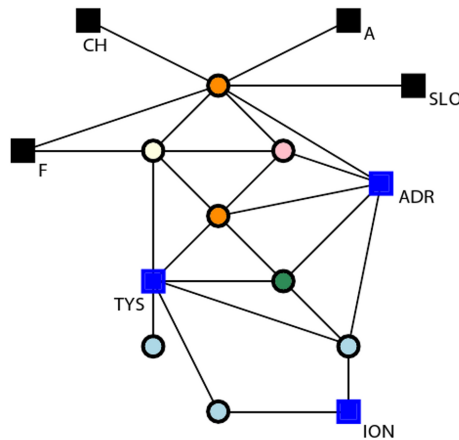


Figure 5.42 Adjacency graph with ancillary relations. Sea areas are marked as blue squares, outside nations as black squares.

The ancillary information is used here to keep outside relations intact. Every relation depicted in Fig. 5.42 must be assigned to an edge on the schematised outline O . Should a

characteristic point on the original outline precede an ancillary anchor point, the internal anchor point of the first order must be reassigned to the preceding edge that is now carrier of that external relation. in the example this is the case for the area of Type 3 in that case: Liguria. The internal anchor points of the first order are projected onto the schematised outline in the following manner (Alg.5.2):

Algorithm 5.2 SchematizeSubdivision(S)

Require: subdivision S that is one connected component with first-order anchor points only
Output: schematisation of S with BC curves for internal boundaries

- 1: Obtain outline polygon P and interior polylines $C_1 \dots C_n$ from S
- 2: Shift P such that p_1 (its first vertex) is a diametrical point
- 3: For each first order anchor point a do
- 4: Compute clockwise distance $d(a)$ from p_1 to a along the boundary of P
- 5: Let O be schematised outline of P produced by Reimer-Meulemans algorithm
- 6: For each first order anchor point a do
- 7: Compute position $\text{pos}(a)$ along boundary of O that has distance $d(a) \cdot |O|/|P|$ from matched vertex
- 8: For each polyline C_i do
- 9: Fit a Bezier curve BC_i
- 10: Transform BC_i to match $\text{pos}(a_1)$ and $\text{pos}(a_2)$ where a_1 and a_2 are the first-order anchor points at the ends of C_i
- 11: While BC_i intersects something do
- 12: *c.i.* Modify BC_i to move away from intersection
- 13: **return** outline O_s and $BC_1 BC_n$

Require: \mathcal{G} is a planar graph, Δ is the threshold distance, dt is the temperature decrease

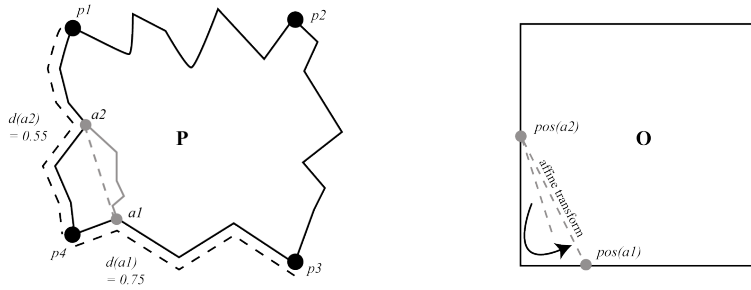


Figure 5.43 Illustration of the reprojection process.

Polyline schematisation with cubic Bézier curves. The extracted polylines are schematised by redrawing them with a fitted cubic BC. For our example we used a modified version of the fitting algorithm proposed by Masood and Ejaz [189] using a part-wise directed Hausdorff distance as error measure for each control point. The underlying idea

of the curve fitting algorithm is to work from starting positions for the control points determined from the polyline to be fitted and then do incremental adjustments to improve their positions. Starting and end points of the polyline to be fitted are the starting and end points of the BC. By measuring the maximum and minimum straight distance from the polyline to the baseline connecting start and end points, we get values $d1$ and $d2$. The starting positions of control points are obtained by extrapolating the line from the baseline to two times the distance d (Fig. 5.44).

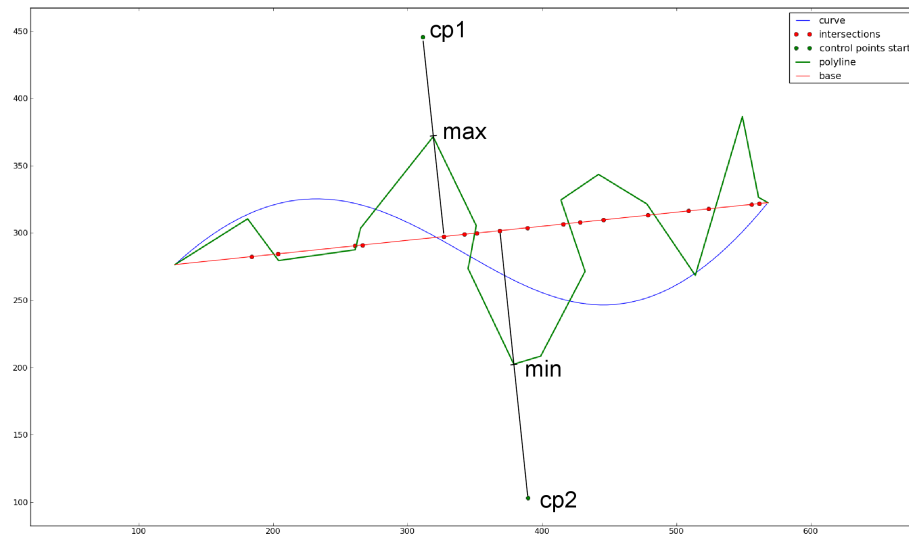


Figure 5.44 Starting points for curve fitting.

This BC is then scaled to the projected APs and translated with the projected APs as new starting and endpoint via affine transformation. The BC is then checked for intersections with itself, the outline and BCs already inserted. Using the pseudo-local control property of BCs, the control point closest to the intersection is moved stepwise until the intersection is remedied and minimal distances between graphical objects are reached.

Results. The final schematisation result is depicted in Fig. 5.45. The internal topological situation is the same one as with the input data (Fig. 5.46). In the case of Type 3 (peripheral areas characterised by a very neutral age profile depicted in tan) region, which is coterminous with the landscape of Liguria, the implicitly expected neighbourhood to France as well as the sea is kept. The colours correspond to the Type-colour pairings of the ESPON-Atlas. Table 1 shows the absolute and relative areas of output and input regions, ignoring the Vatican and San Marino. The relative areas are provided as percentage of the whole depicted land mass respectively. We note that at least for this example, the relative area sizes changes are all well below 2% with a mean of 0.80% and a standard deviation of 0.46%. For a schematisation that is by definition taking great liberties

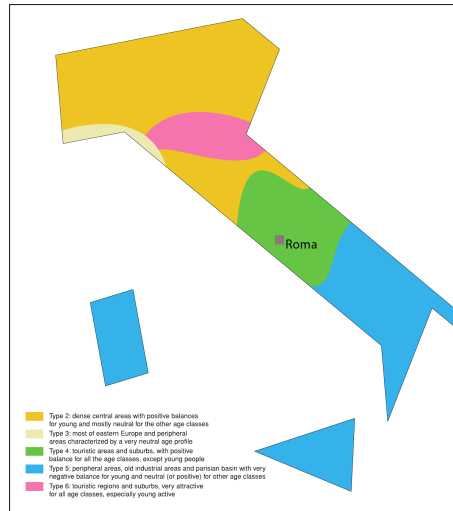


Figure 5.45 Schematisation result.



Figure 5.46 Schematisation result overlaid with input geometries.

with geometry, and which does not explicitly treat area preservation as constraint, this is remarkably faithful to the original graphical structure.

It has been shown that the approach is able to automatically produce a schematisation with BCs that keeps all functional geometric relations while visually highlighting its nature as schematisation. For the data used, the computation was fast as there were only two conflicts that needed to be resolved. The convex hull property of BCs states that a

Table 5.5 . Comparison between output and input area sizes.

| Region | Input[km^2] | Input [%] | Output[km^2] | Output[%] | $\Delta[km]$ | $\Delta[\%]$ |
|----------|-----------------|-----------|------------------|-----------|--------------|--------------|
| Type 2 | 127436.6 | 42.28 | 117774.09 | 41.85 | -9661.93 | -0.44 |
| Type 3 | 5411.55 | 1.8 | 6387.69 | 2.27 | -976.14 | 0.47 |
| Type 4 | 43649.6 | 14.48 | 41707.7 | 14.82 | -1941.9 | 0.34 |
| Type 5 | 55825.61 | 18.52 | 54366.45 | 19.32 | -1459.16 | 0.8 |
| Type 6 | 19543.16 | 6.48 | 21634.03 | 7.69 | 2090.87 | 1.2 |
| Sicily | 25576.41 | 8.49 | 19336.8 | 6.87 | -6239.61 | -1.62 |
| Sardinia | 23938.97 | 7.94 | 20235.75 | 7.19 | -3703.22 | -0.75 |
| Total | 301381.9 | 100 | 281443.09 | 100 | -29934.79 | 0 |

BC is contained within the convex hull of its control polygon, i. e. if the control polygons do not overlap, the resulting BCs will be intersection free. This was used to inform the insertion strategy, inserting all BCs with same degree APs without conflicts first and then placing the burden of conflict resolution on the shortest remaining segments, where changes do impact the overall result less. This can be interpreted as that the proposed anchor point/insertion order strategy is able to eliminate many potential conflicts before they even arise. Further development can concentrate on coping with more complex conflicts by such a divide and conquer strategy. We see such a first success as indicator that BCs can be fruitfully used to visually and geometrically characterize subdivisions for categorical maps in automated mapping

Chapter 6

Stenomaps

Whereas all preceding chapters were occupied with modelling and operationalising implicit and tacit procedural knowledge from traditional cartographic products, this chapter shows how to go beyond tradition. This chapter offers a further extension of the cartographic design space by providing a new method of transforming two-dimensional polygonal representations into smoothly curving one-dimensional linear features or *glyphs*. This form of extreme geometric abstraction we term the *stenomap*, from the Greek *stenos* meaning ‘narrow’ and a direct analogy with stenography – the transformation of letter form into shorthand symbols. The creative process behind shows that the methods and procedures described in the preceding chapters are generally valuable tools for geo-visualisation. They represent attempts of gaining insight into the cartographic design process itself. This resonates with the meta-goal set out in the introduction in Chapter 1.

While in this chapter we mostly report on the technicalities of the generation of stenomaps, the arguably hardest efforts remain more or less undocumented: the modelling process. Stenomaps evolved from an iterative design process to answer the question whether an area-line collapse is visually possible at all. An effort that started with a copious amount of design studies created manually by Herman Haverkort. These designs were discussed thoroughly and at length in informal user studies until some agreement was reached of how the glyphs should look like to remain effective place holders for their parent area. These discussions at first suffered greatly from a lack of terminology. The modelling experience documented in the preceding chapters allowed to focus on the relevant principles and showed ways of discussing the design elements. Without the experience from the preceding work, it would not have been possible to find a way from graphical idea to geometric algorithm and back. What follows below should be read in that light.

The stenomap (as we now know) comprises a series of smoothly curving linear glyphs that each represent both the boundary and the area of a polygon (Fig. 6.1). Stenomaps are inspired in part by some of the work of the 20th century cubist and abstract expressionist artists, including Picasso and Pollock, who explored radical transformations of the

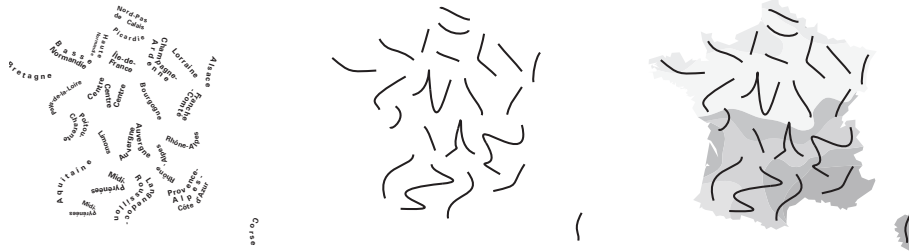


Figure 6.1 Three map-like diagrams (stenomaps) of France using glyphs.

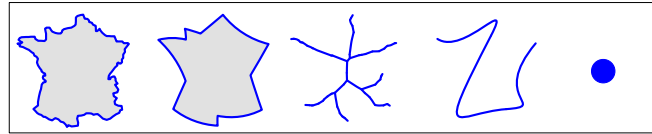


Figure 6.2 Increasing the abstraction of France. From left to right: (a) untransformed polygon, (b) curved schematization, (c) pruned medial axis, (d) stenomap glyph, (e) dot.

depiction of form that were still able to capture something of its essence.

Organization. We present an efficient algorithm to automatically generate these open, C^1 -continuous splines from a set of input polygons. Feature points of the input polygons are detected using the medial axis to maintain important shape properties. We use dynamic programming to compute a planar non-intersecting spline representing each polygon's base shape. The results are stylised glyphs whose appearance may be parameterised and that offer new possibilities in the ‘cartographic design space’. We compare our glyphs with existing forms of geometric schematisation and discuss their relative merits and shortcomings. We describe several use cases including the depiction of uncertain model data in the form of hurricane track forecasting; minimal ink thematic mapping; and the depiction of continuous statistical data.

We first discuss the design choices for the glyphs used in stenomaps (Section 6.1). Then we give an efficient algorithm to automatically generate these glyphs from a polygon through medial axis detection (Section 6.2 and 6.3). We propose a scoring function which encourages the one-dimensional curve to describe both the boundary and area implied by the polygon. There are different possibilities for the types of glyphs computed (Section 6.4) and we describe user-parameters that help explore the possibility-space. We discuss several use-cases (Section 6.5) to explore the role that stenomap abstraction can have in the depiction of geospatial data. Finally, we conclude with a discussion and possible directions for future work (Section 6.6).

Why an area-to-line transformation? We provide several arguments for considering area-to-line transformations. Fig. 6.2 displays an ordered sequence of transformations of a polygon increasing in their abstraction. While generalising polygon boundaries is common (Fig. 6.2(b)), and often valuable, it is constrained by the topological arrangement of adjacent polygonal units along common boundaries. Transformation to a zero-dimensional point feature (Fig. 6.2(e)) frees up graphical space, however, topological relationships and most geographic context is lost in the process. Area-to-line transformation is most commonly achieved via medial axis generation (Fig. 6.2(c)), but while useful as an intermediate step for shape characterisation it has limited cartographic value and may be confused with genuine linear features such as river or road networks. The more smoothly curved stenomap glyphs (Fig. 6.2(d)) capture something of the form of the polygon boundary while being independent of adjacent polygon geometry and freeing up graphical space for other representations.

Background. The representation of outlines has received significant attention within the field of cartography. Both straight-line and curve schematisation, as well as simplification, have been well studied. Well known results in cartographic generalisation such as linear simplification (e.g., [87, 145, 301]) maximise the information maintained when reducing the level of detail. Automated cartographic generalisation (for foundational terms and state of the art see, [59, 62, 180]) is driven by intricate knowledge of the target scale or Level of Detail of the map product (for example [37]). By contrast, the focus of schematisation is to minimise detail while maximising task-appropriateness of the visualisation [182]. Straight-line schematisations (for example [55, 74]) have mainly focussed on orientation-restricted representations. Similarly, curved schematisation (e.g., [292]) has focussed on fixing the type of curve.

Representing shapes using curves has also been considered in other research fields, such as computing tangent-continuous paths for cutting tools (e.g., [89, 136]). Mi *et al.* [196] take an alternative approach, deconstructing a shape into parts to find the required abstraction.

Bézier curves, first described in 1959 [76], are a family of smooth curves described by a set of control points. As the control points define the tangents at the end points of the curve, Bézier curves can be used to create C^1 - or C^2 -continuous splines. Fitting a Bézier spline to a polygonal line can not be optimized in closed form, however iterative algorithms exist (e.g., [189, 247]). Stone and DeRose [267] show how to determine the existence of self-intersections in a cubic Bézier curve.

The medial axis, introduced by Blum [30], is a way to describe the skeleton of a polygon. As the medial axis is not stable under small transformations, various pruning algorithms have been proposed [12, 13, 26, 258]. Only maintaining the parts describing the main features of the polygon gives rises to a more stable version of the medial axis. In computer vision, shock graphs have recently gained considerable attention as this extended structure built on top of the medial axis can be used for automated shape recognition (e.g., [184, 286]).

Space-filling curves are regularly structured curves that fully cover a n -dimensional space. These curves can be seen as “[mapping] a one-dimensional space onto a higher-

dimensional space.” [304]. Recently, the use of space-filling curves to display hierarchical or complex datasets has gained attention (e.g., [9, 275]). In contrast to space-filling curves, our approach focusses on a curve that covers only a part of the area while still sufficiently describing it.

6.1 Design choices

Reducing a polygon to a line inevitably reduces its expressiveness. Hence, if we desire such an abstraction, careful thought should go into the formation of this line. In this section we discuss the design choices made when developing stenomaps.

C^1 -continuous. The glyphs we create are (along single strokes) C^1 -continuous. The continuity of the curve gives a hand-drawn appearance stimulating the perceived inexactness of the geometry. Using smooth swipe-like, near casual representations promotes an attention shift to the actual data, further emphasizing the imprecision in the geometry. For a discussion on C^x -continuity see Section 6.2.

Complexity. All glyphs should be presented using as few curves as possible. The curves should sufficiently describe the polygon at hand, but no excess information should be provided. We target our stenomaps at data not tied to an exact location. As exact geographic information is unimportant and excess information reduces the efficiency of the map, glyphs should have the lowest possible complexity. All attention should be focussed on the main data presented.

Area and boundary. Representing a polygon by a linear smooth glyph reduces the expressive power compared to the original two-dimensional polygon. Whereas a polygon implicitly describes both the area and the boundary, this is less clear for an open curve. In the case of elongated polygons both area and boundary representation give overlapping requirements. A curve following the “central axis” suitably describes both. For compact polygons, however, the requirements contradict (see Fig. 6.3). A partial boundary representation lacks the implied volume of the polygon, whereas a “central axis” is unable to properly represent the shape of the polygon. We note that a trade-off exists between representing the boundary and the area. We require the maximum minimum distance to the curve to be optimized while also sufficiently representing the boundary.

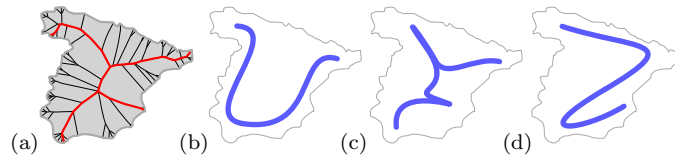


Figure 6.3 Representing Spain as a glyph. (a) Polygon and (pruned) medial axis. (b) Border representation. (c) Collapse to medial axis. (d) Trade-off between border and area.

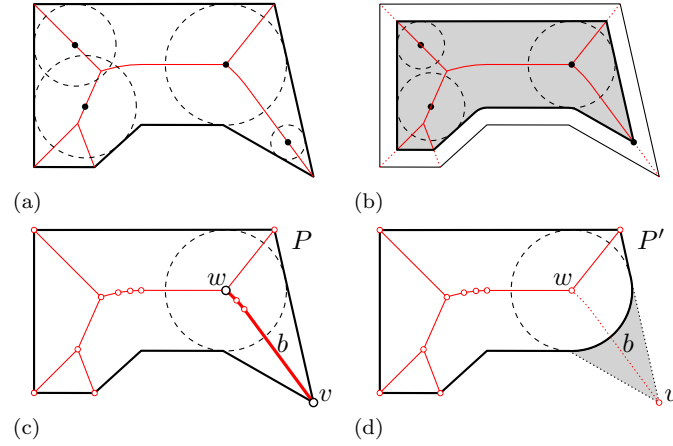


Figure 6.4 (a) Four maximally inscribed circles. The center points of all maximally inscribed circles form the medial axis (red). (b) Reducing the radius of all maximally inscribed circles negatively offsets P . (c) An end-branch b with parent w and leaf v . (d) Area contributed by the end-branch b .

6.2 Technical preliminaries

Medial axis. The *medial axis transform* was first introduced by Blum [30] and is defined for a polygon P as the closure of the set of points with two or more closest points located on the boundary of P . This set is usually simply referred to as the *medial axis* and is a subset of the edges implied by the edge-based Voronoi diagram [73]. The medial axis is a unique description of the shape of P . Each point on the medial axis is associated with a maximally inscribed circle of P (see Fig. 6.4(a)) and the union of all circles fully covers P . More specifically, there is a one-to-one correspondence between the medial axis including the radii of all maximal inscribing circles and the polygon being represented. This representation makes it easy to compute offset polygons by changing the radius of all inscribed circles by a fixed constant c (see Fig. 6.4(b)). A negative offset (essentially shrinking the polygon) can result in several connected components. Maintaining a minimum circle radius of $r \geq 0$ prevents such fragmentation.

Our input is a simply connected polygon P . (Note, though, that our algorithms could easily be extended to polygons with holes.) The medial axis M of a simply connected polygon is a tree. A *leaf* of M is a vertex of degree one and is located on the boundary of the input polygon. An *end-branch* b is a maximal sequence of edges connected via vertices of degree two, where at least one of the two end points is a vertex of degree one (see Fig. 6.4(c)). An end-branch has two end points, one of which is a leaf, the other is a *parent* (which could simultaneously also be a leaf). An end-branch b is *pruned* by removing of the edges of the graph with degree one and two vertices of b from the

medial axis. If we reconstruct the polygon belonging to the pruned medial axis we obtain a locally smoothed polygon P' . The *contributed area* of an end-branch is the area of $P - P'$ (see Fig. 6.4(d)). A pruned medial axis can be used for a variety of purposes and hence there exists a significant amount of literature which discusses various pruning measures and methods [12, 26, 207, 253, 258].

Visibility graphs. Given a set of points S , the visibility graph is the union of all edges between any pair of points in S that can see each other. We use a specific instance of the visibility graph where visibility is defined by the polygon P and the set S consists of all vertices of P . Two points can see each other if the straight-line connection between them is fully contained in the interior or the boundary of P . We use this visibility graph to compute shortest Euclidean paths in P .

Bézier splines. A cubic Bézier curve can be fit “optimally” to a given polygonal line using iterative Newton-Raphson approximation [247]. Similarly, with the help of *dynamic programming*, a series of cubic Bézier curves can be fit optimally to a polygonal line or a polygon [292].

Splines (the concatenations of Bézier curves) can have different degrees of continuity. A spline is C^x -continuous if the derivative of degree x of the spline exists and is a continuous function. When a Bézier spline is C^1 -continuous (smooth), the control points of consecutive curves line up (see Fig. 6.5(a)). Consequently, fitting curves to different parts of the polygonal line is no longer independent and, therefore, dynamic programming can not guarantee an optimal solution. If we reduce the allowed solution space, by fixing the required tangents at all vertices, the fitting of different curves is independent once more. We require the tangents at each vertex to be perpendicular to the bisector (see Fig. 6.5(b)). The start- and end-vertex have no well defined tangents, but no continuity is required here either. While fixing tangents beforehand is not required to compute a smooth spline, if tangents are not fixed, computing an *optimal* series of curves is hard.

6.3 Algorithm

We describe an algorithm to compute a linear, C^1 -continuous glyph G representing a simple input polygon P . Depending on the desired design, different types of glyphs can be generated (see Section 6.4).

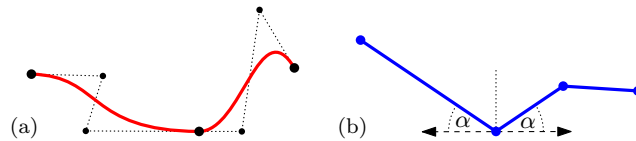


Figure 6.5 (a) C^1 -continuous curves have a continuous derivative. The control points of consecutive curves line up. (b) Fixing the required tangent beforehand allows for a dynamic programming solution.

Algorithm 6.1 ComputeGlyph(P)

Require: P is a simple polygon**Ensure:** G is a glyph of P , strictly positioned inside P

- {Find feature points}*
 - 1: Create the medial axis M of P
 - 2: Prune M to obtain feature points of P
 - {Obtain glyph region}*
 - 3: Trim branches of M
 - 4: Simplify P based on M
 - {Find backbone}*
 - 5: Compute all paths between feature points
 - 6: Find the backbone B visiting all feature points
 - {Create glyph}*
 - 7: Fit a smooth spline to B to obtain glyph G
-

Our algorithm consists of four distinct steps. First, we detect feature points that define the characteristic shape of P . Second, we compute the region in which the glyph should be located. Third, we determine the base shape of the glyph by finding a polygonal line (the *backbone*) that represents the polygon well. The shape of the backbone determines the shape of the final glyph to a large degree. Hence we describe two different approaches which result in radically different backbones. In the final step we fit a cubic Bézier spline to the backbone. Again, there are several possibilities, resulting in different types of glyphs. If the input is planar, our algorithm can be run in parallel on all polygons. See Algorithm 6.1 for a summary. We explain all steps in detail below.

6.3.1 Feature points

To maintain the characteristic shape of the input polygon P , we first detect the main *feature points*. We take a geometric point of view and use the pruned medial axis for feature recognition. Our method is based on the work by Bai and Latecki [12], who use area as a measure to guide the pruning. Area is relatively outlier- and noise-insensitive and is also used as a measure in cartographic simplification [301], making it suitable for our purposes.

The method by Bai and Latecki computes for each end-branch the size of the area that it contributes to P . By repeatedly pruning the end-branch that contributes the least amount of area to P the medial axis can be reduced to its main features. The algorithm by Bai and Latecki compares area loss to the previous, already reduced, incarnation of the polygon. As a consequence it may reduce large subtrees by iteratively removing small sections of the area. To prevent important features from being pruned prematurely we maintain the total area that has been pruned in each subtree. We maintain this information in the leaves and parent nodes and update it in amortized constant time when pruning an end-branch. Each edge is pruned only once and we can compute the area lost in $O(n)$

time, so the total pruning process takes $O(n^2)$ time. The leaves of the pruned medial axis correspond to the main features.

When displaying a subdivision (e.g., countries in Europe) we typically desire a similar complexity level across the map. To achieve this we admit only pruning steps that remove subtrees of a given maximum size. That is, any single prune action is not allowed to remove a branch representing a subtree larger than a user-specified percentage of the average polygon area in the map. The pruning process stops when this constraint is violated or when only a single path is left.

As discussed in Section 6.1, elongated polygons and compact polygons require a different level of detail. To facilitate this we introduce an extra factor measuring the compactness of a polygon. Specifically, we use the squared length of the longest path in the medial axis divided by the area of the polygon as a size independent description of compactness (see Fig. 6.6). Any measure using boundary length instead of the longest path in the medial axis would be more sensitive to local noise. The local area loss accepted in a single prune action is limited by: $0.25 * \alpha * avgArea * longestPath^2 / polygonArea$, where $0 \leq \alpha \leq 1$ is a user-defined parameter.

6.3.2 Regions

We now compute the region P' within which the glyph is contained. To make the glyphs clearly distinguishable we require these to be located strictly within the polygon they represent. Where possible a minimum distance to the boundary of the polygon is guaranteed. Using a modified offset operator ensures that a minimum area is maintained within which the glyph can be fit. A regular offset can cause the polygon to become disconnected and may collapse entire branches (see Fig. 6.7(a)). The modified offset operator uses the radius information stored in the medial axis. We first retract all end-branches of the medial axis by a given percentage (we use 30%). That is, we measure the length of the end-branch, and starting at the leaf vertex remove all vertices and edges until the summed length of the removed edges equals 30% of the original end-branch length. If the next edge induces a percentage larger than 30%, we shorten that edge and introduce a new leaf vertex.

Now we apply a modified negative offset to the radii stored for the inscribed circles of the medial axis. We reduce the radii of all inscribed circles by a constant – as in a regular

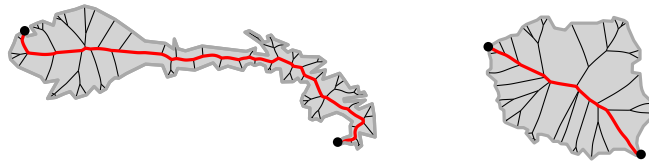


Figure 6.6 The ratio between the longest path and the surface area gives a description of the compactness of a polygon. Both polygons are scaled to the same surface area.

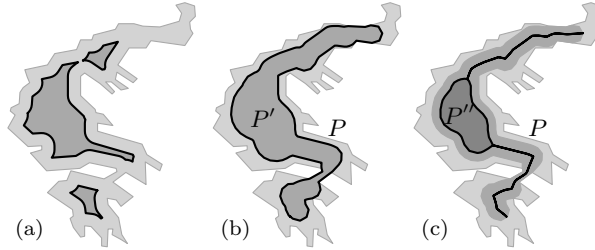


Figure 6.7 (a) A regular offset may cause branches to collapse and disconnect the polygon. (b) The offset polygon P' defines the space for the glyph. (c) The (possibly degenerate) polygon P'' for the backbone.

offset – unless this forces a radius to drop below a given threshold. In this case we set the radius to the threshold to prevent a collapse of the polygon (inscribed circles with an initial radius smaller than the threshold are simply maintained). Using a strictly positive threshold ensures a single connected polygon, using a threshold of zero can result in a degenerate polygon. The union of all reduced circles uniquely describes the negatively offset polygon. It can be computed in a single traversal of the medial axis. Our offset does not retract end-branches as all circles are maintained.

The region P' for the glyph is a negatively offset polygon with a strictly positive minimum radius (Fig. 6.7(b)) to ensure that the curve can turn without intersecting itself or the boundary. Inside the region P' we compute a second offset polygon P'' (Fig. 6.7(c)) in which the *backbone* of the glyph is located (see Section 6.3.3). When the backbone is turned into a smooth glyph we require some additional space for smoothing and hence the backbone needs to lie in a strictly smaller region than the region of the glyph. Here we do not require a strictly positive minimum radius and, hence, P'' may be degenerate.

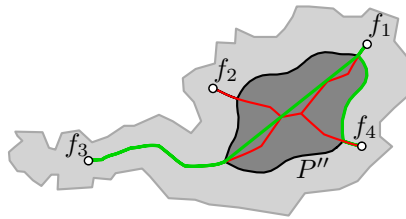


Figure 6.8 Consecutive feature points (e.g., f_4, f_1) are connected by a boundary path. Other pairs (e.g., f_1, f_3) are connected by the shortest Euclidean path inside P'' .

6.3.3 Backbone

A *backbone* is a planar straight-line graph that visits all feature points and describes the polygon well. We consider two types of backbones: simple paths and trees. Backbones are polygonal representations of the glyphs and are used as base shape for the final glyphs (see Section 6.4).

Path-backbone. Our input is the offset polygon P'' and the feature points cyclically ordered around P (see Fig. 6.8). We aim to find a good simple polygonal path visiting all feature points which stays inside or on the boundary of P'' . To do so we first connect any pair of feature points with a path. This path follows the boundary of P'' if it connects two consecutive feature points. For all other pairs we compute the shortest Euclidean path inside P'' using the visibility graph [73].

As discussed in Section 6.1 the final glyph, and thus the backbone, should represent both area and boundary of the polygon. We represent this dual requirement by a linear trade-off between the percentage of boundary covered and the maximum distance to the curve from any point in the polygon. Let $s_{boundary}$ and s_{area} be the boundary and area score respectively and $0 \leq \beta \leq 1$ a user-set parameter. The score of the backbone is defined as $(1.0 - \beta) * s_{boundary} + \beta * s_{area}$.

The boundary score $s_{boundary}$ represent the percentage of the boundary of the original polygon that is covered by an offset of the backbone. Similarly, the area-score s_{area} is the maximum minimum distance to the backbone as a percentage of the maximum minimum distance to the polygon boundary (see Fig. 6.9). As an approximation of the maximum minimum distance we take the maximum minimum distance of any point on the medial axis to the backbone.

Given the computed paths between any pair of feature points and the described weighing scheme, we find the optimal, simple path visiting all feature points. Finding such a path is NP-hard, but as the number of feature points is very small we can use a brute-force approach.

As the backbone is computed using a scoring function we can introduce additional factors to influence the result. For example, our framework implements a penalty function to prevent duplicating parts of the path as well as a sea- or map-border preference.

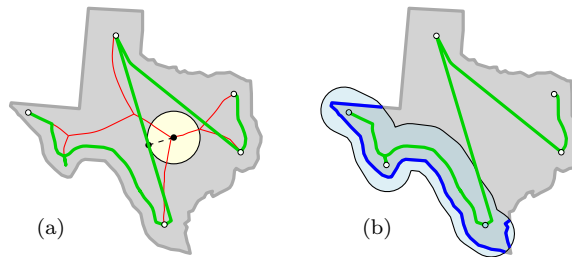


Figure 6.9 (a) Maximum minimum distance for any point on the medial axis to the backbone. (b) Boundary covered by a subset of the backbone.

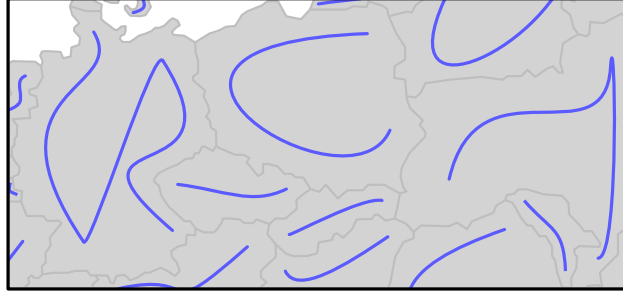


Figure 6.10 Example of simple glyphs. Outlines are supplied for reference.

Ensuring the boundary of a map is covered may be preferential if the shape of the subdivision is familiar, but separate polygons are less recognizable. All the figures presented in this paper were, however, created without the use of these additional parameters.

Tree-backbone. Path-based glyphs achieve a high level of abstraction. Sometimes a more complex structure may be desirable that better captures the shape and the area of the polygon. We also consider backbones based on trees. Tree-backbones are computed directly from the offset polygon P' . We turn the boundary of P' into an undirected graph and detect cycles using depth-first search. Cycles are opened by disconnecting and shortening one of the edges in a cycle.

6.3.4 Glyphs

The backbone is a concise and abstract representation of the input polygon. In the final step we polish the appearance of the backbone using smooth, C^1 -continuous curves. As the essential shape is already determined by the backbone there is a large degree of artistic freedom in this last step. Several types of glyphs can be created, possibly designed to fit the application at hand. In the next section we describe the glyphs that are implemented within our framework.

6.4 Glyph types

Different glyphs can be fit onto a backbone and here we discuss three options.

6.4.1 Simple

We fit a simple, C^1 -continuous, cubic Bézier spline to a path-backbone. The simplicity of the design makes this glyph most suitable for cartographic applications. To keep the complexity of the final glyph low, we minimize the number of Bézier curves (see Fig. 6.10).

The overall spline should use as few curves as possible while staying within a given error-bound err_{max} . For each single curve c representing a polygonal line p , we define its

error e_c as the maximum minimum distance between c and p . The error of a set of curves C is $\max_{c \in C}(e_c)$. We use dynamic programming to minimize the number of Bézier curves used to represent the polygonal line while staying within the error-bound [292].

There may be many different splines, using the minimum amount of curves, that stay within the given error-bound of the polygonal line. Therefore, as a secondary objective function for the dynamic program, we compute the average distance d_c of a curve to the polygonal line. To this end, we compute the average of the squared distances between regularly sampled points along the polygonal line and the curve.

We define the cost c of a curve as $1 + d_c/(n * err_{max}^2)$, where n is the number of vertices of the polygonal line. As each allowed curve has an error of at most err_{max} , the average squared distance d_c is at most err_{max}^2 . The number of curves used to represent the polygonal line can never exceed $n - 1$, hence the total cost implied by the fit of the used curves can never exceed one. As a consequence, the result has the minimum number of Bézier curves and has, for all solutions with this number of Bézier curves, the curves with on average the best fit. To prevent curve intersections and self-intersections we set the cost $c = \infty$ if an intersection occurs.

6.4.2 Locally intersecting

As an alternative to simple, C^1 -continuous cubic Bézier splines we let ourselves be inspired by the work of Picasso (“One-Liners”) [214]. We forgo smooth transitions between consecutive curves and instead create an appearance of smooth behavior by connecting two consecutive Bézier splines with an additional *swirl* (see Fig. 6.11).

We again use a dynamic program to find the optimal set of fitted Bézier curves. As there is no dependency between consecutive curves, we do not need to fix tangents at the vertices beforehand. For any two consecutive curves connecting at a vertex v , we compute the distance d_{vP} from v to the polygon P . We then create an additional cubic Bézier curve (the swirl) whose start- and end-tangents meet up with the previous and next Bézier curve, respectively. To ensure that the swirl is fully located in the polygon the second and third control points of the curve are positioned at a distance $0.75 * d_{vP}$ from the first respectively fourth control point. We again disallow intersecting curves.

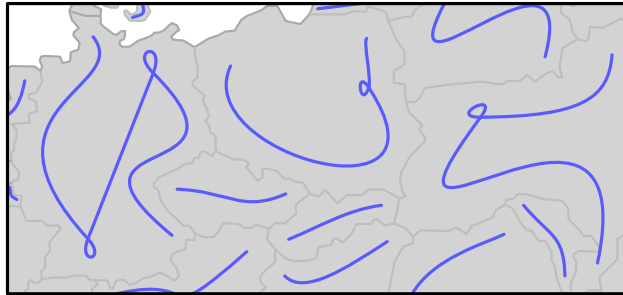


Figure 6.11 Example of locally intersecting glyphs.

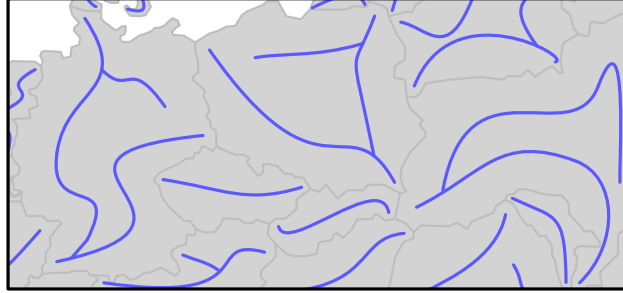


Figure 6.12 Example of tree-based glyphs.

In some cases swirls may be undesirable. When curves meet at a too shallow or too sharp angle a swirl may look unnatural and a C^1 -continuous connection would be preferred. Let C and D be two consecutive curves connected at a vertex v . Let t_C and t_D be the tangents of C respectively D at v . We define α as the minimal angle between t_C and t_D . We only add a swirl if $\pi/6 \leq \alpha \leq 5\pi/6$. Otherwise, we force C and D to be C^1 -continuous. This creates an interdependency between subproblems and, hence, we cannot claim that the dynamic program computes the optimal solution. In practice, however, the results are quite satisfactory.

6.4.3 Tree-based

The final alternative are glyphs based on tree-backbones. Such glyphs can describe area more concisely, but they are also more complex than glyphs based on path-backbones (see Fig. 6.12).

Our input is a tree-backbone B . We say that the leaf of the longest end-branch is the *root* of B . In case that B has only two leaves, the root is the top leftmost leaf. Let the *turning angle* $t_{e,f}$ between two edges e, f on a path p be defined as $\pi - \text{angle}(e, f)$ if e and f have a common vertex and 0 otherwise. The turning angle t_p of a path p is $\sum_{e,f \in p} t_{e,f}$. Let P be the set of paths of minimum size that cover B , where all paths $p \in P$ go strictly down in the tree and $\sum_{p \in P} t_p$ is minimized. For each path $p \in P$ we fit a cubic Bézier spline using the edge-based Voronoi diagram to ensure different splines do not intersect [292]. Different splines might not connect at endpoints. We extend splines using a straight line matching the end-tangent to ensure all splines are connected.

6.5 Cartographic applications

We first in Section 6.5.1 present a formal discussion on the relation of stenomaps to the existing cartographic design space. Section 6.5.2 to 6.5.4 explore three use cases for stenomaps.

6.5.1 Stenomaps as thematic maps

The wealth of expressive and effective visualisations in thematic cartography has been subject to numerous efforts of systematisation. The most fundamental of these systematisations is Jacques Bertin's *Semiology of Graphics* [28]. Bertin postulates that the effectiveness of any diagram is based on the degree of structural equivalence that can be reached between data and the visual variables. For the case of maps the most powerful variables, the two planar dimensions, are more or less fixed by geographic coordinates. Any information beyond geometry (thematic *elevation*) must be expressed by encodings using the remaining visual variables known as *retinal variables* or color-pattern variables. The retinal variables are shape, orientation, color, texture, value, size. Each has a maximum in the structural equivalence of the scale level it can express, further limited by the geometric primitive (point, line or area, i.e., *implantation*) it is applied to. The levels of organizations are Association or Disassociation, Selection, Order and Quantity. The Length of a given variable is different for each implantation. Length denotes the number of possible variations that can be used while still allowing selective perception. Bertin discusses each retinal variable and its potential Length thoroughly and with many examples, including special cases and precise instructions on maximizing differentiation. The effects on expressiveness when using multiple retinal variable encodings simultaneously were discussed by [263]. For a discussion of the concept of Disassociation and its effects see [224]. More encyclopedic taxonomies of the actually realised design space were proposed by [111] or [148] for example, which form the baseline of more current works like [166].

The classic space of possible and realised cartographic visualisations [111, 166] divides the topological structure into discrete and continuous phenomena, further subdivid-

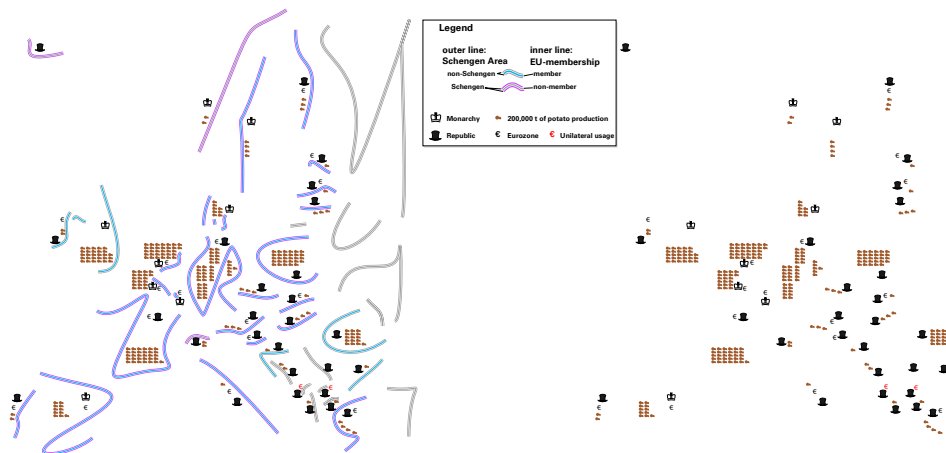


Figure 6.13 Potato production, monarchies, the Eurozone and the Schengen accords in the European Union, with and without glyphs.

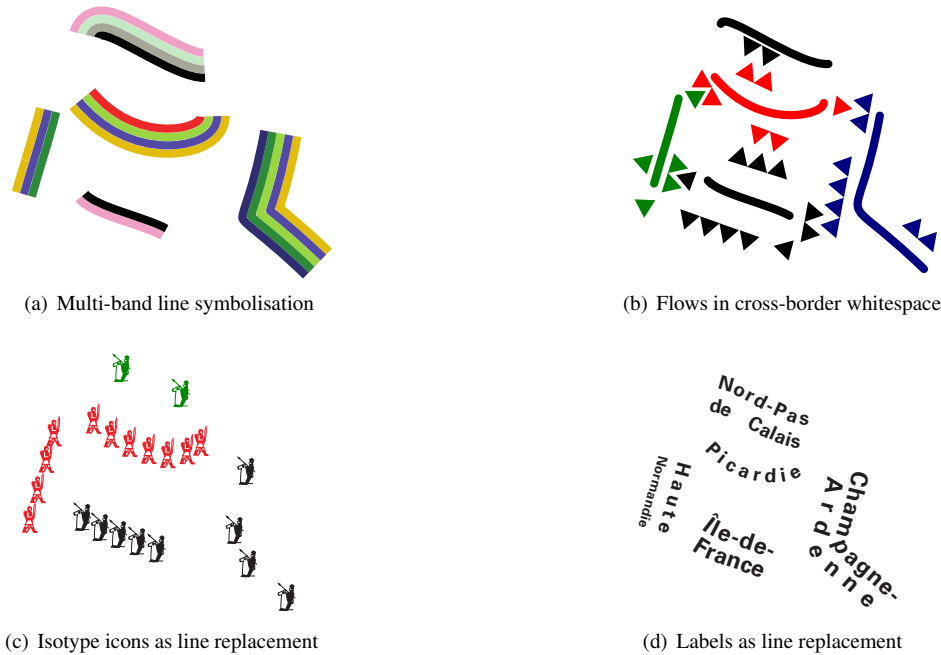


Figure 6.14 Design choices for stenomaps.

ing the discrete phenomena into points, lines and areas. Hence, discrete geographic areas can be expressed only by some form of polygonal subdivision. Stenomaps break that contention and show that it is possible to represent discrete areas with cartographic lines. We observe three major changes:

I boundary lines vanish

II area fills vanish

III implantation change from area to line for discrete area objects from the basemap

These changes reduce the visual complexity of the map by reducing the number of control points [182] as well as the amount of “ink” used [28]. Furthermore, change I has the following immediate effects:

- actual locations of boundaries become fuzzy, limiting the accuracy of placement and the ability to conduct measurements in the plane
- adjacency topology becomes fuzzy
- empty bands of expected width 2ϵ become available around discrete areas. Due to isthmuses (see Fig. 6.7) the theoretical lower bound for width is $2 \cdot width_{min}^{polygon}$, i.e.

twice the minimal discernable width of polygons, = $0.6mm$ for b/w and = $0.8mm$ for color depictions [126].

Effects of change II are:

- maximum selective length for each retinal variable, except shape and orientation is reduced by 1 each. This decreases the degrees of freedom for choosing retinal variables by 4. The reason for this effect can be interpreted as a function of the drawing space real estates that color, texture, value and size need to work at full efficiency.
- maximum selective length for orientation is raised from 0 to 2, as the area implantation does not allow selective variation of orientation at all.
- The net change in degrees of freedom for variation of retinal variables for selective perception is thus -2 .
- figure-ground separation is amplified over the whole map [28]

As the three implantations are highly selective themselves, change III frees up the area implantation for some other feature type to be added, but lessens the degree of freedom for other phenomena to be depicted with cartographic lines. The gain of white space due to both I and II drastically increases the potential to place further map elements in a high-contrast environment. This decreases visual interaction by simultaneous contrast and color mixing effects. Color can be chosen individually for different implantations. The map in Fig. 6.13(left) makes use of that effect to display multiple set memberships while having full access to the color space for the point symbols and quantitative data. We can conclude that in cases where the negative consequences of the implantation change *Area* \rightarrow *Line* such as fuzzy boundaries and adjacencies are not crucial, stenomaps could be used just as well as other maps types like choropleth maps. In cases where displaying sharp administrative boundaries is detrimental to the intended message, stenomaps offer a new cartographic arrangement with improved figure-ground separation, lower complexity, an additional layer-slot for area depictions and a band of white space around the glyphs.

6.5.2 Use case: variations on glyphs as cartographic lines

In this section, we examine the design possibilities for visual variation of glyphs as cartographic lines. On a fundamental level, glyphs inherit the basic and combinatorial traits of the line implantation, a formal discussion of which we forgo. As visual shorthand for discrete area objects, i.e. in application in a stenomap, we provide some further exploration of design possibilities. Stenomaps do not assume the existence of a separate base map layer. Succinctly, the usual constraints stemming from the base map that line features are limited by, do not apply. This allows a much higher degree of variation in pattern and width of the line features. One example is to create multi-band representations such as Fig. 6.14(a). Here, multi-set membership and even configurations of set-membership are displayed by colored repetitions of the basic glyphs. Though there are natural limits, these

are less strict than in regular maps, due to the white space gained by the area-boundary collapse. Special care must be taken not to vary the width of the glyphs too much, lest the perception as an areal subdivision be dissolved. The same care must be taken regarding brightness (value) differences. Fig. 6.13(left) makes use of the variation of pattern as well as color. Specifically, the effect of vibration is used following the parametrisation of [28], not unlike a Moiré-pattern, to highlight the Schengen-participants (signatories to a cross-border migration treaty) who are also EU-members. Note that the lower contrast pairings do not produce the same effect. Such use of vibration is generally not advisable for areas and presents another advantage of stenomaps. The glyphs in this figure give a strong sense of location, as can best be seen when making the comparison with the same map solely containing data (see Fig. 6.13(right)).

While Fig. 6.13(left) makes use of the space formerly occupied by boundaries by placing point symbols and quantitative information, another possible application is to depict cross-border flows (Fig. 6.14(b)). This technique is best suited for the case of planar flow graphs and can reintroduce topology information that was made imprecise by the area collapse. The Vienna Method of Pictorial Statistics (e.g., [204]), later known as *Isotype*, was most often used over very sparse base maps or on plain white paper. Stenomaps are a natural environment where Isotype icons can dwell and prosper. They can be applied like

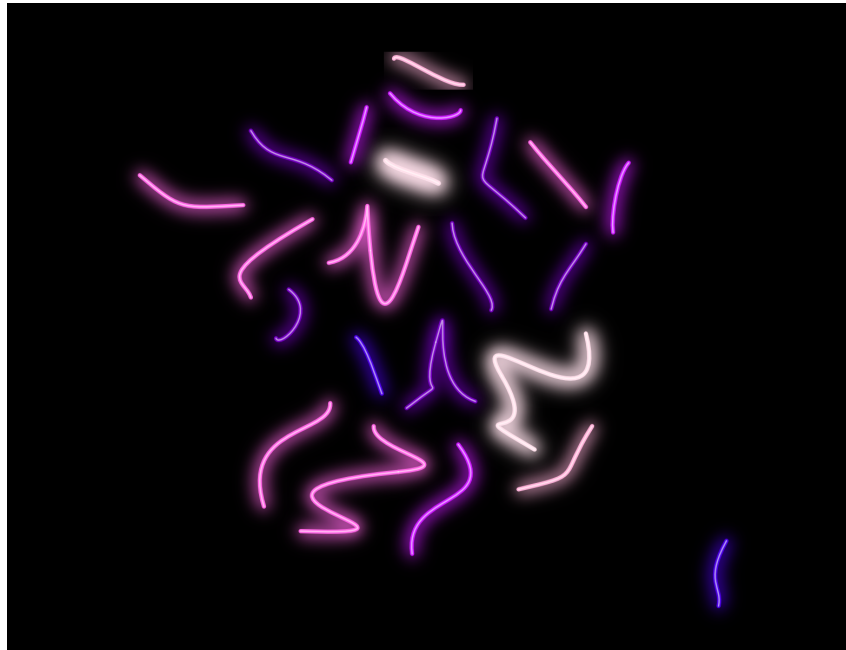


Figure 6.15 Energy consumption in the Regions of France 2010. Data source: Electrical Energy Statistics for France 2010, Réseau de transport d'électricité 2011.

regular carto-diagrams as in Fig. 6.13(left) or even be used to utterly replace glyphs by repetition. The latter technique is limited in cases where the low frequency of icons starts to dissolve the individual glyph, as is exemplified by the green elements in Fig. 6.14(c).

As has been mentioned, stenomaps abscond from regular base maps and thus have no or very few labels. Either through aesthetic choice or informational necessity, the glyphs can be replaced with the toponyms of the collapsed area features, as shown in Fig. 6.14(d). Note that the geometric algorithm itself could also be used for proper labeling of areas. The parametrisation must then be adjusted to yield curves of low complexity close to the backbone of the polygon (Fig. 6.7).

If used as polygon boundaries, cartographic lines can traditionally be used to adumbrate specific area fills. These techniques using hachures for cartographic “hemlines” or repetition for copper-engraving-style waterlining, can be inverted in usage to make glyphs more expressive. Such an inverted hemline as both an adumbration of the area as well as thematic expression was used in Fig. 6.15. The same effect could be applied by inverted waterlining or hachures, which themselves leave ample amount for further variation. Due to the high contrast environment of stenomaps, said variations are much more poignant and discernible than in regular maps.

6.5.3 Use case: spatial uncertainty

As an example of uncertain data we investigate the display of hurricane path predictions (see Fig. 6.17). Presenting these kinds of two dimensional spatial probability data is critical in many applications. Besides hurricane data, thought may be given to flood predications or dispersion of toxic gas plumes. When presenting spatial data on these types of phenomena (we focus on hurricane paths) often only a small part of the information can be presented on the map. While a lot of information may be known about the probabilities, several problems make their effective display challenging. We discuss two problems: selective perception and the illusion of accuracy.

An efficient map requires that the data being conveyed are presented as clearly as possible. To this end the main data presented should be clearly distinguishable from the additional information displayed, such as geography. One of the aspects that ensures *selective perception* is implantation. Using different implantations can enhance the presentation of the main data, hence, improving the effectiveness of the map. When displaying



Figure 6.16 Solar potential in Europe for horizontally placed PV-modules. Data source: PVGIS 2012.



Figure 6.17 Hurricane Katrina Prediction. Probability that center of storm will pass within 75 statute miles. Datasource: NOAA Hurricane Center.

probability information on regular maps, however, both the geography and the two dimensional probability data are polygons. To allow the information to be clearly separated we would desire different implantations to be used. Obtaining different implantations can be achieved by abstracting either of the two data sources. By reducing the geography instead of the probability information we prevent a radical reduction of the information presented, but ensure a high selective perception.

A critical problem when displaying probabilistic data is the *illusion of accuracy*. Maps inherently provide a sense of perceived accuracy which is at odds with the inexactness of the data being provided. For predictions a high level of information should be supplied, but extracting any exact localized conclusions should be prevented. To achieve this often the known data are abstracted, reducing a hurricane path to the single path that is most likely. Abstracting the data, however, results in a radical information loss, reducing the effectiveness of the map to portray the spatial data. The conventional way of addressing this problem of depicting uncertain data is to consider ways of symbolising the uncertainty in the data (hurricane track probabilities in this case), but the stenomap provides an alternative approach. By simplifying the geography instead of the data, we maintain all information present in the data, but prevent users from making possibly erroneous precise inferences. The extreme abstraction of glyphs limits interpretation to generalised regional spatial patterns that reflect the uncertainty in the data. More precise inferences of location are not possible as area and state borders are not exactly described.

stronger sense of positioning of the data. This effect is even further amplified as colors are visually interpreted as more uniform within each polygon. Stenomaps introduce a new, less intrusive way to give a reference to location (see Fig. 6.16(b)) without implying discrete changes at boundaries. By removing the need to close off areas, the continuity of the described phenomena is better maintained. The inexactness of glyphs ensures that no exact location can be matched with the data. Nevertheless, similar to river networks, glyphs instill a sense of location allowing for comparisons between maps.

6.6 Discussion and future work

Evaluation. The use of linear features to represent polygons is an intriguing new concept that gives rise to stenomaps. We presented an algorithm for the automated construction of stenomaps and discussed a variety of use cases. The results are convincing and visually pleasing. It is, however, unclear how effective stenomaps are. To gauge the usability of stenomaps user studies should be performed in future work. A first step could be to test the recognizability. It should be tested if the proposed glyphs maintain sufficient information for users familiar with the input. After recognizability, task appropriateness should be tested for the different use cases. This will be harder to measure as the glyphs are dissimilar from existing techniques, thereby risking a bias towards more familiar methods. However, task-based evaluation, such as estimation of hurricane damage probabilities over space could provide a useful means of comparison with conventional techniques. Testing the usability of this new method would give a better insight in the strengths and weaknesses of the method; possibly spurring further development.

Methodology. The generation of glyphs can be steered using two different parameters. First, by changing the level of pruning of the medial axis the complexity of the final glyph can be determined. Second, the computed backbone can be set to better represent area or boundary. The interplay of these variables allows for a large range of design options (see Fig. 6.19). These options allow map designers more choice over the shape of the glyphs. However, the question arises if it is possible to define a base setting appropriate for most maps. This is already partially the case as differently shaped polygons within one map are presented using the same settings. Preliminary experiments, however, show that a standard base setting across different maps is unlikely as different maps require different levels of detail. Subdivisions with uniquely shaped polygons require less exact detail than more uniformly shaped subdivisions (e.g., the difference between the states of the USA and the countries of Europe).

The medial axis as a shape-descriptor is very suitable for the creation of glyphs. It allows both feature points to be detected and an efficient computation of the available space. The medial axis is a representation of the polygon space, however it is not necessarily a fair sample. In parts where the inscribed circles are large the medial axis may be far removed from sections of the polygon. Thus, the medial axis may be a false sample when computing the maximum minimum distance to the backbone (Section 6.3.3). Misrepresenting the area of the polygon can result in visual artifacts as sections of the polygon may

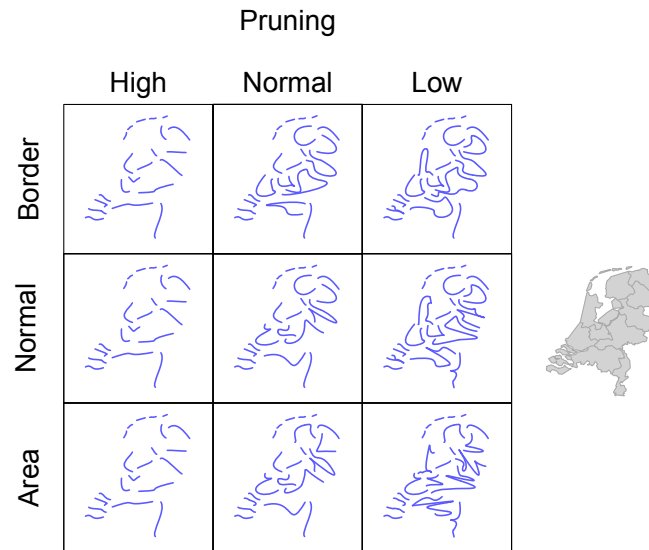


Figure 6.19 A sample of the parameter space defined by the user parameters affecting complexity and polygon representation.

not be taken into account. The boundary representation that is part of the scoring function counteracts these effects. Though misrepresentation is unlikely, future work might investigate if other distance measures can give a better representation of the area.

Glyphs. Glyph representations allow a significant abstraction from the original input. This level of abstraction is a main feature of the stenomap, but also brings forth new considerations. The representation of polygons through glyphs is very useful when information about a subdivision is shown. The extreme level of abstraction, however, implies that glyphs maintain their meaningfulness only while in context. When less context is present a larger amount of detail should be maintained in the glyphs. Displaying more detail within the glyph, however, reduces the advantage of using glyphs. Another consideration introduced by the extreme abstraction of glyphs is their uniqueness. As glyphs are highly abstracted, similarly shaped polygons may end up with a near similar glyph. While glyphs are distinguishable through their positioning in the subdivision, having uniquely shaped glyphs may be beneficial in some maps where lookup tasks are important. Similar shapes create a visual connection, which might counteract the data being presented. For future work it would be interesting to see if unique glyphs can be guaranteed. Taking similarity into account during the creation of glyphs is likely undesirable when fast computation is essential, since it introduces dependencies between subproblems and inhibits parallel computation.

The minimal information maintained in glyphs is still sufficient to give an inexact description of the input shape. It can be argued that the main strength of glyphs is bound

by their subconscious relation to the original input shapes. There is a danger that when the user has no knowledge about those shapes, glyphs could lose part of their strength. We would argue, however, that the glyph in itself becomes a representation of the shape that is sufficient for many tasks where precise geometry of polygonal regions is not central. Glyphs supply sufficient information even when the input division may not be well known (for example Fig. 6.15).

Through their simplicity glyphs make an interesting case for user interaction. Clearly, glyphs can be used as an additional visualization tool. Glyphs reduce the visual input complexity, which can be beneficial when a high-level overview is required. Their smoothness and simplicity, however, also makes glyphs intriguingly suitable for swipe interaction. Through swipe gestures item selection or map interaction could be achieved. For this use case, unique glyphs would be required.

Stenomaps are very efficient when exact boundaries of a subdivision are not needed but a general representation of the shape is helpful. They also offer several unique graphical variations that are applicable to various common use-cases. But by their intended nature of being a one-dimensional visual shorthand for a two-dimensional object they are still tied to size differences of the input polygons. Succinctly, they share the problems of polygons when directly trying to display quantities by size modification. However, as they are one-dimensional, they conceptually offer the opportunity to address this fundamental limitation of cartography. Thus, future work might explore if it is feasible to ensure that all glyphs have equal length. As glyphs are independent of each other this could, for example, allow for distortion-free cartograms. However, it is unclear whether such an approach would be feasible. First, different sized polygons might coexist in a map (e.g., Luxembourg and Russia). Using too small glyphs would be unsuitable for large polygons, whereas too large glyphs could quickly fill up small polygons. Second, even given equal length, glyph shape still affects the visual saliency. Nevertheless, stenomaps might point the way towards a distortion-free solution of the value-by-area problem.

Chapter 7

Conclusion

In this thesis we presented both procedures as well as results of analysing and modelling cartographic design principles for automated map generation. We also implemented several algorithms that follow these principles. Our implementations range from isolated fact-finding optimisations and map generation for National Mapping Agencies to elements for a fully developed web-mapping production chain. Furthermore we illustrated how the individual observations and findings can instruct future efforts of modelling the large design space of thematic maps and geo-visualisation.

7.1 Main findings

Labelling. We presented a fully parametrised multi-criteria model for the problem of point feature labelling that fulfils more cartographic criteria than all other extant literature and industry solutions. Using a complexity model based on raster encoding of base map detail, we presented an efficient algorithm that outperforms all currently available methods. We also presented our advances in the realm of polygon labelling. For labelling individual islands outside their border, we presented a straightforward algorithm, informed by our modelling, that can surpass all other extant solutions. Further on, we introduced the problem of archipelago labelling. Here we show how computational geometry and cartographic modelling can work in unison even during the modelling stage by comparing manual label placements to optimal placements for various distance measures.

Chorematic diagrams. In Chapters 4 and 5 we studied chorematic diagrams. Chorematic diagrams are a special kind of map-like diagram that lie at the intersection of thematic maps and schematised maps using only a reduced set of thematic expressions. We introduced a holistic cartographic modelling process based on work by Berlyant and applied it to all chorematic diagrams published in the journal *Mappemonde*. The modelling process resulted in textual descriptions and measurements that were pushed further towards mathematical formalisation into a system of cartographic generalisation constraints and a

taxonomy. The main finding here is, that indeed chorematic diagrams are diverse but can be grouped into statistically significant classes. These classes make the mapping from task to specific parametrisation of constraints easier. While not all aspects of chorematic diagrams could be fully modelled down to the correct parametrisations and evaluation functions yet, the most prevalent classes (SM & AM) of chorematic diagrams are now well enough understood to be automatically created. Furthermore, we introduced the general form of an evaluation function for chorematic merit which seems attainable. More importantly, we argued that chorematic merit is a subset of cartographic merit, so that the general form of the evaluation function would remain the same.

Schematisation and generalisation. We provided the first rigorous, contextualising definition of schematisation and schematised maps. We introduced the *cartographic line frequency* as a complexity measure for maps and schematisations and indicated that for schematisations it must replace the radical law of generalisation as guiding measure. We also provided the first taxonomy of schematisation operators including their link back to the established generalisation operators, making clear how much larger than angular restriction the design space of schematisations is. This helped us to smooth the way for our and other researchers current and future efforts on curved schematisation. Our systematisation of schematisation operators also allows to find other areas in need of algorithmic work. We closed one of those gaps by introducing the first cartographic area-line collapse for true areal features with Stenomaps in Chapter 6.

We also presented and implemented an algorithm for the aggregation and caricature of medium scale urban areas from highly detailed input data. The results were better matches for the actual urban areas compared to the manually produced dataset. They also are proof that schematisation and generalisation approaches can be combined.

7.2 Looking forward

Labelling. Regarding automated labelling of maps there are some more or less obvious incremental advances that our work suggests. There are also some long term changes in research directions, that we think are important. Our advances for point feature labelling could be easily combined with a sliding model, most likely making the results virtually indistinguishable from manual label placement. Further advances for point features such as labelling in dynamic environments for navigation systems are already investigated by other researchers. For labelling islands outside their boundary, it is not entirely clear whether more involved distance measures might lead to even better results. The placement of labels for archipelagos is just beginning to be fully understood as design and algorithmic problem. The general label placement research paradigm has proven successful. The greatest challenges for automated labelling lie ahead though, in the form of moving beyond the concentration on label *placement*. We mentioned in Chapter 2 that the actual cartographic lettering problem comprises four major areas, of which placement is just one. Choosing task-appropriate subsets of toponyms and automatically generating a typeface scheme including hierarchies of objects and so forth would be an enormous

advance. But we first need to understand much more about the tasks that maps are constructed for. Can we hope to continue studying labelling in isolation, thereby gaining incremental insight into (task, labelling) mappings? Or can we only make progress once we understand task modelling for maps as a whole much better?

Chorematic diagrams. Chorematic diagrams remain an exciting and rich object of study. We hope our results are the start and not the end of research into the subject. From our modelling, several questions are already raised. Can we come up with a harmony function that measures overall map harmony by measuring adherence to rules of visual balance and harmony for individual map elements? Are the promising experiences made in multi agent map generalisation the best way to approach that problem? If yes, then chorematic diagrams could indeed be the testbed for the whole of harmony in cartography. What is harmonious in chorematic diagrams must be so in all maps without the inverse necessarily being true. Algorithmically, many improvements are still needed, especially the run-times of the current approaches are too high for interactive and on-the-fly generation of chorematic visual summaries. What are the respective theoretical lower bounds for the diversity of geometric tasks? What short-cuts can we, must we take? Our research into the generation of territorial outlines also raises questions of general interest. As many territorial outlines of other schematised maps seem to make use of similar visual strategies, is there something profound about human visual cognition to be learned? Are we really looking at all the details of a given coastline in regular maps or are 7-20 vertices always enough? Such insight need not be restricted to geographic data. How much information do we actually need to positively identify arbitrary 2D shapes visually? We already have enough tools at hand to create user studies that we will hopefully conduct in the future to approach these and other functionality and usability problems.

Thematic maps. Advancing the automation of thematic maps is in our view one of the most crucial tasks left for generalisation research. The demand for up-to-date specialised geoinformation is growing everyday, but practical automation has been treading water for nearly twenty years. Just as thematic maps are two-layered (base-map and thematic layer) so is the problem. The first open problem is the generation of appropriate base maps. If we were to identify the most pressing needs, then river generalisation rises to the top. Current digital maps basically do not provide the cartographical backbone of yesteryear: the river network depicted as a tree-graph with smooth, curved lines. While it could be fruitful to empirically measure the benefits that a well-generalised river network has on contextualising the thematic information, practical algorithms are more sorely needed. Quite understandably, national mapping agencies are still concentrating on their intricate hydrological databases for large-scale mapping. River network generalisation for medium and small scales, though, is foremost a visual operation, not so much one for hydrographic engineers. We are hopeful, that approaches from curved schematisation and graph drawing can be combined to yield useful medium and small scale river networks. This presumes of course, a proper cartographic modelling. So far this remained a desideratum, and printed, let alone formalised, cartographic lore is scant.

The big successes of the label placement paradigm leads us to wonder if we cannot transpose label placement strategies to other cartographic production problems. The most

obvious candidate would be page layout: whereas graphic designers need to take into account the changing tastes, maps are functional artefacts that are allowed to be repetitious. Especially for GIS produced thematic maps, users without proper design training need to generate map layouts by the millions every day, without any geometric assistance. Using the graphically defined cartographic guidelines, we could treat the elements of a map such as legend, scale bar and so forth, as labels. With the proper parametrisation, the three subtasks of label placement could just as well help to automatise map layout. Such investigations seem to be both economically very attractive as well as scientifically laudable.

The most fundamental problems arise regarding the scale-dependent modelling of thematic geodata. It seems that every subject matter such as geology, migration, income, age, air speed and so forth needs to be studied separately, as semantics and geometry are so thoroughly interwoven. If we cannot develop a general method of thematic generalisation purely based on geometry, can we at least devise a general cartographic modelling procedure for thematic data and their links to forms of graphical expression?

In this thesis we aimed at laying the groundwork for exactly such a modelling procedure.

Bibliography

- [1] *Történelmi Világtlasz*. Cartographia, 2001.
- [2] E. H. L. Aarts and P. J. M. van Laarhoven. A new polynomial-time cooling schedule. In *Proc. of the IEEE Int. Conf. on CAD-85*, pages 206–208, 1985.
- [3] R. Adams and L. Bischof. Seeded region growing. *Pattern Analysis and Machine Intelligence, IEEE Transactions on*, 16(6):641–647, 1994.
- [4] M. Agrawala and C. Stolte. Rendering effective route maps: improving usability through generalization. In *SIGGRAPH '01: Proceedings of the 28th annual conference on Computer graphics and interactive techniques*, pages 241–249, New York, NY, USA, 2001. ACM.
- [5] J. Ahn and H. Freeman. A program for automatic name placement. *Cartographica*, 21(2-3):101–109, 1984.
- [6] A. Alvim and E. Taillard. Popmusic for the point feature label placement problem. *European Journal of Operational Research*, 192(2):396–413, 2009.
- [7] S. Anand, S. Avelar, J. M. Ware, and M. Jackson. Automated schematic map production using simulated annealing and gradient descent approaches. In *Proc. of 15th Annual GIS Research UK Conference*, pages 11–13, 2007.
- [8] S. Anand, J. M. Ware, and G. Taylor. Generalisation of large-scale digital geographic datasets for mobilegis applications. In *Dynamic and Mobile GIS Investigating Changes in Space and Time*. CRC Press, 2007.
- [9] D. Auber, C. Huet, A. Lambert, B. Renoust, A. Sallaberry, and A. Saulnier. Gospermap: Using a gosper curve for laying out hierarchical data. *IEEE Transactions on Visualization and Computer Graphics*, 19(11):1820–1832, 2013.
- [10] B. Baella, M. Pla, C. Brewer, D. Burghardt, B. Battenfield, J. Gaffuri, K. Tóth, D. Käuferle, et al. Generalisation in practice within national mapping agencies. *Abstracting Geographic Information in a Data Rich World*, pages 329–391, 2014.

- [11] G. Bahrenberg, E. Giese, and J. Nipper. *Statistische Methoden in der Geographie Band 2 Multivariate Statistik*. Teubner, 1992.
- [12] X. Bai and L. Latecki. Discrete skeleton evolution. In *Energy Minimization Methods in Computer Vision and Pattern Recognition*, pages 362–374. Springer, 2007.
- [13] X. Bai, L. Latecki, and W.-Y. Liu. Skeleton pruning by contour partitioning with discrete curve evolution. *IEEE Transactions on Pattern Analysis and Machine Intelligence*, 29(3):449–462, 2007.
- [14] A. Bailly. Los Angeles 1992: Chronique d’Émeutes Annoncées. *Mappemonde*, 2:48–49, 1993.
- [15] S. Balley, B. Baella, S. Christophe, M. Pla, N. Regnauld, and J. Stoter. Map specifications and user requirements. In *Abstracting Geographic Information in a Data Rich World. Methodologies and Applications of Map Generalisation*. Springer, 2014.
- [16] T. Barkowsky, L. J. Latecki, and K.-F. Richter. Schematizing maps: Simplification of geographic shape by discrete curve evolution. In *Spatial Cognition II - Integrating abstract theories, empirical studies, formal models, and practical applications*. Springer, 2000.
- [17] M. Barrault. A methodology for placement and evaluation of area map labels. *Computers, Environment and Urban Systems*, 25(1):33–52, 2001.
- [18] M. Barrault and F. Lecordix. An automated system for linear feature name placement which complies with cartographic quality criteria. In *Proc. AutoCarto 12*, 1995.
- [19] L. Barth. *Das Merkbild im Erdkundeunterricht*. Volk und Wissen, 1960.
- [20] L. Barth and A. Brucker. *Merkbilder im Geographienterricht*. Volk und Wissen, 1991.
- [21] C. Batardy. La berry antique -de la carte au modèle-chorème. *Revue Archéologique du Centre de la France*, 43:253–258, 2004.
- [22] G. D. Battista, P. Eades, R. Tamassia, and I. G. Tollis. Algorithms for drawing graphs: An annotated bibliography. *Computational Geometry: Theory and Applications*, 4 (5):235–282, 1994.
- [23] M. Beard. Constraints on rule formation. In *Map Generalization: Making Rules for Knowledge Representation*. Longman, 1991.
- [24] K. Been, E. Daiches, and C. Yap. Dynamic map labeling. *Visualization and Computer Graphics, IEEE Transactions on*, 12(5):773–780, 2006.

- [25] G. B. Benko and U. Strohmayer. A view on contemporary french human geography. *GeoJournal*, 31(3):227–238, November 1993.
- [26] A. Beristain, M. Graña, and A. Gonzalez. A pruning algorithm for stable voronoi skeletons. *Journal of Mathematical Imaging and Vision*, 42(2-3):225–237, 2012.
- [27] A. M. Berlyant. *Kartograficeskij metod issledovanija (Cartographic Methodology of Investigation)*. Moskva Univers., 1978.
- [28] J. Bertin. *Graphische Semiologie. Diagramme, Netze, Karten*. Gruyter, 1973.
- [29] Å. Björck. Numerical methods in matrix computations. *Texts in Applied Mathematics*, 2015.
- [30] H. Blum. A transformation for extracting new descriptors of shape. *Models for the perception of speech and visual form*, 19(5):362–380, 1967.
- [31] J. Bollmann and W. G. Koch, editors. *Lexikon der Kartographie und Geomatik: Vol. 1*. Spektrum Akademischer Verlag, 2001.
- [32] J. Bollmann and W. G. Koch, editors. *Lexikon der Kartographie und Geomatik: 2 Bände*. Spektrum Akademischer Verlag, 2002.
- [33] J. Bollmann and W. G. Koch, editors. *Lexikon der Kartographie und Geomatik: Vol. 2*. Spektrum Akademischer Verlag, 2002.
- [34] S. Bourgarel. Espaces de sant et structures spatiales en guyane. *MappeMonde*, 94, 2:46–47, 1994.
- [35] K. Brassel and R. Weibel. A review and conceptual framework of automated map generalization. *International Journal of Geographical Information Systems*, 2:229–244, 1988.
- [36] C. Brewer. *Designing better Maps: A Guide for GIS users*. Environmental Systems Research, 2005.
- [37] C. Brewer and B. Battenfield. Mastering map scale: balancing workloads using display and geometry change in multi-scale mapping. *Geoinformatica*, 14:221–239, 2010.
- [38] G. Brodal and R. Jacob. Dynamic planar convex hull. In *Proc. 43rd Annual IEEE Symposium on Foundations of Computer Science*, 2002.
- [39] M. Bruneau and L. Marcotte. Les États de l’asie du sud-est continentale. persistance du modèle en aur éoles concentriques. *MappeMonde*, 1:4–8, 1991.
- [40] R. Brunet. *Les Phénomènes de Discontinuité en Géographie = Dresch, J (ed.) Mémoires er Documents Vol. 7*. CNRS, 1967.

- [41] R. Brunet. Spatial systems and structures. a model and a case study. *Geoforum*, 6:95–103, 1975.
- [42] R. Brunet. La composition des modèles dans l’analyse spatiale. *L’Espace Géographique*, 8, 4:253–265, 1980.
- [43] R. Brunet. *La carte : mode d’emploi*. Fayard-Reclus, February 1987.
- [44] R. Brunet. Building models for spatial analysis. *L’Espace Géographique*, 1(1):109–123, 1993.
- [45] R. Brunet. Mémoire et identité: La géographie au baccalauréat, et auparavant. *MappeMonde*, 56:15–18, 1999.
- [46] R. Brunet. *Le Déchiffrement Du Monde. Théorie et pratique de la géographie*. Belin, Paris, 2001.
- [47] R. Brunet. Models in geography? A sense to research. *Cybergeo: European Journal of Geography*, page DOI : 10.4000/cybergeo.4288, 2001.
- [48] R. Brunet. Lignes de force de l’espace européen. *MappeMonde*, 02:14–19, 2002.
- [49] R. Brunet. D’une erreur commune à propos de cartes et de modèles, commentaire sur l’article de Patrick Poncet Quel fond de carte pour l’Australie. *M@ppemonde*, 2, 2004.
- [50] R. Brunet. *Le développement des territoires : formes, lois, aménagement*. Editions de l’Aube, June 2005.
- [51] R. Brunet and J.-C. Boyer. *Les villes européennes: rapport pour la Datar, Délégation à l’aménagement du territoire et à l’action régionale*. La documentation française, 1989.
- [52] R. Brunet and O. Dollfus. *Mondes nouveaux*, volume 1 of *Géographie Universelle*. Hachette-Reclus, 1990.
- [53] A. S. Bryk and S. W. Raudenbush. Heterogeneity of variance in experimental studies: A challenge to conventional interpretations. *Psychological Bulletin*, 104:386–404, 1988.
- [54] H. Bucher and C. Schlömer. Die neue Raumordnungsprognose des BBR. *Raumforschung und Raumordnung*, 64 (3):206–212, 2006.
- [55] K. Buchin, W. Meulemans, and B. Speckmann. A new method for subdivision simplification with applications to urban-area generalization. In *Proceedings of the 19th ACM SIGSPATIAL GIS*, pages 261–270, 2011.

- [56] M. Buchin, A. Driemel, M. van Kreveld, and V. Sacristán. An algorithmic framework for segmenting trajectories based on spatio-temporal criteria. In *Proceedings of the 18th SIGSPATIAL International Conference on Advances in Geographic Information Systems*, pages 202–211. ACM, 2010.
- [57] Bundesanstalt für Bodenforschung. Bodenkarte der Bundesrepublik Deutschland 1:1000000. map, 1963.
- [58] W. Bunge. *Theoretical Geography. Second revised and enlarged edition*. Gleerup, Lund, 1966.
- [59] D. Burghardt, C. Duchêne, and W. Mackaness, editors. *Abstracting Geographic Information in a Data Rich World - Methodologies and Applications of Map Generalisation*. Springer, 2014.
- [60] D. Burghardt, C. Duchêne, and W. Mackaness. Major achievements and research challenges in generalisation. In *Abstracting Geographic Information in a Data Rich Worlds. Methodologies and Applications of Map Generalisation*. Springer, 2014.
- [61] J. E. Burt and G. M. Barber. *Elementary Statistics for Geographers, second edition*. Guilford, 1996.
- [62] B. Battenfield and R. McMaster, editors. *Map Generalization - Making Rules for knowledge Representation*. Longman, 1991.
- [63] S. J. Butzler, C. A. Brewer, and W. J. Stroh. Establishing classification and hierarchy in populated place labeling for multiscale mapping for the national map. *Cartography and Geographic Information Science*, 38(2):100–109, 2011.
- [64] L. Carstensen. A comparison of simple mathematical approaches to the placement of spot symbols. *Cartographica*, 24(3):46–63, 1987.
- [65] O. Chaudhry and W. A. Mackaness. Automatic identification of urban settlement boundaries for multiple representation databases. *Computers, environment and urban systems*, 32(2):95–109, 2008.
- [66] J.-P. Cheylan, J.-P. Deffontaines, S. Lardon, and H. Théry. Les chorèmes: un outil pour l'étude de l'activité agricole dans l'espace rural? *MappeMonde*, 4/90:2–4, 1990.
- [67] D. Chiara, V. Del Fatto, R. Laurini, M. Sebillio, and G. Vitiello. A choreme-based approach for visually analyzing spatial data. *Journal of Visual Languages and Computing*, doi:10.1016/j.jvlc.2011.02.001, 2011.
- [68] F. Chirié. Automated name placement with high cartographic quality: City street maps. *Cartography and Geographic Information Science*, 27(2):101–110, 2000.
- [69] J. Christensen, J. Marks, and S. Shieber. An empirical study of algorithms for point-feature label placement. *Transactions on Graphics*, 14:203–232, 1995.

- [70] P. Claval. Hérodote and the french left. In *Geopolitical Traditions: A century of geopolitical thought*. Routledge, 2000.
- [71] H. Clout. Book review articles: Vive la géographie! Vive la géographie française! *Prog Hum Geogr*, 16(3):423–428, September 1992.
- [72] A. Cook and C. Jones. A prolog rule-based system for cartographic name placement. *Computer Graphics Forum*, 9(2):109–126, 1990.
- [73] M. de Berg, O. Cheong, M. van Kreveld, and M. Overmars. *Computational Geometry: Algorithms and Applications*. Springer, 3rd edition, 2008.
- [74] M. de Berg, M. van Kreveld, and S. Schirra. A new approach to subdivision simplification. In *Proceedings of the 12th International Symposium on Computer-Assisted Cartography*, volume 4, pages 79–88, 1995.
- [75] M. de Berg, M. van Kreveld, and S. Schirra. Topologically correct subdivision simplification using the bandwidth criterion. *Cartography and Geographic Information Systems*, 25(4):243–257, 1998.
- [76] P. De Casteljaou. Outillages méthodes calcul. Technical report, A. Citroën, 1959.
- [77] R. de Maximy. Chorème et chorématique. In *La Cartographie en débat: Représenter ou convaincre*. Karthala, Paris, 1995.
- [78] B. De Mente. *Elements of Japanese design*. Tuttle Publishing, 2006.
- [79] J. E. De Muth. *Basic Statistics and Pharmaceutical Statistical Applications, Second Edition*. CRC Press, 2006.
- [80] V. del Fatto. *Visual Summaries of Geographic Databases by Chorems*. Thèse de doctorat en informatique, INSA de Lyon, Apr. 2009. Co-tutelle avec Université di Salerno, Italie.
- [81] T. Dey. Improved bounds for planar k-sets and related problems. *Discrete Computational Geometry*, 19(3):373–382, 1998.
- [82] C. Didelon. Modernisation du chemin de fer indien: Entre intégration et accroissement des disparités régionales. *MappeMonde*, 62:22–25, 2001.
- [83] G. Djament-Tran and C. Grataloup. E pluribus urbibus una: Modéliser les trajectoires de villes. *M@ppemonde*, 2010.
- [84] J. Doerschler and H. Freeman. A rule-based system for dense-map name placement. *Communications of the Association of Computing Machinery*, 35(1):68–79, 1992.
- [85] J. Döllner. Non-photorealistic 3d geovisualization. In *Multimedia Cartography*, pages 229–240. Springer, 2007.

- [86] D. Dörschlag, I. Petzold, and L. Plümer. Placing objects automatically in areas of maps. In *Proc. The 23rd Internat. Cartographic Conf. (ICC'03)*, 2003.
- [87] D. Douglas and T. Peucker. Algorithms for the reduction of the number of points required to represent a digitized line or its caricature. *Cartographica*, 10(2):112–122, 1973.
- [88] D. L. Dow. *The Effects of Symbol Iconicity on the Integration of Spatial Knowledge Acquired from the Fly-through Navigation of Simulated Environments*. PhD thesis, University of California, Santa Barbara, 2001.
- [89] R. Drysdale, G. Rote, and A. Sturm. Approximation of an open polygonal curve with a minimum number of circular arcs and biarcs. *Computational Geometry: Theory and Applications*, 41(1-2):31–47, 2008.
- [90] S. Dühr. *The visual language of spatial planning : exploring cartographic representations for spatial planning in Europe*. Routledge, Abingdon, UK, 2007.
- [91] C. A. Duncan, D. Eppstein, M. T. Goodrich, S. G. Kobourov, and M. Löffler. Planar and poly-arc lombardi drawings. In *Graph Drawing*, pages 308–319. Springer, 2012.
- [92] C. A. Duncan, D. Eppstein, M. T. Goodrich, S. G. Kobourov, and M. Nöllenburg. Lombardi drawings of graphs. In *Graph Drawing*, pages 195–207. Springer, 2011.
- [93] D. Duthel and G. Puel. Gèographie, l'Èpreuve du bac est-elle nulle? *MappeMonde*, 56:5–9, 1999.
- [94] G. Dutton. Scale, sinuosity, and point selection in digital line generalization. *Cartography and Geographic Information Science*, 26(1):33–54, 1999.
- [95] D. Ebner, G. W. Klau, and R. Weiskircher. Force-based label number maximization. *Vienna, Austria: Vienna University of Technology*, 2003.
- [96] H. Edelsbrunner and E. Welzl. Constructing belts in two-dimensional arrangements with applications. *SIAM Journal on Computing*, 15(1):271–284, 1986.
- [97] S. Edmondson, J. Christensen, J. Marks, and S. Shieber. A general cartographic labeling algorithm. *Cartographica*, 33(4):13–23, 1996.
- [98] D. Eppstein. Planar lombardi drawings for subcubic graphs. In *Graph Drawing*, pages 126–137. Springer, 2013.
- [99] D. Eriksson. A Principal Exposition of Jean-Louis Le Moignes Systemic Theory. *Cybernetics & Human Knowing*, 4, No. 2-3, 1997.
- [100] European Soil Bureau Network, editor. *Soil Atlas of Europe*. European Commission, 2005.

- [101] D. Fahland and H. Woith. Towards process models for disaster response. In *Business Process Management Workshops*, pages 254–265. Springer, 2009.
- [102] D. Fairbairn. Measuring map complexity. *The Cartographic Journal*, 43:224–238, 2006.
- [103] A. Faludi. Territorial cohesion: Old (french) wine in new bottles? *Urban Studies*, 41, 7:1349–1365, 2004.
- [104] R. Ferras. *Atlas Reclus: España/Espagne/Spain*. Fayard/RECLUS, 1986.
- [105] J.-F. Ferrè. Cambodge: alèas historiques et dynamiques spatiales. *MappeMonde*, 94, 1:10–14, 1994.
- [106] T. Foerster. *Web-based Architecture for On-demand Maps -Integrating Meaningful Generalization Processing*. PhD thesis, University of Twente, Faculty of ITC, 2010.
- [107] T. for London. London underground, January 2015.
- [108] M. Formann and F. Wagner. A packing problem with applications to lettering of maps. In *Proceedings of the 7th Annual Symposium on Computational Geometry*, 1991.
- [109] H. Freeman. Computer name placement. In *Geographical Information Systems: Principles and Applications*. Longman, 1991.
- [110] H. Freeman and J. Ahn. On the problem of placing names in a geographic map. *International Journal of Pattern Recognition and Artificial Intelligence*, 1(1):121–140, 1987.
- [111] U. Freitag. *Kartographische Konzeptionen - Cartographic Conceptions*, chapter Die Eigenschaften der Kartographischen Darstellungsformen, pages 115–132. Freie Universität Berlin, 1992.
- [112] T. Freksa, C; Barkowsky and R. Moratz. Schematic maps for robot navigation. In *Spatial cognition II Integrating abstract theories, empirical studies, formal methods and practical applications*, 2000.
- [113] M. Galanda. *Automated Polygon Generalization in a Multi Agent System*. PhD thesis, University of Switzerland, 2003.
- [114] C. Gaudin. La roumanie au crible. *MappeMonde*, 3:42–43, 2001.
- [115] P. Gentelle. *Chine, un atlas économique*. Fayard-RECLUS, 1987.
- [116] B. Giblin-Delvallet. Les effets de discours du grand chorémateur et leurs conséquences politiques. *Hrodote*, 76:22–38, 1995.

- [117] GIP-RECLUS. Mappemonde website. http://www.mgm.fr/english/Mappre_eng.html, 2004. last accessed 24th February 2014.
- [118] GIP-RECLUS. RECLUS shareware website. <http://www.mgm.fr/Shareware.html>, 2004. last accessed 24th February 2014.
- [119] M. Goetz, J. Lauer, and A. Auer. An algorithm based methodology for the creation of a regularly updated global online map derived from volunteered geographic information. In *The Fourth International Conference on Advanced Geographic Information Systems, Applications and Services. GEOProcessing 2012. Valencia, Spain.*, 2012.
- [120] A. H. Goldman. Aesthetic qualities and aesthetic value. *The Journal of Philosophy*, 87(1):pp. 23–37, 1990.
- [121] M. F. Goodchild. Theoretical Geography (1962): William Bunge. In *P. Hubbard, R. Kitchin, and G. Valentine, editors, Key Texts in Human Geography. Los Angeles: SAGE*, pages 9–16, 2008.
- [122] N. Gould and O. Chaudhry. An ontological approach to on-demand mapping. In *In Proceedings of 15th ICA Generalisation Workshop*, 2012.
- [123] P. Gould. *Mental Maps*. Routledge, 2 edition, May 1986.
- [124] P. Grenier. Structures et organisation de l’espace argentin. *MappeMonde*, 88,4:36–40, 1988.
- [125] P. Haggett. *Geography: A Global Synthesis*. Prentice Hall, 4th edition, April 2001.
- [126] G. Hake, D. Grünreich, and L. Meng. *Kartographie Visualisierung raum-zeitlicher Informationen*. Walter de Gruyter, Berlin, New York, 2002.
- [127] D. Hänsgen. Chorematistische kartensprache zwischen franzsischem geodesign und deutscher geopolitik – ein leseversuch. In *Kampf der Karten. Propaganda- und Geschichtskarten als politische Instrumente und Identittstexte*. Herder Institut, 2012.
- [128] M. Haralick and L. Shapiro. Image segmentation techniques. In *Computer Vision Graphics and Image Processing* 29, 1985.
- [129] J. Harding, B. South, M. Freeman, S. Zhou, and A. Babington. Identifying built-up areas for 2011 census outputs. In *Proceedings of the 26th International Cartographic Conference, Dresden.*, 2013.
- [130] J. B. Harley and D. Woodward, editors. *The History of Cartography, Volume 1: Cartography in Prehistoric, Ancient and Medieval Europe and the Mediterranean*. 1987.

- [131] L. Harrie and H. Stigmar. An evaluation of measures for quantifying complexity of a map. In *International Archives of Photogrammetry, Remote Sensing and Spatial Information Sciences Volume XXXVI 4/W45 covering contributions of the Joint Workshop "Visualization and Exploration of Geospatial Data" June 27-29, 2007, Stuttgart, 2007*.
- [132] L. Harrie and H. Stigmar. An evaluation of measures for quantifying map information. *ISPRS Journal of Photogrammetry and Remote Sensing*, 65:266–274, 2010.
- [133] L. Harrie and R. Weibel. Modelling the overall process of generalisation. In *Generalisation of geographic information: Cartographic modelling and applications*. Elsevier Science, 2007.
- [134] T. Hartog and C. de Vasoigne. Les tourisimes dans les départements français d'amérique. *MappeMonde*, 2:21–25, 1999.
- [135] J.-H. Haunert and L. Sering. Drawing road networks with focus regions. *IEEE Transactions on Visualization and Computer Graphics*, 17, 12:2555–2562, 2011.
- [136] M. Heimlich and M. Held. Biarc approximation, simplification and smoothing of polygonal curves by means of Voronoi-based tolerance bands. *International Journal of Computational Geometry and Applications*, 18(3):221–250, 2008.
- [137] M. Hemmer, W. Meulemans, L. Nachmanson, H. Purchase, A. Reimer, M. Roberts, G. Rote, and K. Xu. Automated evaluation of metro map usability. Technical report, Report from Dagstuhl Seminar 13151 Drawing Graphs and Maps with Curves, 2013.
- [138] L. W. Hepple. Géopolitiques de Gauche: Yves Lacoste, Hérodote and French radical geopolitics. In *Geopolitical Traditions: A century of geopolitical thought*. Routledge, 2000.
- [139] A. Hertzog. Musées, espace et identité territoriale en picardie. *MappeMonde*, 66(2):25–28, 2002.
- [140] S. A. Hirsch. An algorithm for automatic name placement around point data. *American Cartographer*, 9 (1):5–17, 1982.
- [141] F. Hong, Z. Zuxun, and D. Daosheng. Quality evaluation model for map labeling. *Geo-Spatial Information Science*, 8(1):72–78, 2005.
- [142] J. Hopcroft and R. Tarjan. Efficient planarity testing. *J. ACM*, 21(4):549–568, Oct. 1974.
- [143] M. Hudon. La Maitrise de L'Espace en Cisjordanie Occupée. *MappeMonde*, 4:43–48, 1991.
- [144] G. Huswit. Helvetica. a documentary about typography, graphic design, and global visual culture. Movie, 09 2007.

- [145] H. Imai and M. Iri. Computational-geometric methods for polygonal approximations of a curve. *Computer Vision, Graphics and Image Processing*, 36(1):31–41, 1986.
- [146] H. Imai and M. Iri. Polygonal approximations of a curve – formulations and algorithms. In G. Toussaint, editor, *Computational Morphology*, pages 71–86. 1988.
- [147] E. Imhof. *Kartographische Geländedarstellung*. Walter de Gruyter, 1965.
- [148] E. Imhof. *Thematische Kartographie*. Walter de Gruyter, 1972.
- [149] E. Imhof. Positioning names on maps. *The American Cartographer*, 2:128–144, 1975.
- [150] E. Imhof. *Schweizerischer Mittelschulatlas, Siebzehnte Auflage*. Lehrmittelverlag des Kantons Zürich, 1976.
- [151] E. Imhof. *Cartographic relief presentation*. ESRI, Inc., 2007.
- [152] M. Jacomy. *I want hue*. Colors for data scientists. web-tool, 2015.
- [153] A. Jain, M. Murty, and P. Flynn. Data clustering: review. *Journal ACM Computing Surveys*, 31(3):264–323, 1999.
- [154] G. F. Jenks. Thoughts on line generalization. In *AutoCarto. American Congress on Surveying and Mapping*, 1979.
- [155] B. Jenny and L. Hurni. Swiss-style colour relief shading modulated by elevation and by exposure to illumination. *Cartographic Journal*, 43(3):198–207, 2006.
- [156] K. S. Johannessen. Rule following and tacit knowledge. *AI & Society*, 2:287–301, 1988.
- [157] C. Jones. Cartographic name placement with prolog. *IEEE Computer Graphics and Applications*, 9(5):34–47, 1989.
- [158] A. Jurio, H. Bustince, M. Pagola, P. Couto, and W. Pedrycz. New measures of homogeneity for image processing: an application to fingerprint segmentation. In *Soft Computing*. Springer, 2013.
- [159] K. G. Kakoulis and I. G. Tollis. A unified approach to automatic label placement. *International Journal of Computational Geometry and Applications*, 13 (1):23–59, 2003.
- [160] T. Kato and H. Imai. The NP-completeness of the Character Placement Problem of 2 or 3 Degrees of Freedom. In *Record of Joint Conference of Electrical and Electronic Engineers in Kyushu*, 1988.
- [161] S. Keller. Artificial intelligence techniques applied to generalization. In *GIS and Generalization. Methodology and Practice*. Taylor & Francis, 1995.

- [162] S. Kirkpatrick. Optimization by simulated annealing: Quantitative studies. *Journal of Statistical Physics*, 34(5):975–986, 1984.
- [163] R. Kitchin and M. Blades. *The Cognition of Geographic Space (International Library of Human Geography)*. I B Tauris & Co Ltd, February 2002.
- [164] G. W. Klau and P. Mutzel. Optimal labeling of point features in rectangular labeling models. *Mathematical Programming*, 94(2-3):435–458, 2003.
- [165] A. Klippel, K.-F. Richter, T. Barkowsky, and C. Freksa. *Map-Based Mobile Services - Theories, Methods and Implementations*, chapter The Cognitive Reality of Schematic Maps, pages 57–74. Springer, 2005.
- [166] M. J. Kraak and F. Ormeling. *Cartography: Visualization of Spatial Data, Second Edition*. Addison Wesley Longman, subsequent edition, 2003.
- [167] Y. Lacoste. *Geographie und politisches Handeln*. Verlag Klaus Wagenbach, 1990.
- [168] Y. Lacoste. Chormatique et gopolitique. *Hrodote*, 69/70:224–259, 1993.
- [169] Y. Lacoste. Les géographes, la science et l’illusion. *Hérodote*, 76:3–21, 1995.
- [170] Y. Lacoste. Es lebe die nation! wozu? In *Geopolitik: zur Ideologiekritik politischer Raumkonzepte*. Promedia, Wien, 2001.
- [171] P. Laube, M. de Berg, and M. van Kreveld. Spatial support and spatial confidence for spatial association rules. In *Headway in Spatial Data Handling Lecture Notes in Geoinformation and Cartography*, 2008.
- [172] F. Lecordix, C. Plazanet, and J.-P. Lagrange. A platform for research in generalization: Application to caricature. *Geoinformatica*, 1:161–182, August 1997.
- [173] S. Lee, M. Sips, and H.-P. Seidel. Perceptually driven visibility optimization for categorical data visualization. *IEEE Transactions on Visualization and Computer Graphics*, 19(10):1746–1757, 2013.
- [174] S. Leutenegger, J. Edgington, and M. Lopez. STR: A simple and efficient algorithm for R-tree packing. Technical report, NASA Langley Research Center, 1997.
- [175] S. Leyk and R. Boesch. Colors of the past: color image segmentation in historical topographic maps based on homogeneity. *Geoinformatica*, 14(1):1–21, 2010.
- [176] Z. Li. Digital map generalization at the age of enlightenment: a review of the first forty years. *Cartographic Journal, The*, 44(1):80–93, February 2007.
- [177] Z. Li and S. Openshaw. A natural principle for the objective generalization of digital maps. *Cartography and Geographic Information Science*, 20:19–29, 1993.
- [178] A. Lipietz. Avoiding megapolization: The battle of Île-de-france. *European Planning Studies*, 3,2:143–154, 1995.

- [179] P. Lüscher and R. Weibel. Exploiting empirical knowledge for automatic delineation of city centres from large-scale topographic databases. *Computers, Environment and Urban Systems*, 37:18–34, 2013.
- [180] A. S. L. T. Mackaness, William A Ruas, editor. *Generalisation of Geographic Information: Cartographic Modelling and Applications (International Cartographic Association)*. Elsevier Science, 1st e edition, April 2007.
- [181] W. Mackaness. Automated cartography in a bush of ghosts. *Cartography and Geographic Information Science*, 33(4):245–256, October 2006.
- [182] W. Mackaness and A. Reimer. Generalisation in the context of schematised maps. In *Abstracting Geographic Information in a Data Rich World. Methodologies and Applications of Map Generalisation*. Springer, 2014.
- [183] W. Mackaness, A. Ruas, and T. Sarjakoski. Observations and research challenges in map generalisation and multiple representation. In *Generalisation of Geographic Information: Cartographic Modelling and Application*. Elsevier, 2007.
- [184] D. Macrini, S. Dickinson, D. Fleet, and K. Siddiqi. Object categorization using bone graphs. *Computer Vision and Image Understanding*, 115(8):1187–1206, 2011.
- [185] R. Marconis. Ambiguités et dérives de la chorématique. *Hérodote*, 76:110–132, 1995.
- [186] D. M. Mark. Competition for map space as paradigm for automated map design. *GIS/LIS Proceedings 90, Anaheim, California, November 7-10*, 1:97–105, 1990.
- [187] D. M. Mark and F. Csillag. The nature of boundaries on 'area-class' maps. *Cartographica*, 26(1):65–77, 1989.
- [188] J. Marks and S. Shieber. The computational complexity of cartographic label placement. Technical report, Harvard university, Cambridge, 1991.
- [189] A. Masood and S. Ejaz. An efficient algorithm for robust curve fitting using cubic Bezier curves. In *Advanced Intelligent Computing Theories and Applications*, LNCS 6216, pages 255–262, 2010.
- [190] A. Melkman. On-line construction of the convex hull of a simple polyline. *Information Processing Letters*, 25(1):11–12, 1987.
- [191] G. Menschick and C. Sitte. La géographie française - nachhilfe für Österreich? einige bemerkungen zu einer neuen generation französischer geographieschulbücher (insbesondere für die 'terminale' dem vorbereitungsjahr für die matura/bac). *GW-Unterricht*, 65:45–58, 1997.
- [192] W. Meulemans. *Similarity Measures and Algorithms for Cartographic Schematization*. PhD thesis, Technical University Eindhoven, 2014.

- [193] W. Meulemans, A. van Renssen, and B. Speckmann. Area-preserving subdivision schematization. In *Geographic Information Science, 6th International Conference, GIScience 2010, Zurich, Switzerland, September 2010 Proceedings*, 2010.
- [194] E. Meyer. Type de contact village-plantation À sri lanka (1840-1940). *Mappe-Monde*, 4:33–37, 1992.
- [195] E. Meynen, editor. *Multilingual Dictionary of Technical Terms in Cartography*. Franz Steiner Verlag for the International Cartographic Association, 1973.
- [196] X. Mi, D. DeCarlo, and M. Stone. Abstraction of 2D shapes in terms of parts. In *Proceedings of the 7th International Symposium on Non-Photorealistic Animation and Rendering*, pages 15–24, 2009.
- [197] J. Mirloup. Approche de la région centre en neuf chorèmes. *Indicateurs de l'économie du Centre*, 21:3–11, 1998.
- [198] E. Mollard. La différenciation spatiale de l'Économie de plantation. *MappeMonde*, 2:45–47, 1993.
- [199] E. Mollard. Les dissymétries d'usages d'une delta. *MappeMonde*, 1:22–26, 2000.
- [200] M. S. Monmonier. *Computer-Assisted Cartography: Principles and Prospects*. Prentice, 1982.
- [201] K. Mote. Fast point-feature label placement for dynamic visualizations. *Information Visualization*, 6(4):249–260, 2007.
- [202] I. Muehlenhaus. The design and composition of persuasive maps. *Cartography and Geographic Information Science*, 40(5):401–414, 2013.
- [203] J. Neumann, editor. *Multilingual Dictionary of Technical Terms in Cartography*. Saur, 1994.
- [204] O. Neurath. *Gesellschaft und Wirtschaft. Bildstatistisches Elementarwerk*. Bibliographisches Institut Leipzig, 1931.
- [205] M. Nöllenburg. A survey on automated metro map layout methods. 2014.
- [206] S. Nundy, B. Lotto, D. Coppola, A. Shimpi, and D. Purves. Why are angles misperceived? *PNAS*, 97:5592–5597, 2000.
- [207] R. Ogniewicz and O. Kübler. Hierarchic voronoi skeletons. *Pattern recognition*, 28(3):343–359, 1995.
- [208] R. Ogrissek, editor. *Brockhaus abc Kartenkunde*. VEB F.A. Brockhaus Verlag, Leipzig, 1983.
- [209] R. Ogrissek. *Theoretische Kartographie. Eine Einführung*. VEB Hermann Haack, Gotha, 1987.

- [210] F. Ormeling. Brunet and the revival of french geography and cartography. *The Cartographic Journal*, pages 20–24, 1992.
- [211] S. Pal and N. Pal. Segmentation using contrast and homogeneity measures. *Pattern Recognition Letters*, 5(4):293–304, 1987.
- [212] D. Peters and K. Richter. Taking off to the third dimension -schematization of virtual environments-. *International Journal of SPatial Data Infrastructure Research*, 3:20–37, 2008.
- [213] R. Phillips and L. Noyes. An investigation of visual clutter in the topographic base of a geological map. *Cartographic Journal*, 19(2):122–132, 1982.
- [214] P. Picasso and S. Galassi. *Picasso's One-Liners*. Artisan, 1997.
- [215] I. Pinto and H. Freeman. The feedback approach to cartographic areal text placement. In *Advances in Structural and Syntactical Pattern Recognition, Lecture Notes in Computer Science 1121*. Springer, 1996.
- [216] P. Poncet. Quel fond de carte pour l'australie? *M@ppemonde*, 2, 2004.
- [217] H. C. Purchase, J. Hamer, M. Nöllenburg, and S. G. Kobourov. On the usability of lombardi graph drawings. In *Graph Drawing*, pages 451–462. Springer, 2013.
- [218] D. Purves and B. Lotto. *Why We See What We Do Redux: A Wholly Empirical Theory of Vision*. Sinauer Associates, Inc., 2010.
- [219] P. Ramsay. (Much) Faster Unions in PostGIS 1.4. blog, January 2009. post by PostGIS developer.
- [220] P. Raposo. Piece by piece: A method of cartographic line generalization using regular hexagonal tessellation. In *AutoCarto 2010 Fall Conference Proceedings*, 2010.
- [221] W.-D. Rase and M. Sinz. Kartographische Visualisierung von Planungskonzepten. *Kartographische Nachrichten*, 43:139–145, 1993.
- [222] N. Regnauld and R. B. McMaster. A synoptic view of generalisation operators. In *Generalisation of Geographic Information: Cartographic Modelling and Applications*. Elsevier, 2007.
- [223] A. Reimer. Understanding chorematic diagrams: Towards a taxonomy. *The Cartographic Journal*, 47:330–350, 2010.
- [224] A. Reimer. Squaring the Circle? Bivariate Colour Maps and Jacques Bertins Concept of Disassociation. In *International Cartographic Conference*, pages 3–8, 2011.

- [225] A. Reimer and C. Kempf. Efficient derivation and caricature of urban settlement boundaries for 1:250k. In *17th ICA Workshop on Generalisation and Multiple Representation, Vienna, Austria, 23rd September 2014*, 2014.
- [226] A. Reimer and W. Mackaness. Taxonomy validation for chorematic diagrams. *under review*, NN:NN, 2015.
- [227] A. Reimer and W. Meulemans. Parallelity in chorematic territorial outlines. In *14th ICA Workshop on Generalisation and Multiple Representation, Paris, France*, 2011.
- [228] A. Reimer, P. Neis, M. Rylov, S. Schellhorn, G. Sagl, B. Resch, J. Porto, and A. Zipf. Erfahrungsbericht: Crisis mapping zum taifun hayán. In *Proceedings Geoinformatik 2014*, 2014.
- [229] A. Reimer, M. Rylov, C. Kempf, and P. Neis. Assigning Scale Equivalencies to OpenStreetMap Polygons. In *AutoCarto, International Symposium on Automated Cartography 2014, Proceedings*, 2014.
- [230] A. Reimer, A. van Goethem, M. Rylov, M. van Kreveld, and B. Speckmann. A formal approach to the automated labelling of groups of features. *CCartography and Geographic Information Science (accepted)*, 2015.
- [231] A. Reimer and C. Volk. An approach for using cubic bézier curves for schematizations of categorical maps. *Geographic Information on Demand 15th Workshop of the ICA commission on Generalisation and Multiple Representation, Zürich, 12-13 September 2010*, 2012.
- [232] A. Reimer and R. Westerholt. Schematization for the analysis of geolocated microblog messages. In *AutoCarto, International Symposium on Automated Cartography 2014, Proceedings*, 2014.
- [233] B. Resch, F. Hillen, A. Reimer, and W. Spitzer. Towards 4d cartography-four-dimensional dynamic maps for understanding spatio-temporal correlations in lightning events. *The Cartographic Journal*, 50(3):266–275, 2013.
- [234] P. Revell, N. Regnault, and G. Bulbrooke. Ordnance Survey VectorMap District: Automated Generalisation, Text Placement and Conflation in Support of making Public Data Public. *International Cartographic Conference ICC 2011, Paris.*, 2011.
- [235] V. Rey, O. Groza, I. Ianoş, and M. Patroescu. *Atlas de la Roumanie*. Montpellier-Paris, 2000.
- [236] M. J. Roberts. *Underground Maps Unravelling*. 2012.
- [237] A. Ruas and J.-P. Lagrange. Data and knowledge modelling for generalization. In *GIS and Generalization. Methodology and Practice*. Taylor & Francis, 1995.

- [238] M. Rylov and A. Reimer. A comprehensive multi-criteria model for high cartographic quality point-feature label placement. *Cartographica: The International Journal for Geographic Information and Geovisualization*, 49(1):52–68, 2014.
- [239] M. Rylov and A. Reimer. Improving label placement quality by considering basemap detail with a raster-based approach. *Geoinformatica*, pages DOI:10.1007/s10707-014-0214-6, 2014.
- [240] M. Rylov and A. Reimer. A practical algorithm for the external annotation of area features. *The Cartographic Journal*, page DOI: 10.1179/1743277414Y.0000000091, 2014.
- [241] M. Rylov and A. Reimer. An efficient algorithm for pairwise line labeling of geographic boundaries. *Cartographic Perspectives*, pages (tba, accepted), 2015.
- [242] A. Saalfeld. Area-preserving piecwise affine mappings. In *Proceedings of the 17th annual symposium on computational geometry SCG 01*, 2001.
- [243] I. Sacareau. Mise en tourisme et dynamique spatiale au népal. *MappeMonde*, 2:12–16, 2000.
- [244] L. T. Sarjakoski. Conceptual models of generalisation and multiple representation. In *Generalisation of geographic information: Cartographic modelling and applications*. Elsevier Science, 2007.
- [245] W. Scharfe. The development of consciousness in cartography of mass media maps. In *International Conference on Mass Media Maps. Approaches, Results, Societal Impact, Berlin June 19-21, 1997 - Proceedings -*, 1997.
- [246] V. Schmidt-Seiwert, L. Porsche, and P. Schön, editors. *ESPON ATLAS Mapping the structure of the European territory*. Federal Office for Building and Regional Planning, 2006.
- [247] P. Schneider. An algorithm for automatically fitting digitized curves. In *Graphic Gems*, pages 612–626. Academic Press Professional, 1990.
- [248] C.-D. Schönwiese. *Praktische Statistik für Meteorologen und Geowissenschaftler*. Bontraeger, 2013.
- [249] M. Schreyer and G. Raidl. Letting ants labeling [sic] point features. In *Proc. IEEE Congress on Evolutionary Computation (CEC '02)*, 2002.
- [250] M. Sester. Generalization based on least squares adjustment. *International Archives of Photogrammetry and Remote Sensing*, 33(B4):931–938, 2000.
- [251] M. Sester and B. Elias. Relevance of generalisation to the extraction and communication of wayfinding information. In *Generalisation of geographic information: Cartographic modelling and applications*. Elsevier Science, 2007.

- [252] J. P. Shaffer. Multiple hypothesis testing. *Annual Review of Psychology*, 45:561–84, 1995.
- [253] D. Shaked and A. Bruckstein. Pruning medial axes. *Computer Vision and Image Understanding*, 69(2):156–169, 1998.
- [254] M. Shamos. *Computational Geometry*. PhD thesis, Dept. of Computer Science, Yale University, 1978.
- [255] C. E. Shannon and W. Weaver. *The Mathematical Theory of Communication*. The University of Illinois Press, 1964.
- [256] L. Shao and H. Zhou. Curve fitting with Bézier cubics. *Graphical Models and image processing*, 58:223–232, 1996.
- [257] L. Shapiro and G. Stockmann. *Computer Vision*, chapter Image segmentation, pages 279–325. Prentice-Hall, 2001.
- [258] W. Shen, X. Bai, R. Hu, H. Wang, and L. Latecki. Skeleton growing and pruning with bending potential ratio. *Pattern Recognition*, 44(2):196–209, 2011.
- [259] J. F. Shupe, editor. *National Geographic Atlas of the World, Revised Sixth Edition*. National Geographic Society, 1995.
- [260] M. Sivignon. Chorèmes: éléments pour un débat. *Hérodote*, 76:93–109, 1995.
- [261] T. Slocum, R. McMaster, F. Kessler, and H. Howard. *Thematic Cartography and Geovisualization, Second Edition*. Prentice Hall, 2009.
- [262] R. A. Smith. *Using Geospatial Metadata and Expert Systems for the Partial Automation of the Cartographic Design Process*. PhD thesis, University of Georgia, 2012.
- [263] E. Spiess. Eigenschaften von Kombinationen graphischer Variablen. *Grundsatzfragen der Kartographie*, pages 280–293, 1970.
- [264] S. Steiniger and R. Weibel. Relations and structures in categorical maps. In *8th ICA Workshop on generalisation and Multiple Representation, A Coruna (Spain), July 7-8th, 2005*, 2005.
- [265] S. Steiniger and R. Weibel. Relations among map objects in cartographic generalization. *Cartography and Geographic Information Science*, 34:175–197, 2007.
- [266] G. Stiens. *Prognostik in der Geographie*. Westermann, 1996.
- [267] M. Stone and T. DeRose. A geometric characterization of parametric cubic curves. *ACM Transactions on Graphics*, 8(3):147–163, 1989.

- [268] J. Stoter, D. Burghardt, C. Duchêne, B. Baella, N. Bakker, C. Blok, M. Pla, N. Regnauld, G. Touya, and S. Schmid. Methodology for evaluating automated map generalization in commercial software. *Computers, Environment and Urban Systems*, 33(5):311–324, 2009.
- [269] J. Stoter, M. Post, V. van Altena, R. Nijhuis, and B. Bruns. Fully automated generalization of a 1:50k map from 1:10k data. *Cartography and Geographic Information Science*, 41(1):1–13, 2014.
- [270] T. Strijk and M. van Kreveld. Practical extensions of point labeling in the slider model. *Geoinformatica*, 6(2):181–197, 2002.
- [271] G. Sun, Y. Liu, W. Wu, R. Liang, and H. Qu. Embedding temporal display into maps for occlusion-free visualization of spatio-temporal data. In *Pacific Visualization Symposium (PacificVis), 2014 IEEE*, pages 185–192, March 2014.
- [272] C. Taillard and V. tu Lâp. *Atlas du Viêt-Nam*. Reclus, 1994.
- [273] E. Taillard and S. Voss. Popmusic: Partial optimization metaheuristic under special intensification conditions. In *Essays and Surveys in Metaheuristics*. Springer, 2001.
- [274] P. Tainz. Chorème. *Lexikon der Kartographie und Geomatik*, 1, 2001.
- [275] S. Tak and A. Cockburn. Enhanced spatial stability with hilbert and moore tree-maps. *IEEE Transactions on Visualization and Computer Graphics*, 19(1):141–148, 2013.
- [276] A. C. Tamhane. Multiple comparison in model i one-way anova with unequal variances. *Communications in Statistics-Theory and Methods*, pages 15–32, 1977.
- [277] H. Théry. *Brazil. A chorematical atlas*. Fayard/RECLUS, 1986.
- [278] H. Théry. Chronochorèmes et paléochorèmes: la dimension temporelle dans la modélisation graphique. *Modèles Graphiques et Représentations Spatiales*, pages 41–63, 1990.
- [279] G. Thieme and H.-D. Laux. Soziale und ethnische Konflikte im Restrukturierungsprozess: Die Unruhen vom Frühjahr 1992 in Los Angeles. *Erdkunde*, 49:315–334, 1995.
- [280] I. Thomas, C. Cotteels, J. Jones, and D. Peeters. Revisiting the extension of the Brussels urban agglomeration: new methods, new data new results? *Belgeo. Revue belge de géographie*, 1-2(1-2), 2012.
- [281] F. Töpfer. *Kartographische Generalisierung*. VEB Hermann Haack, Gotha, 1974.
- [282] F. Töpfer and W. Pillewitzer. Das Auswahlgesetz, ein Mittel zur kartographischen Generalisierung. *Kartographische Nachrichten*, 14:117–121, 1964.

- [283] F. Töpfer and W. Pillewizer. The principles of selection. *Cartographic Journal, The*, 3(1):10–16, 1966.
- [284] A. Torun and A. Ulubay. Database driven cartographic visualization of vmap database. In *Proceedings of ISPRS 2004, Istanbul*, 2004.
- [285] G. Touya and A. Reimer. Inferring the Scale of OpenStreetMap Features. In *OpenStreetMap in GIScience: experiences, research, applications*. Springer, 2015.
- [286] N. Trinh and B. Kimia. Skeleton search: Category-specific object recognition and segmentation using a skeletal shape model. *International Journal of Computer Vision*, 94(2):215–240, 2011.
- [287] E. Tufte. *The visual display of quantitative information*. Graphics Press, 1983.
- [288] S. van Dijk, M. van Kreveld, T. Strijk, and A. Wolff. Towards an evaluation of quality for names placement methods. *International Journal of Geographical Information Science*, 16(7):641–661, 2002.
- [289] T. van Dijk, A. van Goethem, J.-H. Haunert, W. Meulemans, and B. Speckmann. Accentuating focus maps via partial schematization. In *Proceedings of the 21st ACM SIGSPATIAL International Conference on Advances in Geographic Information Systems*, pages 418–421. ACM, 2013.
- [290] T. C. van Dijk, A. van Goethem, J.-H. Haunert, W. Meulemans, and B. Speckmann. Map schematization with circular arcs. In *Geographic Information Science*, pages 1–17. Springer, 2014.
- [291] C. van Elzakker. *The use of maps in the exploration of geographic data*. PhD thesis, Universiteit Utrecht / International Institute for Geo-Information Science and Earth Observation, 2004.
- [292] A. van Goethem, W. Meulemans, A. Reimer, H. Haverkort, and B. Speckmann. Topologically safe curved schematization. *The Cartographic J*, 50(3):276–285, 2013.
- [293] A. van Goethem, W. Meulemans, B. Speckmann, and J. Wood. Exploring curved schematization. In *Pacific Visualization Symposium (PacificVis), 2014 IEEE*, pages 1–8. IEEE, 2014.
- [294] A. van Goethem, A. Reimer, B. Speckmann, and J. Wood. Stenomaps: Shorthand for shapes. *IEEE Transactions on Visualization and Computer Graphics*, 2014.
- [295] M. van Kreveld, T. Strijk, and A. Wolff. Point labeling with sliding labels. *Computational Geometry: Theory and Applications*, 13:21–47, 1999.
- [296] W. van Roessel. An algorithm for locating candidate labeling boxes within a polygon. *The American Cartographer*, 16(3):201–209, 1989.

- [297] J. van Smaalen. *Automated Aggregation of Geographic Objects - A New Approach to the Conceptual Generalisation of Geographic Databases*. PhD thesis, Wageningen Universiteit, 2003.
- [298] Various. *Knaurs Grosser Weltatlas = The Times Comprehensive Atlas of the World - Millennium Edition*. Droemersch Verlaganstalt Th. Knaur Nachf., 2000.
- [299] K. Verbeek. *Algorithms for cartographic visualization*. PhD thesis, Faculty of Mathematics and Computer Science, TU/e, 2012.
- [300] O. Verner, R. Wainwright, and D. Schoenefeld. Placing text labels on maps and diagrams using genetic algorithms with masking. *INFORMS Journal on Computing*, 9(3):266–275, 1997.
- [301] M. Visvalingam and J. Whyatt. Line generalisation by repeated elimination of points. *The Cartographic Journal*, 30(1):46–51, 1993.
- [302] M. Visvalingam and P. J. Williamson. Simplification and generalization of large scale data for roads: a comparison of two filtering algorithms. *Cartography and Geographic Information Systems*, 22(4):264–275, 1995.
- [303] P. Waniez. *Les données et le territoire au Brésil*. Universit Paris X Nanterres, 2002.
- [304] M. Wattenberg. A note on space-filling visualizations and space-filling curves. In *IEEE Symposium on Information Visualization*, pages 181–186. IEEE, 2005.
- [305] R. Weibel. Three essential building blocks for automated generalisation. In *GIS and Generalization - Methodology and Practice*. Taylor & Francis, 1995.
- [306] R. Weibel, S. Keller, and T. Reichenbacher. Overcoming the knowledge acquisition bottleneck in map generalization: The role of interactive systems and computational intelligence. In A. Frank and W. Kuhn, editors, *Spatial Information Theory A Theoretical Basis for GIS*, volume 988 of *Lecture Notes in Computer Science*, pages 139–156. Springer Berlin Heidelberg, 1995.
- [307] J. Welkowitz, B. H. Cohen, and R. B. Ewen. *Introductory Statistics for the Behavioral Sciences, sixth edition*. Wiley, 2006.
- [308] L. Williams. The effects of target specification on objects fixated during visual search. *Acta Psychologica*, 27:355–360, 1967.
- [309] S. Wilson. Are London Riots Any Different Than L.A. Riots? UCLA Professor Says Blacks Are 'Similarly Oppressed' In UK. online, 2011. <http://www.laweekly.com/informer/2011/08/09/are-london-riots-any-different-than-la-riots-ucla-professor-says-blacks-are-similarly-oppressed-in-uk>.
- [310] W. Witt, editor. *Lexikon der Kartographie*. Franz Deuticke, Wien, 1979.

- [311] W. Wojtach. Reconsidering perceptual content. *Philosophy of Science*, 76(1):22–43, 2009.
- [312] A. Wolff. Drawing subway maps: A survey. *Informatik-Forschung und Entwicklung*, 22(1):23–44, 2007.
- [313] A. Wolff, L. Knipping, M. van Kreveld, T. Strijk, and P. Agarwal. A simple and efficient algorithm for high-quality line labeling. In *Innovations in GIS VII: Geo-Computation 11*, 2001.
- [314] A. Wolff and T. Strijk. A map labeling bibliography, 2009.
- [315] C. Wood. Effects of brightness difference on specific map-analysis tasks: An empirical analysis. *Cartography and Geographic Information Science*, 21(1):15–30, 1994.
- [316] C. H. Wood. A descriptive and illustrated guide for type placement on small scale maps. *The Cartographic Journal*, 37(1):5–18, 2000.
- [317] J. Wood, P. Isenberg, T. Isenberg, J. Dykes, N. Boukhelifa, and A. Slingsby. Sketchy rendering for information visualization. *Visualization and Computer Graphics, IEEE Transactions on*, 18(12):2749–2758, 2012.
- [318] C. Wu and B. Buttenfield. Reconsidering rules for point-feature name placement. *Cartographica*, 28(1):10–27, 1991.
- [319] M. Yamamoto, G. Camara, and L. Lorena. Tabu search heuristic for point-feature cartographic label placement. *Geoinformatica*, 6(1):77–90, 2002.
- [320] P. Yoeli. The logic of automated map lettering. *Cartographic Journal*, 9 (2):99–108, 1972.
- [321] U. Zahn, editor. *Diercke Weltatlas, 3. aktualisierte Auflage*. Westermann, 1992.
- [322] J. Zighed, R. Abdesselam, and A. Hadgu. Topological comparisons of proximity measures. In *Advances in Knowledge Discovery and Data Mining Lecture Notes in Computer Science 7301*, 2012.
- [323] S. Zoraster. Integer programming applied to the map label placement problem. *Cartographica*, 23(3):16–27, 1986.
- [324] S. Zoraster. Practical results using simulated annealing for point feature label placement. *Cartography and Geographic Information Science*, 24(4):228–238, 1997.

Summary

Cartographic Modelling for Automated Map Generation

For many applications, maps are the most effective visualisation of geographic phenomena. Automated map generation, once thought to be impossible, has celebrated great successes in recent years. These successes were concentrated on large-scale topographic map production and roadmap-style web-maps. Many more specialised map types, especially from the realm of thematic maps, remain challenges both interesting and relevant. The previous efforts were especially successful when the crucial design specifications were well understood and properly formalised. When these preconditions were met, algorithmic and technical refinement could take over. In this thesis we investigate several areas of cartographic design specifications that have so far been mostly neglected. We concentrate on cartographic modelling for map labelling and medium-scale map generation. We put a special focus on automated schematisation for chorematic diagrams.

In Chapter 2 of this thesis, we investigate automated label placement. We conclude that previous efforts did not take into account many of the design principles that are relevant for actually producing maps. Most importantly, we show that by modelling the relationship between labels beyond simple overlaps, readability and legibility can be greatly improved and thus higher text densities reached. Implicitly, this suggests that treating labelling problems as maximum independent set of rectangles is insufficient for map production. Furthermore, we investigate the labelling of islands and groups of islands. We present an efficient algorithm for the labelling of individual islands outside their boundary and propose a framework for further investigating the design principles that cartographers used to label groups of islands.

In Chapter 3 of this thesis, we discuss cartographic schematisation in the context of automated generalisation. We argue that schematisation is much more content driven than current generalisation approaches and thus a crucial stepping stone towards thematic map generation. We provide the first rigorous and contextualising definition of schematisation. We also investigate the relationship of the well-known generalisation operators and schematisation operations. We conclude that schematisation operators can be presented in a taxonomy that allows to identify areas in need of further research. We introduce the *cartographic line frequency* as a measure for the content-density of a map, that replaces scale as the governing measure for schematisations. Underscoring the relation between

schematisation and generalisation, we close this chapter with an schematisation-based approach for generating caricatures of urban areas for Ordnance Survey's Strategi medium scale map product.

Chapter 4 represents the first part of our investigation of chorematic diagrams. Chorematic diagrams are thematic schematisations, that is schematised maps used to display thematic content such as population density instead of roads and routes. This makes them attractive candidates to explore thematic map generation. Chorematic diagrams use a limited set of cartographic expressions and a peculiar style. We conducted a broad investigation using multiple methods, including qualitative text analysis and quantitative, statistical methods. Our investigation highlights how the specific attributes of chorematic diagrams are linked to their ideological and organisational background. Furthermore we show with statistical high certainty that chorematic diagrams can be grouped into distinct classes. We further provide descriptive statistical measures to better describe these classes.

In Chapter 5 we investigate the cartographic design principles that are observably driving the look and feel of published chorematic diagrams. Such aesthetic qualities are commonly understood to be difficult to formalise and are also known as *tacit knowledge*. We formalise such tacit knowledge by moving from very general observations towards a more formal constraint-based model of chorematic diagrams. Most importantly, we conclude that the three main aesthetic principles of chorematic diagrams are lucidity, abstractness and harmony. We move on to show ways how each of these can be further subdivided and potentially measured. We present two studies that are concerned with validating and parametrising individual constraint measures.

In Chapter 6 we present Stenomaps: the first area-to-curve collapse technique for true areal features. Stenomaps fill one of the gaps in the schematisation taxonomy identified in Chapter 3. A stenomap comprises a series of smoothly curving linear glyphs that each represent both the boundary and the area of a polygon. We present an efficient algorithm to automatically generate these open, C1-continuous splines from a set of input polygons. Feature points of the input polygons are detected using the medial axis to maintain important shape properties. We use dynamic programming to compute a planar non-intersecting spline representing each polygon's base shape. Stenomaps show that our approach to cartographic modelling is not bound to emulate existing techniques, but can be applied to widen the cartographic design space. We describe several use cases for stenomaps including the depiction of uncertain model data in the form of hurricane track forecasting; minimal ink thematic mapping; and the depiction of continuous statistical data.

Curriculum Vitae

Andreas Reimer was born on the 9th of April, 1980 in the British Sector of West Berlin. He finished pre-university secondary education in 1999 at the Freiherr-vom-Stein Oberschule in Berlin-Spandau, Germany. He was a short term career soldier from 1999-2001, successfully completing squad leader and reserve officer training. In 2008, he received his degree of Diplom-Geograph (*cum laude*) from the Humboldt University in Berlin, Germany, with a minor in cartography from the Free University Berlin. After stays at the German Research Centre for Geosciences GFZ in Potsdam, Germany, and the Computer Science Department of Humboldt University, he is now working at the GIScience Group of the Geography Department of Heidelberg University, Germany.